

VOLUME XLIV

SPRING 2008

GEMS & GEMOLOGY



*Paraíba-type Tourmaline from
Mozambique*

History of Diamond Treatments

Purple Diamonds

THE QUARTERLY JOURNAL OF THE GEMOLOGICAL INSTITUTE OF AMERICA



pg. 14



pg. 40

EDITORIAL

- 1 The Dr. Edward J. Gübelin Most Valuable Article Award

FEATURE ARTICLES

- 4 Copper-Bearing (Paraiba-type) Tourmaline from Mozambique

Brendan M. Laurs, J. C. (Hanco) Zwaan, Christopher M. Breeding, William B. (Skip) Simmons, Donna Beaton, Kenneth F. Rijdsdijk, Riccardo Befi, and Alexander U. Falster

The geology, mining, and properties are described for this tourmaline, which typically yields bright Paraiba-like blue-to-green hues on heat treatment.

- 32 A History of Diamond Treatments



Thomas W. Overton and James E. Shigley

Reviews the history, characteristics, and identification of diamond color and clarity enhancement techniques.

NOTES AND NEW TECHNIQUES

- 56 Natural-Color Purple Diamonds from Siberia

Sergey V. Titkov, James E. Shigley, Christopher M. Breeding, Rimma M. Mineeva, Nikolay G. Zudin, and Aleksandr M. Sergeev

A gemological and spectroscopic investigation of rare purple diamonds from Siberia to better understand their color and its causes.

REGULAR FEATURES

- 66 Lab Notes

Aquamarine with kelp-like inclusions • Diamond with repeating growth/dissolution features • First CVD synthetic diamond submitted for Dossier grading • Interesting filled voids • Glass with devitrified inclusions • White clam pearl with original shell • Large baroque multicolored conch pearl • Green synthetic sapphire with vibrant blue inclusions • High-temperature heat-treated zircon

- 74 Gem News International

Tucson report • Emerald-bearing gem pockets from North Carolina • Spessartine from Loliondo, Tanzania • Gem-quality afghanite and haüyne from Afghanistan • A blue manganaxinite • Gem news from Myanmar • Gems on the market in Taunggyi, Myanmar • Large gem pocket discovered in San Diego County, California • Green sodic plagioclase from East Africa • A blue topaz with 2500+ facets • An imitation "elephant pearl" • An interesting synthetic sapphire • Lead glass-filled color-change sapphire • Myanmar Gem Emporium offerings for 1992–2007 • Conference reports

- 95 2008 Gems & Gemology Challenge

- 97 Book Reviews

- 100 Gemological Abstracts



pg. 71



pg. 83

GEMS & GEMOLOGY.

*is pleased to announce
the winners of the*



The first-place article was “Durability Testing of Filled Emeralds” (Summer 2007), a long-term study of the stability and durability of nine common emerald-filling substances. Receiving second place was “Serenity Coated Colored Diamonds: Detection and Durability” (Spring 2007), which examined a new multi-layer diamond coating technique that produces evenly distributed, natural-looking fancy colors. Third place went to “Latest-Generation CVD-Grown Synthetic Diamonds from Apollo Diamond Inc.” (Winter 2007), a report on the company’s latest products, which showed significant improvements in size, color, and clarity.

The authors of these three articles will share cash prizes of \$2,000, \$1,000, and \$500, respectively. Following are brief biographies of the winning authors.

*as voted by the journal’s readers.
We extend our sincerest thanks to all
the subscribers who participated
in the voting.*

● *First Place*

DURABILITY TESTING OF FILLED EMERALDS

Mary L. Johnson



Mary L. Johnson

Mary L. Johnson is the principal of Mary Johnson Consulting in San Diego, California. Formerly manager of research and development at GIA, Dr. Johnson received her Ph.D. in mineralogy and crystallography from Harvard University.

●● *Second Place*

SERENITY COATED COLORED DIAMONDS: DETECTION AND DURABILITY

Andy H. Shen, Wuyi Wang, Matthew S. Hall, Steven Novak, Shane F. McClure, James E. Shigley, and Thomas M. Moses



Andy H. Shen



Wuyi Wang

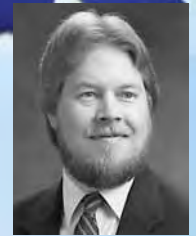
Andy H. Shen is a research scientist at the GIA Laboratory in Carlsbad, California. Dr. Shen holds a Ph.D. from Cornell University and has conducted



research in mineral physics in the United States, Germany, and the United Kingdom for more than 15 years. **Wuyi Wang** is manager of research projects at the GIA Laboratory in New York. Dr. Wang holds a doctorate in geology from the University of Tsukuba in Japan. He has considerable research experience in diamond geochemistry and diamond treatment. **Matthew S. Hall** is manager of identification services at the GIA Laboratory in New York. Mr. Hall has a bachelor's degree in geology from Franklin and Marshall College and a master's in geology and geochemistry from the University of Maryland. **Steven Novak** is senior specialist at the Evans Analytical Group in East Windsor, New Jersey. Dr. Novak has a Ph.D. in geology from Stanford University. **Shane F. McClure** is director of identification services at the GIA Laboratory in Carlsbad. Well-known for his many articles and lectures on gem identification, Mr. McClure is coeditor of *G&G's* Lab Notes section. **James E. Shigley** is distinguished research fellow at the GIA Laboratory in Carlsbad. The editor of the *Gems & Gemology in Review* series and contributing editor to the journal, Dr. Shigley received his doctorate in geology from Stanford University. **Thomas M. Moses** is senior vice president of the GIA Laboratory and Research, New York.



Matthew S. Hall



Steven Novak



Shane F. McClure



James E. Shigley



Thomas M. Moses

●●● *Third Place*

LATEST-GENERATION CVD-GROWN SYNTHETIC DIAMONDS FROM APOLLO DIAMOND INC.

Wuyi Wang, Matthew S. Hall, Kyaw Soe Moe, Joshua Tower, and Thomas M. Moses

Wuyi Wang, **Matthew S. Hall**, and **Thomas M. Moses** were profiled in the second-place entry. **Kyaw Soe Moe**, formerly a research technician at the GIA Laboratory in New York, holds a bachelor's degree in geology from the University of Yangon in Myanmar. Mr. Moe resides in West Melbourne, Florida. **Joshua Tower**, senior scientist at Apollo Diamond Inc. in Boston, has 20 years of experience in crystal growth, materials characterization, and semiconductor metrology. Mr. Tower received a bachelor's degree from Middlebury College and a master's degree from the University of Maryland, both in physics.



Kyaw Soe Moe



Joshua Tower

Congratulations to Dr. Edward Blomgren of Owls Head, New York, whose ballot was drawn from the many entries to win a three-year subscription to *GEMS & GEMOLOGY*, and copies of the two *GEMS & GEMOLOGY IN REVIEW* volumes, *COLORED DIAMONDS* and *SYNTHETIC DIAMONDS*.



COPPER-BEARING (PARAÍBA-TYPE) TOURMALINE FROM MOZAMBIQUE

Brendan M. Laurs, J. C. (Hanco) Zwaan, Christopher M. Breeding, William B. (Skip) Simmons,
Donna Beaton, Kenneth F. Rijdsdijk, Riccardo Befi, and Alexander U. Falster

Copper-bearing tourmaline from Mozambique was first recovered in 2001, but its Cu content was not recognized until 2003, and it was not widely sold with its Mozambique origin disclosed until 2005. It has been mined from alluvial deposits in an approximately 3 km² area near Mavuco in the eastern portion of the Alto Ligonha pegmatite district. Most of the production has come from artisanal mining, with hand tools used to remove up to 5 m of overburden to reach the tourmaline-bearing layer. The stones exhibit a wide range of colors, typically pink to purple, violet to blue, and blue to green or yellowish green. Heat treatment of all but the green to yellowish green stones typically produces Paraíba-like blue-to-green hues by reducing absorption at ~520 nm caused by the presence of Mn³⁺. The gemological properties are typical for Cu-bearing tourmaline (including material from Brazil and Nigeria); the most common inclusions consist of partially healed fractures and elongate hollow tubes. With the exception of some green to yellow-green stones, the tourmalines examined have relatively low Cu contents and very low amounts of Fe and Ti. Mechanized mining is expected to increase production from this region in the near future.

Copper-bearing tourmaline, in bright blue-to-green hues, is one of the most sought-after colored stones in the gem market. Soon after its discovery in Brazil's Paraíba State in the late 1980s (Koivula and Kammerling, 1989), the material gained notoriety for its beautiful "neon" colors, and prices escalated rapidly. Additional deposits were found in Paraíba and in neighboring Rio Grande do Norte State during the 1990s (Shigley et al., 2001). Then, in 2001, Cu-bearing tourmaline was discovered in Nigeria (Smith et al., 2001). At least three Nigerian localities were subsequently recognized (Furuya and Furuya, 2007; Breeding et al., 2007). The newest source of Cu-bearing tourmaline is Mozambique, which was first described in 2004 (Wentzell, 2004). Eventually, the gem trade learned that the source was the Mavuco (or Chalaua) area in the Alto Ligonha pegmatite district. It is probably the world's largest known

deposit of Cu-bearing tourmaline, and the "neon" blue and green shown by the finest stones closely resembles the most sought-after material from Paraíba (figure 1). Mavuco actually produces a wide variety of colors, including unusual deep purple amethyst-like hues and steely violetish blues (figure 2). Of the several hundred kilograms of tourmaline rough mined to date in the Mavuco area, about 10% show blue-to-green Paraíba-like colors without heat treatment (M. Konate, pers. comm., 2007).

The Cu-bearing tourmaline from this area may have been sold initially as Brazilian material (in various countries around the world, including Brazil), since the Mozambique origin was not correctly and

See end of article for About the Authors and Acknowledgments.
GEMS & GEMOLOGY, Vol. 44, No. 1, pp. 4–30.
© 2008 Gemological Institute of America



Figure 1. Copper-bearing tourmaline from Mozambique is found as alluvial pebbles (upper left, approximately 11 g) and is faceted into a variety of bright colors, including the most desirable “neon” blue and green. The center stone in the ring weighs approximately 5 ct, and the other faceted tourmalines weigh 6.73–15.77 ct; the blue teardrop in the center and the stone in the ring have been heat treated. Ring courtesy of The Collector Fine Jewelry, Fallbrook, California, and loose stones courtesy of Barker & Co. and Pala International; photo © Harold and Erica Van Pelt.

widely marketed until the September 2005 Hong Kong International Jewelry Fair (Abduriyim and Kitawaki, 2005; Abduriyim et al., 2006). Although most dealers agree that the Mozambique material’s blue-to-green colors are typically somewhat less saturated than those of its Brazilian counterpart, the lower price and greater availability have helped fuel this tourmaline’s continued popularity. The larger number of eye-clean stones in the 20–60 ct range has also created excitement (“Mozambique Paraiba tourmaline hot in Tucson,” 2007; Wise, 2007). The largest clean faceted “neon” blue Paraiba-type stone from Mozambique known to these authors weighs 88.07 ct (figure 3).

Mavuco lies on the eastern side of the Alto Ligonha pegmatite district, which is well known for producing superb gem material and/or specimens of tourmaline, beryl, topaz, and other species (e.g., Bettencourt Dias and Wilson, 2000). Most of the Alto Ligonha pegmatites are located west of Ligonha

River, whereas the Cu-bearing tourmaline deposit is on the east side. Even further east, the Monapo-Nacala area is another source of pegmatite minerals,

Figure 2. Ranging from 10.66 to 16.50 ct, these stones show some of the vivid colors seen in Cu-bearing tourmaline from Mozambique. All are reportedly unheated. Courtesy of Barker & Co. and Pala International; photo by Robert Weldon.

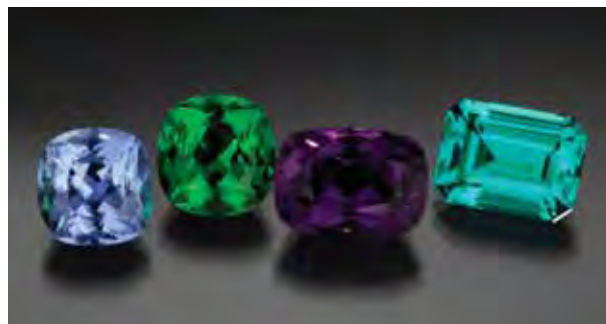




Figure 3. At 88.07 ct, this is the largest faceted “neon” blue Paraiba-type tourmaline from Mozambique that the authors have seen (heated stone, courtesy of Mozambique Gems). A 1 ct diamond is shown for scale (courtesy of GIA). Photo by Robert Weldon.

including alluvial tourmaline (Correia Neves et al., 1972; Petsch, 1985), but no Cu-bearing material is known from there.

To date, Cu-bearing tourmaline from Mozambique has been described most thoroughly by Abduriyim et al. (2006), Milisenda et al. (2006), Furuya and Furuya (2007), and Rondeau and Delaunay (2007). All of these authors have presented chemical analyses, and some illustrated how trace-element chemistry can be used to separate the Mozambique tourmalines from their Brazilian and Nigerian counterparts. The present article introduces additional chemical data for the Mozambique material and characterizes the gemological properties in detail. Information on the geology and mining was gathered by authors BML and JCZ during a five-day visit to the Mavuco area in August-September 2007. These authors were guided by Mozambique Gems Ltd., which filed the first mining claim in the area for the Paraiba-type tourmaline and has been preparing for a major mechanized operation.

HISTORY

Tourmaline, in a variety of vivid colors, was first recovered from the Mavuco area in 2001 by local farmers (M. Konate, pers. comm., 2007). In 2003, Moses Konate (current owner of Mozambique Gems) sold a parcel of this tourmaline in the United States, and was subsequently informed that it con-

tained traces of copper. As with Paraiba-type tourmaline from other localities, some of the stones turned bright blue to blue-green when heated to moderate temperatures. Mozambique then joined Brazil and Nigeria as the world’s only known sources of this attractive tourmaline.

Soon, about 300 local people were working a small area for the tourmaline. In July 2004, Mr. Konate filed a 300-hectare claim, and eventually others surrounded this concession with a series of larger claims. During the ensuing mining rush, Mr. Konate secured his claim from illegal mining and assembled four overseas partners to help finance a mechanized mining operation. In preparation for this operation, the group secured the permits needed for mining, performed mapping and exploration, and undertook an environmental impact study. They have also helped the local community by providing employment, sharing electricity from their generator, and assisting with the construction of a medical clinic in Mavuco.

Prior to the discovery of the tourmaline, fine crystals of aquamarine and quartz were recovered from miarolitic cavities in nearby pegmatites during the mid-1980s to the late 1990s. Some of this mining was actually done on the northwest portion of Mozambique Gems’ present claim, but the tourmaline was not recognized at the time because the alluvial layer that hosts it was buried by up to several meters of overburden.

LOCATION AND ACCESS

The mining area is located in northeastern Mozambique, in Nampula Province, adjacent to the village of Mavuco (figure 4). Measured in a straight line, Mavuco is located approximately 95 km south-southwest of the city of Nampula, from which the mining area can be reached in a sturdy vehicle in 2½–3 hours. The route follows a paved road 80 km to the village of Murrupula, and then 86 km of dirt road to a crossing located nearly halfway between the villages of Iuluti (or Luluti) and Chalaua. From the crossing, a dirt track proceeds a few more kilometers to the mining area.

The Mavuco region marks a gradual transition from the lower coastal plains in the southeast toward the higher plateaus in the northwest. The mining area is rather flat, but a few kilometers to the south are a pair of prominent granite monoliths (inselbergs or kopjes) with an altitude of approximately 600 m that are collectively known as Mt. Muli. *Mavuco* means *lakes*, in reference to low



Figure 4. Cu-bearing tourmalines are found in northeastern Mozambique, in Nampula Province, near the village of Mavuco. From Nampula, Mavuco can be reached via Murrupula.

areas near Mt. Muli that fill with water during the rainy season. For much of the year, though, water must be carried from seasonal streams to Mavuco by local entrepreneurs on bicycles.

Mavuco has a tropical humid climate, with a dry period in winter. The average temperature in Nampula Province varies from ~23°C (73°F) in April to ~28°C (82°F) in October–December; average rainfall varies from 15–25 mm (an inch or less) in the period May–September, to 250–260 mm (about 10 inches) in January–February (Slater, 2006). The vegetation consists of open savanna, and farmers use much of the land around the mining area to grow crops such as cassava, maize, beans, cashew nuts, and various fruits.

GEOLOGY

The basement rocks in the Mavuco area form part of the Mozambique Belt (1100–800 million years old [Ma]), which extends from the Mediterranean Sea down to central Mozambique (Lächelt, 2004).

This orogenic belt hosts rich gem and mineral wealth over a large area from Mozambique through Tanzania and Kenya (Bettencourt Dias and Wilson, 2000). In northern Mozambique, the basement consists primarily of strongly metamorphosed gneisses (migmatites) that were mainly deformed during the Pan-African tectonic event (800–550 Ma). During the period 600–410 Ma, these rocks were intruded by granitoids and rare-element granitic pegmatites (e.g., Pinna et al., 1993; Lächelt, 2004; figure 5). Most of the pegmatites were emplaced within approximately 200 km of Alto Ligonha. Since the 1930s, they have been mined for a variety of commodities, including rare metals (Li, Be, Nb, and Ta), industrial minerals (quartz, mica, feldspar, and clay), and gems such as tourmaline and beryl (Bettencourt Dias and Wilson, 2000; Lächelt, 2004).

The Mavuco area is tropically weathered and mostly covered by deep lateritic soil. Recent regional-scale geologic mapping, carried out by Mozambique's National Directorate of Geology and supported by the World Bank, shows that the principal rock types

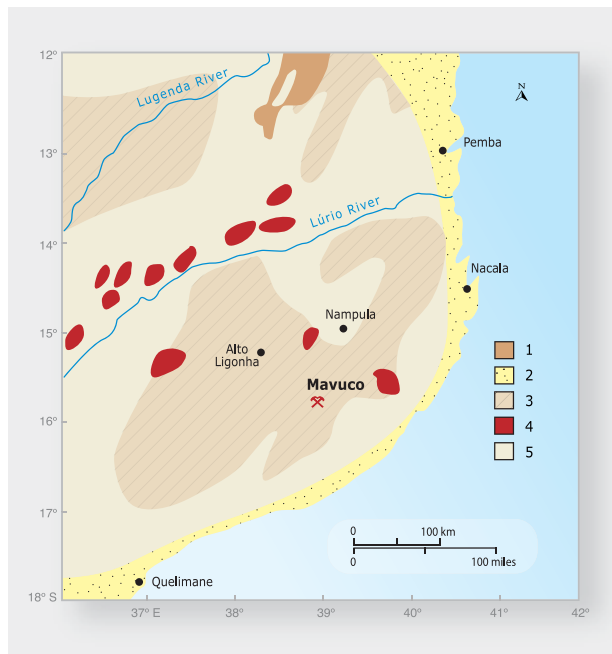


Figure 5. The area where the Cu-bearing tourmalines are found lies on the eastern side of the well-known Alto Ligonha pegmatite district. This geologic sketch map shows the principal tectonic-geologic units: (1) rift of the East African Rift System; (2) Mesozoic and Cenozoic sedimentary rocks; (3) pegmatite fields; (4) Pan-African intrusions; (5) Mozambican areas, part of the Mozambique Belt and mostly remetamorphosed during the Pan-African tectonic event. Modified after Lächelt (2004).

consist of various types of gneiss (mapped as the Nantira/Metil Group by Pinna et al., 1986), as well as the granites of Mt. Muli and Mt. Iulüti (figure 6).

Simple granitic pegmatites locally crosscut the basement rocks and form quartz-rich outcrops where the host gneisses are exposed at the surface (particularly common in the northwest portion of Mozambique Gems' claim). They consist of milky, rose, and/or clear, transparent quartz, pink K-feldspar, and black tourmaline, with rare micas and sometimes beryl. Although these pegmatites are found quite close to the area mined for Cu-bearing tourmaline, they are not the source of this material, as expected from their Li-poor composition.

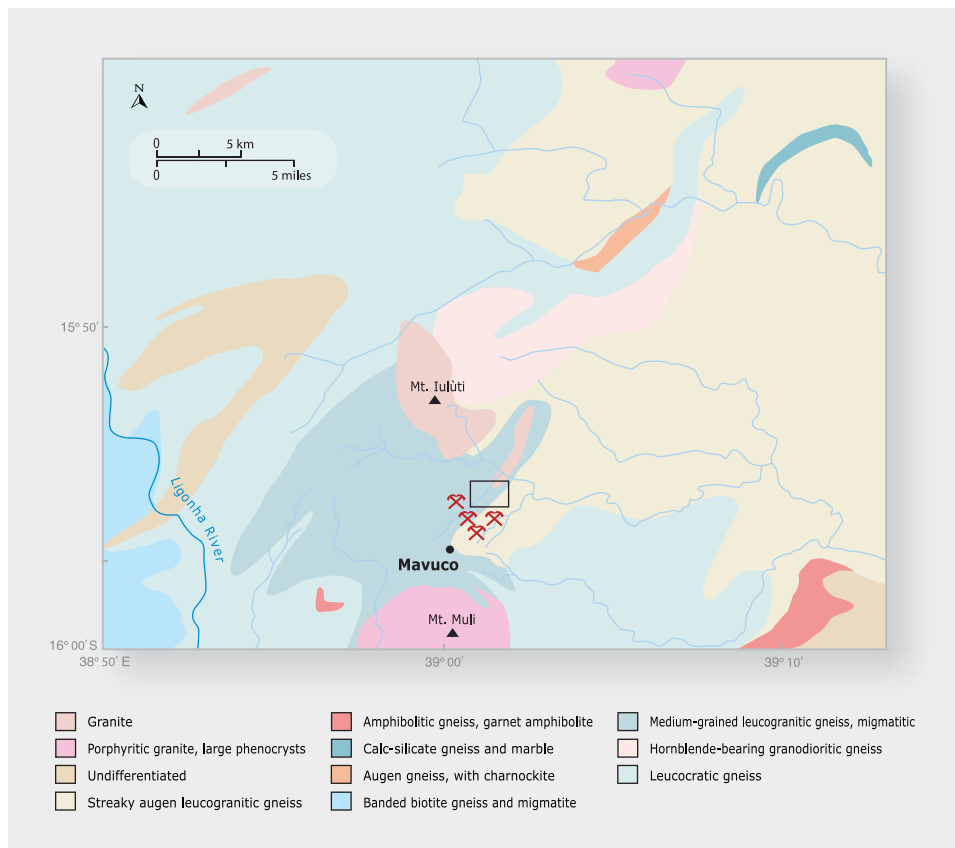


Figure 6. The inferred basement rocks in the Mavuco area are shown on this geologic map. The map is part of an as-yet unpublished regional map that was recently compiled by Mozambique's National Directorate of Geology as part of an ongoing project financed by the World Bank. The Cu-bearing tourmaline deposit is situated approximately between two granitic massifs, Mt. Muli and Mt. Iulüti. The rectangle shows the mining concession of Mozambique Gems Ltd.



Figure 7. This large pit on the Mozambique Gems claim shows a good cross-section of the geology of the deposit (left; photo by B. M. Laurs). The tourmalines are found in a light reddish brown quartz-rich gravel layer on top of light tan weathered bedrock, and underneath a top layer of red-brown clayey soil. The gravel layer can be found between 0.5 m and 5 m below the surface in the Mavuco area. The thickness of the tourmaline-bearing gravel layer is indicated by the men in the image on the right (photo by J. C. Zwaan).



fall into the latter category, although some pieces we encountered still showed traces of striations on the prism surfaces (figure 9).

Figure 8. The tourmaline-bearing layer is a quartz-rich, clast-supported gravel. Many of the clasts are angular, such as the larger (5 cm) quartz pebble toward the right in this image. Photo by J. C. Zwaan.

The Cu-bearing tourmaline has only been found as waterworn pebbles in secondary deposits. The tourmaline-bearing layer (paleoplacer) rests on top of weathered biotite gneiss bedrock, and itself is covered by a red-brown to black tropically weathered horizon (laterite; figure 7). The laterite varies in thickness from approximately 0.5 m near seasonal streams to typically 3–5 m. The tourmaline-bearing gravel layer is generally between several centimeters and 1 m thick and ranges from light gray to red-brown. The latter color is due to the weathering of iron-bearing materials, which has locally stained the clasts and interstitial clays within the gem-bearing layer. Available exposures of this layer showed that it is flat-lying. It is predominantly comprised of fine- to medium-sized gravels (0.2–30 mm) and local pebbles (typically 40–70 mm). The gravels are clast-supported, showing an open-worked matrix (i.e., containing many empty spaces, and in places no matrix at all). The individual pebbles are typically coated with a red clayey silt (figure 8). The gravels consist mainly of milky to transparent quartz; less common are partially weathered feldspar and black or colored tourmaline. The gravels are dominated by subangular clasts (>90%), with the balance subrounded to rounded. The colored tourmalines





Figure 9. Copper-bearing tourmalines from Mozambique are found as waterworn pebbles that only rarely show traces of striations on the prism surfaces. This selection of larger rough—some with evidence of striations—was taken from a 1 kg parcel of unheated Cu-bearing tourmaline seen in Nampula. Photo by J. C. Zwaan.

MINING

The Cu-bearing tourmaline recovered thus far comes from an approximately 3 km² area near Mavuco (figure 10). Informal diggers have done most of the mining on the south and east sides of Mozambique Gems' 300-hectare mining concession. The area that has been explored/mined for the tourmaline is roughly bounded by coordinates 15°54'–15°57' S and 39°00'–39°03' E, at elevations between 150 m (near seasonal streams) and 200 m above sea level. The extent of the tourmaline-bearing horizon has not yet been determined, although during the visit by BML

and JCZ miners reported encountering only black tourmaline on some edges of the mined area, leading them to search elsewhere.

The artisanal miners use picks and shovels to dig through the hard laterite in search of the gem-bearing layer (figure 11). They remove the tourmaline pebbles by hand while digging through the gravels with a pick (figure 12). Although many gems are probably overlooked in the process, water for washing the gravel is scarce or unavailable to the artisanal miners during most of the year, and the material is cemented by clay so dry screening is not feasible. Most of the rough material weighs 2–5 g, although stones up to 10 g are common. Rare pieces are found that attain weights of 100–300+ g.

Mozambique Gems has performed systematic mapping and test pitting of their concession (figure 13), and has completed a comprehensive environmental impact report. At the time of the authors' visit, the company employed 32 workers, mostly from the local area. The company is building a washing plant capable of processing 150–200 tonnes of material per day (figure 14). It is modeled after plants used for recovering alluvial alexandrite in Brazil, and Brazilians are doing the design and construction. The plant will employ water jets to break up the mined material and wash it through a series of three screens with mesh sizes of 2, 1, and 0.5 cm. Material from the three screens will be routed to large tables and then hand-picked for tourmaline.

Mechanized mining will begin when the washing plant is completed, which is projected for mid-2008.



Figure 10. This view of the Mavuco area from the top of Mt. Muli (a few kilometers to the south) shows a portion of the town in the foreground, and the weathered red-brown laterite that denotes the mining area in the background. Photo by B. M. Laurs.



Figure 11. Most of the Cu-bearing tourmaline recovered so far from the Mavuco area has come from artisanal miners. Working in small groups, they use picks and shovels to dig through the laterite overburden in search of the gem-bearing layer. Photo by B. M. Laurs.

Figure 13. Mozambique Gems is digging this test pit to help determine the extent of the tourmaline-bearing layer on their concession. The material from the gem-bearing layer of the pit will be washed, screened, and hand-picked for tourmaline. Photo by B. M. Laurs.



Figure 12. When they reach the tourmaline-bearing layer, the miners search for the gems by digging through the gravels with a pick. Photo by B. M. Laurs.

A bulldozer will excavate a series of elongate pits to reach the tourmaline-bearing layer. The topsoil will be stockpiled, and miners will reclaim each pit before proceeding to the next one. All of the material excavated from the tourmaline-bearing layer will be put through the washing plant. Water will be pumped to the plant from a local stream, and once

Figure 14. This washing plant, constructed by Mozambique Gems, will be able to process 150–200 tonnes of material per day when it is completed. Photo by J. C. Zwaan.





Figure 15. The market in Mavuco is bustling with miners, stone buyers, and salespeople who peddle supplies to the diggers. Photo by J. C. Zwaan.

discharged will be captured by a series of settling ponds to remove the silt. A reservoir will ensure that the washing plant continues to operate when the stream dries out from late September to late December.

A limited amount of mechanized mining has reportedly occurred in the area surrounding the Mozambique Gems claim. The owners of the mineral rights in that area have consolidated their claims and also are making preparations for mechanized mining.

PRODUCTION AND DISTRIBUTION

So far, local diggers are responsible for most of the tourmaline produced from the Mavuco area. The vast majority are Mozambique nationals who came to Mavuco (figure 15) from neighboring Zambezia Province, where most of the Alto Ligonha pegmatites are mined. At the time of the visit by authors BML and JCZ, we estimated that about 600 diggers were active, and 3,000–4,000 people were living in the region. Gem dealers in the area when mining first started said that more than 7,000 people were in the region during the initial gem rush.

The locals typically have contract mining arrangements with West African buyers (figure 16), who support them in exchange for first rights to buy their production. During our visit, one local dealer told us there were at least 200 buyers, and some employed several dozen miners. The tourmalines are brought from the miners to the buyers by “runners,” who are commonly seen going to and from the Mavuco market on motorcycles. The West African buyers then sell the rough to other buyers who come to the Mavuco market (other West Africans, as well as Brazilian and Thai dealers), or in Nampula (where German buyers and other foreigners are also active). In Mavuco the stones may be purchased singly (figure 17), while in Nampula they are commonly offered in parcels weighing from hundreds of grams to a few kilograms. Due to the multiple channels by which the stones



Figure 16. The vast majority of the stone buyers in Mavuco come from West Africa. They purchase the rough material by the gram from the miners, using miniature digital scales. Also present in this photo are Chirindza Henrique (wearing a blue short-sleeved shirt) and Salifou Konate (far right) from Mozambique Gems. Photo by B. M. Laurs.



Figure 17. This intense multicolored bluish violet to pink waterworn tourmaline pebble, which weighs 6 g, was offered for sale at Mavuco. Photos by B. M. Laurs (left) and J. C. Zwaan (above).

arrive on the market, it was impossible to determine the overall production of rough from Mavuco.

Considerable amounts of the tourmaline produced by artisanal miners have been sent to Hong Kong and Germany for cutting. According to Mr. Konate (pers. comm., 2007), the tourmaline obtained so far by Mozambique Gems has been cut in Brazil, where heating is done to the preformed gems. In the future, their production will be channeled directly to large cutting wholesalers and television shopping networks, mainly for U.S. and Japanese markets.

While in Nampula, authors BML and JCZ examined two parcels of rough material (one about 1 kg and the other 400 grams) that were reportedly unheated goods mined from the Mavuco area. They showed a variety of colors, clarities, and sizes (again, see figure 9), with some weighing as much as 30 g. We purchased a selection of smaller samples from the 1 kg parcel for analysis (figure 18), some of which later proved to be imitations: bluish green manufactured glass, yellowish green fluorite, and amethyst. According to one dealer who has visited the Mavuco area (F. Hashmi, pers. comm., 2007), bluish green glass frequently appears in rough parcels offered for sale throughout East Africa. Amethyst is used as an

imitation because it resembles the color of Cu-bearing tourmaline that commonly heat-treats to “neon” blue colors. During our trip, Mr. Konate mentioned that pieces of “tumbled” amethyst are produced by shaking them in an empty soda bottle until they take on a worn appearance. Milisenda et al. (2006) also documented a non-Cu-bearing tourmaline crystal and a flame-fusion synthetic ruby “pebble” that were represented as being Mozambique Cu-tourmaline.

Figure 18. These unheated waterworn pebbles (0.3–1.1 g) were obtained in Nampula for characterization as part of this study. Three of the samples proved to be imitations: an amethyst (the somewhat triangular purple fragment on the left), a very light yellowish green fluorite (the rectangular piece just to the right of center), and a very light bluish green manufactured glass (below the fluorite). Photo by Kevin Schumacher.





Figure 19. Mozambique Cu-bearing tourmaline pebbles commonly are of a single color, yielding cut stones with even color distribution (here, 6.75–15.77 ct). All but the blue faceted stone are unheated. Courtesy of Barker & Co. and Pala International; photo © Harold & Erica Van Pelt.

While much of the tourmaline rough is monochromatic and yields stones of a single hue (figure 19), some pieces show noticeable color zoning, commonly in irregular patterns (figure 20). A small number of dramatic multicolored stones have been cut from the color-zoned material (figure 21). Since heat treatment reduces the violet/purple hue (see below), such stones are highly unlikely to have been heated. Most of the faceted tourmaline from Mavuco weigh 1–4 ct. Stones weighing 5–20 ct are produced occasionally, and clean faceted gems in the 20–60+ ct range are rare but nevertheless more common than among Paraíba-type tourmalines from other localities.

Figure 21. This 2.55 ct faceted Cu-bearing tourmaline from Mozambique shows striking color zoning. The presence of purple and violet in this stone strongly indicates that it is unheated. Courtesy of Mayer and Watt, Maysville, Kentucky; photo by Robert Weldon.



Figure 20. Some of the rough tourmaline have vivid color zoning. The stones shown here, which are all unheated, range from 6 to 11 g. Courtesy of Barker & Co. and Pala International; photo by C. D. Mengason.

MATERIALS AND METHODS

For this study, we examined 106 samples of Mozambique Cu-bearing tourmaline, including 59 pieces of rough (0.1–4.1 g) and 47 faceted stones (0.40–17.49 ct). All the rough samples were transparent and suitable for faceting or cabbing; at least two windows were polished on each. The rough consisted of 17 samples obtained by authors BML and JCZ from a local dealer in Nampula, who represented them as unheated tourmaline from the Mavuco area (again, see figure 18); and 21 pairs of samples (42 total) donated by two U.S. dealers to show the effects of heat treatment (e.g., figure 22). The faceted samples included 12 unheated stones (e.g., figure 23) and 11 pairs (22 total) of unheated/heated stones (figure 24) that were tested at the Netherlands Gemmological Laboratory (NGL); as well as 13 unheated tourmalines that were examined at the GIA Laboratory in New York (figure 25). All the faceted samples were obtained from U.S. dealers, who had purchased the material from reliable suppliers as coming from Mozambique. Mavuco is the only known source of Cu-bearing tourmaline in Mozambique.

The two plates from each of the 21 unheated/heated pairs of rough were cut from the same piece of rough. One of the dealers (Bill Barker) heated one sample from each pair in air to 530°C for three hours. To minimize thermal shock, he packed the samples in plaster-of-paris powder and raised and lowered the temperature gradually. After heating, these samples were soaked in warm oxalic acid at GIA for several days to remove iron staining and improve the observation and comparison of colors. Mr. Barker selected



Figure 22. Each pair of parallel-polished plates shown here (0.98–7.15 ct) was sliced from the same piece of rough. The segments on the left in each pair are unheated, and those on the right were heated to 530°C for three hours. These slices formed part of the study suite of samples examined before and after heating. Gift of Barker & Co. and Pala International, GIA Collection nos. 37519–37540; photo by J. C. Zwaan.

the 11 unheated/heated pairs of cut stones to show the typical effects of heat treatment on the coloration of these tourmalines; the stones in each pair are similar in size and shape, but they were not faceted from the same piece of rough. Mr. Barker informed us that he brought the heated samples in each pair to 550°C for three hours.

Testing at NGL was done on all the rough samples and on 34 of the faceted samples described above; included were standard gemological properties and energy-dispersive X-ray fluorescence (EDXRF) spectrometry. Instruments and methods used for determination of standard gemological properties included a Rayner refractometer (yttrium aluminum garnet prism) with a near sodium-equivalent light source to measure refractive indices and birefringence; hydrostatic determination of specific gravity; a calcite dichroscope for observation of pleochroic colors; four-watt long- and short-wave UV lamps used in a darkened room to observe fluorescence; a Nikon Eclipse E600 POL polarizing microscope; and both standard daylight and incandescent illumination for the observation of colors. An Eagle mProbe EDXRF spectrometer was used to analyze the composition of one surface-reaching inclusion, as well as the composition of a rough sample that proved to be an imita-

tion, and to survey the chemistry of the sediment in which the tourmalines are found. In addition, Raman spectroscopy of inclusions in 26 samples (7 unheated cut stones, and 7 heated and 12 unheated pieces of

Figure 23. These Cu-bearing tourmalines from Mozambique (1.69–3.76 ct), which were characterized for this report, show a wide range of natural, unheated colors. Courtesy of Barker & Co. and Pala International; photo by J. C. Zwaan.



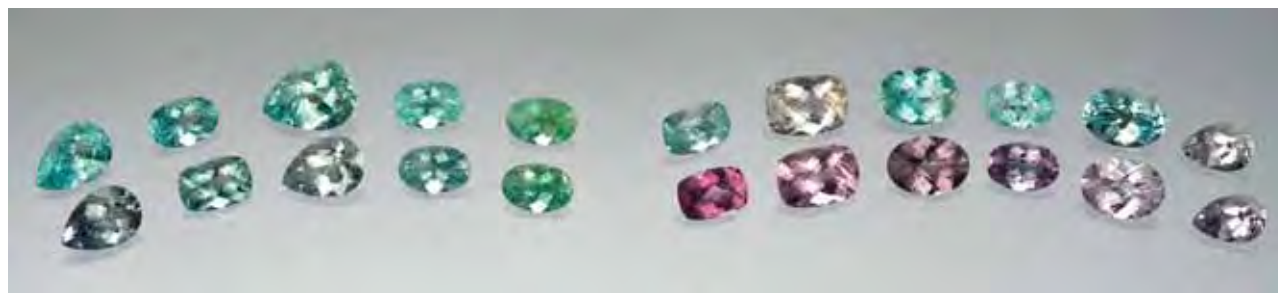


Figure 24. These faceted Cu-bearing tourmalines (0.42–0.85 ct) were carefully selected to show typical colors before (bottom row) and after (top row) heat treatment. The sample pairs were not cut from the same pieces of rough. Courtesy of Barker & Co. and Pala International; photo by Robert Weldon.

rough) was performed by JCZ at the CCIP French Gemmological Laboratory in Paris using a Renishaw Invia instrument with 514 nm laser excitation.

The examination of 13 faceted stones at the GIA Laboratory in New York included determination of standard gemological properties, as well as polarized UV-Vis-NIR spectroscopy using a Perkin-Elmer Lambda 950 spectrophotometer with a calcite polarizer over the range 250–850 nm with a resolution of 1 nm. Gemological testing included daylight-equivalent (D65) light for color and a GIA Duplex II refractometer for RI and birefringence. Methods for deter-

mining SG, pleochroism, fluorescence, and internal features were comparable to those used at NGL. The GIA Laboratory in Carlsbad performed Vis-NIR absorption spectroscopy (400–1000 nm range) on the 21 unheated/heat-treated pairs of polished rough, using a Hitachi U4001 spectrometer with a slit width of 2.0 nm, data collection interval of 1.0 nm, and scan speed of 120 nm/min. Spectra were collected at room temperature using an unpolarized light beam focused through the parallel polished samples.

The quantitative chemical composition of all 59 rough samples was measured by electron micro-

Figure 25. These unheated Cu-bearing tourmalines from Mozambique were also studied for this report. The 1.28–3.02 ct stones on the left are courtesy of Pala International; the less common colors on the right (3.71–17.49 ct, top; 80.54 ct, bottom) are courtesy of Fine Gems International. Photos by Robert Weldon.

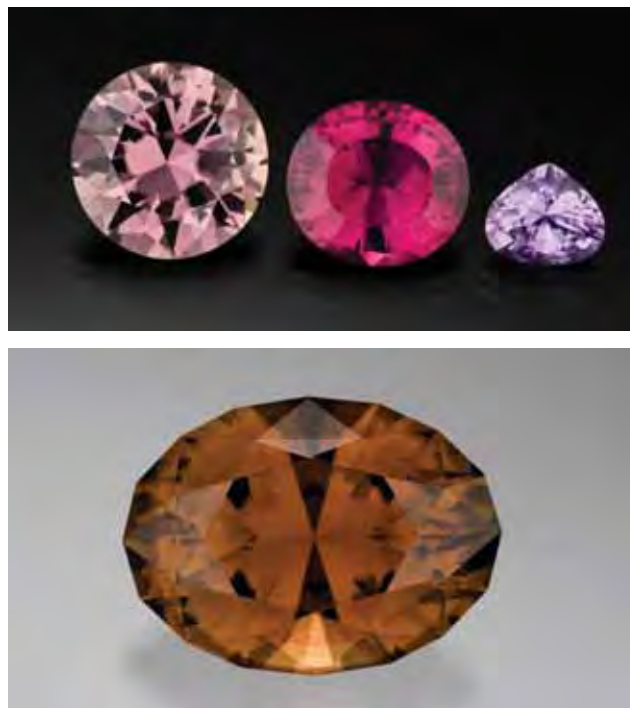


TABLE 1. Physical properties of Cu-bearing tourmaline from Mavuco, Mozambique.

Properties	Unheated (no. samples)				Heated (no. samples)	
	16	29	14	15	26	6
Color (standard daylight)	Very light to medium purple to reddish purple; very slightly grayish to strong saturation	(Medium) light (violetish) blue to (medium) light (bluish) violet; grayish to moderately strong saturation	Light bluish green to light greenish blue; most often moderately strong and strong saturation	Very light to medium green to yellowish green; moderately strong to vivid saturation	Light bluish green to light greenish blue; moderately strong to strong saturation	Light to medium green
Color (incandescent light)	(Purplish) pink	Light (grayish) green to light (greenish) gray	Same	Same	Same	Same
Pleochroism	Weak to strong	Weak to distinct	Weak to distinct	Weak to strong	Weak to distinct	Weak to distinct
e-ray	Pink, pale yellow, brownish/pinkish orange, purple	Light (grayish) pink, gray to green, light brown	Light greenish gray to (grayish) green	Light gray to grayish green, green to bluish green	Light gray, grayish green, yellowish to bluish green	Light (greenish) gray to grayish green
o-ray	Medium(-light) purple to violet to pink, violetish blue	Light blue to violet (greenish) blue	Light bluish green to green	Medium (yellowish) (greenish) blue	Light bluish green to (yellowish) green	Light to medium
RI						
n_o	1.638–1.640	1.638–1.642	1.638–1.640	1.640–1.643	1.638–1.643	1.639–1.643
n_e	1.620–1.622	1.619–1.623	1.620–1.621	1.620–1.623	1.618–1.623	1.620–1.623
Birefringence	0.018–0.020	0.018–0.020	0.018–0.020	0.018–0.021	0.018–0.020	0.019–0.020
SG	3.01–3.06	3.01–3.06	3.03–3.09	3.06–3.09	3.03–3.07	3.06–3.09
UV fluorescence (long- and short-wave)	Inert except for two samples ^a	Inert	Inert	Inert	Inert; 13 faint blue to long-wave	Inert; two faint blue to long-wave
Internal features	<ul style="list-style-type: none"> Partially healed fissures (“fingerprints”) with isolated two-phase (liquid-gas) inclusions, with irregular, wispy/thready, and triangular shapes, also in almost pinpoint size Partially healed fissures with “trichites,” reflective thin films, and long, spiky inclusions Hollow tubes, long and generally thin and narrow, oriented parallel to the c-axis, occasionally in discrete planes or forming “walls”; may be stained yellow to red-brown and contain hematite Straight growth zoning Color zoning (one sample) Mineral inclusions (not common): quartz, both isolated and within fluid inclusions; lepidolite; and sodic plagioclase 				In addition to the features listed for the natural colors: <ul style="list-style-type: none"> Minute cracks, usually small, with discoid and more elongated shapes, appearing milky or brownish, depending on the lighting (Larger) voids in partially healed fissures may appear frosty and dried out 	

^a A brownish reddish purple stone (figure 25, top right—far left sample) fluoresced weak white to long-wave UV; an orangy brown stone with reddish purple components (figure 25, bottom) fluoresced white under the girdle to short-wave UV and irregular weak yellow to long-wave UV.

probe at the University of New Orleans. Data were collected using an ARL-SEMQ electron microprobe with 15 kV (for sodium) and 25 kV accelerating voltages, 15 nA beam current, and a 3 μm beam diameter. The measurements were calibrated with natural mineral and synthetic compound standards, and a ZAF correction procedure was applied to the data.

Trace-element chemical data of all the rough samples were measured quantitatively at the GIA Laboratory in Carlsbad using a Thermo X Series ICP-MS (inductively coupled plasma-mass spectrometer) joined to a New Wave UP-213 laser-ablation sampling system. The laser operated at a wavelength of 213 nm with He as the carrier gas (flow rate of ~1 liter/minute). Laser-ablation parameters were as follows: 40 μm spot diameter, ~10 J/cm² laser energy density (fluence), 7 Hz repetition rate, and 25 second laser dwell time. For calibration, NIST SRM 610, 612, and 614 glass reference materials (Pearce et al.,

1996) were used as external standards, and boron was used as an internal standard. An average B concentration for elbaite tourmaline of 3.26 wt.% was obtained from Deer et al. (1974).

In the course of this testing, four pebbles obtained in Mozambique by authors BML and JCZ proved to be imitations. The amethyst, light yellowish green fluorite, and light bluish green manufactured glass (again, see figure 18) purchased from one of the parcels were initially detected during microprobe analysis. A piece of light green rough that was obtained directly from one of the miners at the pits was identified as fluorite during gemological testing at NGL.

GEMOLOGICAL PROPERTIES

The gemological properties of the rough and cut tourmalines are summarized in table 1, with details described below.



Figure 26. This unheated tourmaline (4.13 ct) shifted from grayish blue in fluorescent light (left) to grayish green in incandescent light (right). Photos by J. C. Zwaan.

Visual Appearance and Color. The rough tourmaline seen in Mozambique by the authors consisted of well-rounded waterworn pebbles (again, see figures 9 and 17–19) and broken fragments, in various colors including blue or violet, very light blue, strong greenish blue, purple, and green (for complete color descriptions, see the *G&G* Data Depository at www.gia.edu/gemsandgemology). Typically the color was evenly distributed, although we did see strong color zoning in some of the rough. One greenish blue piece had a pink core; other green-blue samples showed pinkish purple zones, while one blue-green crystal section had a dark green rim. On one side of a violetish blue sample, a gradual transition to greenish blue was observed. In some waterworn pebbles, portions of the original crystal faces could be recognized. Most of the material were transparent, but we also saw heavily included stones.

The cut and rough (most facetable, some cabochon quality) tourmalines we studied showed a wide variety of colors (again, see figures 22–25). The main color groups (in daylight-equivalent illumination) of the unheated samples were purple to reddish purple, blue to bluish violet, bluish green to

greenish blue, and green to yellowish green. Color banding was observed only rarely in our samples. Many of the heated tourmalines were bluish green to greenish blue, colors produced from blue-to-violet starting material (figure 22). Some of our heated samples were green, which resulted from heating darker green or yellowish to slightly bluish green stones (see again figure 22 and “UV-Vis-NIR Spectroscopy” below). The dichroism of the cut tourmalines varied from weak to strong.

When viewed in incandescent light, the unheated light blue to violet tourmalines appeared light green to gray (figure 26). Most of the purple stones appeared pink and purplish pink or red in incandescent light. However, there was no obvious color change shown by a light purple piece of rough and a medium, slightly grayish purple cut stone.

Physical Properties. Nearly 80% of the stones tested showed refractive indices of $n_o = 1.638\text{--}1.641$ and $n_e = 1.619\text{--}1.622$, with a birefringence ranging between 0.018 and 0.020. Although overlapping, some green tourmalines showed slightly higher average values of $n_o = 1.640\text{--}1.643$ and $n_e = 1.621\text{--}1.622$, with a birefringence of 0.019–0.021.

Figure 27. In Cu-bearing tourmaline from Mavuco, partially healed fissures show a wide variation in appearance, as illustrated in these unheated samples. They commonly occur as “trichites,” consisting of flat and irregularly fluid-filled cavities that are connected by thin capillaries (left, magnified 65×). Some of the cavities are larger and less flat, with obvious bubbles when viewed with transmitted light (center; magnified 40×). In some of the fissures, isolated two-phase (liquid-gas) inclusions were abundant (right, magnified 65×). Photomicrographs by J. C. Zwaan.



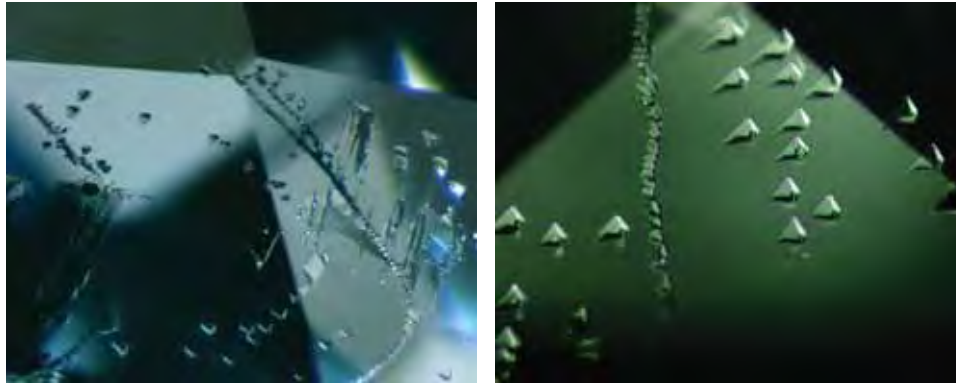


Figure 28. This partially healed fissure in an unheated tourmaline has a network of oriented triangular two-phase (liquid-gas) inclusions, with some isolated and others in close array (left, magnified 75×). Higher magnification clearly shows the bubbles present in each triangular inclusion (right, magnified 100×). Photomicrographs by J. C. Zwaan.

Specific gravity values ranged from 3.01 to 3.09. The majority of the stones had an SG between 3.04 and 3.06, while the green tourmalines showed slightly higher values of 3.06–3.09.

All but two of the tourmalines that were represented as unheated were inert to long- and short-wave UV radiation. Almost half of the known heat-treated stones fluoresced a faint blue to long-wave UV, and nearly half of those also fluoresced very faint blue to short-wave UV.

Microscopic Characteristics. The rough and cut samples ranged from very slightly to heavily included. The main internal characteristics in both the heated and unheated samples were partially healed fissures (showing various stages of healing), fluid inclusions, and growth tubes (commonly stained). In addition, numerous minute cracks were seen in many of the heated stones.

Fluid Inclusions, Growth Tubes, and Cracks. The most conspicuous inclusions consisted of partially healed fissures, which exhibited wide variations in appearance (figure 27). Often they occurred as “trichites” (i.e., fluid-filled cavities connected by networks of very thin capillaries). The capillaries were irregular and coarse, wispy, or thread-like. The cavities were typically flattened and irregularly shaped (figure 27, left), but more equidimensional (or less flattened) cavities were often present. In the larger cavities, a bubble could sometimes be seen in transmitted light (figure 27, center). Some partially healed fissures were marked by abundant isolated two-phase (liquid-gas) inclusions (figure 27, right). Typically these inclusions were irregular and wispy, but in some cases triangular shapes were predominant, either isolated or in groups (figure 28). Some partially healed fissures contained very small, pin-point-sized features that could be resolved as two-phase inclusions under 200× magnification. The

two-phase inclusions showed low relief, with bubbles that were small relative to the size of the inclusion, indicating that they are rich in liquid water (e.g., Samson et al., 2003). Occasionally, they contained small doubly refractive minerals as well (see “Mineral Inclusions” below).

More-or-less parallel-oriented and interconnected flat channels and long, spiky inclusions—apparently representing a relatively early discontinuation of fracture healing—were occasionally encountered (figure 29). Hollow tubes, oriented parallel to the c-axis, were quite common (figure 30). They were present as one or two isolated tubes in “clean” stones, but also occurred more abundantly, occasionally even forming “walls” of parallel tubes in straight or slightly wavy planes. Both the narrow

Figure 29. Subparallel-oriented and interconnected flat channels and long, spiky inclusions, such as seen here in an unheated tourmaline, are occasionally encountered. These features appear to represent an early discontinuation of fracture healing. Photomicrograph by J. C. Zwaan; magnified 55×.



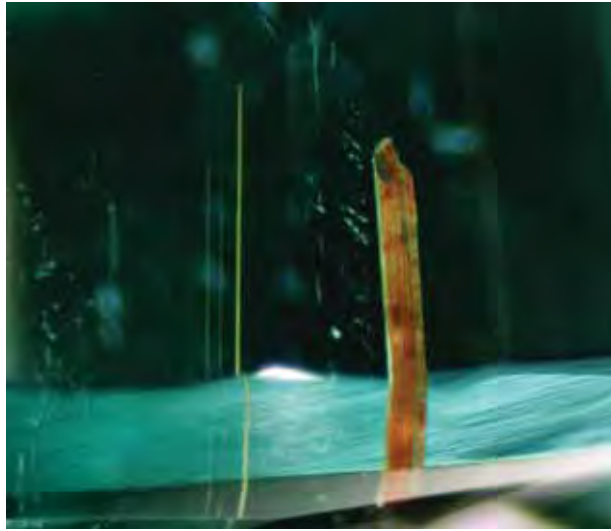


Figure 30. Hollow tubes are quite common in the tourmaline, typically very thin but occasionally much thicker (and flattened), and often stained yellow to red-brown. They occur in parallel orientation in this unheated stone. Photomicrograph by J. C. Zwaan; magnified 36 \times .

and the thicker tubes, which at first glance might be confused with a mineral inclusion, turned out to be hollow. Many of the tubes were stained yellow to red-brown. Raman analysis identified a fine-grained reddish brown substance inside relatively

Figure 31. Minute and slightly larger cracks were common in most of the heated tourmalines, showing both discoid and more elongated shapes. When viewed with darkfield illumination, they often appear as milky stress fractures or otherwise translucent areas. Photomicrograph by J. C. Zwaan; magnified 16 \times .



thick tubes in three stones as hematite (again, see figure 30).

Most of the unheated stones, regardless of how heavily they were included, did not contain many fractures. Only two of the polished rough fragments and one faceted stone were heavily fractured.

Although most of the above features occurred in both unheated and heated stones, some different characteristics were seen in the latter material. Abundant minute cracks were present in all but one (which was only slightly included) heated stone examined (figure 31). These minor cracks were usually small and often discoid, although more elongated cracks also occurred. When viewed with darkfield illumination, they appeared as milky and translucent stress fractures, which became reflective when viewed along the fracture plane. In brightfield or transmitted light they were often invisible, or showed a brownish tinge when viewed along the fracture plane.

In heat-treated stones, the larger voids in partially healed fissures often appeared somewhat frosty (especially close to the surface), as if they had dried out during the heating process (figure 32). This is supported by the fact that no bubbles could be detected in them. In one unheated/heated sample pair, the untreated part had irregular cavities filled with liquid (figure 33, left), whereas the treated half had cavities

Figure 32. In the heat-treated tourmalines, the larger cavities in partially healed fissures often appeared somewhat frosty, which indicates that the fluid dried out during the heating process. Photomicrograph by J. C. Zwaan; magnified 40 \times .



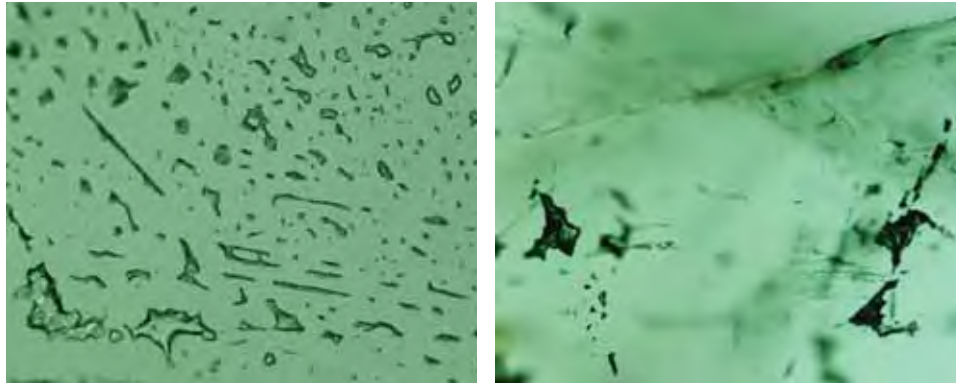


Figure 33. The unheated portion of one tourmaline slice (left) contains irregular-shaped cavities filled with liquid. However, in the portion subjected to heat treatment (right), the cavities appear dark in transmitted light, which indicates that they are empty. Photomicrographs by J. C. Zwaan; magnified 100 \times .

with the same shape that appeared dark in transmitted light, and were therefore empty (figure 33, right). Some of the smaller fluid inclusions survived the relatively low-temperature heat treatment.

Mineral Inclusions. Small, mostly rounded to sub-angular, transparent grains of quartz were identified in five of the samples by a combination of optical means and Raman analysis. Quartz occurred as isolated grains (figure 34), but also connected to—and captured within—fluid inclusions.

Flakes of lepidolite were identified by Raman analysis in six tourmalines (figure 35); in two instances they formed “booklets.” In all cases, Raman analysis gave a perfect fit with reference spectra for lepidolite, but also a good fit with polyolithionite. As lepidolite, once considered a dis-

tinct mineral, has been redefined as a lithium-bearing mica in the polyolithionite-trilithionite series (Kogure and Bunno, 2004; Brigatti et al., 2005), *lepidolite* seems an appropriate general name for these inclusions.

A few transparent, irregular-to-rounded grains in an otherwise clean yellowish green tourmaline were identified by Raman analysis as sodic plagioclase (figure 36). The spectra showed a close resemblance to those of both oligoclase and albite, with two grains showing the best fit for albite (see, e.g., Mernagh, 1991).

In one very clean green tourmaline, small grains with very low relief, hardly visible with a loupe, appeared to form a trail through the stone. The grains were too deep and too small for Raman analysis; they were tentatively identified as tourmaline, based on their low relief and moderate pleochroism, which was shown clearly by one crystal located somewhat closer to the surface.

Figure 34. The isolated transparent crystal on the left, close to a partially healed fissure in a heat-treated tourmaline, was identified as quartz. Photomicrograph by J. C. Zwaan; magnified 50 \times .

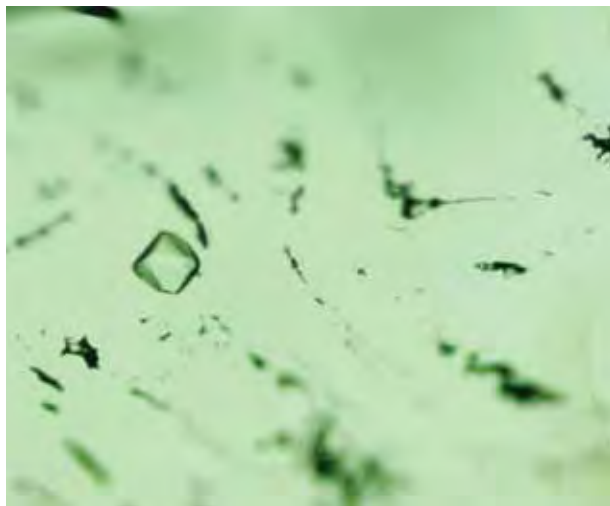


Figure 35. Flakes of lepidolite were occasionally encountered, as seen in this unheated tourmaline (left). In contrast to quartz, these flakes show high-order interference colors when viewed with crossed polarizing filters (right). Photomicrographs by J. C. Zwaan; magnified 50 \times .

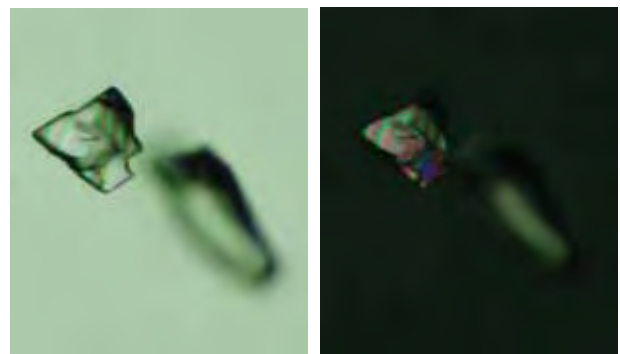




Figure 36. Rounded and irregularly shaped sodic plagioclase crystals, probably albite, were found in only one yellowish green (unheated) sample, and are therefore considered a rare inclusion in tourmaline from Mavuco. Photomicrograph by J. C. Zwaan; magnified 50x.

CHEMICAL COMPOSITION

Table 2 presents average chemical analyses for representative samples of the various colors of the tourmaline; a complete listing of all analyses is available in the G&G Data Depository. For table 2, we selected the most appropriate analytical technique for each element reported, whereas all data obtained from both techniques are provided in the G&G Data Depository. Chemical analysis indicated that all the tourmalines were elbaite with CuO and MnO concentrations ranging up to 0.66 wt.% (LA-ICP-MS) and 3.09 wt.% (microprobe), respectively. The most abundant trace elements were Bi (extremely vari-

TABLE 2. Average chemical composition of representative unheated Cu-bearing tourmalines from Mozambique.^a

Chemical composition	Pink (no. 511-7)	Purple (no. 5u)	Violet ^b (no. 1u)	Greenish blue (no. 510-6)	Bluish green (no. 510-3)	Green (no. 511-5)	Yellowish green ^c (no. 17u)
Oxide (wt.%)							
SiO ₂	36.59	36.68	36.64	36.68	36.62	36.63	36.71
B ₂ O ₃ calc.	10.97	10.90	10.88	10.97	10.97	10.96	10.95
Al ₂ O ₃	42.27	41.23	40.81	42.20	42.19	41.97	41.95
MnO	0.26	2.20	2.55	0.41	0.01	0.92	1.28
CuO	0.07	0.16	0.11	0.30	0.54	0.54	0.21
CaO	0.10	0.01	0.02	0.16	0.92	0.12	0.00
Li ₂ O calc.	1.98	1.70	1.71	1.94	2.04	1.90	1.81
Na ₂ O	2.39	2.10	2.26	2.21	1.63	2.30	2.15
H ₂ O calc.	3.23	3.32	3.32	3.24	3.28	3.23	3.33
F	1.18	0.93	0.91	1.16	1.05	1.16	0.94
Trace elements (ppm)							
Be	6.8	3.7	5.2	6.6	96.2	79.5	4.9
Mg	6.6	1.0	bdl	1.4	bdl	10.7	3.6
K	175	105	46.0	191	76.3	209	171
Ti	122	61.4	19.7	38.9	15.0	356	292
V	0.3	1.0	0.7	0.7	0.7	1.3	2.2
Cr	8.8	3.5	bdl	4.8	4.2	8.2	3.0
Fe	bdl	53.1	bdl	bdl	bdl	5775	895
Ni	0.6	3.7	1.1	0.3	bdl	0.3	0.9
Zn	1.4	2.5	0.6	1.4	0.6	188	30.0
Ga	617	335	312	517	624	247	380
Ge	4.6	4.8	4.6	5.9	6.8	20.8	8.1
Nb	1.4	0.8	0.7	1.4	bdl	bdl	0.5
Mo	bdl	0.9	bdl	0.7	bdl	1.0	2.4
Sn	12.1	4.0	1.3	4.0	0.3	3.3	6.4
Ta	bdl	bdl	bdl	0.7	0.6	bdl	bdl
Pb	10.0	5.7	6.7	10.4	292	128	8.8
Bi	38.4	24.3	209	61.3	3445	3163	53.2

^aAnalyses of oxides by electron microprobe (except for CuO, analyzed by LA-ICP-MS): average of 4–5 analyses per sample. For complete electron-microprobe analyses, including the calculated ions per formula unit, see the G&G Data Depository. Analyses of trace elements by LA-ICP-MS; average of two analyses per sample (not in same locations as the oxide analysis points). Abbreviation: bdl = below detection limit.

^bThis is the unheated sample (no. 1) used for the absorption spectrum in figure 39 (top).

^cThis is the unheated sample (no. 17) used for the absorption spectrum in figure 39 (bottom).

able, exceptionally up to 9,286 ppm), Fe (up to 5,854 ppm), Ga (up to 674 ppm), Zn (up to 512 ppm), and Ti (up to 497 ppm). While significant amounts of Fe were present in the green stones, the other colors contained extremely low amounts in most cases (i.e., below the detection limit of the instrument, ~40 ppm). Another important tourmaline chromophore, Ti, was also depleted in those colors.

As expected, no consistent differences were noted in the composition of the sample pairs before and after heating (since the heating affects the oxidation state of the chromophoric elements, not their concentration). Some minor variations between pieces from a single slice occurred, but these were most likely due to inherent heterogeneity. Differences in color between samples, however, were accompanied by distinct variations in composition. In general, unheated violet stones (and their heated “neon” blue counterparts) contained noticeably lower concentrations of Ti, Fe, and Zn—and higher concentrations of Bi—than all the green samples. Ranges in the concentrations of Mn, Cu, Ga, and Pb were relatively similar for stones of both the violet and green colors.

Meaningful trends in the chemical data could be discerned by plotting Cu vs. Fe+Ti (whereas too much scatter resulted from plotting Mn vs. Fe+Ti). The average chemical data for all samples analyzed (both unheated and heated) are shown in figure 37,

grouped according to color. Most of the green samples had distinctly higher contents of Fe+Ti than the other colors. All of the color groups showed considerable overlap in Cu contents; the lowest Cu contents were measured in some of the pink to pinkish purple samples.

Figure 38 plots the same elements for *only* the before-and-after heated sample pairs (again, see figure 22) according to their color. As expected, samples before and after heating commonly exhibit differences in composition due to preexisting chemical heterogeneity. Although it is not possible to clearly indicate specific sample pairs on this diagram, average chemical analyses of all samples are available in the G&G Data Depository. The green to yellow-green samples had the highest Fe+Ti contents and did not show appreciable changes in color with heating. The blue to bluish green tourmalines contained less Fe+Ti; heating of those samples made the original hues greener or more intense. The violetish blue to purple samples had the lowest Fe+Ti values and showed the greatest change with heating, becoming blue to bluish green.

UV-VIS-NIR SPECTROSCOPY

Figure 39 shows the Vis-NIR absorption spectra for two pairs of polished slabs, before and after heating. The chemical analyses of these samples (before

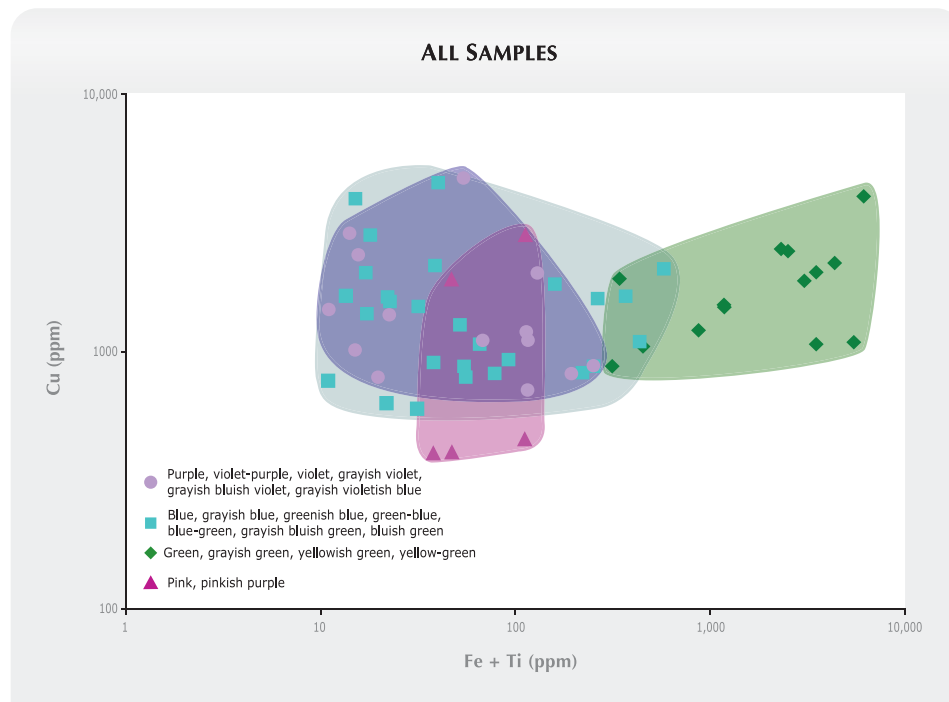


Figure 37. This plot of Cu vs. Fe+Ti shows the average chemical data for all tourmaline samples analyzed in this study, according to the four main color groups. Due to large variations in composition, both axes use a logarithmic scale. The green to yellowish green samples have the highest Fe+Ti contents, and therefore would not be expected to change color with heat treatment. Some of the pink to reddish purple samples also would not be expected to change to the “neon” green or blue colors due to their low Cu contents.

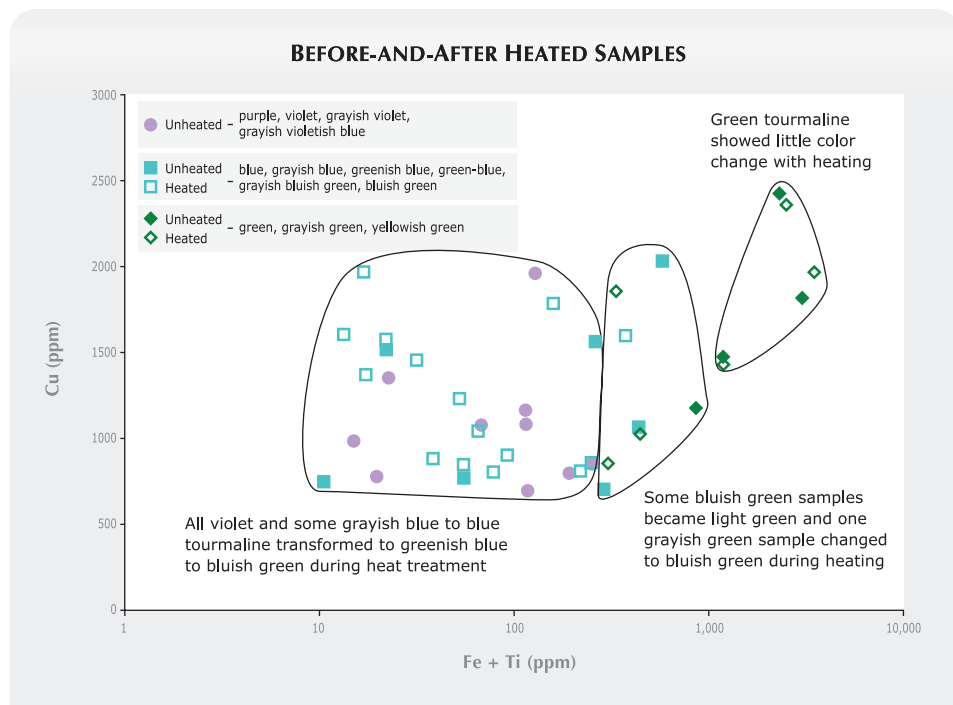


Figure 38. The same elements plotted in figure 37 are shown again here, for only the tourmaline pairs before and after heat treatment that shared the same piece of rough (see figure 22). Since this sample set has less variation in Cu content (because it is smaller), a logarithmic scale is not necessary for the Y-axis. The samples with the highest Fe+Ti contents (green to yellowish green) did not change color, whereas the others became blue to bluish green (or, in the case of those that were originally blue to green, became more intense) with heating.

heating) are provided in table 2. All the samples showed two distinctive broad bands centered at ~700 and ~900 nm, caused by Cu^{2+} absorption (Abduriyim et al., 2006). In addition, the unheated, violet-colored tourmalines also exhibited a broad absorption between ~500 and ~550 nm due to Mn^{3+} , causing a transmission window at ~400–430 nm that produced the violet color. This band was very weak or absent in both the unheated and heated “neon” blue samples, as well as in most of the green stones. In addition to the Cu^{2+} absorption bands, many of the green tourmalines (both heated and unheated) showed small peaks at ~415 nm and a broad band at ~325 nm, which Rossman and Mattson (1986) attributed to Mn^{2+} and $\text{Mn}^{2+}\text{-Ti}^{4+}$ intervalence charge transfer (IVCT), respectively.

Reduction of the Mn^{3+} absorption band was the major change noted as the result of heating of the violet and darker blue tourmaline samples (see, e.g., figure 39, top). Most of the green samples showed little change in Vis-NIR absorption after heating (see, e.g., figure 39, bottom).

Spectra for various natural-color faceted Cu-bearing tourmalines from Mozambique are shown in figure 40.

DISCUSSION

Gemological Properties. Wentzell (2004), Wentzell et al. (2005), and Liu and Fry (2006) documented a

“reverse” color change in Cu-bearing tourmaline from Mozambique. Unlike the usual alexandrite effect, these “reverse” stones showed warm coloration in daylight (purple) and cool colors (gray–bluish green to greenish blue) in incandescent light. However, many of our samples appeared violetish blue to pale blue in daylight and greenish gray to grayish green in incandescent light. Thus, those samples were not changing from warm to cool colors, but rather from “cool” to “less cool” colors—which, in principal, is the same mechanism as in alexandrite. It is interesting to note that the purple tourmalines we studied shifted color in the normal direction, from purple to purplish pink/red.

The measured RI and SG values (table 1) show a slightly wider range than the values for Mozambique Cu-bearing tourmaline presented by Milisenda et al. (2006) and Abduriyim et al. (2006), with significantly higher refractive indices for the green tourmalines, and lower overall specific gravity values for the blue-to-violet and bluish green tourmalines. While our Mozambique samples generally showed overlapping values with Cu-bearing tourmalines from other localities, blue to blue-green and yellowish green to green material from Mina da Batalha, Brazil, may show slightly higher SG values, up to 3.11 and 3.12, respectively (Fritsch et al., 1990; Abduriyim et al., 2006). One blue-green stone from that mine

showed some different properties: birefringence of 0.025, and a specific gravity of 3.12. The values of the light blue Cu-bearing tourmalines from the Alto dos Quintos mine in Brazil show complete overlap, whereas the (light) blue to bluish green stones from the Mulungu mine in Brazil show higher SG values (3.08–3.13; Shigley et al., 2001; Abduriyim et al., 2006). Violetish blue and blue to bluish green Cu-bearing tourmalines from Nigeria exhibit considerable overlap (see Smith et al., 2001; Abduriyim et al., 2006), but may have SG values up to 3.10. The similarity in properties between Cu-bearing tourmaline from the various

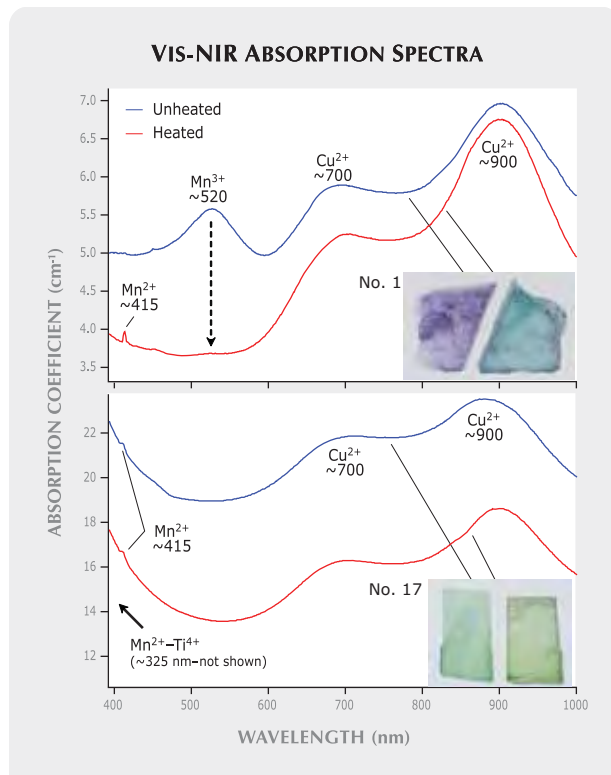
localities, and the initial difficulty in separating them, contributed to the desire by some in the trade to refer to all of these tourmalines by the trade name “Paraíba” (see box A).

This is the first detailed description of inclusions in copper-bearing tourmaline from Mozambique. Abduriyim et al. (2006) mentioned the presence of liquid inclusions, two-phase (liquid-gas) inclusions, and healed fractures, while Milisenda et al. (2006) mentioned trichites and the presence of hollow tubes, generally filled with a brownish substance. The statement made by Abduriyim et al. (2006) that in faceted stones these tubes may be indicative of tourmalines from Nigeria (because they are not common in Mozambique stones) is not supported by this study. Of 47 faceted tourmalines studied, 29 contained hollow tubes (i.e., a majority of the stones, nearly 62%).

Lepidolite, quartz, and feldspar have not been reported as mineral inclusions in Cu-bearing tourmaline from Brazil or Nigeria (e.g., Fritsch et al., 1990; Shigley et al., 2001), although Abduriyim et al. (2006) did report “hexagonal mica platelets” in Cu-bearing tourmaline from Nigeria. In any case, these minerals should probably not be considered locality-specific inclusions, since they have been encountered in elbaite from many different sources (see, e.g., Koivula, 2005). Consistent with the findings of Milisenda et al. (2006), we did not see any copper platelets in our samples, as were documented in Brazilian material by Brandstätter and Niedermayr (1994).

Abundant minute cracks were obvious in almost 90% of the heat-treated stones but in only a few of the unheated samples; they were probably caused by stress released during heating. The larger fluid inclusions, or the ones closer or connected to the surface, were the least stable to heating and therefore most prone to leakage and decrepitation, which may explain their “frosty” appearance when viewed with darkfield illumination. These features, together with the minute cracks that always accompanied them, were seen in more than 20% of the heated stones and in none of the unheated stones, so they are good indicators of heat treatment. Only one heated stone did not show either of these features. In addition, a faint blue fluorescence to long-wave UV may be indicative of heat treatment, although it was not visible in all heat-treated stones (table 1) or in any of the samples examined by Milisenda et al. (2006). All but two of the unheated stones we examined were inert to UV radiation.

Figure 39. Vis-NIR absorption spectra are shown for two pairs of polished tourmaline slabs, before and after heating. In the top spectra, the reduction of the Mn^{3+} absorption with heating (in the absence of significant Ti- and Fe-related absorptions) results in a dramatic change from violet to blue-green. In the bottom spectra, the yellowish green color changed very little due to strong Mn^{2+} - Ti^{4+} absorption. The spectra have not been offset vertically. Sample thicknesses: 3.36 and 3.80 mm (unheated and heated, top) and 1.42 and 1.85 mm (unheated and heated, bottom). Inset photos by C. D. Mengason.



UV-VIS-NIR ABSORPTION SPECTRA

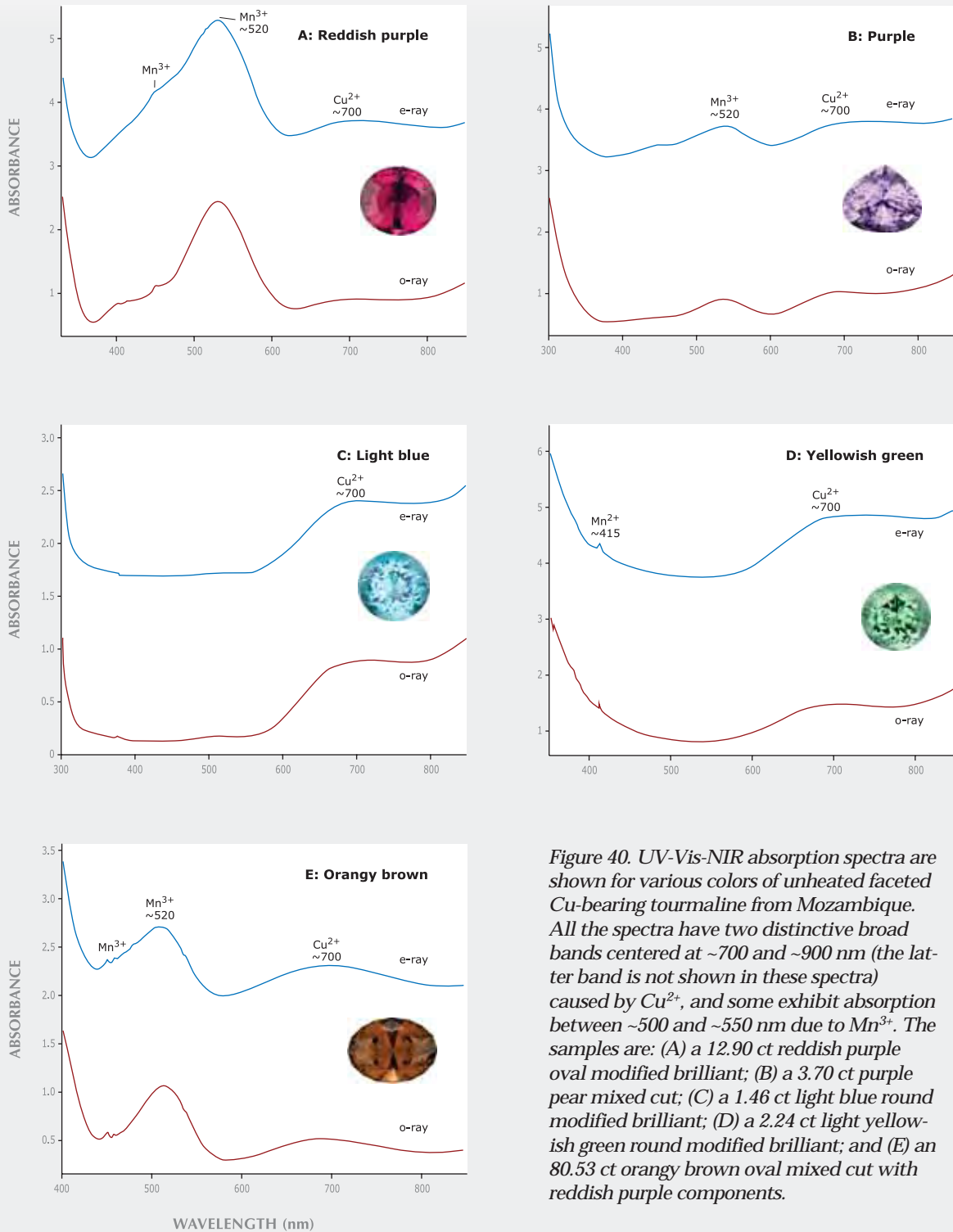


Figure 40. UV-Vis-NIR absorption spectra are shown for various colors of unheated faceted Cu-bearing tourmaline from Mozambique. All the spectra have two distinctive broad bands centered at ~700 and ~900 nm (the latter band is not shown in these spectra) caused by Cu²⁺, and some exhibit absorption between ~500 and ~550 nm due to Mn³⁺. The samples are: (A) a 12.90 ct reddish purple oval modified brilliant; (B) a 3.70 ct purple pear mixed cut; (C) a 1.46 ct light blue round modified brilliant; (D) a 2.24 ct light yellowish green round modified brilliant; and (E) an 80.53 ct orange brown oval mixed cut with reddish purple components.

BOX A: NOMENCLATURE ISSUES

“Paraíba tourmaline” is a trade name that was originally used to describe brightly colored blue-to-green Cu- and Mn-bearing elbaite from Mina da Batalha in Paraíba State, Brazil. After similar tourmalines were found in other areas of Brazil (Rio Grande do Norte State), as well as in Nigeria and Mozambique, gem laboratories were asked to identify material from the various sources for their clients. Initially, using semi-quantitative EDXRF chemical analysis, the laboratories were not able to separate the localities. Further research quantifying the trace elements using LA-ICP-MS has produced a reliable technique for distinguishing nearly all Cu-bearing tourmalines from Brazil, Nigeria, and Mozambique.

The trade, however, had become accustomed to calling the “neon” blue-to-green tourmalines “Paraíba” regardless of their origin. In January 2007, the Laboratory Manual Harmonization Committee (consisting of representatives from the AGTA Gemological Testing Center—U.S., CISGEM—Italy, GAAJ Laboratory—Japan, GIA Laboratory—U.S., GIT Gem Testing Laboratory—Thailand, Gübelin Gem Lab and SSEF Swiss Gemmological Institute—Switzerland) published LMHC Information Sheet no. 6, which defines Paraíba tourmaline as

a blue (electric blue, neon blue, violet blue), bluish green to greenish blue or green elbaite tourmaline, of medium to high saturation and tone, mainly due to the presence of Cu and Mn of whatever geographical origin. The name of the tourmaline variety ‘Paraíba’ is derived from the Brazilian locality where this gemstone was first mined.

Two wording options are provided—one where the report uses “Paraíba” as a variety designation, and one where it is used as a trade name. Most member labs of LMHC have opted to use “Paraíba” as a trade name.

One consequence of the above decision (which is different from what the LMHC decided earlier in 2006, when they did not define saturation and tone; compare Abduriyim et al., 2006) is that certain colors that were part of the original Paraíba output were excluded, notably violet to reddish purple and yellowish green. Although violet stones can often be heat-treated to produce the blue-to-green varieties, an awkward situation has arisen in which Cu- and Mn-bearing elbaite of this color may get a country-of-origin designation of Brazil, and still not be considered a Paraíba tourmaline.

Another nomenclature issue concerns the saturation and tone of the blue-to-green color that is necessary for the “Paraíba” trade name. This issue became particularly important with the availability of significant amounts of Mozambique Cu-bearing tourmalines showing either desaturated or light to very light colors, particularly after being cut into smaller sizes. The saturation necessary for a blue-to-green Cu-bearing tourmaline to be considered “Paraíba” does not have widespread agreement. At the time this article was prepared, the LMHC was working on a consistent definition for these saturation levels. Meanwhile, some dealers have bypassed the problems related to both geographic origin and coloration by referring to the material as cuprian tourmaline.

In cases where a stone does not have sufficient saturation, is too light in tone, or is not considered the proper hue to be called “Paraíba,” some labs will issue a report indicating that it is a Cu- and Mn-bearing tourmaline. There is no universal agreement on the level of copper (and manganese) necessary for a tourmaline to be considered “Cu- and Mn-bearing,” and given the increase in sensitivity of modern analytical techniques such as LA-ICP-MS, such criteria should be carefully reviewed for consistency between laboratories.

Chemical Composition and UV-Vis-NIR Spectroscopy. The Paraíba-type tourmalines from Mozambique are characterized by low Fe and Ti concentrations and relatively low-to-moderate amounts of Cu. As outlined below, their attractive coloration is due to a combination of these chemical features. Overall, the composition of our samples is comparable with the data presented by Milisenda et al. (2006), but we mea-

sured lower values for Cu and Mn than were reported by Abduriyim et al. (2006). Note that anomalously higher copper values of 2.08–3.21 wt.% CuO were measured by Abduriyim et al. (2006) in only a few highly saturated greenish blue to bluish green samples from Mozambique; they are not representative of the typical tourmaline composition (A. Abduriyim, pers. comm., 2008). Consistent with data previously

recorded by LA-ICP-MS at GIA (248 analyses on 122 samples; unpublished GIA data), all the samples analyzed for this study fell within the following ranges: 0.05–0.66 wt.% CuO, 0.01–3.09 wt.% MnO, 10–497 ppm Ti, and from below detection limit to 5854 ppm Fe.

The coloration of Mozambique Cu-bearing tourmaline is controlled, for the most part, by a combination of the concentrations and oxidation states of Cu, Mn, Fe, and Ti (Wentzell et al., 2005; Abduriyim et al., 2006; Milisenda et al., 2006; Rondeau and Delaunay, 2007). The vast majority of the samples analyzed showed strong Cu²⁺ absorptions centered at ~700 and 900 nm, and contained relatively high amounts of Mn. In the absence of significant amounts of Fe and Ti, and when the manganese occurs as Mn²⁺, the tourmalines show an attractive “neon” blue color without heating. If, however, the manganese is present as Mn³⁺ (the more common oxidation state), a strong absorption at ~520 nm causes the stones to appear violet to pink.

Heat treatment of Cu- and Mn-bearing tourmaline has long been known to significantly change the color of many stones. This occurs simply by reducing the oxidation state of Mn in the stone, from Mn³⁺ (which causes violet-pink coloration) to Mn²⁺ (not a strong chromophore in tourmaline), but the resultant color also depends on the amount of Fe and Ti present. Most of the violet Mozambique Cu-bearing tourmaline contains little Fe and Ti. Heat treatment of such material removes the Mn³⁺ absorption at ~520 nm, creating a transmission window from ~400 to 580 nm that yields a “neon” blue color (figure 39, top). Heat treatment of a similar stone containing significant Ti and Fe will produce green coloration due to Mn, Ti, and Fe, producing broad absorptions at ~325, ~420, and 710 nm. The resulting transmission window at ~550 nm is responsible for the green color.

Many unheated green samples have substantially more Fe and Ti than the violet samples, and much of the manganese is already in the Mn²⁺ state. In such material, the Mn, Ti, and possibly Fe IVCT absorptions are naturally present and combine with the Cu²⁺ bands to produce a green color. Heating these stones results in little to no color modification, as shown in the bottom of figure 39.

Thus, it should be possible to predict the effects of heat treatment of Cu-bearing tourmalines from Mozambique by measuring their Ti and Fe concentrations. UV-Vis spectroscopy, which directly

reflects the composition, can also be used to predict the response to heating (Milisenda, 2007).

GEOLOGIC ORIGIN OF CU-BEARING TOURMALINE FROM MOZAMBIQUE

The authors' observations of the tourmaline-bearing layer revealed sedimentary structures and a clast-supported matrix that suggest a fluvial origin (i.e., deposited by a stream or river). The dominance of angular clasts indicates a short transport distance (probably less than 10 km) for most of the quartz in the matrix. It also suggests the importance of mechanical weathering and hillslope transportation. However, the sub- to well-rounded quartz and tourmaline clasts had longer transport distances and transit times.

The dominance of angular clasts suggests that fluvial transport was spasmodic (i.e., it occurred only occasionally and then for a short time). The rather coarse grain size (10–30 mm) suggests energetically high hydrodynamic conditions. The open-worked clast-supported fabric of the gravel layer also indicates short transport distances and abrupt rapid deposition. Therefore, the sedimentology and internal architecture of the tourmaline-bearing layer suggest a braided fluvial depositional environment. It is likely that semi-ephemeral to perennial braided streams transported and redistributed alluvial materials down-valley during high discharge events (wet seasons) of relatively short duration.

It can be concluded that the tourmaline-bearing layer is an accretional unit deposited by slope processes and redistributed fluvially. Much of the angular material may be derived from the local simple granitic pegmatites (some aquamarine-bearing) that cross-cut the basement rocks. Also, the angular material may have been derived upstream from the hinterland valleys and transported downhill through spasmodic flash floods (distances on the order of 10 km or less).

The rounded tourmalines and quartz (<10%) were transported longer in terms of both time and distance, and perhaps were redistributed and concentrated several times. Given the known fairly localized occurrence of the Cu-bearing tourmaline in this part of Mozambique, its origin must relate to the catchment area of the fluvial units and to the former presence of pegmatite source rock upstream. Based on the size of the current catchment, we infer that these (sub)rounded clasts represent maximum transport/reworking distances on the order of 100



Figure 41. Cu-bearing tourmaline from Mozambique (here, 14.53 ct and heated) is being showcased by innovative jewelry designs. The 18K white gold pendant is accented by black and red spinel, yellow sapphire, tsavorite, and diamond. Courtesy of Carley McGee-Boehm, Carley Jewels, San Diego, California; photo by Robert and Orasa Weldon.

km. To the northwest, this falls well within the boundaries of the Alto Ligonha pegmatite district (compare with figure 5). However, since no Cu-bearing tourmaline is known from previously worked deposits in that district (primary or alluvial), the materials from Mavuco were apparently derived from pegmatites that were quite unusual compared to those currently known in the area. Also, the transport direction of the sediments depended on

the topography, which directly resulted from the regional tectonics/geology of the area at the time that the original pegmatites eroded. The direction that the rivers flow today may not have been the same when the tourmaline-bearing sediments were eroded and deposited.

The site of tourmaline deposition depended on the local topography and slope direction, and it may be no coincidence that the deposit is located in the area between the granitic hills of Mt. Muli to the south and Mt. Iuluti to the north. This arrangement of the resistant granitic rocks, combined with the regional northeast-southwest structure of the basement, may have created ideal topographic conditions for channeling the sediments derived from the original pegmatites into their present position. In addition, this may have prevented the tourmaline from being dispersed over long distances, even during the reworking that is suggested by their rounded nature.

CONCLUSION

Copper-bearing tourmaline from Mozambique is notable for its variety of bright colors, availability in relatively large quantities, and impressive number of large clean stones. Although most of the material does not attain the saturation of the famous Paraíba tourmaline from Brazil, the Mozambique deposit has helped make Cu-bearing tourmaline more affordable and also has popularized its use in fine jewelry (figure 41). It is expected that the material will become even more widely available in the near future, as mechanized mining becomes more prevalent. Further exploration could turn up additional reserves in the Mavuco area, particularly through systematic test pitting over a larger area than has currently been mined. Wider-scale exploration throughout the eastern part of the Alto Ligonha pegmatite district may also result in the discovery of new areas for this tourmaline.

ABOUT THE AUTHORS

Mr. Laurs is editor of Gems & Gemology at GIA in Carlsbad. Dr. Zwaan is director of the Netherlands Gemmological Laboratory, and curator of minerals and gems, at the National Museum of Natural History "Naturalis," Leiden, the Netherlands. Dr. Breeding is research scientist at the GIA Laboratory in Carlsbad. Ms.

Beaton and Mr. Belfi are staff gemologists at the GIA Laboratory in New York. Dr. Rijdsdijk is researcher and sedimentologist at the Netherlands Institute of Applied Geosciences TNO, Delft, the Netherlands. Dr. Simmons is professor of mineralogy and university research professor, and Mr. Falster is senior research technologist, at the University of New Orleans, Louisiana.

ACKNOWLEDGMENTS

The authors are grateful to Moses Konate, Salifou Konate, and Chirindza Henrique (Mozambique Gems, Nampula) for providing logistical support in the field and access to the mining property, as well as supplying information and donating samples for research. They also appreciate the cooperation and assistance of company partners Saint Clair Fonseca Jr., Daniel Trinchillo, Burkhard Pohl, and Marcus Budil. Additional samples were loaned or donated by Bill Barker (Barker & Co., Scottsdale,

Arizona), Bill Larson (Pala International, Fallbrook, California), and Robert Kane (Fine Gems International, Helena, Montana). Dirk van der Marel (National Museum of Natural History "Naturalis," Leiden) is thanked for preparing maps and for general assistance. Access to Raman facilities was provided to one of the authors (JCZ) by the CCIP French Gemmological Laboratory, Paris. We also thank Farooq Hashmi (Intimate Gems, Jamaica, New York) for providing helpful information and discussions after his 2006 trip to the mining area.

REFERENCES

- Abduriyim A., Kitawaki H. (2005) Cu- and Mn-bearing tourmaline: More production from Mozambique. *Gems & Gemology*, Vol. 41, No. 4, pp. 360–361.
- Abduriyim A., Kitawaki H., Furuya M., Schwarz D. (2006) "Paraiba"-type copper-bearing tourmaline from Brazil, Nigeria, and Mozambique: Chemical fingerprinting by LA-ICP-MS. *Gems & Gemology*, Vol. 42, No. 1, pp. 4–21.
- Bettencourt Dias M., Wilson W.E. (2000) Famous mineral localities: The Alto Ligonha pegmatites, Mozambique. *Mineralogical Record*, Vol. 31, pp. 459–497.
- Brandstätter F., Niedermayr G. (1994) Copper and tenorite inclusions in cuprian-elbaite tourmaline from Paraiba, Brazil. *Gems & Gemology*, Vol. 30, No. 3, pp. 178–183.
- Breeding C.M., Rockwell K., Laurs B.M. (2007) Gem News International: New Cu-bearing tourmaline from Nigeria. *Gems & Gemology*, Vol. 43, No. 4, pp. 384–385.
- Brigatti M.F., Caprilli E., Malferrari D., Medici L., Poppi L. (2005) Crystal structure and chemistry of trilithionite-2M2 and polyolithionite-2M2. *European Journal of Mineralogy*, Vol. 17, No. 3, pp. 475–481.
- Deer W.A., Howie R.A., Zussman J. (1994) *An Introduction to the Rock Forming Minerals*. Longman Group, London, 528 pp.
- Fritsch E., Shigley J.E., Rossman G.R., Mercer M.E., Muhlmeister S., Moon M. (1990) Gem-quality cuprian-elbaite tourmalines from São José da Batalha, Paraiba, Brazil. *Gems & Gemology*, Vol. 26, No. 3, pp. 189–205.
- Furuya M., Furuya M. (2007) *Paraiba Tourmaline—Electric Blue Brilliance Burnt into Our Minds*. Japan Germany Gemmological Laboratory, Kofu, Japan, 24 pp.
- Gübelin E.J., Koivula J.I. (2005) *Photoatlas of Inclusions in Gemstones*, Vol. 2. Opinio Publishers, Basel, Switzerland, 829 pp.
- Kogure T., Bunno M. (2004) Investigation of polytypes in lepidolite using electron back-scattered diffraction. *American Mineralogist*, Vol. 89, pp. 1680–1684.
- Koivula J.I., Kammerling R.C., Eds. (1989) Gem News: Unusual tourmalines from Brazil. *Gems & Gemology*, Vol. 25, No. 3, pp. 181–182.
- Lächelt S. (2004) *The Geology and Mineral Resources of Mozambique*. National Directorate of Geology, Maputo, Mozambique, 515 pp.
- Liu Y., Fry B.A. (2006) A colorimetric study of a tourmaline from Mozambique which shows a reverse alexandrite effect. *Journal of Gemmology*, Vol. 30, No. 3/4, pp. 201–206.
- Mernagh T.P. (1991) Use of the laser Raman microprobe for discrimination amongst feldspar minerals. *Journal of Raman Spectroscopy*, Vol. 22, No. 8, pp. 453–457.
- Milisenda C.C. (2005) A new source of cuprian tourmalines. *Gemmologie: Zeitschrift der Deutschen Gemmologischen Gesellschaft*, Vol. 54, No. 2–3, pp. 63–64.
- Milisenda C.C. (2007) Paraiba tourmaline revisited. *30th International Gemmological Conference*, Moscow, Russia, July 15–19, p. 76.
- Milisenda C.C., Horikawa Y., Emori K., Miranda R., Bank F.H., Henn U. (2006) Neues Vorkommen kupferführender Turmaline in Mosambik [A new find of cuprian tourmalines in Mozambique]. *Gemmologie: Zeitschrift der Deutschen Gemmologischen Gesellschaft*, Vol. 55, No. 1–2, pp. 5–24.
- Mozambique Paraiba tourmaline hot in Tucson (2007) *Jewellery News Asia*, No. 272 (April), p. 56.
- Pearce N.J.G., Perkins W.T., Westgate J.A., Gorton M.P., Jackson S.E., Neal C.R., Chenery S.P. (1996) Application of new and published major and trace elements data for NIST SRM 610 and NIST SRM 612 glass reference materials. *Geostandards Newsletter*, Vol. 20, No. 2, pp. 115–144.
- Petsch E.J. (1986) Riesen in Rot, Grün und Blau—Die Turmalin-Vorkommen in Mocambique. *Mineralientage München 85—Turmalin*, Oct. 18–20, Munich, Germany.
- Pinna P., Marteau P., Becq-Giraudon J.-F., Manigault B. (1986) *Notice Explicative de la Carte Géologique à 1/1 000 000 de la République Populaire du Mozambique (1986)*. BGRM, Orléans, France, 261 pp. (includes geologic map).
- Pinna P., Jourde G., Calvez J.Y., Mroz J.P., Marques J.M. (1993) The Mozambique Belt in northern Mozambique: Neo-proterozoic (1100–850 Ma) crustal growth and tectogenesis, and superimposed Pan-African (800–550 Ma) tectonism. *Precambrian Research*, Vol. 62, pp. 1–59.
- Rondeau B., Delaunay A. (2007) Les tourmalines cuprifères du Nigeria et du Mozambique [Cuprian tourmalines from Nigeria and Mozambique]. *Revue de Gemmologie*, No. 160, pp. 8–13.
- Rossman G.R., Mattson, S.M. (1986) Yellow, Mn-rich elbaite with Mn-Ti intervalence charge transfer. *American Mineralogist*, Vol. 71, pp. 599–602.
- Samson I., Anderson A., Marshall D. (2003) *Fluid Inclusions, Analysis and Interpretation*. Mineralogical Association of Canada Short Course Series, Vol. 32, 374 pp.
- Shigley J.E., Cook B.C., Laurs B.M., Bernardes de Oliveira M. (2001) An update on "Paraiba" tourmaline from Brazil. *Gems & Gemology*, Vol. 37, No. 4, pp. 260–276.
- Slater M. (2006) *Globetrotter Travel Map – Mozambique*, 3rd ed. New Holland (Publishers) Ltd., London, UK.
- Smith C.P., Bosshart G., Schwarz D. (2001) Gem News International: Nigeria as a new source of copper-manganese-bearing tourmaline. *Gems & Gemology*, Vol. 37, No. 3, pp. 239–240.
- Wentzell C.Y. (2004) Lab Notes: Copper-bearing color-change tourmaline from Mozambique. *Gems & Gemology*, Vol. 40, No. 3, pp. 250–251.
- Wentzell C.Y., Fritz E., Muhlmeister S. (2005) Lab Notes: More on copper-bearing color-change tourmaline from Mozambique. *Gems & Gemology*, Vol. 41, No. 2, pp. 173–175.
- Wise R.W. (2007) Mozambique: The new Paraiba? *Colored Stone*, Vol. 20, No. 2, pp. 10–11.



A HISTORY OF DIAMOND TREATMENTS

Thomas W. Overton and James E. Shigley

Although various forms of paints and coatings intended to alter the color of diamond have likely been in use for almost as long as diamonds have been valued as gems, the modern era of diamond treatment—featuring more permanent alterations to color through irradiation and high-pressure, high-temperature (HPHT) annealing, and improvements in apparent clarity with lead-based glass fillings—did not begin until the 20th century. Modern gemologists and diamantaires are faced with a broad spectrum of color and clarity treatments ranging from the simple to the highly sophisticated, and from the easily detected to the highly elusive. The history, characteristics, and identification of known diamond treatments are reviewed.

For as long as humans have valued certain materials as gems, those who sell them have sought ways to make them appear brighter, shinier, and more attractive—to, in other words, make them more salable and profitable. From the earliest, most basic paints and coatings to the most sophisticated high-pressure, high-temperature (HPHT) annealing processes, the history of diamond treatments parallels that of human advancement, as one technological development after another was called upon to serve the “King of Gems” (figure 1). And, much as the pace of human technological advances accelerated in the past hundred-plus years, gemologists of the 20th century witnessed the introduction of gem treatments that the earliest diamond merchants could scarcely have imagined—and that literally reshaped the world of contemporary diamantaires.

Because of their potential to deceive, gem treatments, including those applied to diamond, have long had an aspect of fraud about them, whether a treatment was intended to mask or remove color (e.g., figure 2); to add, enhance, or alter color (e.g., figure 3); or to change other characteristics such as apparent clarity. That being said, there have also

been long periods, both ancient and modern, when diamond treatments were conducted in the relative open, and their practitioners were regarded by some as experts and even artists. Gem treatments, it must be recognized, are neither good nor bad in themselves—fraud comes about only when their presence is concealed, whether by intent or by negligence. This fact places a specific responsibility for full treatment disclosure on all those handling gem materials, and most especially on those selling diamonds, given their long and enduring value. That responsibility is one of knowing and understanding what happens as a result of treatment, having the expertise to recognize treated stones when they are encountered, and knowing when suspect stones should be examined by properly equipped gem-testing laboratories.

This article is not intended to be a complete review of the history of diamond treatments, as such

See end of article for About the Authors and Acknowledgments.
GEMS & GEMOLOGY, Vol. 44, No. 1, pp. 32–55.
© 2008 Gemological Institute of America



Figure 1. Once rarely-seen collectors' items, colored diamonds are now widely available as a result of a variety of treatments that can change off-color stones to attractive hues. Shown here is a collection of jewelry set with treated-color diamonds. The "cognac" diamond in the ring is 1.07 ct; the blue diamond in the brooch is 0.85 ct and is set with 0.60 ct of purple diamonds; the stud earrings contain 1.74 ct of green diamonds and 0.30 ct of yellow diamonds; the hoop earrings contain 0.95 ct of colored diamonds. All the colored diamonds were treated by irradiation. Composite of photos by azadphoto.com; courtesy of Etienne Perret.

an endeavor could easily fill a book (see, e.g., Nassau, 1994; Shigley, 2008). Rather, it is intended to provide a broad overview of the subject and a resource for those wishing to delve further into the literature. Information presented is derived from the published literature and the authors' (primarily JES) experience with diamond testing. The subject will be addressed in roughly chronological order, with the discussions divided by color and clarity treatments.

COLOR TREATMENTS

Paints and Coatings. *Early History.* The coating, dyeing, and painting of gems to alter their appearance is an ancient practice, and one that likely started soon after human beings began valuing minerals for personal adornment. The first use of diamond as a gemstone was almost certainly in India (e.g., figure 4), probably well before any contact with Western cultures around the Mediterranean, as Indian lapidary arts in the Indus Valley were already fairly advanced by the second millennium BC (Krishnan and Kumar, 2001). Whether treatment of diamonds there was as common as with other gems is another matter, however. Diamonds were objects of great religious and cultural significance in ancient India (see, e.g., Brijbhusan, 1979), and there were strong taboos against altering them in any way (Tillander,

1995). Further, as with many other things in India, diamonds were classified by color according to a rigid caste system (Brijbhusan, 1979; Tillander, 1995), and consequently there must have been strong social pressure against altering a stone's color. This hardly means it did not occur, of course. Since colorless stones occupied the highest caste, there would have been strong *economic* incentives to find ways to reduce the apparent color of off-color

Figure 2. A blue coating on a yellowish diamond can neutralize its bodycolor and make it appear more colorless. Variations on this treatment have been used for centuries. Photomicrograph by John I. Koivula; magnified 5x.

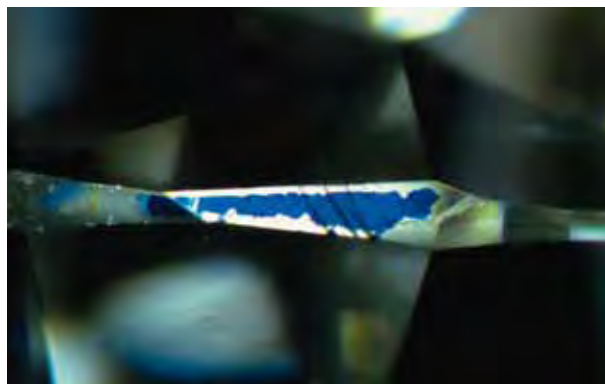




Figure 3. This attractive green diamond (3.06 ct) owes its color to irradiation. Photo by Robert Weldon.

stones—though the party responsible no doubt risked much in doing so. Gill (1978), for example, reported the historic use of ultramarine in India to improve the color of yellowish stones, as well as of other pigments to produce apparent colors.

Diamonds were largely unknown to the early Greeks. Ball (1950) placed the arrival of diamonds in Greece no earlier than about the fifth century BC (and then only as “the rarest of curiosities,” p. 242), and in Rome at about 65 BC. Although Pliny mentioned the dyeing and foiling of a variety of gems, diamond is not among them. Instead, his discussion of diamond is largely confined to its resistance to fire and blows—though not goat’s blood, which was reputed to soften it* (Ball, 1950). Nevertheless, diamond crystals were used on occasion in jewelry during this period, so it is likely that some enterprising jewelers were painting and coating them as well, since dyeing is known to have been a common practice with other gems during this period (Ball, 1950).

Although cleaving of octahedral diamond crystals to create various simple shapes (usually point cuts) may have taken place as much as 2,000 years ago (Tillander, 1995), true cutting and polishing to create new shapes and facet arrangements is thought to have evolved slowly beginning some time in the 14th century (Balfour, 2000). As cutting techniques developed, and early diamond manufacturers learned which methods best improved brilliance and color, it is likely that different types of coatings followed closely behind. It is interesting to note that one of the oldest surviving accounts of early diamond cutting, by Italian master jeweler Benvenuto Cellini (Cellini, 1568), also contains

detailed instructions on how to improve a diamond’s appearance by applying various substances to the pavilion surface.

Cellini told the story of a large diamond that had been given by Holy Roman Emperor Charles V to Pope Paul III, which Cellini was commissioned to mount. Interestingly, not only was the coating of diamonds legal at this time, it was also such an accepted practice that Cellini conducted the coating in the presence of several of his colleagues in order to impress them with his artistry. He applied a mixture of pure gum mastic, linseed oil, almond oil, turpentine, and lampblack to the base of the stone, and so “seemed to remove from it any internal imperfections and make of it a stone of perfect quality” (p. 39). The results were dramatic enough that his audience declared that he had increased the value of the diamond from 12,000 to 20,000 scudi (the forerunner of the modern Italian lira).

Cellini also described how the appearance of yellow diamonds could be improved by replacing the lampblack with indigo (a blue dye): “[I]f it be well applied, it becomes one colour, neither yellow as heretofore nor blue owing to the virtue of the tint, but a variation, in truth, most gracious to the eye” (p. 36).

The mastic/lampblack recipe is one that appears to have been employed for several centuries, as it is described by Thomas Nichols in his 1652 work, *A Lapidary, or, The History of Pretious [sic] Stones*. Yet, a review of the literature does not seem to indicate that matters progressed much beyond this until the mid-20th century. There is a passing mention of coating diamonds in John Hill’s annotated translation of Theophrastus’ *History of Stones* (1774), among several other works (see Nassau, 1994), but little else. Although the recipes changed as the science of chemistry evolved (potassium permanganate [KMnO₄] was commonly used in the late 1800s [see Gill, 1978], and aniline blue [a histological stain] was popular in the early 1900s [“Gemmology. . .,” 1940]), the same basic approach was still being used well into the 20th century (see, e.g., “Gemological glossary,” 1934; Briggs, 1935; Crowningshield, 1959).

*Nassau (1994) traced this curious myth, which persisted for over 1,500 years, to a recipe in an Egyptian papyrus dating to about 400 AD (though copied from a much older version). Dipping in goat’s blood was actually the last step in a quench-crackling process in preparation for dyeing crystalline quartz. Over the ensuing centuries, this use with quartz was apparently confused with other colorless gems, including diamond.



Figure 4. These untreated Mogul-cut diamonds (9.27 and 9.54 ct) may be from India's Golconda region, possibly fashioned several centuries ago. Photo by Nicholas Del Re.

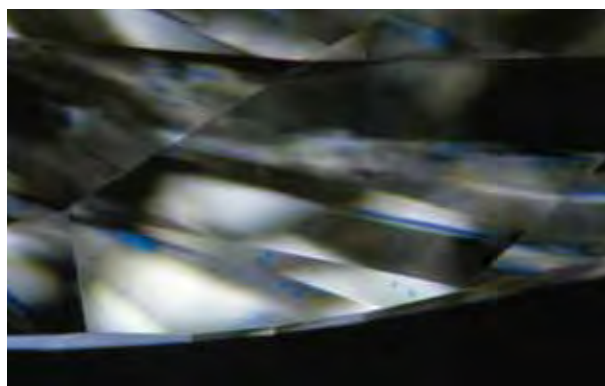
Contemporary Treatments. It was not until the 1950s that modern technology began replacing these centuries-old methods. Following up on a report in *The Gemmologist* the previous year ("Improved gem brilliancy. . .," 1949), Gübelin (1950) described experiments with sputter-coated fluoride thin films (CaF_2 , BaF_2 , MgF_2) in combination with a titanium oxide substrate and a protective silica top coating in order to increase light transmission, brilliance, and color appearance in gems, including diamond (e.g., figure 5). These optical coatings had been developed for military purposes during World War II in order to obtain improved performance from binoculars, bombsights, periscopes, and similar optical devices (MacLeod, 1999), and they were the subject of numerous patents in the post-war years (e.g., Moulton and Tillyer, 1949, which mentions possible use on gem materials). The process is carried out in a vacuum chamber containing a cathode of the coating material and a substrate that serves as the anode. Positively charged ions of the coating material flow across the chamber in gaseous form and adhere to the substrate (Quorum Technologies, 2002).

Among other effects produced by these coatings, Gübelin (1950) stated, "slightly yellowish tinted diamonds may appear blue-white" (p. 246). It is interesting to note that he reports the best results were obtained when the coatings were applied to the top of the stone. However, this also resulted in anomalous refractometer readings (i.e., the RI of the coating rather than that of the diamond, which is over the limit of a standard refractometer), and the appearance of an obvious iridescent film on the crown and table. Diamond treaters apparently recognized these problems as well, and coated diamonds seen in the trade over the ensuing years had such coatings

applied only to their pavilions or girdles (Miles, 1962).

Schlossmacher (1959) reported seeing such coated diamonds in the German gem center of Idar-Oberstein, and Miles (1962, 1964) reviewed GIA's experiences while grading diamonds at the Gem Trade Laboratory in New York City. Miles also described several practical visual means by which these coated "near-colorless" diamonds could be recognized by gemologists. Most stones were treated with a bluish coating in order to mask (or compensate for) light yellow bodycolors and thereby create a more colorless appearance. Several treaters were performing coatings with varying degrees of skill, and Miles reported that at least one company was actively offering its services to the New York diamond trade. As the technology advanced and treaters became more experienced, detection of these coated stones became a serious challenge (Miles, 1962). Although U.S. Federal Trade Commission (FTC) guidelines issued in 1957 required jewelers to disclose coated diamonds ("Jewelry industry . . .," 1957), the rules were widely ignored. The problem became so serious that in 1962 the New York State Legislature was forced to pass a law making the sale of coated diamonds without disclosure a criminal offense (see Overton, 2004, and references therein for a more detailed discussion of the legal elements of treatment disclosure). This law had the effect of forcing the practice outside of mainstream markets, though diamonds with such coatings are still periodically seen in the GIA Laboratory. Sheby (2003), for

Figure 5. A sputtered coating—visible here as indistinct dark spots on the bezel and upper girdle facets—has been applied to this 5.69 ct pear-shaped diamond. Such colored spots are a classic feature of sputter coatings intended to create a more colorless appearance in off-color stones. Photomicrograph by Vincent Cracco; magnified 23 \times .



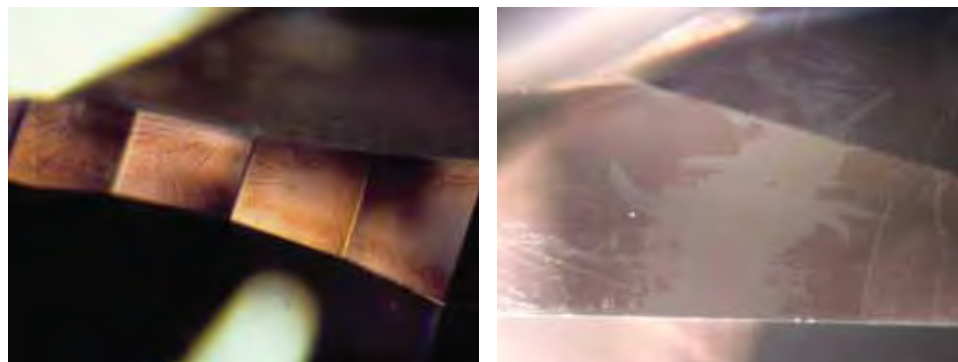


Figure 6. The diamond on the left proved to be a cape stone with a pink coating on the girdle. Note the iridescence and irregular surface features. At right, scratches in the pink coating on this stone are also indicative of this treatment. Photomicrographs by Andrew Quinlan, left (magnified 63×), and Wuyi Wang, right (100×).

example, described a yellowish diamond coated with a blue material to improve its apparent color, similar to those reported 40 years earlier by Miles.

Although it was known that these thin film coatings could also mimic fancy colors (see Schiffman, 1969; Crowningshield, 1975), such color-coated diamonds were not seen in meaningful numbers until fairly recently. In fact, even natural fancy-color diamonds were virtually unknown to most consumers until the 1980s and '90s (Shor, 2005). Pink diamonds were among the first natural fancy colors to gain widespread attention, so it is not surprising that pink-coated diamonds began to appear in the late 1990s (figure 6). Crowningshield and Moses (1998), Evans et al. (2005), and Wang et al. (2006) all described recent examples of polished diamonds colored pink by sputter-coated thin films. Epelboym et al. (2006) reported seeing both pink- and orange-coated diamonds that were possibly colored by a silica film doped with gold rather than the fluoride coatings previously in use. Shen et al. (2007) described a method by which a wide variety of colors could be produced using multiple microthin coatings of varying chemistries. In this same article, Shen et al. reported that the GIA Laboratory was also seeing an increase in diamonds colored pink by coating with calcium fluoride (CaF_2).

Despite all these advances, however, traditional methods of painting and coating have not disappeared, and examples have appeared on occasion in the trade. Crowningshield (1965) reported on assistance GIA gave to law enforcement authorities who were prosecuting a jeweler for selling painted diamonds. Fryer (1983) related an interesting (and no doubt distressing for the parties involved) story of a large natural-color pink diamond being switched for a yellowish stone that had been painted with pink nail polish. Other methods, such as coloring girdle facets with permanent markers and solutions made from colored art pencils, have also been seen (S. McClure, pers. comm., 2008).

Identification. Most coated diamonds can be identified by an experienced gemologist, provided the opportunity exists to examine the entire stone with a gemological microscope. Typically, coatings betray themselves through the presence of spots, scratches, uneven color concentrations, and similar surface irregularities, in addition to iridescent reflections and interference-related colors (again, see figures 5 and 6); these latter features are best seen with reflected light. In addition, diamonds that are coated to appear more colorless often display an unnatural grayish or bluish cast, which can make color grading difficult to impossible (Sheby, 2003). Paler colors present a greater challenge, but immersion in methylene iodide can help reveal color concentrations in surface areas. “Near-colorless” coatings are necessarily more difficult to detect than those intended to impart a bodycolor to the diamond, especially if they are applied to very small areas of the stone, as is often the case. Visual detection of surface coatings on melee-sized diamonds can also present greater difficulties.

When available, Nomarski differential interference contrast microscopy (Sato and Sasaki, 1981; Robinson and Bradbury, 1992) can enhance the visibility of irregularities such as scratches or uneven coatings on facet surfaces (e.g., figure 7). If destructive testing is permitted, applying a polishing powder with a lower hardness than diamond (such as corundum powder) to the facets will produce scratches and thus reveal the presence of a surface coating.

Advanced methods, such as scanning electron microscopy (which can examine the coated areas at much higher magnification) and chemical analysis (which can reveal the presence of elements that do not occur naturally in diamond), will provide definitive confirmation when any doubt remains.

The durability of diamond coatings varies considerably depending on the substances used and how they are applied. Simple paints can be wiped off or removed with solvents such as alcohol and

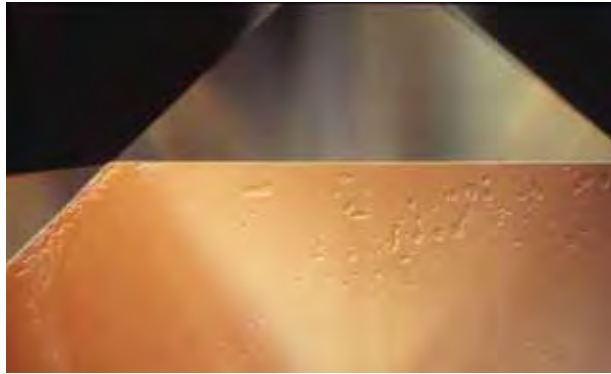


Figure 7. It is clear from this Nomarski image that a coating has been applied to the table of this diamond. Photomicrograph by John I. Koivula; magnified 30 \times .

acetone. Optical coatings are more durable, but they can still be scratched or removed with acids; they are also unstable to some jewelry repair processes (Shen et al., 2007), as are paints.

Synthetic Diamond Thin Films. Finally, a word must be said about the potential use of synthetic diamond thin films on natural diamond. Koivula and Kammerling (1991) reported an experiment in which boron-doped synthetic diamond was deposited as a thin coating by chemical vapor deposition (CVD) on several colorless faceted diamonds, which became dark bluish gray as a result (see also Fritsch and Phelps, 1993). Although there is no indication that this process has ever seen commercial use, recent advances in—and commercialization of—CVD diamond synthesis (see, e.g., Wang et al., 2003, 2005b, 2007; Martineau et al., 2004) mean that it remains a possibility. Such a diamond coating might be far more durable than anything previously seen on the market. As an illustration, CVD diamond coatings applied to machine tools can typically extend the useful life of such tools by 10–50 times (CVD Diamond Corp., 2007). In light of this, and the fact that such a coating would be chemically homogeneous with the coated stone, identification methods such as the polish test and chemical analysis might not be reliable means of detection.

Irradiation. The era of artisanal diamond treatments came to an end shortly after the turn of the 20th century. In 1896, French scientist Henri Becquerel accidentally discovered radioactivity while performing experiments with phosphorescence (Becquerel, 1896). Seeking to measure the phosphorescent reaction of a sample of the mineral zippeite [potassium uranyl sulfate; $K_2UO_2(SO_4)_2$] on a set of photograph-

ic plates, Becquerel found that the uranium in the sample had exposed the plates before the experiment even began. Further research by Marie and Pierre Curie led to the discovery of the element radium in 1898. Radium's intense radioactivity made it a useful source of radiation for experimentation by subsequent researchers, one of whom was an English scientist named Sir William Crookes (box A).

In 1904, Crookes presented a paper to the Royal Society of London detailing his experiments exposing diamonds to radium, both to its radioactive emissions and to direct contact (Crookes, 1904). While the former had no lasting effect, packing the stones in radium bromide gave them a bluish green to green color after several months. As might be expected, this discovery created an immediate stir in the nascent gemological community.

Over the ensuing decades, a series of researchers repeated Crookes's experiments (as did Crookes himself; see, e.g., Crookes, 1914; Lind and Bardwell, 1923a,b; Dollar, 1933). Their work established that the color change was due to alpha radiation, that the color was confined to a very shallow surface layer of the diamond, and that the green or blue-green color could be changed to various shades of yellow to brown by sufficient heating.

However, Crookes and other researchers also discovered that radium treatment of diamonds created long-lasting residual radioactivity that could present a health risk (Crookes, 1914), which effectively limited any legitimate commercial use of this method. Although these treated diamonds (some of which were colored by exposure to other radioactive isotopes such as ^{241}Am or ^{210}Pb) were occasionally seen in the trade anyway, they remained for the most part no more than scientific curiosities and are encountered today only very infrequently (see, e.g., Hardy, 1949; Crowningshield, 1961; Webster, 1965; Henn and Bank, 1992; Ashbaugh and Moses, 1993; Reinitz and Ashbaugh, 1993). It is worth noting, though, that they can remain radioactive for periods of up to several hundred years.

Radium and similar materials were not the only sources of radiation that might be used to treat diamonds, however. In the early 1930s, Professor Ernest Lawrence at the University of California at Berkeley developed a device that became known as the cyclotron, which could accelerate charged atomic particles to high velocities using a magnetic field (e.g., Lawrence, 1934). Through the 1940s and into the 1950s, various researchers experimented with

BOX A: SIR WILLIAM CROOKES

Sir William Crookes (1832–1919) was one of the great Victorian men of science (figure A-1). His life was characterized by wide-ranging, enthusiastic research across multiple fields, from hard sciences such as physics and chemistry to more philosophical work in spiritualism and metaphysics (see D'Albe, 1923; this brief biography is adapted from that book). Although he is known in gemology for his discovery of the effects of radiation on diamond near the end of his life, Crookes had already had a long and distinguished career as a chemist and physicist prior to this work.

Crookes was educated at the Royal College of Chemistry in London. His initial studies in inorganic chemistry received a great boost after Gustav Kirchhoff and Robert Bunsen published their pioneering work on spectroscopy in 1860 (Kirchhoff and Bunsen, 1860). Using their methods, Crookes was able to identify a new element, thallium, in 1861 during an analysis of pyrite ore used for making sulfuric acid. This discovery cemented his reputation and led to his election to the Royal Society in 1863. In the 1870s, Crookes turned his attention to cathode rays, cathode-ray tubes, and cathodoluminescence, and his work in this area remains the foundation of the field, though some of his theories about these discoveries were later shown to be in error. (Crookes believed cathode rays were a new, fourth state of matter rather than electrons.)

In chemistry, he contributed greatly to the evolution of spectroscopy, and published a wide range of papers and treatises on the subject. Much of his chemical research was directed toward practical questions of the day, and he was a recognized authority on water quality and public sanitation (a notable pamphlet, which he published in 1876, was *The Profitable Disposal of Sewage*).

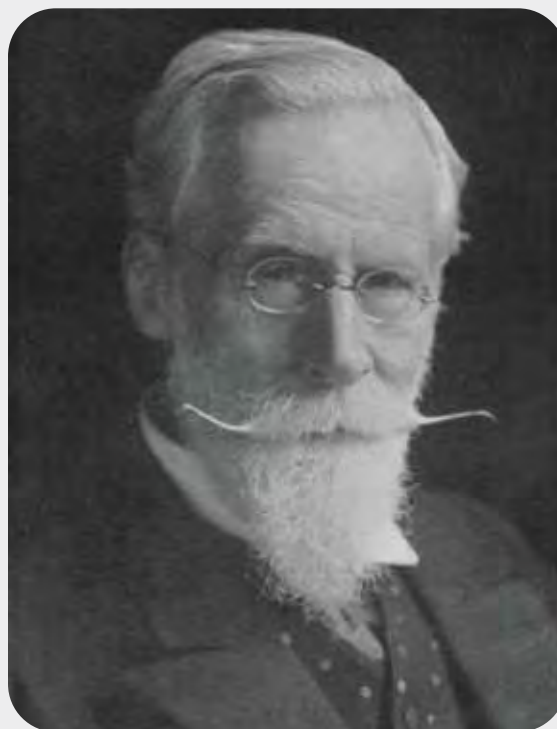
Crookes also had an interest in diamonds, and in 1896 he toured the Kimberley mines in South Africa as a guest of De Beers (Crookes, 1909). His research into the luminescence of minerals naturally led him to experiment with radioactivity after Becquerel's discovery that same year. He continued studies in this field almost up to the time of his death. In addition to his work with diamonds, he also achieved the

first separation of protactinium (Pa) from uranium, and invented a simple device for detection of radioactivity, the spintharoscope.

Crookes's dabblings in Victorian mysticism (e.g., Crookes, 1874), which led him to conduct a series of séances and form relationships with noted mediums, were viewed with some consternation by his colleagues and nearly led to his expulsion from the Royal Society. History has been kinder, however, and these works have come to be seen as merely another sign of his indefatigable energy and insatiable curiosity.

Crookes was knighted in 1897 and appointed to the Order of Merit in 1910. He died in London on April 4, 1919, and is buried in Brompton Cemetery.

Figure A-1. Sir William Crookes is best known in gemology for his discovery of the effects of radiation on diamonds. Photo by Ernest H. Mills, approx. 1911.



exposing diamonds to cyclotron radiation, usually alpha particles, deuterons (^2H nuclei), and protons (e.g., Cork, 1942; Ehrman, 1950; Pough and Schulke, 1951; Pough, 1954, 1957). The diamonds turned various shades of blue-green, green, yellow, and brown,

though the yellow-to-brown colors were eventually determined to be the result of heating caused by the bombardment. The stones did become radioactive, but only for a short period afterward. The colors were confined to near-surface layers—though visibly

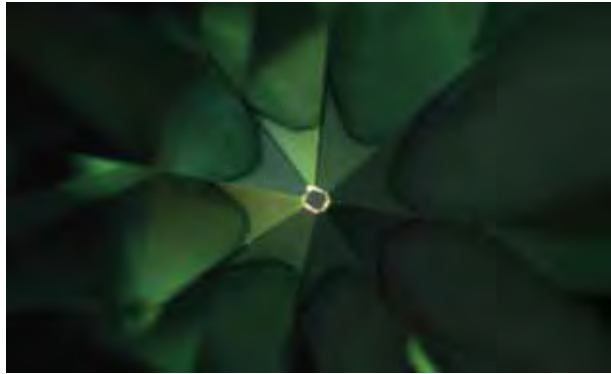


Figure 8. The distinctive feature around the culet of this irradiated diamond, commonly referred to as the umbrella effect, is a tell-tale sign of treatment in a cyclotron. The umbrella effect is not a result of the cyclotron beam striking the culet, but rather the girdle area; its appearance at the culet is caused by internal reflections. Photomicrograph by John I. Koivula; magnified 10 \times .

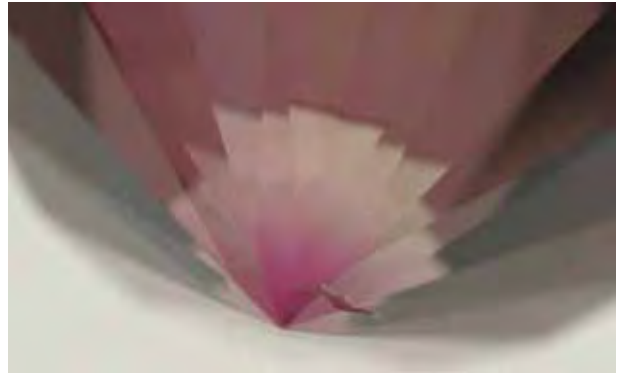


Figure 9. Lower-energy electron irradiation in a linear accelerator can create a thin layer of color beneath the pavilion facets which, because of internal reflections within the diamond, also appears as a concentration of color at the culet of the stone. In this instance, the color concentration is rather intense, which would not be the case if the thin layer of induced color was less saturated. Photomicrograph by Wuyi Wang; magnified 5 \times .

deeper than those seen with radium-treated stones—and were also induced in strongly defined color concentration patterns related to the facet arrangement (e.g., figure 8), since color was created only where the beam of radiation struck the diamond. The commercial applications of these treated colors were obvious, and cyclotron-treated diamonds soon appeared in significant numbers in the market, with sometimes embarrassing results (box B).

Early linear accelerators (linacs) were also used to bombard diamonds with electrons (Clark et al., 1956a,b; Pough, 1957). However, as the energies were relatively low (on the order of 0.5–3.0 MeV; Dyer 1957; Schulke, 1961), the beam did not completely penetrate the stone, and the color was also confined to thin layers beneath facet surfaces that were exposed to the radiation (e.g., figure 9; Collins, 1982; Fritch and Shigley, 1989).

As nuclear reactors became more commonplace in the 1950s, these too were used to irradiate diamonds (Dugdale, 1953). However, because neutrons—which make up the most significant portion of radiation from nuclear fission—can completely penetrate even a large stone, the resulting green color was created more uniformly throughout the diamond (i.e., a “bodycolor”) rather than being confined to thin zones near the surface (Dyer, 1957; Pough, 1957). Likewise, when more powerful linacs came into common usage in the 1960s and 1970s, the higher-energy electrons (10–15 MeV; Ashbaugh, 1988) that were generated with these devices were also able to create uniform color (Parsons, 1996). Without the tell-tale facet-related color concentra-

tion patterns of early electron irradiation, these treated diamonds would prove to be a significant identification challenge, requiring the use of advanced spectroscopic techniques.

Diamonds can also be colored by exposure to gamma ray emissions from a radionuclide such as ⁶⁰Co, similar to that used to sterilize food products and medical equipment (Dyer, 1957; Pough, 1957; Ashbaugh, 1988). Although the process has been known from the early days of diamond irradiation, it is rarely used because it is much slower than other methods, typically taking several months (Collins, 1982). It is worth noting here that the gamma rays do not themselves color the diamond; rather, they generate secondary electrons as they pass through the stone, and these electrons induce color in the same fashion as those from a linac (Collins, 1982).

Nowadays, the most common methods are neutron irradiation in a reactor and high-energy electron irradiation in a linac (e.g., Nassau, 1994). The process selected will depend on the exposure time, costs, potential damage to the diamond, and the treated colors desired.

Radiation-induced color in diamond is the result of damage caused as the radiation (whether neutrons or charged particles) passes through the stone. Collisions between these particles and the carbon atoms create vacant positions in the atomic lattice by knocking the carbon atoms out of their normal positions (Collins, 1982). These vacancies give rise to a broad region of absorption in the visible and near-infrared regions of the spectrum (and a sharp peak at 741 nm, known as the GR1 band), thus creating a

BOX B: THE IRRADIATED DEEPEDENE

Out of all the uncounted carats of diamonds subjected to one treatment or another, perhaps none is more famous than a large yellow stone named after the country estate of the Bok family outside Philadelphia. The Deepdene (figure B-1), as it is known, is believed to have been mined in South Africa in the 1890s (*The Deepdene Diamond*, 1997; Balfour, 2000; most information here is taken from these two references). Consistent with this source, its original color is thought to have been a dark cape (Pough, 1988). The Boks purchased the stone from Los Angeles diamond dealer Martin Ehrmann, who would, interestingly enough, later conduct a series of early experiments in diamond irradiation (Ehrmann, 1950; there is no evidence Mr. Ehrmann was involved in treating the Deepdene). The Boks sold the stone to Harry Winston in 1954.

Sometime in 1955, Dr. Frederick Pough was hired to cyclotron irradiate and anneal the diamond and thereby intensify its yellow color (Pough, 1980, 1988). Dr. Pough was then a recognized authority on the subject and had, perhaps not coincidentally, just published an article on diamond irradiation in *Jewelers' Circular-Keystone* (Pough, 1954). Afterwards, the stone was repolished slightly to remove obvious signs of treatment, specifically the umbrella effect (again, see figure 8).

The diamond was next seen when it came up for auction in 1971. Before the sale, Christie's had engaged two gemological laboratories to determine an origin of color, and both reported that it was untreated. After the sale, this conclusion was disputed by famed gemologist Dr. Edward Gübelin, and it was then sent to the Gem Testing Laboratory in London, where Basil Anderson concurred with Dr. Gübelin's opinion, and to New York, where Robert Crowningshield (who had seen the diamond before it was treated) confirmed Dr. Gübelin's original doubts. The sale thus had to be rescinded and the diamond returned to its owners. Controversy over this incident would simmer for another decade. Not until the 1980s did Dr. Pough come forward to publicly confirm that he had irradiated the stone (e.g., Pough, 1988).

There is some uncertainty in the literature as to when, exactly, Dr. Pough learned of the controversy,



Figure B-1. The Deepdene diamond (currently 104.53 ct), which was irradiated and heated in 1955 to intensify its yellow hue, is perhaps the most famous treated-color diamond in the world. Photo courtesy of Christie's.

and how long he waited to come forward. Both Balfour (2000) and a later auction catalog (*The Deepdene Diamond*) suggest that he was not aware of the debate for some time afterward, perhaps not until the early 1980s. Pough himself did not clear up this ambiguity in a *Lapidary Journal* article a few years later (Pough, 1988) and further insisted that the controversy was “foolish and hardly seems to matter” (p. 29).

In fact, Dr. Pough was aware of the controversy all along. In an interview with GIA Library director Dona Dirlam in 2004 (Pough, 2004), he described how he was contacted shortly after Dr. Gübelin's examination of the diamond in 1971, and how he confirmed to Dr. Gübelin that he had irradiated the stone. Only a confidentiality agreement with the party who had commissioned the treatment prevented him from going public at the time.

The Deepdene came up for sale again in 1997—this time with full disclosure—and was sold to diamond dealer Lawrence Graff for \$715,320.

blue-to-green coloration (Walker, 1979; Collins, 1982; Clark et al., 1992). The strength of the overall broad GR1 absorption, and thus the saturation of the induced color, is directly related to the amount of

radiation received (Clark et al., 1956a). Under conditions of extreme exposure, the induced color can become so dark that it appears black, though the blue or green hue can usually still be seen by holding

the treated diamond over a strong light source such as a fiber-optic cable (e.g., Moses et al., 2000; Boillat et al., 2001).

Heating of most irradiated diamonds above about 500°C in an inert atmosphere will change the blue-to-green colors to brownish or orangy yellow to yellow or, rarely, pink to red (e.g., figure 10). This is the result of radiation-induced vacancies migrating through the lattice and pairing with nitrogen to create new color centers, such as H3 (503.2 nm) and H4 (496 nm) for yellow to orange, and N-V⁰ (637 nm) for pink to red (Collins, 1982). These color alterations are accompanied by specific features in the visible and luminescence spectra of treated diamonds that aid in the identification of the treatments (see, e.g., Collins, 1978, 1982, 2001, 2003; Clark et al., 1992).

Identification. Recognition of laboratory-irradiated (and sometimes heated) faceted colored diamonds has been a major focus of gemological research since the early 1950s (Scarratt, 1982). For example, Crowningshield (1957) reported on the detection of treated yellow diamonds by means of an absorption band at 5920 Å (592 nm) seen in the desk-model spectroscope. The availability of more sensitive spectrometers has since refined the location of this band to 595 nm and established a number of other identifying clues (Scarratt, 1982; Woods and Collins, 1986; Fritsch et al., 1988; Clark et al., 1992; Collins, 2001).

Although initially believed to be diagnostic of laboratory treatment, a weak 595 nm band was subsequently found in the spectra of some natural-color diamonds. This discovery, along with the increasing abundance and variety of treated-color diamonds in the market, led gemological researchers to realize that identifying treated diamonds would require more comprehensive study of both known natural-color and known treated-color stones, and the collection of a database of their gemological properties (color, UV fluorescence, absorption spectrum, and other visual features) and more sophisticated spectral information (visible, infrared, and luminescence). Correct identification, when possible, requires an evaluation of all of these factors. Thus, even today, many artificially irradiated diamonds cannot be identified by a gemologist with standard gem-testing equipment, and they must be submitted to a laboratory for an “origin of color” determination.

Diamonds with a blue-to-green bodycolor present a special identification problem, since their



Figure 10. A broad array of colors are currently achievable by exposure to radiation. All of these diamonds (0.12–1.38 ct) were color treated by irradiation and—except for the black, blue, and green stones—subsequent heat treatment. Photo by Robert Weldon.

color may be due to natural radiation exposure. Some rough diamond crystals display a very thin (several microns) green surface coloration due to exposure to natural alpha-particle radiation in the earth. If green naturals are left on the finished stone, these can contribute to a green face-up color, but this layer is often mostly or completely removed during the faceting process. Natural diamonds with a saturated blue-to-green bodycolor are very rare, but they do exist; perhaps the best example is the famous 41-ct Dresden Green diamond (Kane et al., 1990; see also King and Shigley, 2003). Despite work over the past five decades, identifying origin of color in these cases remains very challenging for gemological researchers, and still it is not always possible for gem-testing laboratories to conclusively establish whether a green diamond is or is not

laboratory irradiated unless it can be examined from the rough through the faceting process.

HPHT Annealing. The most important recent treatment of diamonds involves annealing them at high pressure and high temperature to either lighten off-color stones or create certain fancy colors. Although the commercial uses of this process in the jewelry trade were not realized until the late 1990s, scientists had recognized more than 30 years earlier that treatment under such conditions could change diamond color.

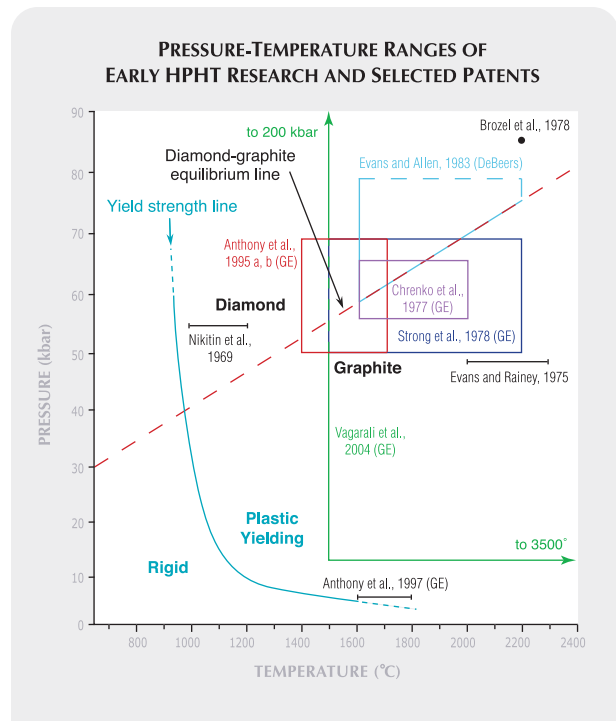
In the late 1960s, Soviet researchers reported experiments in which HPHT treatment both removed color from light yellow diamonds and turned yellow and yellow-green diamonds predominantly green (Nikitin et al., 1969). A few years later, Evans and Rainey (1975) successfully induced yellow color in colorless type Ia diamonds. Research by Chrenko et al. (1977) at General Electric (GE) and by Brozel et al. (1978) at the University of Reading, England, demonstrated that HPHT treatment could change the aggregation state of nitrogen impurities in diamond. Changes from single substitutional nitrogen (Ib) to nitrogen aggregates (Ia), and from Ia to Ib, were both possible under the right conditions of temperature and pressure and the appropriate starting diamond. By altering these nitrogen-containing optical defects, and thereby changing how they caused the diamond to absorb portions of the spectrum of incident light, the process altered the color of the stone. Figure 11 illustrates the relative experimental conditions of this early work, as well as that of later researchers.

In the late 1970s, researchers at GE obtained two U.S. patents on processes for removing yellow and yellow-brown color from type I diamonds, again by converting type Ib nitrogen to type Ia (Strong et al., 1978, 1979; see also Schmetzer, 1999a,b). Type Ib nitrogen creates a broad absorption below about 560 nm toward the ultraviolet, leading to an observed strong yellow color (Collins, 1980, 1982). Type IaA and IaB nitrogen aggregates, however, absorb only in the infrared, so converting Ib nitrogen to aggregated form would remove most of the yellow hue (provided, of course, that other nitrogen-based color centers, such as H3 and N3, were not created in the process). Parallel work by De Beers Industrial Diamond Division led to a similar patent a few years later (Evans and Allen, 1983). Commenting on these discoveries, Nassau (1984, p. 129) said, “The possible commercial significance of these experi-

ments regarding the decolorizing of natural or synthetic yellow diamonds is not yet clear.”

In the early 1990s, GE researchers apparently also discovered that HPHT treatment could be used to strengthen (i.e., improve strength and hardness by reducing lattice defects) colorless CVD synthetic diamond, which is type IIa (i.e., without detectable nitrogen and boron) and incidentally also reduce the color in stones with a brown component (Anthony et al., 1995a,b, 1997). Similar work was ongoing with other groups. In their report on synthetic dia-

Figure 11. This carbon phase diagram illustrates the diamond-graphite stability field (defined by the dashed red equilibrium line) and the plastic yield limit of diamond (solid blue line). Diamond is the stable form of carbon above the diamond-graphite equilibrium line, whereas graphite is stable below this line. The high pressures of the HPHT process are required to prevent diamond from converting to CO₂ gas or graphitizing while heated to the high temperatures needed to change the color. Diamond is rigid to the left of the yield-strength line, whereas it can plastically deform under conditions corresponding to those to the right of this line. Pressure-temperature ranges of early HPHT experiments and selected patents are also shown. Note that the upper pressure limit of Evans and Allen (1983) was undefined. Modified from DeVries (1975) and Schmetzer (1999b).



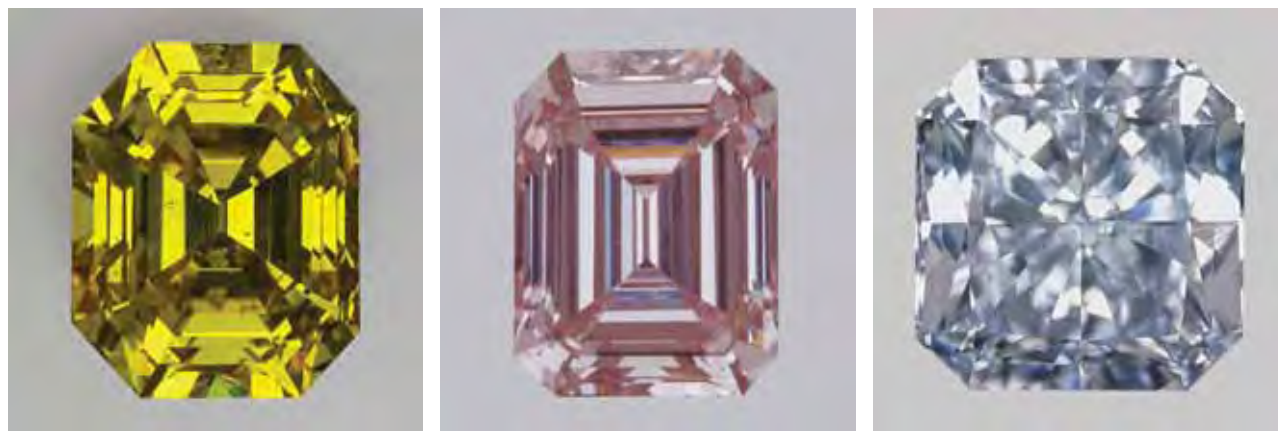


Figure 12. These examples illustrate some of the fancy colors that can be produced by HPHT treatment of type Ia (left), type IIa (center), and type IIb (right) diamonds. Photos by Robison McMurtry, left; C. D. Mengason, center; Jessica Arditi, right.

monds from Russia, Shigley et al. (1993) examined three greenish yellow to yellow samples that had been HPHT treated to alter their color. In 1997, Reinitz and Moses reported on several yellow-green diamonds submitted to the GIA laboratory that displayed features later considered indicative of HPHT treatment (Reinitz et al., 2000). Again, the commercial possibilities of the HPHT process were not clear to those in the trade, though there was some limited speculation (K. Scarratt, as reported in Even-Zohar, 1994). This latter report followed up on claims by Russian scientists that yellowish Ib diamonds could be made whiter by conversion to type IaAB, as discussed above, but there is no evidence that this process has ever seen commercial use. Treated-color yellow-to-green diamonds continued to appear on the market in the late 1990s (Van Bockstael, 1998; Henn and Millisenda, 1999).

Despite more than three decades of research, along with technical publications and patents, the trade was taken by surprise in March 1999 when GE and Lazare Kaplan International (LKI) announced the commercial use of the HPHT process to remove color from type IIa diamonds (Rapaport, 1999). This development caused substantial controversy and criticism, especially since the initial press release asserted that the stones would be “indistinguishable” from natural diamonds (Moses et al., 1999; Schuster, 2003). Some of this criticism was blunted after GE and LKI agreed to laser inscribe their diamonds and work with GIA and other industry groups to establish reliable means of identification, though GE initially refused to release specific details about the process itself. The need for proper detection criteria became even more critical after a few treated diamonds with their identifying laser inscriptions removed began

appearing later that year (Moses et al., 1999).

Fortunately, gemological researchers were not as ill-prepared as the trade for this development, and reports by Schmetzer (1999a), Collins et al. (2000), Fisher and Spits (2000), and Smith et al. (2000), among others, did much to clear the confusion about what GE was doing. What mystery remained around the GE process began to dissipate in October 2001, as related patent applications began to be published (Vagarali et al., 2001, 2004). Although GE’s initial work involved removing color from type IIa brown diamonds (Smith et al., 2000), subsequent developments by GE and others have led to the production of a wide range of colors in both type II (pink or blue; Hall and Moses, 2000, 2001) and type I (orangy yellow, yellow, to yellow-green; e.g., Henn and Millisenda, 1999; Reinitz et al., 2000; Deljanin et al., 2003; Hainschwang et al., 2003) diamonds (e.g., figure 12).

The exact mechanism of the color change in brown diamonds is still a subject of debate. Although brown color in natural diamonds was once believed to be associated with plastic deformation of the carbon lattice (see, e.g., Wilks and Wilks, 1991; Fritsch, 1998), it is now thought that this is not entirely correct, as the lattice deformation is not affected by the HPHT process even though the brown color is removed. Recent research has suggested a link between brown color and vacancies and vacancy-related extended defects (e.g., Bangert et al., 2006; Fisher et al., 2006). Such extended defects can give rise to an absorption spectrum similar to that of brown type IIa diamonds.

It is believed (Collins, 2001) that the absorptions responsible for blue and pink colors are not a result of the HPHT process, but rather are preexisting, and

the blue or pink color is revealed only when the predominant brown component is removed, as the resulting stones show certain properties similar to natural-color blue and pink stones (Hall and Moses, 2000, 2001). Yellow-green to green colors in HPHT-treated stones are the result of vacancies pairing with nitrogen to form H2 and H3 centers, while pure yellows can be created from type Ia diamonds through disaggregation to type Ib nitrogen (Collins, 2001; Hainschwang et al., 2003). Processes to remove color from type IaB brown diamonds have also shown some promise (Van Royen et al, 2006).

Other U.S. companies as well as treatment facilities in Russia, Sweden, and Korea have since entered the market with their own products (e.g., Henn and Millisenda, 1999; Smith et al., 2000; Reinitz et al., 2000; Deljanin et al., 2003; Wang and Moses, 2004; Wang et al., 2005a). When combined with irradiation (e.g., Wang et al., 2005a), colors across nearly the entire visible spectrum can be achieved for type I and type II diamonds, and such treated-color diamonds have now become nearly ubiquitous in the market (e.g., Perret, 2006; again, see figure 10). Further, unlike paints and coatings, the colors of HPHT-treated diamonds are permanent to standard jewelry manufacturing, wear, and repair situations.

Identification. The identification of HPHT-treated diamonds, especially through standard gemological testing, remains a challenge (Collins, 2006). Although these stones may occasionally display distinctive visual features that can be seen with magnification (such as graphitized inclusions or internal cleavages, or damaged surfaces [figure 13]; see Moses et al., 1999; Gelb and Hall, 2002), in general these indicators either are not always present or are not adequate to fully establish a stone's correct identity. Type IIa diamonds—which comprise the vast majority of colorless HPHT-treated diamonds—are relatively easy to identify by their short-wave UV transparency with simple equipment like the SSEF Diamond Spotter (Chalain et al., 2000; Hänni, 2001), but further testing is still necessary to determine if a stone is natural or treated color. The De Beers DiamondSure instrument (Welbourn et al., 1996) will also “refer” type IIa stones, but it cannot make a definitive identification of treatment (and the cost is out of the reach of most gemologists).

When the proper laboratory equipment is available, a variety of spectroscopic clues can identify HPHT treatment (Newton, 2006). Some of the earliest work in this area actually began in the 1980s at

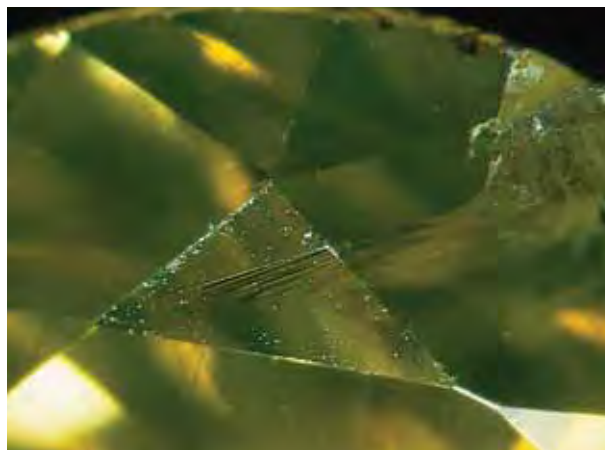


Figure 13. This 0.52 ct green-yellow diamond shows abraded facet edges and frosted facets, indicative of HPHT treatment. Typically, such features will be polished off before a stone is offered for sale. Photomicrograph by Shane Elen; magnified 15 \times .

the De Beers DTC Research Centre (Fisher and Spits, 2000). This and subsequent research (see, e.g., Chalain et al., 1999, 2000, 2001; Collins et al., 2000; De Weerd and Van Royen, 2000; Smith et al., 2000; Vins, 2002; Collins, 2003; Novikov et al., 2003), helped establish various features seen with infrared and, particularly, low-temperature photoluminescence (PL) spectroscopy as reliable indicators of treatment. The relative strength of the N-V luminescence at 575 and 637 nm when excited by a 514.5 nm laser has been found to be useful for type IIa diamonds (Collins, 2001). It is very important to note, though, that it is the *combination* and relative strength of various defects that is key to identification, rather than the mere presence or absence of a single type of defect (Newton, 2006). For this reason, definitive identification requires testing in a properly equipped gemological laboratory. In general, the precise methods and criteria of identification are considered proprietary by most labs.

Low-Pressure, High-Temperature Annealing. Heat treatment under low pressures can be used to create black diamonds by inducing large-scale graphitization within surface-reaching fractures (Hall and Moses, 2001; Notari, 2002). First seen in the early 2000s, these diamonds are now common enough to greatly outnumber natural black stones on the market (Cheung and Liu, 2007). In general, these treated-color black diamonds are not difficult to identify. Strong illumination will reveal graphite inclusions confined to fractures, in contrast to the random “salt and pepper” appearance of natural black

stones (Hall and Moses, 2001; Notari, 2002). They also generally lack the pitted and knotted surface features common in natural black diamonds, and they can display a characteristic surface iridescence. As with other treatments, though, melee-sized stones can be difficult to fully characterize.

As a review of this section, figure 14 shows a graphic representation of the range of treated colors now available in the market, through coating, irradiation, HPHT treatment, and low-temperature annealing.

CLARITY TREATMENTS

Laser Drilling of Inclusions. One effect of the dramatic increase in the supply of diamonds in the late 19th and early 20th centuries (largely due to discoveries in South Africa) was a desire to rank them by perceived quality factors, and one obvious criterion was clarity.

Diamonds with visible dark inclusions were not as highly valued as those that were eye-clean. This trend led to the development of various methods to rate a diamond's clarity—the most commonly used today being the GIA grading scale (e.g., Liddicoat, 1955)—and the presence of eye-visible inclusions became a matter of economics as well as aesthetics.

Until the invention of the diamond saw, there was no way to remove a dark inclusion deep in a stone short of polishing or cleaving away large amounts of material—obviously an unattractive and uneconomic solution. The diamond saw allowed manufacturers to cut through a stone and essentially “slice out” dark inclusions, but even this was not always economic, as it might require dividing an otherwise profitable piece of rough into two much less valuable stones, or the inclusion might be so large that slicing it out would result in too much loss of material.



Figure 14. Shown here are examples of the wide range of treated-color diamonds now available on the market. Colors across the entire visible spectrum are now achievable with the proper starting material and combination of treatments. Colors shown are based on what has been seen to date, and other colors may appear in the future. Figure by Christopher M. Breeding.

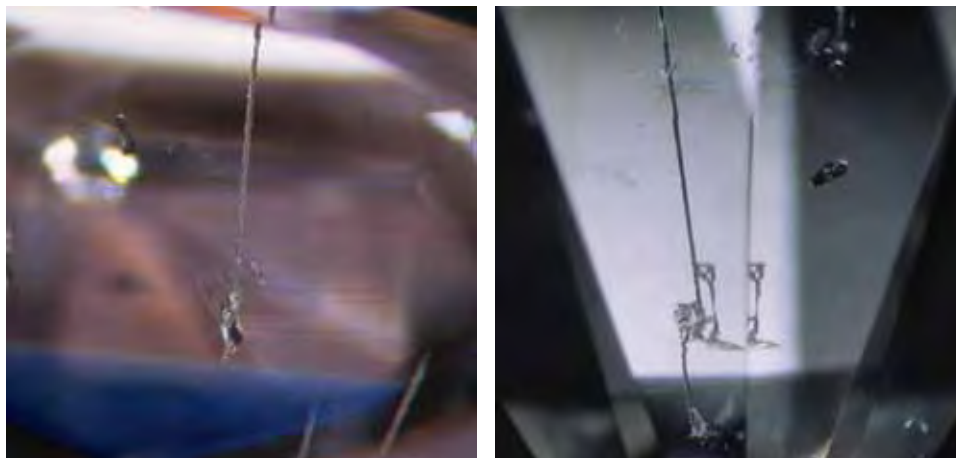


Figure 15. The laser drill holes in these diamonds serve as a conduit from the diamond's surface to mineral inclusions, which have been lightened or removed by acid boiling. Photomicrographs by Shane McClure (left) and John I. Koivula (right); both magnified 10 \times .

Dark inclusions in diamond are generally composed of graphite or sulfide minerals, or other, iron-containing mineral phases (Kammerling et al., 1990; Titkov et al., 2003), most of which can be dissolved by strong acids. Diamonds have long been boiled in acid for cleaning purposes after faceting (to remove lap metal and other debris, particularly from bruted girdles), and diamond manufacturers surely noticed that this process also often removed surface-reaching dark inclusions. In the early 1960s, a more thorough process, referred to as *deep-boiling*, was conducted under pressure in order to force the acid deeper into surface-reaching cleavages (Rapaport, 1987). When such a cleavage was connected to a dark inclusion, the acid would be able to bleach it to a lighter color or remove it entirely. However, this process did not affect dark inclusions sealed inside the stone. The industry had to wait a few more years before technology provided a solution.

For most of history, diamonds could only be manufactured using mechanical means: cleaving, sawing, grinding, and polishing. This began to change in the 1970s, following the development of lasers of relatively low cost and sufficiently high power to vaporize diamond (see Caspi, 1997). Although laser sawing, kerfing, and bruting would not become established in the trade until the 1980s, as early as 1970 Crowningshield reported that lasers were being used as part of a process to bleach or dissolve dark inclusions. Further, he mentions having heard rumors about this process for several years before seeing an actual laser-drilled diamond. This timing is significant because it was less than 10 years after the invention of the laser in 1960 (Cooper, 1991). Laser drilling proved to be the first widespread treatment ever used to alter the clarity of polished “colorless” diamonds.

One of the earliest trade reports of the process gives credit for its invention to Louis Perlman of

Perlman Brothers in New York, who—allegedly—first tested his idea in collaboration with technicians at Raytheon Co. in Massachusetts in 1963 (Ward, 1972). This would have been shortly after a report appeared in the trade press about GE researchers using a laser to drill 0.02-inch-diameter holes into an industrial diamond (“A beam of light . . .,” 1962). It is unknown whether this report gave Perlman the idea, but it seems likely that some in the trade made the connection.

The basic laser-drilling process is relatively simple. A 1064 nm solid-state neodymium-doped YAG laser is used to vaporize a tiny channel from the surface down to a dark inclusion using a pulsed, focused beam. Because the absorption of diamond at 1064 nm is negligible (i.e., the beam will normally pass through the diamond without effect), the process must be started by marking the target spot with dark ink. The ink will absorb enough heat to convert the underlying diamond to graphite, which is then converted to carbon dioxide gas. Once the graphite conversion begins, the process is self-sustaining (Cooper, 1991). With this open conduit to the inclusion, the diamond can be deep-boiled in acid to bleach or remove the internal feature (figure 15).

Although Perlman’s first efforts were not successful, by 1969 he had refined the process sufficiently for commercial use (Ward, 1972). By the early 1970s, it was widely enough available to members of the trade that refinements and alternatives were already being discussed (see, e.g., Crowningshield, 1971; Lenzen, 1973, 1974), and the ethics of the process and its disclosure were already creating controversy (Leadbeater, 1972; Alexander, 1973; Eyles, 1973; Pagel-Theisen, 1976).

The FTC rules in place at the time did not require disclosure of laser drilling (as it was a permanent treatment; see Overton, 2004), but many in the

trade still felt that it should be disclosed to consumers anyway (“Lasering. . .,” 1980). The controversy would persist until the early 2000s, when the FTC finally updated its disclosure rules to require it (Overton, 2004).

Refinements in laser technology allowed more precise drilling and smaller, less-visible channels, but the basic process went unchanged until the end of the 20th century. In the early 2000s, examples of several new methods began to appear. The first, referred to as *KM treatment* (KM stands for *kiduah meyuhad*, or “special drill” in Hebrew), opened channels from dark inclusions to the surface not by burning through the diamond but rather by using the focused heat of the laser to expand (or even create) feathers around the inclusion (McClure et al., 2000; Horikawa et al., 2001). The process was sufficiently controllable that a series of tiny step-like cleavages could be created in order to take the shortest route to the surface. In some stones, the treatment created irregular worm-like channels with some resemblance to natural etch channels (McClure et al., 2000) or sugary disk-like features with irregular boundaries (Cracco and Kaban, 2002).

Variations in the appearance of drill holes and the internal features they reach continue to be seen (e.g., Astuto and Gelb, 2005), and as laser drilling is a versatile tool, it is likely that new permutations will arise in the future. Diamonds that display evidence of what seems to be accidental laser damage—that is, laser-created holes that do not connect to any inclusions—have also been noted (S. McClure, pers. comm., 2008).

Laser drilling is a permanent treatment, since there is obviously no way to replace the diamond burned out of the drill hole. (However, the drill hole can be glass filled to make it less apparent.) Some in the trade do not consider laser drilling a treatment at all but rather an additional step in the manufacturing process, though the consensus of diamond trade organizations is otherwise, and—as mentioned above—current FTC guidelines require that laser drilling be disclosed as a treatment. The presence of laser-drilled channels is also recorded as a clarity feature on typical diamond grading reports.

Identification. From a gemological standpoint, the detection of conventional laser drilling is straightforward, since the drill hole is easily visible with a gemological microscope provided the entire stone can be examined. When a drill hole is absent (e.g., with the KM treatment), recognition of laser action

on inclusions can be more difficult, but it is not terribly challenging if one is familiar with the characteristic features (McClure et al., 2000). Note, however, that even melee-sized diamonds can be laser drilled, and it may not be practical to examine every stone in a large parcel.

Glass Filling of Surface-Reaching Cleavages. Like coating and painting, the use of oils and waxes to hide surface-reaching cracks and improve luster is an ancient practice, at least with colored stones. Wax treatment of jade, for example, has been detected in Chinese artifacts more than 2,500 years old (Qiu et al., 2006), and the oiling of emeralds has been recorded at least as far back as the 14th century (Nassau, 1994).

Diamonds, however, seem to have escaped such filling treatments until recently. Because of diamond’s very high refractive index, filling with a low-RI material—such as the oils used in emerald filling—would not significantly reduce the visibility of a crack. Diamond filling likely had to wait until modern chemistry could supply fillers with sufficiently high RIs. Although lead-oxide glasses have been known since antiquity, their maximum RIs are around 1.7 (Newton and Davidson, 1989), well below that of diamond. Modern lead-bismuthate glass, however, can have an RI well into the 2-plus range (Dumbaugh, 1986). When such a glass is forced into surface-reaching cracks, the improvement in apparent clarity can be dramatic (figure 16; see Kammerling et al., 1994, for a discussion of the optics of glass filling).

It is not generally known exactly when the commercial filling of diamonds with high-RI glass began, but it appears to have been invented in Israel by diamond dealer Zvi Yehuda in the mid-1980s. The first published reports of the treatment appeared in 1987 (e.g., Koivula, 1987), but several sources (e.g., Rapaport, 1987; Everhart, 1987a,b) stated that Mr. Yehuda had been treating stones with this process since 1981. This would mean that such filled diamonds might have been in circulation for more than five years without having been detected by either dealers or gemological laboratories—possible, but unlikely given that diamonds are carefully examined during the quality grading process and the treatment was detected almost simultaneously by a variety of parties during 1987 (as discussed in Koivula, 1987; Koivula et al., 1989).

Although the exact details of the filling process and the formulas of the fillers are proprietary (and



Figure 16. Introduction of a glass filler into this 0.30 ct diamond's cleavage cracks produced a dramatic change in apparent clarity (before filling, left; after filling, right). Photomicrographs by John I. Koivula.

closely guarded), there is general agreement that the diamonds are filled in a vacuum or near-vacuum so as to evacuate the air from surface-reaching cracks (see Nelson, 1993; Nassau, 1994; Kammerling et al., 1994). Because of the low melting point of the glass, ordinary laboratory equipment can be used to melt the filler materials and mix in the diamonds (Nassau, 1994).

Initial controversy over this treatment was intense, with a few diamond bourses going so far as to ban filled stones altogether, and many others threatening expulsion for any member who sold filled stones without disclosing the treatment (Everhart, 1989; Shor, 1989). The situation was further complicated by the fact that within five years there were a number of firms marketing filled diamonds and filling services. Competing claims in the trade press regarding the detectability, durability, and effectiveness of various methods made it very difficult for diamond dealers to know what to believe.

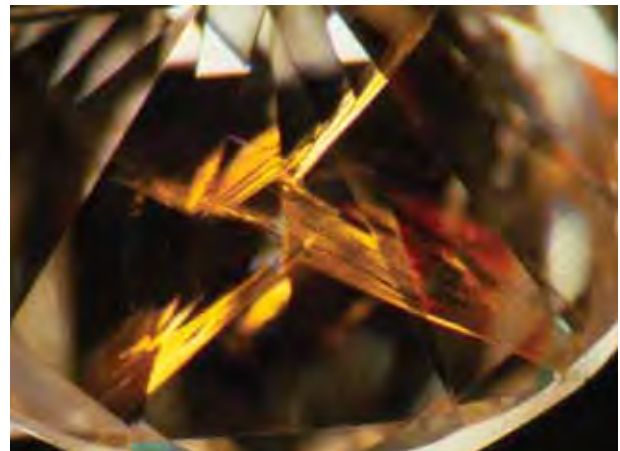
Gemologists quickly determined reliable methods to detect fillings in diamonds based on straightforward examination with a microscope: flow structures, gas bubbles, a “crackled” texture, and, most prominently, different “flashes” of color seen with brightfield and darkfield illumination (e.g., Koivula et al., 1989; Hänni, 1992; Scarratt, 1992; Schlüssel, 1992; Kammerling et al., 1994; Sechos, 1994; McClure and Kammerling, 1995; figure 17). Although some manufacturers would subsequently claim that their filling process did not show one or another of these features, particularly the flash effect, further research determined that, in fact, all filled stones on the market at the time could be identified by this approach.

The precise mechanism behind the flash effect has itself been the subject of some discussion. Although early reports referred to it as an interfer-

ence-related phenomenon, Nelson (1993) showed that it was actually the result of differences in dispersion between the diamond and the filling material (see also Kammerling et al., 1994). Nelson (1995) later speculated that the flash effect could be eliminated by using a filling material with an RI curve that closely matched—but did not intersect with—that of diamond in the visible range. However, there has been no evidence that this approach was ever adopted by those performing the treatment.

One drawback of the glass-filling process is that it may result in a lower color grade for the diamond, something that was noted almost immediately after treated stones began showing up in the market (e.g., Koivula et al., 1989). This side effect is believed to result from the color of the filler, as lead-bismuthate

Figure 17. The intersecting cleavage cracks in this diamond have been filled with a high-RI glass, but the bright flash-effect colors betray the presence of the filler. Photomicrograph by Shane F. McClure; magnified 5 \times .



glasses are frequently yellow when seen in large pieces. In some rare filled diamonds, fairly thick areas of filler have shown a yellow color (Kammerling et al., 1994). Although this effect is undesirable with colorless to near-colorless diamonds, it does raise the possibility that colored fillers could be used to add or enhance color in off-color stones. However, only a few such stones have been reported. Yeung and Gelb (2003, 2004) described two diamonds that had been colored pink by a filling substance (see, e.g., figure 18), though the results were generally poor and the treatment was easily detected with magnification. There are some reports of natural fancy-color diamonds having been glass filled (see, e.g., Sechos, 1995), but these appear to be less common since there is more acceptance of lower clarity grades in colored diamonds.

Glass filling is not a permanent treatment, but it is stable under normal conditions of wear and use of jewelry (Kammerling et al., 1994). However, because of the relatively low melting point of the glass, it can be damaged during jewelry repair if the diamond is subjected to substantial direct heat, as from a jeweler's torch or during repolishing (Crowningshield, 1992; Kammerling et al., 1994; Shigley et al., 2000).

Identification. The detection of glass filling is normally a matter of examination with a gemological microscope to identify the features discussed above:

Figure 18. This 1.02 ct diamond is colored by a pink residue in the large fractures that reach the surface through the crown. The actual bodycolor of the diamond is near-colorless. Photo by Elizabeth Schrader.

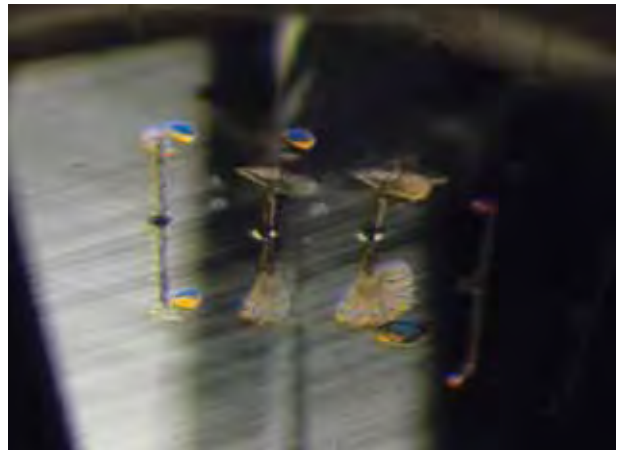


Figure 19. The drill holes in this laser-drilled diamond have been filled with high-RI glass to reduce their visibility. Note the flash-effect colors around the filling. Photomicrograph by John I. Koivula; magnified 25 \times .

flow structures, trapped gas bubbles, crackled textures, and—most importantly—flash-effect colors. Detection of flash effects is best conducted with fiber-optic illumination, which provides an intense, focused beam of light (Kammerling et al., 1994; McClure and Kammerling, 1995).

COMBINED TREATMENTS

It is important for the gemologist to remember that, in most cases, there is little to prevent a treator or manufacturer from employing more than one process to achieve a desired result. In recent years, quite a few examples of combined treatments have been reported. Laser drilling and glass filling are perhaps the most commonly combined processes (figure 19), common enough to scarcely merit mention in the literature. These may be used in concert simply to disguise the drill holes or because a particular stone has both dark inclusions and clarity features that can be made less visible, but examples have been seen in which the combination of treatments made possible results that would not have been achievable using either process in isolation. Crowningshield (1993) reported on a diamond in which a large feather under the table had been glass filled after a laser was used to open a channel to the surface. Absent the laser drilling, the filling would not have been possible.

As noted above, the use of irradiation followed by moderate-temperature heating began in the 1950s. More recently, irradiation and HPHT annealing have been used in combination. In addition to the pink-to-red stones described by Wang et al. (2005a), Wang et al. (2005c) reported on two orange diamonds that

were likely treated by a similar combination of HPHT annealing, then irradiation, followed by low-temperature annealing.

Other combinations are certainly possible. One of the pink filled stones that Yeung and Gelb (2004) described had been filled both to improve apparent clarity and to induce a pink color. Irradiated glass-filled diamonds have also been seen: Gelb (2005) reported a bluish green diamond that displayed both an obvious color zone around the culet (figure 20) and flash-effect colors from the filler. Gelb and Hall (2005) reported a large yellow diamond that proved to be irradiated, but that also displayed very unusual textures and structures within surface-reaching cracks. They speculated that the diamond might have been glass filled by one party, and then irradiated by another party unaware of the filling, which was damaged by the post-irradiation annealing necessary to create the yellow color.

SYNTHETIC DIAMONDS

Though not directly addressed in this article, which focuses on natural diamonds, it is important to note that gem-quality synthetic diamonds are potential candidates for all of these color and clarity enhancement processes. Irradiation and heating treatments have already been used to produce red, pink, and green colors in synthetic diamonds (Moses et al., 1993; Shigley et al., 2004; Schmetzer, 2004), just as

Figure 20. This 1.22 ct round brilliant diamond shows both an obvious color zone at the culet and flow structures from glass filling. It was apparently subjected to artificial irradiation followed by glass filling treatment. Photomicrograph by Thomas Gelb; magnified 30 \times .

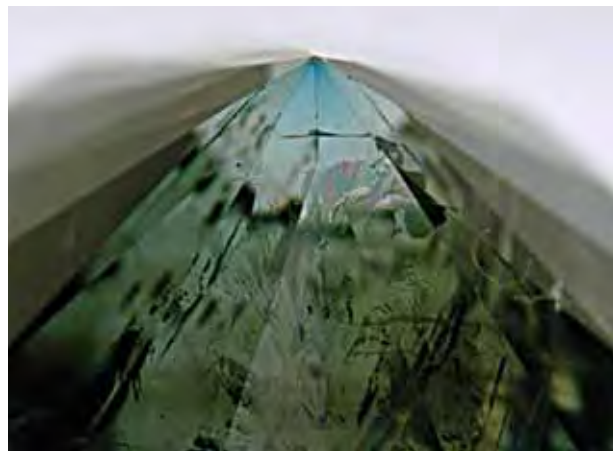


Figure 21. Recent developments in diamond treatment have made previously rare diamond colors much more available to jewelry designers. This platinum engagement ring contains a 1.57 ct HPHT-treated orange diamond. Photo by Ralph Gabriner; courtesy of Etienne Perret.

they are used with their natural counterparts. Shigley et al. (1993) described several synthetic diamonds whose colors had been modified by HPHT annealing. Wang et al. (2005a) discussed the use of HPHT treatment to improve the color of CVD synthetic diamonds. Application of these color treatments does not necessarily make the diamonds more difficult to recognize as being synthetic, however.

Although synthetic diamonds exhibiting evidence of laser drilling or glass filling have not been reported, there is no reason why these processes could not be used, especially since the metallic flux inclusions often present in (and characteristic of) HPHT synthetics could conceivably be removed by acid boiling after laser drilling to open a channel to the surface.

THE FUTURE OF DIAMOND TREATMENT

The wide variety of treatments now available on the market presents both opportunities for designers (e.g., figure 1 and figure 21) and an ongoing challenge to all those who handle diamonds. While “low-tech” treatments such as glass filling and laser drilling can be identified with sufficient training, the days when a diamond’s color could be presumed natural after rinsing in alcohol to remove possible paints are gone forever.

There are several treatments that are not discussed in this article because there is no evidence that they are used widely, if at all, in the trade at this time. These include, for example, ion implantation to produce a thin surface layer of color (e.g., Moses et al., 2000) and foil backing, which—though common centuries ago—has largely died out for use with diamonds, and is more properly considered a lapidary technique (e.g., Cellini, 1568).

The most likely areas of future development lie in further combination of treatments and advanced coating materials. New combinations of irradiation and heating may expand the possible starting material that can be converted to gem-quality diamond. In addition, some laboratories have seen evidence of laser drilling to reportedly mask signs of HPHT treatment (Bates, 2004). Future generations of surface coatings will likely be more durable, and the observa-

tion of film damage, the most reliable method used now for detection, may become less useful. Newer coatings may be applied to laser-drilled and/or glass-filled diamonds, since such treatments are typically used on lower-quality diamonds that are more difficult to sell in their untreated state. Such coatings could interfere with detection of laser drill holes or flash-effect colors, making these stones more difficult to fully identify, especially in smaller sizes. CVD synthetic diamond thin films may also see commercial use as a coating on natural diamond, as CVD methods evolve and become more economic.

For all treatment types, identification using standard gemological techniques will likely grow even more difficult. Working in the modern diamond market will continue to require constant vigilance and the assistance of a professional gemological laboratory.

ABOUT THE AUTHORS

Mr. Overton is managing editor of *Gems & Gemology*, and Dr. Shigley is GIA Distinguished Research Fellow, at GIA in Carlsbad.

ACKNOWLEDGMENTS

The authors wish to thank Dr. Christopher M. (Mike) Breeding,

Dino DeGhionno, Dona Dirlam, Dr. Sally Eaton-Magaña, Scott Guhin, John I. Koivula, Shane McClure, Caroline Nelms, Terri Ottaway, Duncan Pay, Robert Weldon, and Clara Zink of GIA Carlsbad; and Dr. Wuyi Wang and Matthew Hall of GIA New York, for information and assistance. A substantially shorter version of this article serves as the preface to *Gems & Gemology in Review: Treated Diamonds* (Shigley, 2008).

REFERENCES

- Alexander A.E. (1973) Ethics or not, lasers are removing diamond spots. *National Jeweler*, Vol. 68, No. 8, pp. 1, 31, 46.
- Anthony T.R., Banholzer W.F., Spiro C.L., Webb S.W., Williams B.E. (1995a) *Toughened Chemically Vapor Deposited Diamond*. European patent application, open-laid No. 0 671 482 A1, published September 13, 1995.
- Anthony T.R., Fleischer J.F., Williams B.E. (1995b) *Method for Enhancing the Toughness of CVD Diamond*. U.S. patent 5,451,430, issued September 19, 1995.
- Anthony T.R., Banholzer W.F., Spiro C.L., Webb S.W., Williams B.E. (1997) *Method of Enhancing the Toughness of CVD Diamond*. U.S. patent 5,672,395, issued September 30, 1997.
- Ashbaugh C.E. (1988) Gemstone irradiation and radioactivity. *Gems & Gemology*, Vol. 24, No. 4, pp. 196–213.
- Ashbaugh C.E., Moses T.M. (1993) Lab Notes: Another radioactive diamond. *Gems & Gemology*, Vol. 29, No. 1, p. 49.
- Astuto J., Gelb T. (2005) Lab Notes: Diamond with unusual laser drill holes. *Gems & Gemology*, Vol. 41, No. 2, p. 170.
- Balfour I. (2000) *Famous Diamonds*, 4th ed. Christie, Manson and Woods, London.
- Ball S.H. (1950) *A Roman Book of Precious Stones*. Gemological Institute of America, Los Angeles.
- Bangert U., Barnes R., Hounscome L.S., Jones R., Blumenau A.T., Briddon P.R., Shaw M.J., Öberg S. (2006) Electron energy loss spectroscopic studies of brown diamonds. *Philosophical Magazine*, Vol. 86, No. 29–31, pp. 4757–4779.
- Bates R. (2004) How should labs treat treatment? *JCK*, Vol. 175, No. 2, pp. 134–135.
- A beam of light has been used to strike holes in diamonds (1962) *Jewelers' Circular-Keystone*. Vol. 133, No. 6, p. 78.
- Becquerel A.H. (1896) Sur les radiations émises par phosphorescence [On the radiations emitted by phosphorescence]. *Comptes Rendus Hebdomadaires des Séances de l'Académie des Sciences* [Weekly reports of the meetings of the Academy of Science of France], Vol. 122, pp. 420–421.
- Boillat P.Y., Notari F., Grobon C. (2001) Luminescences sous excitation visible des diamants noirs irradiés: Les luminescences d'arêtes [Luminescence of irradiated black diamonds under visible light excitation: Luminescence of edges]. *Revue de Gemmologie*, No. 141/142, pp. 37–41.
- Briggs H.E. (1935) A coated "emerald." *Gems & Gemology*, Vol. 1, No. 9, p. 254.
- Brijbhushan J. (1979) *Masterpieces of Indian Jewellery*. Taraporevala, Mumbai.
- Brozel M.R., Evans T., Stephenson R.F. (1978) Partial dissociation of nitrogen aggregates in diamond by high temperature-high pressure treatments. *Proceedings of the Royal Society A: Mathematical and Physical Sciences*, Vol. 361, No. 1704, pp. 109–127.
- Caspi A. (1997) Modern diamond cutting and polishing. *Gems & Gemology*, Vol. 33, No. 2, pp. 102–121.
- Cellini B. (1568/1967) *The Treatises of Benvenuto Cellini on Goldsmithing and Sculpture*. Transl. by C. R. Ashbee, Dover Publications, New York.
- Chalain J.-P., Fritsch E., Hänni H. (1999) Detection of GE POL diamonds: A first stage. *Revue de Gemmologie a.f.g.*, No. 138/139, pp. 30–33.
- (2001) Diamants de type IIa et traitement HPHT: identification. [Type IIa diamonds and HPHT treatment: Identification]

- Revue de Gemmologie a.f.g.*, No. 141/142, pp. 50–53.
- (2000) Identification of GE/POL diamonds: A second step. *Journal of Gemmology*, Vol. 27, No. 2, pp. 73–78.
- Cheung C., Liu Q. (2007) Lab Notes: Unusual natural-color black diamond. *Gems & Gemology*, Vol. 43, No. 1, pp. 52–53.
- Chrenko R.M., Tuft R.E., Strong H.M. (1977) Transformation of the state of nitrogen in diamond. *Nature*, Vol. 270, No. 5633, pp. 141–144.
- Clark C.D., Ditchburn R.W., Dyer H.B. (1956a) The absorption spectra of natural and irradiated diamonds. *Proceedings of the Royal Society of London A*, Vol. 234, No. 1198, pp. 363–381.
- Clark C.D., Ditchburn R.W., Dyer H.B. (1956b) The absorption spectra of irradiated diamonds after heat treatment. *Proceedings of the Royal Society of London A*, Vol. 237, No. 1208, pp. 75–89.
- Clark C.D., Collins A.T., Woods G.S. (1992) Absorption and luminescence spectroscopy. In J. E. Field, Ed., *The Properties of Natural and Synthetic Diamond*, Academic Press, London, pp. 35–79.
- Collins A.T. (1978) Investigating artificially coloured diamonds. *Nature*, Vol. 273, No. 5664, pp. 654–655.
- (1980) Vacancy enhanced aggregation of nitrogen in diamond. *Journal of Physics C: Solid State Physics*, Vol. 13, No. 14, pp. 2641–2650.
- (1982) Colour centres in diamond. *Journal of Gemmology*, Vol. 18, No. 1, pp. 37–75.
- (2001) The colour of diamond and how it may be changed. *Journal of Gemmology*, Vol. 27, No. 6, pp. 341–359.
- (2003) The detection of colour-enhanced and synthetic gem diamonds by optical spectroscopy. *Diamond and Related Materials*, Vol. 12, No. 10/11, pp. 1976–1983.
- (2006) Identification technologies for diamond treatments. *Gems & Gemology*, Vol. 42, No. 3, pp. 33–34.
- Collins A.T., Kanda H., Kitawaki H. (2000) Colour changes produced in natural brown diamonds by high-pressure, high-temperature treatment. *Diamond and Related Materials*, Vol. 9, No. 2, pp. 113–122.
- Cooper M. (1991) Laser technology in the diamond industry. In Cooke P., Caspi A., Eds., *International Diamond Technical Symposium Proceedings*, Tel Aviv, Oct. 20–24, CSO Valuation AG, London, pp. 6–1–6–16.
- Cork J.M. (1942) Induced color in crystals by deuteron bombardment. *Physical Review*, Vol. 62, No. 1/2, pp. 80–81.
- Cracco V., Kaban H. (2002) Gem Trade Lab Notes: Internal laser drilling update. *Gems & Gemology*, Vol. 38, No. 2, pp. 164–165.
- Crookes W. (1874) *Researches into the Phenomena of Spiritualism*. Two Worlds Publishing Co., London.
- (1876) *The Profitable Disposal of Sewage*. Pamphlet publ. by the author, London, 18 pp.
- (1904) On the action of radium emanations on diamond. *Proceedings of the Royal Society of London*, Vol. 74, pp. 47–49.
- (1909) *Diamonds*. Harper & Brothers, London.
- (1914) On acquired radio-activity. *Philosophical Transactions of the Royal Society of London A*, Vol. 214, pp. 433–445.
- Crowningshield G.R. (1957) Spectroscopic recognition of yellow bombarded diamonds and bibliography of diamond treatment. *Gems & Gemology*, Vol. 9, No. 4, pp. 99–104, 117.
- (1959) Highlights at the Gem Trade Laboratory in New York: New colors in treated diamonds. *Gems & Gemology*, Vol. 9, No. 9, p. 268.
- (1961) Highlights at the Gem Trade Laboratory in New York: Radium-treated diamonds. *Gems & Gemology*, Vol. 10, No. 8, p. 242.
- (1965) Developments and highlights at the Gem Trade Laboratory in New York: More painted diamonds. *Gems & Gemology*, Vol. 11, No. 10, pp. 310–311.
- (1970) Developments and highlights at the Gem Trade Laboratory in New York: Laser beams in gemology. *Gems & Gemology*, Vol. 13, No. 7, pp. 224–226.
- (1971) Developments and highlights at the Gem Trade Laboratory in New York: Drilled diamonds. *Gems & Gemology*, Vol. 13, No. 12, pp. 370–371.
- (1975) Developments and highlights at the Gem Trade Laboratory in New York: A painted blue diamond. *Gems & Gemology*, Vol. 15, No. 4, pp. 124–125.
- (1992) Gem Trade Lab Notes: More on damage to fracture-filled diamonds in cutting and cleaning. *Gems & Gemology*, Vol. 28, No. 3, p. 193.
- (1993) Gem Trade Lab Notes: Laser-assisted filling in diamond. *Gems & Gemology*, Vol. 29, No. 1, pp. 48–49.
- Crowningshield G.R., Moses T.M. (1998) Diamond colored by pink coating. *Gems & Gemology*, Vol. 43, No. 2, pp. 128–129.
- CVD Diamond Corp. (2007) Machining carbon fiber, machining fiberglass, and machining G10. www.cvddiamond.com/Applications.shtml [date accessed: 8/23/07].
- D'Albe E.E.F. (1923) *The Life of Sir William Crookes*. T. Fisher Unwin, London.
- De Weerd F., Van Royen J. (2000) Investigation of seven diamonds, HPHT treated by NovaDiamond. *Journal of Gemmology*, Vol. 27, No. 4, pp. 201–208.
- The Deepdene Diamond* (1997) Magnificent Jewels auction catalog, November 20, Christie's, Geneva.
- Deljanin B., Semenets E., Woodring S., DelRe N., Simic D. (2003) HPHT-processed diamonds from Korea. *Gems & Gemology*, Vol. 39, No. 3, pp. 240–241.
- DeVries R.C. (1975) Plastic deformation and “work hardening” of diamond. *Materials Research Bulletin*, Vol. 10, No. 11, pp. 1193–1199.
- Dollar A.T.J. (1933) Radium and the colour of diamonds. *The Gemmologist*, Vol. 2, No. 19, pp. 213–217.
- Dugdale R.A. (1953) The colouring of diamonds by neutron and electron bombardment. *British Journal of Applied Physics*, Vol. 4, No. 11, pp. 334–337.
- Dumbaugh W.H. (1986) Heavy metal oxide glasses containing Bi₂O₃. *Physics and Chemistry of Glasses*, Vol. 27, No. 3, pp. 119–123.
- Dyer H.B. (1957) Artificial coloration of diamond. *The Gemmologist*, Vol. 26, No. 316, pp. 193–199.
- Egyes G. (1973) See definite advantages to laser-treated stones. *National Jeweler*, Vol. 68, No. 10, pp. 1, 41.
- Ehrmann M.L. (1950) Bombarded diamonds. *Gems & Gemology*, Vol. 6, No. 10, pp. 295–297, 318.
- Epelboym M., Zaitsev A., Simic D., Deljanin D. (2006) Preliminary study on new generation of coated diamonds with limited color stability. EGL USA Group of Laboratories, November 14, www.eglcanada.ca/media/Summary_of_observation_on_COATED_DIAMONDS.pdf.
- Evans D.J., Fisher D., Kelly C.J. (2005) Coated pink diamond—A cautionary tale. *Gems & Gemology*, Vol. 41, No. 1, pp. 36–41.
- Evans T., Allen B.P. (1983) *Diamond Treatment*. U.S. patent 4,399,364, issued August 16, 1983.
- Evans T., Rainey P. (1975) Changes in the defect structure of diamond due to high temperature + high pressure treatment. *Proceedings of the Royal Society A: Mathematical and Physical Sciences*, Vol. 344, No. 1636, pp. 111–130.
- Even-Zohar C. (1994) An interview with Kenneth Scarratt: Making diamonds whiter. *Mazzal U'Bracha*, Vol. 10, No. 58, pp. 50–58.
- Everhart J. (1987a) Industry warned of new treatments used on diamonds. *National Jeweler*, Vol. 82, No. 17, pp. 98, 114.
- (1987b) Diamond dealers balk at disclosure of new treatment. *National Jeweler*, Vol. 33, No. 2, pp. 1, 86.
- (1989) Diamond treatment that removes flaws hits U.S. market. *National Jeweler*, Vol. 31, No. 17, pp. 1, 33.
- Fisher D., Spits R.A. (2000) Spectroscopic evidence of GE POL HPHT-treated natural type IIa diamonds. *Gems & Gemology*, Vol. 36, No. 1, pp. 42–49.

- Fisher D., Evans D.J.F., Glover C., Kelly C.J., Sheehy M.J., Summerton G.C. (2006) The vacancy as a probe of the strain in type IIa diamonds. *Diamond and Related Materials*, Vol. 15, No. 10, pp. 1636–1642.
- Fritsch E. (1998) The nature of color in diamond. In G. E. Harlow, Ed., *The Nature of Diamonds*, Cambridge University Press, Cambridge, UK, pp. 23–47.
- Fritsch E., Phelps A.W. (1993) Type IIb diamond thin films deposited onto near-colorless natural gem diamonds. *Diamond and Related Materials*, Vol. 2, No. 2/5, pp. 70–74.
- Fritsch E., Shigley J.E. (1989) Contribution to the identification of treated colored diamonds with peculiar color-zoned pavilions. *Gems & Gemology*, Vol. 25, No. 2, pp. 95–101.
- Fritsch E., Shigley J.E., Stockton C.M., Koivula J.I. (1988) Detection of treatment in two unusual green diamonds. *Gems & Gemology*, Vol. 24, No. 3, pp. 165–168.
- Fryer C. (1983) Gem Trade Lab Notes: Painted pink diamond—the big switch. *Gems & Gemology*, Vol. 19, No. 2, pp. 112–113.
- Gelb T. (2005) Irradiated and fracture-filled diamond. *Gems & Gemology*, Vol. 41, No. 1, p. 46.
- Gelb T., Hall M. (2002) Altered vs. natural inclusions in fancy-color diamonds. *Gems & Gemology*, Vol. 38, No. 2, pp. 252–253.
- Gelb T., Hall M. (2005) Diamond, fracture filled, with varying results. *Gems & Gemology*, Vol. 41, No. 2, pp. 164–165.
- Gemmology for beginners (1940) *The Gemmologist*. Vol. 10, No. 110, pp. 18–22.
- Gemological glossary (1934) *Gems & Gemology*, Vol. 1, No. 6, pp. 167–168.
- Gill J.O. (1978) A study of colored diamonds, part 2. *Jewelers' Circular-Keystone*, Vol. 149, No. 7, pp. 131–132.
- Gübelin E.J. (1950) New process of artificially beautifying gemstones. *Gems & Gemology*, Vol. 6, No. 8, pp. 243–254.
- Hainschwang T., Katrusha A., Vollstaedt H. (2003) HPHT treatment of different classes of type I brown diamonds. *Journal of Gemmology*, Vol. 28, No. 5/6, pp. 261–273.
- Hall M., Moses T.M. (2000) Lab Notes: Blue and pink HPHT-annealed diamonds. *Gems & Gemology*, Vol. 36, No. 3, pp. 254–255.
- Hall M., Moses T.M. (2001) Lab Notes: Update on blue and pink HPHT-annealed diamonds. *Gems & Gemology*, Vol. 37, No. 3, pp. 215–216.
- Hänni H.A. (1992) Identification of fissure-treated gemstones. *Journal of Gemmology*, Vol. 23, No. 4, pp. 201–205.
- Hänni H.A. (2001) Gemmologische Kurzinformationen: Eine neue Lichtquelle von kurzwelligem UV-Licht für den SSEF IIa Diamond Spotter™ zum Nachweis des Diamanttyps IIa [Gemological Briefs: A new source of short-wave UV light for the SSEF IIa Diamond Spotter™ for the detection of type IIa diamond]. *Gemmologie: Zeitschrift der Deutschen Gemmologischen Gesellschaft*, Vol. 50, No. 1, pp. 57–58.
- Hardy J.A. (1949) Report on a radioactive diamond. *Gems & Gemology*, Vol. 6, No. 6, pp. 167–170.
- Henn E., Bank H. (1992) Gemmologische Kurzinformationen: Radioaktive, künstliche bestrahlte schwarze Diamanten [Gemological Briefs: Radioactive, artificially treated black diamonds]. *Zeitschrift der Deutschen Gemmologischen Gesellschaft*, Vol. 41, No. 2/3, p. 63.
- Henn U., Milisenda C.C. (1999) Gemmologische Kurzinformationen: Ein neuen Typ farbbehandelter Diamanten [Gemological Briefs: A new type of color-treated diamond]. *Gemmologie: Zeitschrift der Deutschen Gemmologischen Gesellschaft*, Vol. 48, No. 1, pp. 43–45.
- Hill J. (1774) *Theophrastus's History of Stones. With an English Version, and Notes, Including the Modern History of the Gems Described by the Author, and of Many Other of the Native Fossils*, 2nd ed. Published by the author, London.
- Horikawa Y. (2001) Identification of a new type of laser treatment (KM treatment) of diamonds. *Journal of Gemmology*, Vol. 27, No. 5, pp. 259–263.
- Improved gem brilliancy by special coatings claimed (1949) *The Gemmologist*, Vol. 18, No. 212, pp. 73–76.
- Jewelry industry in motion with 39 new rules (1957) *Jewelers' Circular-Keystone*, Vol. 127, No. 11, pp. 114–123.
- Kammerling R.C., Kane R.E., Koivula J.I., McClure S.F. (1990) An investigation of a suite of black diamond jewelry. *Gems & Gemology*, Vol. 26, No. 4, pp. 282–287.
- Kammerling R.C., McClure S.F., Johnson M.L., Koivula J.I., Moses T.M., Fritsch E., Shigley J.E. (1994) An update on filled diamonds: Identification and durability. *Gems & Gemology*, Vol. 30, No. 3, pp. 142–177.
- Kane R.E., McClure S.F., Menzhausen J. (1990) The legendary Dresden green diamond. *Gems & Gemology*, Vol. 26, No. 4, pp. 248–266.
- King J.M., Shigley J.E. (2003) An important exhibition of seven rare gem diamonds. *Gems & Gemology*, Vol. 39, No. 2, pp. 136–143.
- Kirchhoff G.R., Bunsen R. (1860) Chemical analysis by observation of spectra. *Philosophical Magazine*, Vol. 20, p. 89.
- Koivula J.I. (1987) Gem News: "Filled diamonds." *Gems & Gemology*, Vol. 23, No. 3, pp. 172–173.
- Koivula J.I., Kammerling R.C., Eds. (1991) Gem News: Bluish gray synthetic diamond thin films grown on faceted diamonds. *Gems & Gemology*, Vol. 27, No. 2, pp. 118–119.
- Koivula J.I., Kammerling R.C., Fritsch E., Fryer C.W., Hargett D., Kane R.E. (1989) The characteristics and identification of filled diamonds. *Gems & Gemology*, Vol. 25, No. 2, pp. 68–83.
- Krishnan U.R.B., Kumar M.S. (2001) *Indian Jewellery: Dance of the Peacock*. India Book House, Mumbai.
- Lasering and the ethics issue (1980) *Jewelers' Circular-Keystone*, Vol. 151, No. 9, p. 105.
- Lawrence E.O. (1934) *Method and Apparatus for the Acceleration of Ions*. U.S. Patent 1,948,384, issued Feb. 20.
- Leadbeater P.W. (1972) Does laser treatment improve a diamond? *Australian Gemmologist*, Vol. 11, No. 8, pp. 27–28.
- Lenzen G. (1973) Ein lasergebohrter Diamant-Brilliant [A laser-drilled diamond]. *Zeitschrift der Deutschen Gemmologischen Gesellschaft*. Vol. 22, No. 1, pp. 39–41.
- Lenzen G. (1974) Before and after: An illustrated documentation on laser-drilling of diamond. *Journal of Gemmology*, Vol. 14, No. 2, pp. 69–72.
- Liddicoat R.T. Jr. (1955) Diamond selling practices. *Gems & Gemology*, Vol. 8, No. 6, pp. 165–171.
- Lind S.C., Bardwell D.C. (1923a) The coloring and thermophosphorescence produced in transparent minerals and gems by radium radiation. *American Mineralogist*, Vol. 8, pp. 171–180.
- Lind S.C., Bardwell D.C. (1923b) The coloring of the diamond by radium radiation. *American Mineralogist*, Vol. 8, pp. 201–209.
- Macleod A. (1999) The early days of optical coatings. *Journal of Optics A*, Vol. 1, Supplement, pp. 779–783.
- Martineau P.M., Lawson S.C., Taylor A.J., Quinn S.J., Evans D.J., Crowder M.J. (2004) Identification of synthetic diamond grown using chemical vapor deposition (CVD). *Gems & Gemology*, Vol. 40, No. 1, pp. 2–25.
- McClure S.F., Kammerling R.C. (1995) A visual guide to the identification of filled diamonds. *Gems & Gemology*, Vol. 31, No. 2, pp. 114–119.
- McClure S.F., King J.M., Koivula J.I., Moses T.M. (2000) A new lasering technique for diamond. *Gems & Gemology*, Vol. 36, No. 2, pp. 138–146.
- Miles E.R. (1962) Diamond-coating techniques and methods of detection. *Gems & Gemology*, Vol. 10, No. 12, pp. 355–364, 383.
- Miles E.R. (1964) Coated diamonds. *Gems & Gemology*, Vol. 11, No. 6, pp. 163–168.
- Moses T., Reinitz J., Fritsch E., Shigley J.E. (1993) Two treated-color synthetic red diamonds seen in the trade. *Gems & Gemology*, Vol. 29, No. 3, pp. 182–190.
- Moses T.M., Shigley J.E., McClure S.F., Koivula J.I., Van Daele M. (1999) Observations on GE-processed diamonds: A photo-

- graphic record. *Gems & Gemology*, Vol. 35, No. 3, pp. 14–22.
- Moses T.M., Reinitz I.M., Koivula J.I., Buerki P.B., McClure S.F., Shigley J.E. (2000) Update on the new “Incolor” treated black and green diamonds. *The Loupe*, Vol. 9, No. 4, pp. 16–19.
- Moulton H.R., Tillyer E.D. (1949) *Reflection Modifying Coatings and Articles So Coated and Method of Making the Same*. U.S. Patent 2,466,119, Issued April 5.
- Nassau K. (1984) *Gemstone Enhancement*. Butterworths, London.
- Nassau K. (1994) *Gemstone Enhancement*, 2nd ed. Butterworth-Heinemann, New York.
- Nelson J.B. (1993) The glass filling of diamonds, Part 1: An explanation of the colour flashes. *Journal of Gemmology*, Vol. 23, No. 8, pp. 461–472.
- Nelson J.B. (1995) Scotch tape and a magic box. *Diamond International*, November/December, pp. 47–54.
- Newton R.G., Davison S. (1989) *Conservation of Glass*. Butterworth-Heinemann, London.
- Newton M.E. (2006) Treated diamond: A physicist’s perspective. *Gems & Gemology*, Vol. 42, No. 3, pp. 84–85.
- Nicols T. (1652) *A Lapidary, or, The History of Pretious Stones*. Thomas Buck, Cambridge, 239 pp.
- Nikitin A.V., Samoilovich M.I., Bezrukov G.N., Vorozheikin K.F. (1969) The effect of heat and pressure on certain physical properties of diamonds. *Soviet Physics Doklady*, Vol. 13, No. 9, pp. 842–844.
- Notari F. (2002) Traitement du diamant noir par graphitisation “interne” [Treatment of black diamond by internal graphitization]. *Revue de Gemmologie a.f.g.*, No. 145/146, pp. 42–60.
- Novikov N.V., Katrusha A.N., Ivakhnenko S.A., Zanevsky O.A. (2003) The effect of high-temperature treatment on the defect-and-impurity state and color of diamond single crystal (Review). *Journal of Superhard Materials*, Vol. 25, No. 6, pp. 1–12.
- Overton T.W. (2004) Gem treatment disclosure and U.S. law. *Gems & Gemology*, Vol. 40, No. 2, pp. 106–127.
- Pagel-Theisen V. (1976) On lasered diamonds. *Börsen Bulletin*, September.
- Parsons D.J. (1996) Gem enhancement by electron beam accelerators. Presentation at the 25th International Gemmological Conference, Rayong, Thailand. *JewelSiam*, December/January, pp. 72–78.
- Perret E. (2006) Color treatment of diamonds and their potential in designer jewelry. *Gems & Gemology*, Vol. 42, No. 3, pp. 159–160.
- Pough F.H. (1954) The present status of diamond coloration treatments. *Jewelers’ Circular Keystone*, Vol. 124, No. 8, pp. 76–77, 105–111, 113.
- (1957) The coloration of gemstones by electron bombardment. *Sonderheft zur Zeitschrift der Deutschen Gesellschaft für Edelsteinkunde*, pp. 71–78.
- (1980) Letter to Dr. Alan T. Collins, Jan. 28. Unpublished material on file with authors.
- (1988) More or less: Altering the color of diamonds. *Lapidary Journal*, Vol. 41, No. 2, pp. 28–34.
- (2004) Interview with Dona M. Dirlam. Videorecording, April 5, GIA oral history project, Richard T. Liddicoat Library and Information Center, Carlsbad, CA.
- Pough F.H., Schulke A.A. (1951) The recognition of surface irradiated diamonds. *Gems & Gemology*, Vol. 7, No. 1, pp. 3–11.
- Qiu Z., Wu M., Wei Q. (2006) Study on the wax enhancement for the unearthened jade wares by FTIR technique from ancient tombs of Shang-Zhou period in Henglingshan site of Boluo County, Guangdong Province. *Spectroscopy and Spectral Analysis*, Vol. 26, No. 6, pp. 1042–1045.
- Quorum Technologies (2002) Sputter coating technical brief. Document number TB-Sputter, Issue 1, www.quorumtech.com/Manuals/Current_Technical_Briefs/TB-SPUTTER.pdf.
- Rapaport M. (1987) Diamond treatment—buyers beware. *Rapaport Diamond Report*, Vol. 10, No. 32 (Sept. 4), p. 8.
- Rapaport M. (1999) *Rapaport News Flash*, March 19, pp. 1–6.
- Reinitz I., Ashbaugh C.E. (1993) Lab Notes: Treated green diamond. *Gems & Gemology*, Vol. 29, No. 2, pp. 124–125.
- Reinitz I., Moses T.M. (1997) Lab Notes: Treated-color yellow diamonds with green graining. *Gems & Gemology*, Vol. 33, No. 2, p. 136.
- Reinitz I., Buerki P.R., Shigley J.E., McClure S.F., Moses T.M. (2000) Identification of HPHT-treated yellow to green diamonds. *Gems & Gemology*, Vol. 36, No. 2, pp. 128–137.
- Robinson P.C., Bradbury S. (1992) *Qualitative Polarized-Light Microscopy*. Oxford University Press, Oxford, UK, pp. 94–108.
- Sato K., Sasaki E. (1981) Application of interference contrast microscopy to identify coated diamonds. *Journal of the Gemmological Society of Japan*, Vol. 8, No. 1/4, pp. 139–144.
- Scarratt K. (1982) The identification of artificial coloration in diamond. *Gems & Gemology*, Vol. 18, No. 2, pp. 72–78.
- Scarratt K.V.G. (1992) The clarity enhancement of diamonds. *Diamond International*, No. 19, pp. 45–58.
- Schiffmann C.A. (1969) Coloured diamond—Natural or artificially treated? *Journal of Gemmology*, Vol. 11, No. 7, pp. 233–255.
- Schlossmacher K. (1959) Brillanten mit Farbverbesserungsüberzug [Diamond with color-improving coating]. *Zeitschrift der Deutschen Gesellschaft für Edelsteinkunde*, Vol. 26, pp. 22–23.
- Schlüssel R. (1992) L’identification au microscope des diamants aux cavités artificiellement colmatées à l’aide d’une substance vitreuse [Microscopic identification of diamonds with cavities artificially filled using a vitreous substance]. *Revue de Gemmologie a.f.g.*, No. 111, pp. 15–17.
- Schmetzer K. (1999a) Behandlung natürlicher Diamanten zur Reduzierung der Gelb- oder Braunsättigung [Treatment of natural diamonds for the reduction of yellow or brown coloration]. *Goldschmiede Zeitung*, Vol. 97, No. 5, pp. 47–48.
- (1999b) Clues to the process used by General Electric to enhance the GE POL diamonds. *Gems & Gemology*, Vol. 35, No. 4, pp. 186–190.
- (2004) Letters: Patents on treatment processes for certain colored synthetic diamonds. *Gems & Gemology*, Vol. 40, No. 4, pp. 286–287.
- Schulke A.A. (1961) The artificial coloration of diamond. *Gems & Gemology*, Vol. 10, No. 8, pp. 227–241.
- Sechos B. (1994) Fracture filled diamonds. *Australian Gemmologist*, Vol. 18, No. 12, pp. 379–385.
- Sechos B. (1995) Fracture filled Cognac™ diamond. *Australian Gemmologist*, Vol. 19, No. 2, p. 64.
- Sheby J. (2003) Gem Trade Lab Notes: Coated diamonds. *Gems & Gemology*, Vol. 39, No. 4, pp. 315–316.
- Shen A.H., Wang W., Hall M.S., Novak S., McClure S.F., Shigley J.E., Moses T.M. (2007) Serenity coated colored diamonds: Detection and durability. *Gems & Gemology*, Vol. 43, No. 1, pp. 16–34.
- Shigley J.E., Ed. (2008) *Gems & Gemology in Review: Treated Diamonds*. Gemological Institute of America, Carlsbad, CA.
- Shigley J.E., Fritsch E., Koivula J.I., Sobolev N.V., Malinovsky I.Y., Palyanov Y.N. (1993) The gemological properties of Russian gem-quality synthetic yellow diamonds. *Gems & Gemology*, Vol. 29, No. 4, pp. 228–248.
- Shigley J.E., McClure S.F., Koivula J.I., Moses T.M. (2000) New filling material for diamonds from Oved Diamond Company: A preliminary study. *Gems & Gemology*, Vol. 36, No. 2, pp. 147–153.
- Shigley J.E., McClure S.F., Breeding C.M., Shen A.H.-T., Muhlmeister S.M. (2004) Lab-grown colored diamonds from Chatham Created Gems. *Gems & Gemology*, Vol. 40, No. 2, pp. 128–145.
- Shor R. (1989) Filled diamonds worry dealers. *Jewelers’ Circular-Keystone*, Vol. 159, No. 2, pp. 394–395.
- Shor R. (2005) A review of the political and economic forces shaping today’s diamond industry. *Gems & Gemology*, Vol. 41, No. 3, pp. 202–233.

- Shuster W.G. (2003) *Legacy of Leadership: A History of the Gemological Institute of America*. Gemological Institute of America, Carlsbad, CA, 451 pp.
- Smith C.P., Bosshart G., Ponahlo J., Hammer V.M.F., Klapper H., Schmetzer K. (2000) GE POL diamonds: Before and after. *Gems & Gemology*, Vol. 36, No. 3, pp. 192–215.
- Strong H.M., Chrenko R.M., Tuft R.E. (1978) *Annealing Type Ib or Mixed Type Ia Natural Diamond Crystal*. U.S. patent 4,124,690, issued November 7, 1978.
- Strong H.M., Chrenko R.M., Tuft R.E. (1979) *Annealing Synthetic Diamond Type Ib*. U.S. patent 4,174,380, issued November 13, 1979.
- Tillander H. (1995) *Diamond Cuts in Historic Jewelry*. Art Books Intl., London.
- Titkov S.V., Zudin N.G., Gorshkov A.I., Sivtsov A.V., Magazina L.O. (2003) An investigation into the cause of color in natural black diamonds from Siberia. *Gems & Gemology*, Vol. 39, No. 3, pp. 200–209.
- Vagarali S.S., Webb S.W., Jackson W.E., Banholzer W.F., Anthony T.R. (2001) *High Pressure/High Temperature Production of Colorless and Fancy-Colored Diamonds*. U.S. patent application 20010031237, filed September 28, 1998; published October 18.
- Vagarali S.S., Webb S.W., Jackson W.E., Banholzer W.F., Anthony T.R., Kaplan G.R. (2004) *High Pressure/High Temperature Production of Colorless and Fancy-Colored Diamonds*. U.S. patent 6,692,714, issued February 17.
- Van Bockstael M. (1998) Enhancing low quality coloured diamonds. *Jewellery News Asia*, No. 169, pp. 320, 322.
- Van Royen J., De Weerd F., De Gryse O. (2006) HPHT treatment of type IaB brown diamonds. *Gems & Gemology*, Vol. 42, No. 3, pp. 159–160.
- Vins V.G. (2002) Change of color produced in natural brown diamonds by HPHT-processing. *Proceedings of the Russian Mineralogical Society*, Vol. 131, No. 4, pp. 111–117.
- Walker J. (1979) Optical absorption and luminescence in diamond. *Reports on Progress in Physics*, Vol. 42, No. 10, pp. 1605–1659.
- Wang W., Moses T.M. (2004) Lab Notes: Commercial production of HPHT-treated diamonds showing a color shift. *Gems & Gemology*, Vol. 40, No. 1, pp. 74–75.
- Wang W., Moses T., Linares R., Shigley J.E., Hall M., Butler J.E. (2003) Gem-quality synthetic diamonds grown by the chemical vapor deposition method. *Gems & Gemology*, Vol. 39, No. 4, pp. 268–283.
- Wang W., Smith C.P., Hall M.S., Breeding C.M., Moses T.M. (2005a) Treated-color pink-to-red diamonds from Lucent Diamonds Inc. *Gems & Gemology*, Vol. 41, No. 1, pp. 6–19.
- Wang W., Tallaire A., Hall M.S., Moses T.M., Achard J., Sussmann R.S., Gicquel A. (2005b) Experimental CVD synthetic diamonds from LIMHP-CNRS, France. *Gems & Gemology*, Vol. 41, No. 3, pp. 234–244.
- Wang W., Moses T.M., Pearce C. (2005c) Diamond, orange, treated by multiple processes. *Gems & Gemology*, Vol. 41, No. 4, pp. 341–342.
- Wang W., Gelb T., Dillon S. (2006) Lab Notes: Coated pink diamonds. *Gems & Gemology*, Vol. 42, No. 2, pp. 162–163.
- Wang W., Hall M.S., Moe K.S., Tower J., Moses T.M. (2007) Latest-generation CVD-grown synthetic diamonds from Apollo Diamond Inc. *Gems & Gemology*, Vol. 43, No. 4, pp. 294–312.
- Ward A. (1972) Pique diamonds, treated by lasers, on the increase in world markets. *Jewelers' Circular-Keystone*, Vol. 143, No. 3, pp. 98–100.
- Webster R. (1965) Radio-active diamonds. *Journal of Gemology*, Vol. 9, No. 10, pp. 352–353.
- Welbourn C.M., Cooper M., Spear P.M. (1996) De Beers natural versus synthetic diamond verification instruments. *Gems & Gemology*, Vol. 32, No. 3, pp. 156–169.
- Wilks E., Wilks J. (1991) *Properties and Applications of Diamond*. Butterworth-Heinemann, Oxford, pp. 81–82.
- Woods G.S., Collins A.T. (1986) New developments in spectroscopic methods for detecting artificially colored diamonds. *Journal of Gemology*, Vol. 20, No. 2, pp. 75–82.
- Yeung S.F., Gelb T. (2003) Diamond with fracture filling to alter color. *Gems & Gemology*, Vol. 39, No. 1, pp. 38–39.
- Yeung S.F., Gelb T. (2004) Diamond, fracture filled, to alter color and enhance clarity. *Gems & Gemology*, Vol. 40, No. 2, p. 163.

SPECIAL OFFER! Buy any 12 back issues, and receive a **FREE 25 Year Index!**



Twenty-Five Years at Your Fingertips

Twenty-five years of GEMS & GEMOLOGY means a lot of valuable research. Fortunately, we've got it all—articles, lab notes, gem news, editorials, and book reviews—indexed in this one handy volume. It's an invaluable tool for the serious gemologist, for the far-from-invaluable price of just \$14.95. (\$19.95 internationally) **FREE shipping!**

Order Yours Today!

To order, visit www.gia.edu/gemsandgemology and click on *Ordering and Renewals*. Call 800-421-7250 ext. 7142 within the U.S., or 760-603-4000 ext. 7142.

NATURAL-COLOR PURPLE DIAMONDS FROM SIBERIA

Sergey V. Titkov, James E. Shigley, Christopher M. Breeding, Rimma M. Mineeva, Nikolay G. Zudin, and Aleksandr M. Sergeev

Twelve natural-color purple diamond crystals from Siberia, and seven round brilliants that were faceted from some of these crystals, were studied using spectroscopic methods to better understand their color and its causes. Aspects of their color and the various structural defects in these purple diamonds are due to their post-growth plastic deformation in the earth. All the samples exhibited prominent parallel planar lamellae along which the purple color was concentrated.

Predominantly purple diamonds are quite rare, and few have been documented in the literature. While their color is thought to be due to plastic deformation, the exact nature of the defects responsible for purple coloration is not yet fully understood. With the availability of treated-color purple-to-red diamonds in the marketplace (e.g., Wang et al., 2005), it is important for gemologists to be able to properly identify natural-color purple diamonds, despite their rarity.

Natural-color purple diamonds are usually described with various hue modifiers such as pink, gray, and brown (Hofer, 1998). In the few published gemological reports on purple diamonds, their geographic origin is usually not mentioned (see, e.g.,

Liddicoat, 1977; Hargett, 1990; Hofer, 1998; Moses et al., 2002). However, one recurring source is Russia's Siberia region (see Federman, 1995). Purple diamonds are occasionally found in all the Siberian deposits explored to date, but they are most often recovered from the pipes of the Mir kimberlite field (comprising the Dachnaya, Internatsional'naya (also spelled Internationalaya), Mir, and Sputnik mines). In those mines, they typically account for 1% of all diamonds from the deposits, although as much as 6% of some parcels have been described as purple (Gnevushev et al., 1961; Orlov, 1977; Zintchouk and Koptil', 2003). The majority of purple diamonds from the Siberian deposits are pale, but crystals with more highly saturated purple colors are sometimes found.

To study the cause of color in diamonds with a dominant purple hue, we first characterized 12 purple crystals from Siberia using various spectroscopic methods. The results of earlier electron paramagnetic resonance (EPR) studies of structural deformation defects in these same purple diamonds were reported by Mineeva et al. (2007). That article showed that purple diamonds contain thin mechanical microtwins, which are parallel to octahedral planes and were previously interpreted as slip planes. Optical dichroism was also observed in these purple diamond crystals; this phenomenon is unusual for crystals with cubic symmetry and was investigated using a special spectroscopic technique (Konstantinova et al., 2006). The present article reports the gemological characteristics of faceted purple diamonds and the results of ultraviolet-visible-near infrared (UV-Vis-NIR), Fourier-transform infrared (FTIR), and photoluminescence (PL) spectroscopy on a number of rough and/or faceted samples. For convenience, the diamonds examined

See end of article for About the Authors and Acknowledgments.
GEMS & GEMOLOGY, Vol. 44, No. 1, pp. 56–64.
© 2008 Gemological Institute of America



Figure 1. This group of purplish pink to gray-purple diamonds (0.28–0.85 ct) is representative of similarly colored material recovered from mines in the Mir kimberlite field in Siberia. These particular samples, which were studied for the present report, came from the Internatsional'naya pipe. Photo by C. D. Mengason.

here are usually referred to simply as “purple” diamonds, although the GIA color descriptions of the faceted samples include modifying colors.

BACKGROUND

Over the past 50 years, extensive research has characterized the color centers in natural diamonds (see, e.g., Fritsch, 1998; Collins, 2001). However, the origin of purple coloration has not yet been fully established. The spectra of purple diamonds exhibit a broad absorption band centered at 550 nm (Collins, 1982; Moses et al., 2002), but the cause of this band remains unclear. The band is also observed in the spectra of other fancy-color diamonds, such as red (Shigley and Fritsch, 1993), pink, and pink-brown (King et al., 2002). However, in pink-to-red diamonds, the 550 nm band is typically accompanied by an intense 390 nm band and a strong N3 system (zero-phonon line [ZPL] at 415 nm). The absorption spectra of red diamonds also contain the H3 system, with its ZPL at 503.2 nm (Shigley and Fritsch, 1993). In pink-brown diamonds, the 550 nm band is superimposed on an absorption spectrum that continuously increases in intensity from the red to the blue region of the visible spectrum, which causes the brown coloration. Faceted purple diamonds without a modifying color typically do not show these other features (Moses et al., 2002).

Although several theories about the origin of the purple coloration have been proposed (e.g., Raal, 1958; Gnevushev et al., 1961; Taran et al., 2004), Orlov (1977) showed that purple (as well as pink, in most cases) in natural diamonds is restricted to a set of parallel octahedral planes, which were referred to as slip planes. These “planes” appear to be a result of

natural post-growth plastic deformation of the diamonds, which probably occurred during their transportation from the mantle to the earth's surface by kimberlite magma.

MATERIALS AND METHODS

Twelve natural diamond crystals with a dominant purple color were selected for study by rough-diamond graders of Alrosa (Russia's largest diamond mining and processing company), according to the De Beers color classification system for rough diamonds. These crystals (0.4–1.4 ct) were recovered from the Internatsional'naya kimberlite pipe. Plates of 1.6 mm thickness were cut from two crystals so that the colored lamellae were perpendicular to a cutting plane. All rough crystals and the plates were examined with a binocular microscope using daylight-equivalent illumination. Following spectroscopic analysis (Konstantinova et al., 2006; Mineeva et al., 2007), 10 of the crystals were faceted as round brilliants.

Gemological examination of seven of the round brilliants (figure 1) was conducted at GIA. Experienced graders determined color grades using the standard conditions and methodology of GIA's color grading system for colored diamonds (King et al., 1994). Internal features were observed with a gemological microscope using brightfield and darkfield lighting techniques. Reactions to UV radiation were checked with a conventional four-watt combination long-wave (365 nm) and short-wave (254 nm) lamp. The seven diamonds were also examined with a DiamondView deep-UV (<230 nm) luminescence imaging system. A desk-model spectroscope was

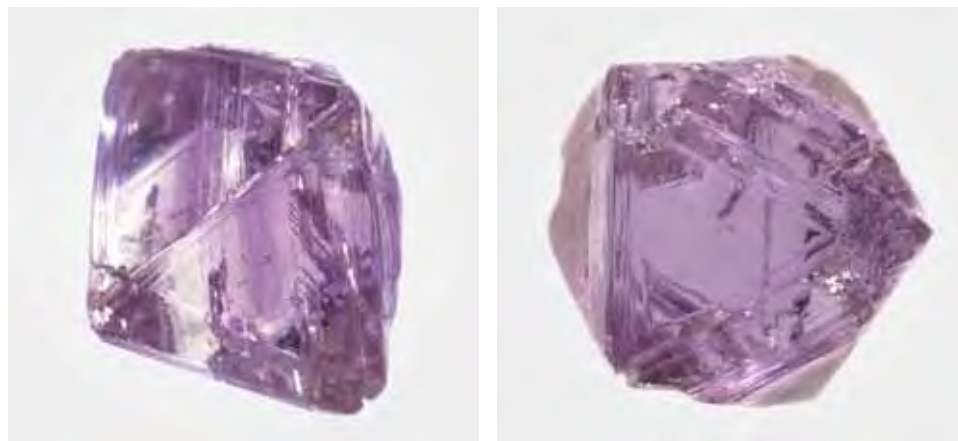


Figure 2. The purple diamond crystals studied exhibited strong parallel color banding, so that in one orientation (left) the color was unevenly distributed, while in the other (right) it appeared much more uniform. Photos by M. A. Bogomolov.

used to view absorption features at room temperature in the visible range.

Infrared spectra of the seven faceted stones were obtained at room temperature at GIA with a Thermo-Nicolet Nexus 670 FTIR spectrometer equipped with KBr and quartz beam splitters. Spectra were collected in the mid-infrared (6000–400 cm^{-1} ; 1 cm^{-1} resolution) and near-infrared (11000–4000 cm^{-1} ; 4 cm^{-1} resolution) ranges. A 6 \times beam condenser was used to focus the beam through the girdle region of the samples, and a total of 1,024 scans per sample were collected to improve signal-to-noise ratios.

Low-temperature photoluminescence spectra of the seven faceted samples were also collected at GIA, using a Renishaw 1000 Raman microspectrometer with an Ar-ion laser at two different laser excitations (488.0 and 514.5 nm). The samples were cooled by direct immersion in liquid nitrogen.

UV-Vis-NIR absorption spectroscopy of the 12 crystals was performed in Russia. Spectra were recorded over the 300–800 nm range with a Perkin Elmer two-beam Lambda 9 spectrometer at liquid

nitrogen (77 K) temperatures using a fabricated cryostat mounted in the spectrometer. The spectral resolution was ~ 0.2 nm.

RESULTS

Visual Observations of the Crystals and Polished Plates. The 12 crystals were purple, with pink, gray, and brown modifiers, and had weak-to-moderate saturation. All displayed an octahedral habit; most also showed thin, rough parallel straight striations with subordinate development of shield-like striations. This indicated that they experienced only minor post-growth dissolution (Orlov, 1977). They also exhibited varying degrees of fracturing or cleavage.

For crystals with native flat faces, we readily observed that the purple coloration was restricted to thin bands parallel to octahedral planes (figure 2, left); between these planes, the diamonds were nearly colorless, with a very light yellowish or pinkish brown hue. When the crystals were examined in a direction perpendicular to these planes, the purple color

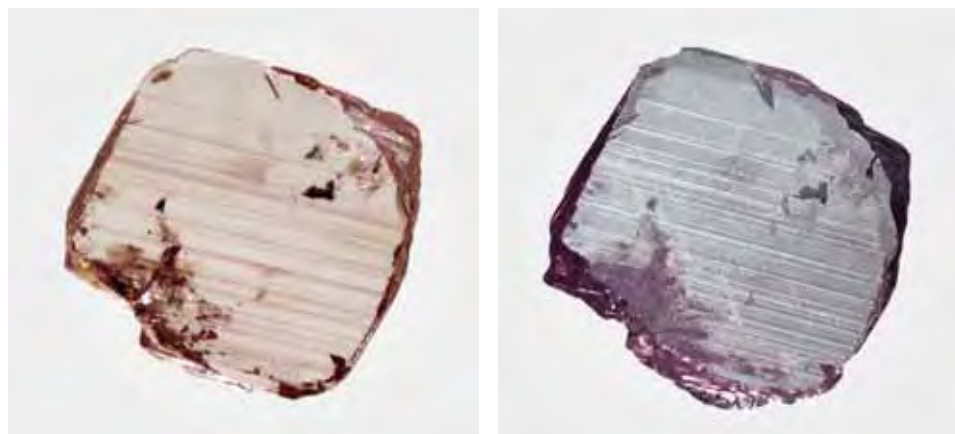


Figure 3. This flat plate (4 \times 4 \times 1.6 mm) cut from one of the diamond crystals shows purple coloration concentrated along thin parallel lamellae (transmitted light, left). When viewed with reflected light (right), the purple lamellae appear as mirror-like reflective sheets. Photos by M. A. Bogomolov.

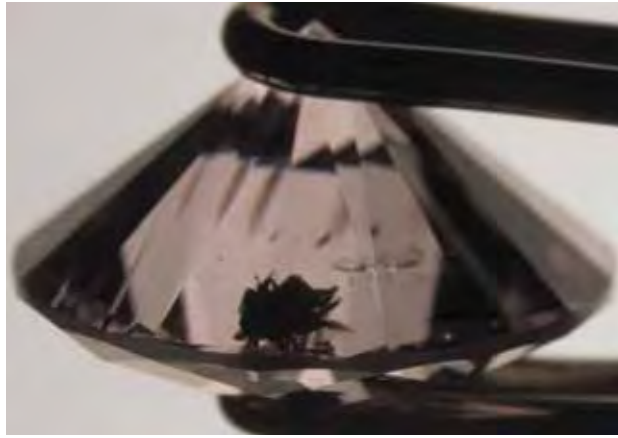


Figure 4. This 0.85 ct Fancy Light gray-purple round brilliant exhibits a dark inclusion of unknown identity. The presence of this inclusion resulted in an I_2 clarity grade. Photomicrograph by J. E. Shigley; magnified 5 \times .



Figure 5. Intersecting sets of purple and brown lamellae can be seen in this 0.43 ct Fancy brownish purple-pink diamond. Photomicrograph by J. E. Shigley; magnified 5 \times .

appeared evenly distributed (figure 2, right). Ten of the 12 crystals contained dark opaque inclusions of undetermined identity.

Study of the flat plates in transmitted light revealed that the purple planes were actually thin lamellae (~0.1 mm in thickness and about 0.1–0.5 mm apart). Typically, these were unevenly distributed throughout the volume of the crystal (figure 3). At crystal surfaces, the colored lamellae were truncated by chains of trigons, a feature that has been reported previously (e.g., Orlov, 1977).

Gemological Examination of the Faceted Samples.

The seven polished diamonds were color graded as follows: one Fancy Light gray-purple, three Fancy pink-purple, one Fancy purple-pink, one Fancy brownish purple-pink, and one Fancy Light purplish pink (again, see figure 1). The difference between the color classifi-

cation of the rough crystals (as predominantly purple) and the color grades of the diamonds faceted from them (three of which were predominantly pink) may be due to some disagreement between the two grading systems in the pink-to-purple continuum. Additionally, the cutting process may play an important role. Not only have significant hue changes from the original rough to the faceted stone been reported in colored diamonds, but the orientation of the table in a color-zoned diamond is also key to its face-up appearance (King et al., 2002).

The clarity grades of the seven round brilliants all fell into the “I” (included) category due to the presence of cleavages and dark inclusions (e.g., figure 4; we did not identify the inclusions). Additionally, we saw clouds of fine particles in most of the samples. All of the diamonds displayed parallel lamellae that appeared purple or brownish purple (figures 5 and 6) and were

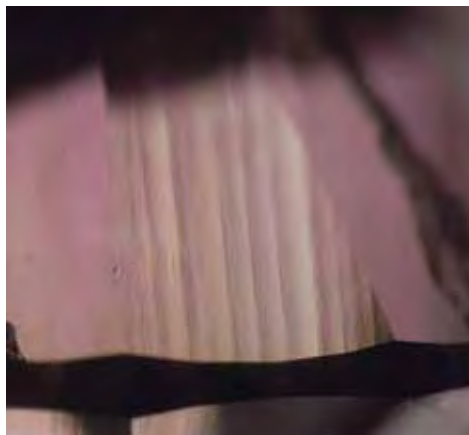


Figure 6. In this 0.53 ct Fancy purple-pink diamond, parallel planes of purple lamellae are separated by zones that are near-colorless to light brown. Photomicrographs by J. E. Shigley; magnified 5 \times (left) and 10 \times (right).



Figure 7. These Diamond-View images reveal the banded appearance of blue fluorescence in the faceted diamonds. In the 0.39 ct sample on the left, the complex sculptured shape of the banding is indicative of the diamond's growth history. The 0.85 ct diamond on the right shows weak green luminescence (due to the H3 defect) along traces that correspond to the purple lamellae. Photos by C. M. Breeding.

more evident in the strongly colored samples (in some instances, these colored lamellae were easily seen with the unaided eye or low magnification; again, see figures 5 and 6). When the diamonds were examined with fiber-optic illumination, green luminescence was commonly visible along the colored planes.

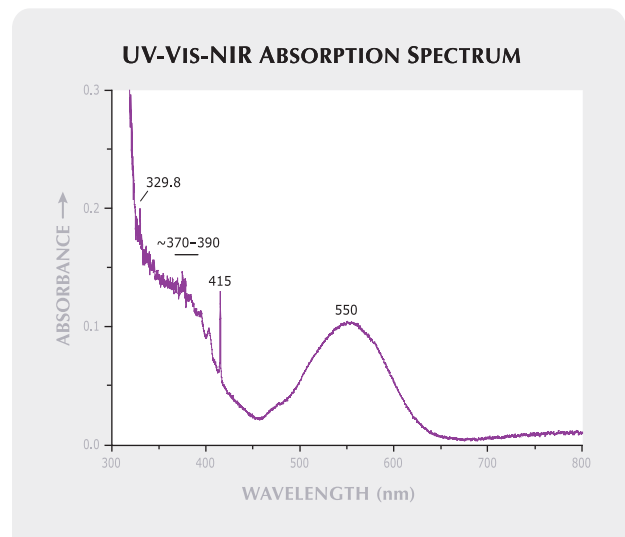
None of the diamonds displayed distinct absorption features when examined with a desk-model spectroscope. When observed in a darkened room, the diamonds fluoresced very weak to weak yellow or were inert to long-wave UV radiation, and fluoresced very weak to weak orangy yellow or were inert to short-wave UV. The DiamondView revealed bright blue luminescence patterns that depicted the complex growth structure of these diamonds (figure 7, left). In addition, H3-related green luminescence banding was seen following the purple lamellae (figure 7, right).

UV-Vis-NIR Absorption Spectroscopy. Figure 8 shows the absorption spectrum at 77 K for a crystal with polished octahedral faces that were parallel to the colored lamellae. The spectrum exhibited increasing absorption below 450 nm and a broad absorption band centered at about 550 nm, which contributes to the purple coloration. A broad band at 370–390 nm and the N3-related ZPL at 415 nm (with weak phonon sidebands at 383, 394, and 403 nm) were superimposed on the increasing absorption below 450 nm. With the exception of the most intensely colored crystal, the N3 center was observed in all the purple diamonds studied, but in very low intensities (sometimes near the detection limit of the spectrophotometer). The exact position of the maximum for the 370–390 nm band was difficult to determine because of overlapping absorption below 450 nm. We believe that it corresponds to a band at 390 nm observed in pink diamonds (Collins, 1982; King et al., 2002). On the background of the absorption

below 450 nm, a sharp ZPL was observed at 329.8 nm; this is due to the N5 center, an electronic transition of the A aggregate of nitrogen (Zaitsev, 2001).

The intensity of the 550 nm band changed noticeably over a series of spectra as the angle between the sample and the beam changed. This phenomenon may be due to the localization of purple coloration within the thin lamellae. For accurate studies of this unusual phenomenon, absorption spectra were recorded using polarized light (Konstantinova et al., 2006). That research found that these purple diamond crystals possessed dichroism (i.e., different absorption of polarized light depending on crystallographic direction), which

Figure 8. This UV-Vis-NIR absorption spectrum of a purple crystal exhibits increasing absorption below 450 nm, the N5 system (ZPL at 329.8 nm), a band at about 380 nm, the N3 system (ZPL at 415 nm), and a broad band centered at about 550 nm.



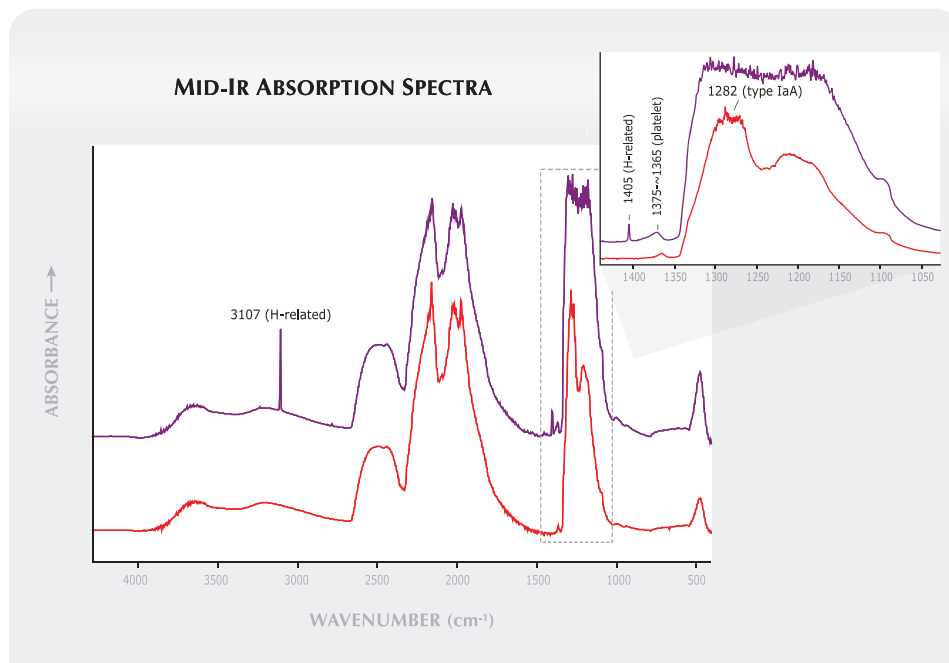


Figure 9. These mid-infrared spectra from two faceted samples (top, 0.53 ct Fancy purple-pink; bottom, 0.85 ct Fancy Light gray-purple) reveal spectral features that are characteristic of type IaA diamonds, which may include hydrogen-related defects (3107 cm^{-1}), platelet features (~1375–1365 cm^{-1}), B-aggregated nitrogen (1175 cm^{-1}), and the dominant A-aggregate of nitrogen (~1282 cm^{-1}). Spectra are offset for clarity.

may be caused by low-symmetry defects in the diamond structure formed during plastic deformation.

Infrared Spectroscopy. All the faceted diamonds proved to be type IaA. Figure 9 presents typical mid-infrared spectra for two of them. Absorption features in the one-phonon region (1400–1000 cm^{-1}) indicate the presence of structural defects involving nitrogen impurity atoms, such as A aggregates along with minor amounts of B aggregates and platelets (polyatomic segregations up to a few microns in size in cubic planes of the diamond lattice, which involve nitrogen and/or carbon atoms; Zaitsev, 2001). Single substitutional nitrogen (associated with type Ib diamond) was not detected in the IR spectra of any of these samples, although it was observed in very low concentrations (20–60 ppb) in the EPR spectra of all the diamond crystals (Mineeva et al., 2007).

Five of the diamonds showed the 4496, 3107, and 1405 cm^{-1} peaks that are associated with a hydrogen structural impurity (see Zaitsev, 2001). However, these peaks were not all present in the IR spectra of the other two samples (e.g., the bottom spectrum in figure 9). In addition, six of the seven faceted diamonds showed H1b and H2 defect centers, and a few showed amber centers in the near-infrared range (figure 10).

Photoluminescence Spectroscopy. The PL spectra revealed the presence of several defect centers (figure 11). The H3 center (503.2 nm) occurred in all the faceted samples (although it was not seen in the UV-

Vis-NIR spectra, likely due to its low concentration). Other centers, including those located at 612 nm (unknown origin), 693 and 700 nm (commonly attributed to nickel and/or hydrogen impurities), 787 nm (unknown origin, although possibly related to hydrogen), and 793 nm (related to nickel) were present in most of the diamonds (see Zaitsev, 2001).

DISCUSSION

The results of this gemological and spectroscopic study of natural-color purple diamonds, when considered with those of previous studies on the same samples (Konstantinova et al., 2006; Mineeva et al., 2007), provides a comprehensive characterization of their defect centers and their relation to the purple color.

Nitrogen-Related Defects. Most of the defects were formed during post-growth plastic deformation, which caused a transformation of some of the most abundant defects in the purple crystals—the A centers, which consist of two nitrogen atoms in nearest-neighbor structural sites. This transformation resulted in the formation of many new centers, such as H3, H2, H1b, amber centers, W7, and M2 defects (the latter two were revealed with EPR spectroscopy; Mineeva et al., 2007). Of the less-commonly described defects in the gemological literature, the W7 center represents a ring consisting of four carbon atoms and two nitrogen atoms on the opposite sites, with one of the nitrogen atoms in the ionized state

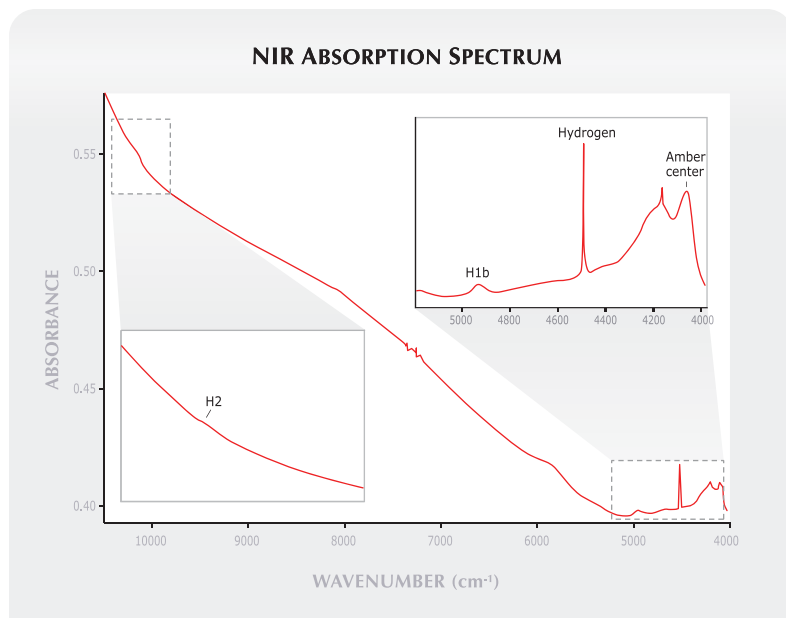


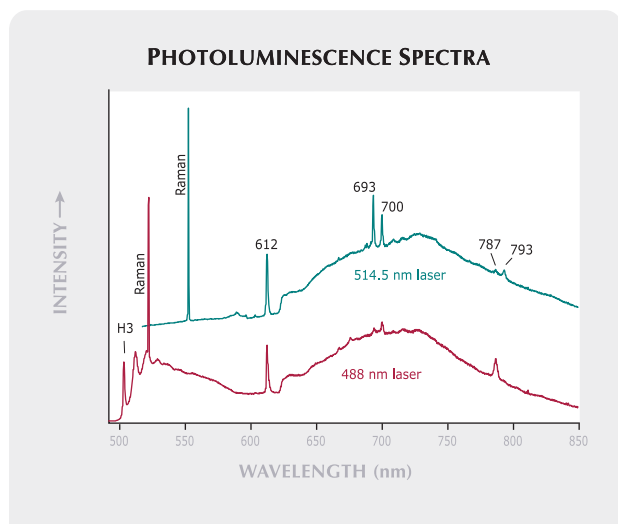
Figure 10. This near-infrared spectrum of a 0.53 ct Fancy purple-pink diamond reveals features due to H2 (~10130 cm^{-1}) and H1b (~4935 cm^{-1}) defects, as well as hydrogen impurities (4496 cm^{-1}) and the amber center (~4300–4000 cm^{-1}).

N^+ . The amber center is considered the optical analogue of the paramagnetic W7 center (Massi et al., 2005). The M2 center involves two nitrogen atoms and eight carbon atoms, which form an octahedron-like polyhedron with nitrogen atoms at opposite corners. Among these various deformation-related centers, the M2 is the most important from a gemological standpoint. This center is characteristic only for

diamonds with absorption spectra that exhibit the 550 nm band. Additionally, both the M2 center and the purple coloration were concentrated within the microtwin lamellae (Mineeva et al., 2007).

H1b, H2, and H3 centers may be produced in diamond by artificial irradiation and subsequent heating (Collins, 2001). The H3 center also has been seen in many natural plastically deformed brown diamonds (Collins, 1982), and it likely accounts for the green luminescence observed in our samples (again, see figure 7, right). However, only a few occurrences of the H2 center in natural plastically deformed diamonds have been reported (e.g., De Weerd and Van Royen, 2001). Natural plastic deformation in the earth may generate vacancies in the diamond structure, including the H1b, and this may be similar to the processes of laboratory irradiation and subsequent annealing (see, e.g., Collins, 2001).

Figure 11. The photoluminescence spectra of this 0.39 ct Fancy Light purplish pink diamond, recorded with 488 and 514.5 nm laser excitations, revealed features due to several defect centers at 503.2 (H3), 612, 693, 700, 787, and 793 nm.



Effects of Lamellae and Dichroism on Coloration.

This and previous studies by many of the same authors have revealed the complicated origin of color in purplish pink to purple diamonds. The coloration is strongly restricted to thin microtwin lamellae, so the color intensity may appear quite different depending on whether a stone is viewed perpendicular or parallel to the lamellae. Additionally, the purplish pink to purple color centers exhibit optical dichroism (Konstantinova et al., 2006). To the best of our knowledge, the absorption anisotropy of the 550 nm band in diamond has previously been reported only by Zaitseva and Konstantinova (1989).



Figure 12. Natural-color purple diamonds, among the rarest of colored diamonds, owe their purple hue to post-growth plastic deformation. These purple and pink-purple diamonds from Siberia weigh 0.73, 0.62, and 0.63 ct, respectively. Photo by M. A. Bogomolov; courtesy Rony Carob Ltd.

Purplish pink to purple diamonds have been observed to shift color when viewed in various lighting conditions (Hofer, 1998) and after cutting (Moses et al., 2002). Hofer (1998) attributed the change in color to differences in the spectral composition and color temperature of the light source. The occurrence of dichroism in these diamonds implies that the viewing direction and the degree of light polarization may also be important. This dichroism may have been a cause of the predominant pink hue in some of the faceted diamonds in this study. In addition, it may be a characteristic feature of not only purple diamonds, but also other diamonds that receive their color from plastic deformation, such as red, pink, and some of the more common pink-brown stones. As with purple diamonds, the optical spectra of those diamonds also show the 550 nm band, and their coloration often is restricted to deformation lamellae with boundaries that exhibit a characteristic mirror-like reflective appearance (Shigley and Fritsch, 1993; King et al., 2002).

Comparison with Treated-Color Purple Diamonds. Natural-color purple diamonds may be easily distinguished from their treated-color counterparts. The coloration in natural purple diamonds is confined to the deformation lamellae, while in treated diamonds reported on thus far it is evenly distributed

REFERENCES

- Collins A.T. (1982) Colour centers in diamond. *Journal of Gemmology*, Vol. 18, No. 1, pp. 37–75.
 Collins A.T. (2001) The colour of diamond and how it may be

or is located in growth zones (Wang et al., 2005).

In the optical spectra of natural purple diamonds, the 550 nm band is not accompanied by sharp peaks at 575 and 637 nm, as are seen in the spectra of treated diamonds. Moreover, the absorption spectra of these natural diamonds with a dominant purple color show dichroism.

CONCLUSIONS

Natural purple coloration in diamond (figure 12) is thought to arise from post-growth plastic deformation in the earth. Using several spectroscopic methods, this study of purple crystals from Siberia and their faceted counterparts revealed various nitrogen-related defects that formed in the diamond lattice during this deformation. The color appearance of purple diamonds is influenced by localization of the coloration within microtwin lamellae and by the optical dichroism of the color centers. On the basis of their spectroscopic properties and gemological characteristics, natural-color purple diamonds may be easily distinguished from their treated-color counterparts.

ABOUT THE AUTHORS

Dr. Titkov (titkov@igem.ru) is leading research scientist and Dr. Mineeva is senior research scientist at the Institute of Geology of Ore Deposits, Petrography, Mineralogy, and Geochemistry of the Russian Academy of Sciences in Moscow. Dr. Shigley is distinguished research fellow, and Dr. Breeding is research scientist, at GIA in Carlsbad. Mr. Zudin is director of Rony Carob Ltd. in Moscow. Mr. Sergeev is a research scientist at the Federal Scientific-Technical Center (Leonid Jakovlevich, Karpov Institute) in Moscow.


ACKNOWLEDGMENTS

The authors thank Dr. M. A. Bogomolov (Moscow State University) and C. D. Mengason (of GIA Carlsbad) for taking the photos. We are also grateful to Dr. A. F. Konstantinova (Institute of Crystallography of the Russian Academy of Sciences) and Prof. L. V. Bershov (Institute of Geology of Ore Deposits, Petrography, Mineralogy, and Geochemistry of the Russian Academy of Sciences) for helpful discussions. This work was supported by grant no. 05-05-64986 from the Russian Foundation of Basic Research.

- changed. *Journal of Gemmology*, Vol. 27, No. 6, pp. 335–339.
 De Weerd F., Van Royen J. (2001) Defects in coloured natural diamonds. *Diamonds and Related Materials*, Vol. 10, No. 3/7, pp. 474–479.

- Federman D. (1995) Purple diamond: Russian delight. *Modern Jeweler*, Vol. 94, No. 9, pp. 19–20.
- Fritsch E. (1998) The nature of color in diamonds. In G. E. Harlow, Ed., *The Nature of Diamonds*, Cambridge University Press, Cambridge, UK, pp. 23–47.
- Gnevushev M.A., Krasov L.M., Dubotovko Y.V., Diakova N.I. (1961) On the color of Yakutian diamonds. In A. A. Menyaylov, Ed., *Proceedings of the Yakutian Branch of Russian Academy of Sciences, Geological Series, Issue 6: Diamonds of Yakutia*, Academic Science Publishing, Moscow, pp. 87–96 [in Russian].
- Hargett D. (1990) Gem Trade Lab Notes: Another purple diamond. *Gems & Gemology*, Vol. 26, No. 2, pp. 154–155.
- Hofer S.C. (1998) *Collecting and Classifying Colored Diamonds: An Illustrated Study of the Aurora Collection*. Ashland Press, New York.
- King J.M., Moses T.M., Shigley J.E., Liu Y. (1994) Color grading of colored diamonds in the GIA Gem Trade Laboratory. *Gems & Gemology*, Vol. 30, No. 4, pp. 220–242.
- King J.M., Shigley J.E., Guhin S.S., Gelb T.H., Hall M. (2002) Characterization and grading of natural-color pink diamonds. *Gems & Gemology*, Vol. 38, No. 2, pp. 128–147.
- Konstantinova A.F., Titkov S.V., Imangazieva K.B., Evdshchenko E.A., Sergeev A.M., Zudin N.G., Orekhova V.P. (2006) Dichroism and birefringence of natural violet diamond crystals. *Crystallography Reports*, Vol. 51, No. 3, pp. 465–471.
- Liddicoat R.T. (1977) Developments and highlights at GIA's lab in Santa Monica: Diamond items of interest. *Gems & Gemology*, Vol. 15, No. 10, pp. 296–299.
- Massi L., Fritsch E., Collins A.T., Hainschwang T., Notari F. (2005) The “amber centers” and their relation to the brown colour in diamond. *Diamond and Related Materials*, Vol. 14, No. 10, pp. 1623–1629.
- Mineeva R.M., Speransky A.V., Titkov S.V., Zudin N.G. (2007) The ordered creation of paramagnetic defects at plastic deformation of natural diamonds. *Physics and Chemistry of Minerals*, Vol. 34, No. 2, pp. 53–58.
- Moses T.M., King J.M., Wang W., Shigley J.E. (2002) A highly unusual, 7.34 ct, Fancy Vivid purple diamond. *Journal of Gemmology*, Vol. 28, No. 5, pp. 7–12.
- Orlov Y.L. (1977) *The Mineralogy of the Diamond*. Wiley Interscience, New York.
- Raal F.A. (1958) A new absorption band in diamond and its likely cause. *Proceedings of the Physical Society of London*, Vol. 71, No. 461, pp. 846–847.
- Shigley J.E., Fritsch E. (1993) A notable red-brown diamond. *Journal of Gemmology*, Vol. 23, No. 5, pp. 259–266.
- Taran M.N., Kvasnytsya V.M., Langer K. (2004) On unusual deep-violet microcrystals of diamonds from placers of Ukraine. *European Journal of Mineralogy*, Vol. 16, No. 2, pp. 241–245.
- Wang W., Smith C.P., Hall M.S., Breeding C.M., Moses T.M. (2005) Treated-color pink-to-red diamonds from Lucent Diamonds Inc. *Gems & Gemology*, Vol. 41, No. 1, pp. 6–19.
- Zaitsev A.M. (2001) *Optical Properties of Diamond: A Data Handbook*. Springer Verlag, Berlin.
- Zaitseva T.M., Konstantinova A.F. (1989) Anisotropy of optical properties of natural diamonds. *Mineralogicheskiy Zhurnal*, Vol. 11, No. 11, pp. 68–73 [in Russian].
- Zintchouk N.N., Koptil' V.I. (2003) *Typomorphism of the Siberian Platform Diamonds*. Nedra, Moscow [in Russian].

NOW AVAILABLE!



GEMS & GEMOLOGY
IN REVIEW


TREATED DIAMONDS

The best of *Gems & Gemology* on the subject of treated diamonds
in one comprehensive research volume

This volume of GEMS & GEMOLOGY IN REVIEW presents a selection of articles and notes that have appeared in the journal since its inception in 1934. Some of the material is from issues long out of print. That means you won't find this information collected anywhere else but here!

- 301 pages of award-winning articles and beautiful, detailed color photography
- More than 70 years of cutting-edge research on the features and identification of treated diamonds
- Editorial commentary by Dr. James E. Shigley,

- GIA Distinguished Research Fellow
- Insights on the past, present, and future of treated diamonds—in the marketplace and the laboratory
- Includes folded chart “Identification of Filled Diamonds.”



This soft-cover book (complete with an attractive slipcase) is now available for \$59.95 (plus shipping).

To order your copy today visit **GEMS & GEMOLOGY** at www.gia.edu or call 800-421-7250, ext. 7142 (outside the U.S.: 760-603-4000, ext. 7142)

EDITORS

Thomas M. Moses and
Shane F. McClure
GIA Laboratory

AQUAMARINE with Kelp-Like Inclusions

At GIA's inaugural Show Service Laboratory in Tucson, Arizona, this past February, we examined a 15.80 ct light greenish blue aquamarine submitted by Lisa Elser of Custom Cut Gems Co., Port Moody, British Columbia. This pear-shaped checkerboard cut, said to be from Pakistan, contained interesting thin bladed inclusions arrayed in patterns reminiscent of kelp. The inclusions were transparent and formed fans with distinctive branches (figure 1, left) that were large enough to be seen with the unaided eye.

Standard gemological testing easily identified the gem as a natural aquamarine. When examined with magnification and polarized light (figure 1, right), the inclusions proved to be birefringent and displayed dramatic interference colors that shifted as the analyzer on the microscope was rotated. Becke line testing indicated that the inclusions had a refractive index somewhat higher than the surrounding beryl host. Because we had never before encountered such inclusions in beryl, we asked the owner for permission to

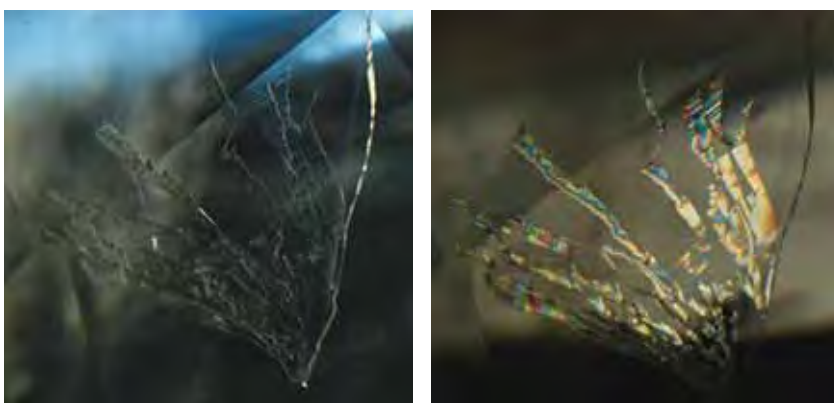


Figure 1. Discovered in an aquamarine that reportedly came from Pakistan, these transparent blades (left) in a distinctive fan-like arrangement were identified as triploidite. The interference colors seen with polarized light (right) proved that the inclusions were birefringent. Field of view 3.0 mm.

bring the stone back to the Carlsbad laboratory for further analysis to conclusively identify them.

In Carlsbad, we used Raman microspectroscopy on one of the inclusion blades, which had been polished through and exposed at the surface of the pavilion. The results indicated triploidite, a monoclinic manganese-iron phosphate that is known to occur in granitic pegmatites. We have encountered triploidite inclusions only once before, in quartz. Since aquamarine is also a known product of granitic pegmatites, however, the inclusion of triploidite in Pakistani aquamarine is geologically reasonable.

We in the laboratory thought it very appropriate to have inclusions of a rare

mineral that resembles fans of kelp in a gem variety known as *aquamarine*.

John I. Koivula and Alethea Inns

DIAMOND with Repeating Growth/Dissolution Features

Diamond crystallization is a complex process. Natural diamonds typically experience multiple stages of growth; it is believed that many also experience episodes of dissolution from one stage to the next (A. R. Lang, "Internal structure," in J. E. Field, Ed., *The Properties of Diamond*, Academic Press, London, 1979, pp. 425–469). Yet whereas the multiple growth stages may be seen

Editors' note: All items are written by staff members of the GIA Laboratory.

GEMS & GEMOLOGY, Vol. 44, No. 1, pp. 66–73.
© 2008 Gemological Institute of America



Figure 2. This square-cut 5.20 ct Fancy brownish greenish yellow diamond experienced multiple growth/dissolution stages during its formation.

with fluorescence or cathodoluminescence imaging as banded structures in the same growth sector, features clearly related to dissolution are less frequently observed and reported. In the New York laboratory, however, we recently examined an unusual diamond with distinctive growth/dissolution features.

The square-cut 5.20 ct diamond in figure 2 was color graded Fancy brown-

ish greenish yellow. Infrared spectroscopy showed that it was a type Ia diamond with a high concentration of nitrogen and structurally bonded hydrogen. Observation with an optical microscope revealed clear octahedral {111} and cubic {100} growth sectors. Clouds of submicron-sized inclusions were spread throughout the cubic growth sector, and the yellow color was more concentrated in the octahedral sector. As a result, this stone displayed patchy color distribution and clear internal graining at the boundaries of the two types of growth sectors.

DiamondView fluorescence imaging revealed multiple growth zones (figure 3). Each fine zone, representing a specific growth stage, either fluoresced greenish yellow or was inert (dark), due to variations in lattice defect configurations. Most of the narrow growth zones were perfectly parallel to one another, with sharp and straight boundaries indicating a repetitive growth process. This process was interrupted at least twice, however, as evidenced by the two areas in figure 3 where several of the greenish yellow and inert bands are discontinuous. These “zigzag” areas were caused by dissolution of the previously formed diamond and subse-

quent additional diamond growth, again with continuous growth zones and curved boundaries following the morphology after dissolution. Faceting produced the “islands” seen in figure 3 (right), remnants of the original growth zone that remained after dissolution, now surrounded by newly precipitated diamond.

The occurrence of dissolution in this diamond strongly indicates that it was subjected to repeated transformation from thermodynamically stable conditions to unstable ones, which may have involved changes in pressure, temperature, system chemistry, or various combinations of these factors. Rarely have we seen such a clear illustration of growth/dissolution features in a diamond.

Wuyi Wang

First CVD SYNTHETIC DIAMOND Submitted for Dossier Grading

Synthetic diamonds grown by the chemical vapor deposition (CVD) technique have been discussed in several recent *Gems & Gemology* articles (W. Wang et al., “Gem-quality synthetic diamonds grown by a chemical vapor deposition [CVD] Method,” Winter 2003, pp. 268–283; P. M. Martineau et al., “Identification of synthetic diamond grown using chemical vapor deposition [CVD],” Spring 2004, pp. 2–25; and W. Wang et al., “Latest-generation CVD-grown synthetic diamonds from Apollo Diamond Inc.,” Winter 2007, pp. 294–312). They have rarely, however, been encountered in the day-to-day grading operations of the lab.

Recently, the Carlsbad laboratory identified a near-colorless CVD synthetic diamond weighing approximately one third of a carat that had been submitted for the standard GIA Diamond Dossier grading report. This is the first CVD product submitted to the Carlsbad lab for a grading service. Previously, all of the CVD samples we examined were received directly from the manufacturer for research purposes (see above references).

Figure 3. These DiamondView fluorescence images clearly illustrate two episodes of growth and dissolution (the jagged, zigzag-shaped zones) in the diamond in figure 2.

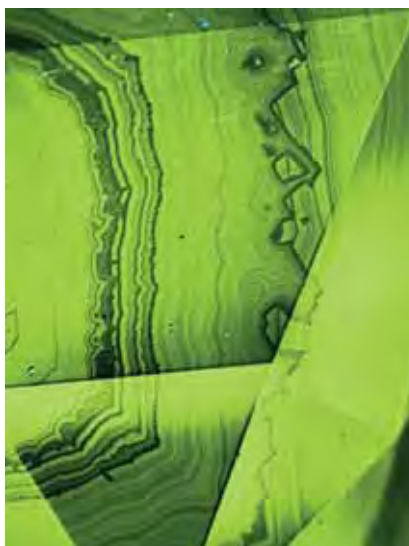




Figure 4. Examination between crossed polarizers revealed an irregular strain pattern in this CVD synthetic diamond, which was submitted to the Carlsbad lab for a grading report. Field of view 3.7 mm.

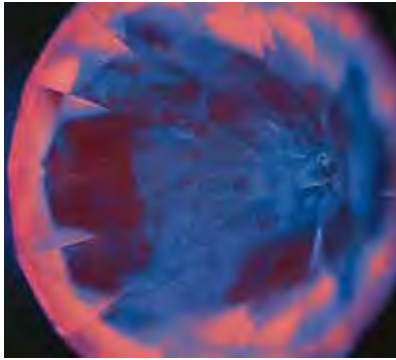


Figure 5. DiamondView imaging of the round brilliant in figure 4 showed an orangy pink fluorescence color with irregular blue zones, similar to the pattern reported previously for CVD synthetic diamonds.

Growth of synthetic diamonds via the CVD method can be accomplished at relatively low pressures, in contrast to the more extreme requirements for growth of high-pressure, high-temperature (HPHT) synthetics. During CVD growth, gaseous interactions result in deposition of synthetic diamond onto a suitable substrate; single-crystal synthetic diamond is the substrate typically used for production of gem-quality material (Wang et al., 2003; Martineau et al., 2004). Element Six of the United Kingdom and Apollo Diamond Inc. of Boston are two well-known producers of gem-quality CVD materials, though only Apollo has produced facetable material for sale to the jewelry trade.

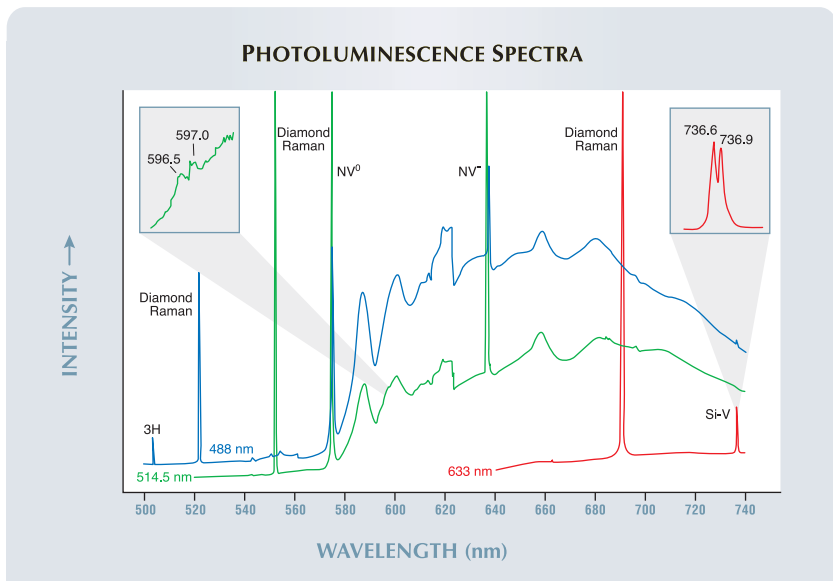
Microscopic examination of the sample submitted for grading revealed numerous feathers and related cavities on the pavilion, which resulted in a clarity grade that fell into the Slightly Included (SI) range. We also observed pinpoints. Between crossed polarizers, the synthetic diamond showed unevenly distributed, high-order interference colors (figure 4)—the first of many similarities we encountered between this sample and those discussed by Wang et al. (2007). It exhibited no visible fluorescence to either long- or short-wave ultraviolet (UV) radiation emitted by a desk-model UV lamp; however,

when subjected to the stronger ultra short-wave UV emissions of the Diamond-View instrument, it showed an overall strong orangy pink to pinkish orange fluorescence (typical of CVD synthetic diamonds), interspersed with patches of blue (figure 5). When viewed through the pavilion, the fluorescence

details became significantly clearer—including red striations that were most prominent in the pink/orange region and concentration of the irregular blue patches toward the culet. These latter features were both described by Wang et al. (2007). The weak blue phosphorescence noted in the DiamondView was also similar to the Wang et al. findings.

FTIR analysis indicated that the synthetic diamond was type IIa, and low-temperature photoluminescence (PL) spectroscopy revealed a classic CVD signature consisting of peak doublets at 736.6/736.9 nm (due to the silicon-vacancy [Si-V] defect) and at 596.5/597.0 nm. PL spectra were collected using four different laser excitations to confirm the presence of these features (for ease of reproduction, only the results for three of these are shown in figure 6). While the 596.5/597.0 nm doublet is still considered unique to CVD synthetic diamonds, the Si-V doublet has been reported in some rare colorless and near-colorless natural diamonds (see C. M. Breeding and W. Wang, “Occurrence of the Si-V defect center in natural colorless gem diamonds,” *Diamonds and Related*

Figure 6. Photoluminescence spectra collected from the near-colorless synthetic diamond at 488, 514.5, and 633 nm laser excitations showed distinctive CVD-related features.



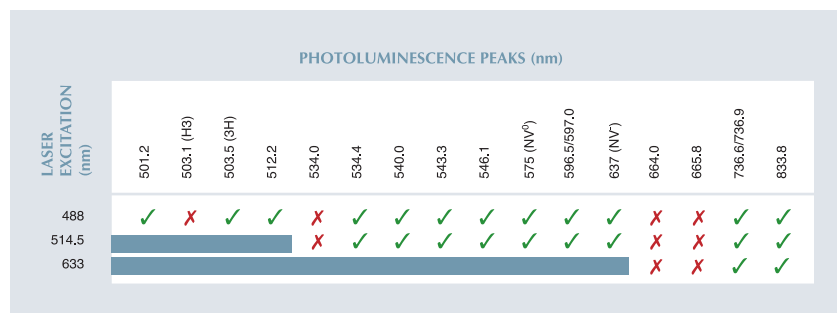


Figure 7. A comparison of PL peaks from analysis of the CVD synthetic diamond in figure 4 and those presented by Wang et al. (2007), using laser excitations at 488, 514.5, and 633 nm, reveals many similarities. A check (✓) indicates that the peak was observed in both studies, whereas an x indicates a lack of correlation; gray portions are regions outside the working range of the specific laser.

Materials, in press). We also observed most of the other peaks presented by Wang et al. (2007), including the 3H (503.5 nm) defect; a comparison of our photoluminescence results with those PL features is shown in figure 7. The results for the fourth laser excitation, at 830 nm, were also generally consistent with those reported by Wang et al. (2007).

Given the many similarities between this synthetic diamond and the Apollo CVD material produced during 2006–2007 (Wang et al., 2007), it is likely that this sample is from a similar generation. Its submission to the lab for Diamond Dossier grading confirms that at least some CVD-grown synthetic diamonds are currently present in the marketplace. Examination by a gemological laboratory remains the most effective way to confidently identify synthetic diamonds.

The sample was returned to the client with a Synthetic Diamond grading report and the words “LABORATORY GROWN” laser inscribed on the girdle, as is GIA’s standard practice.

Karen M. Chadwick and
Christopher M. Breeding

Interesting FILLED VOIDS

Carbonate minerals such as calcite, dolomite, and magnesite are occasionally encountered in emeralds, rubies,

and other gems. As inclusions, the carbonates can provide valuable evidence that the host gem has not been treated.

For gem treatments involving filling with epoxy resins and solder (high lead content) glasses, it is generally believed that lower-quality starting material is first immersed in hydrochloric or oxalic acid to remove foreign matter from surface-reaching cracks and pits to “clean” the gem and make the treatment more effective. If surface-reaching cracks extend to solid mineral inclusions, then those inclu-

sions will also be attacked by the acid—or, in the case of hydrochloric acid and carbonate minerals, totally dissolved so that only a void remains. While most such voids do not show any recognizable form, occasionally we encounter examples with obvious carbonate habits. Recently we examined two gems with such voids. One was a ring-mounted emerald that was reportedly mined at Chivor, near Somondoco, Colombia. It was submitted for gemological examination by Manuel J. Marcial of Emeralds International, Key West, Florida. The other was a 2.58 ct ruby, thought to be from Madagascar, that was provided by E. Gamini Zoysa of Mincraft Co., Mount Lavinia, Sri Lanka.

The emerald hosted two large filled voids as well as a very distinctive light brown translucent mineral with the visual appearance of the very rare carbonate parasite (figure 8). Parasite is known to occur in Colombian emeralds, although it is generally thought to indicate emeralds mined at Muzo (see Winter 1982 Lab Notes, p. 230). The voids next to the mineral inclusion were of very low relief, and each contained a single large, spherical gas bubble. They also had the same general shape as the apparent parasite.

Figure 8. The single gas bubble and the flash-effect colors in each of these two voids prove that the host emerald has been filled. The light brown well-formed crystal has the appearance of the rare carbonate mineral parasite, which is known to occur in Colombian emeralds. Field of view ~5.6 mm.





Figure 9. These bright flash-effect colors provide clear evidence that the host ruby has been filled with a glass that closely matches it in RI. Field of view ~3.5 mm.

With shadowed illumination, flash-effect colors at the edges of the filled voids readily delineated them.

On first inspection, the ruby clearly showed extensive evidence of solder glass filling in the form of bright flash-effect colors (figure 9). More detailed microscopic examination revealed a rhomb-shaped void in the pavilion that contained a single spherical gas bubble, visible just below the girdle (figure 10). As with the void in the emerald, shadowed illumination enhanced the visibility of this feature. Although no actual carbonate inclusions were present in this ruby, the habit of this filled cavity and the well-known vulnerability of carbonate minerals to acid attack made us suspect that the original mineral occupying this void was a carbonate.

John I. Koivula, Shane F. McClure, and Dino DeGhionno

GLASS with Devitrified Inclusions

Glass is a very common gem simulant, and the lab regularly encounters glass specimens—most of them unexciting—in the course of its work. In fall 2007, however, the New York lab-



Figure 10. Measuring approximately 0.56 mm in length and containing a single gas bubble, this rhomb-shaped glass-filled cavity in the 2.58 ct ruby probably once contained a carbonate mineral such as calcite.

oratory received an 11.17 ct ($12.26 \times 12.09 \times 8.66$ mm) round modified brilliant cut that immediately piqued our interest because of the striking asterisk-like arrangements of long fibrous

inclusions it contained (figure 11).

Microscopic examination revealed the presence of several gas bubbles, consistent with a glass. This identification was confirmed by its singly refractive optic character (with slight anomalous double refraction) and Raman and Fourier-transform infrared (FTIR) spectroscopy.

With the sample's over-the-limit refractometer reading and a specific gravity of 4.44, we were able to exclude natural glasses such as obsidian and moldavite, as well as less common natural materials such as Libyan desert glass and tektites. Based on the high clarity and the unusually pure light yellowish green color, we determined that the glass was manufactured. This was supported by energy-dispersive X-ray fluorescence (EDXRF) results indicating an expected strong signal for silicon, as well as zirconium and barium (and moderate strontium), a signature that would be very unusual for natural glass but is

Figure 11. This 11.17 ct specimen of manufactured glass contains several unusual clusters of inclusions.

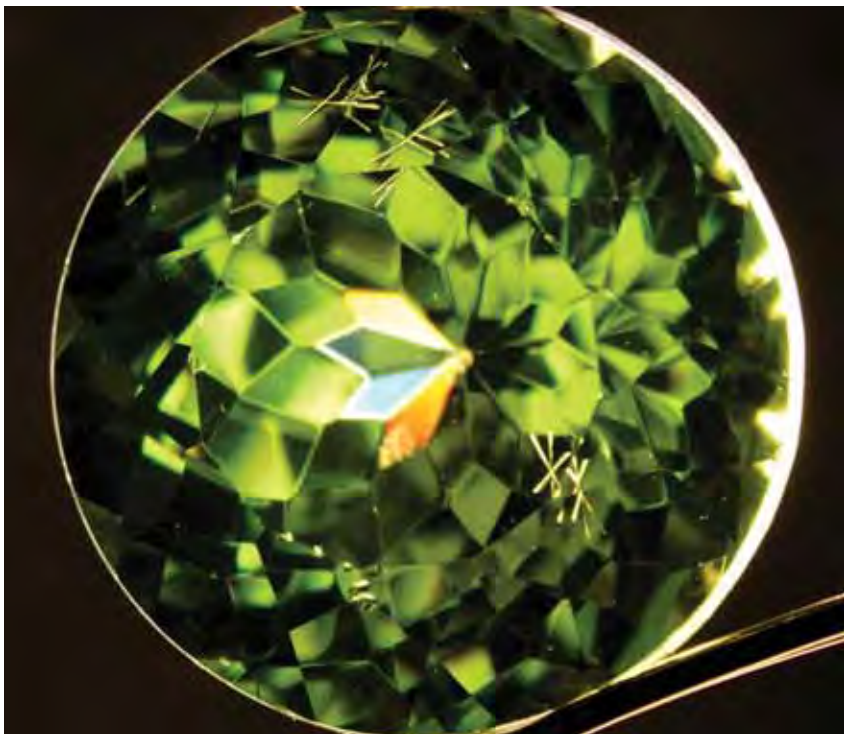




Figure 12. These long, fibrous inclusions were likely formed by devitrification of the glass host. Field of view ~3.1 mm.

not uncommon for some manufactured glasses. The presence of these heavy elements also explained the high RI and SG values.

As the fibrous inclusions had a discernable crystalline character (figure

12), we concluded that they were exsolved from the glass host. Faint growth lines were present at the tips of the fibrous bundles, and crossed polarizing filters showed low-order interference colors. Examination with a calibrated camera microscope indicated that the inclusions had an approximate average length of 1.2 mm and a cross section of about 60 μm .

In our experience, the crystalline inclusions were best explained as the result of partial devitrification (i.e., regions where the glass's amorphous state has locally changed to a crystalline material). Many examples of devitrified inclusions in manufactured glasses have been published in *G&G* (e.g., Lab Notes—Fall 1993, p. 201; Summer 1995, p. 137; Summer 1996, p. 123—and G. Bosshart, “Cobalt glass as a lapis lazuli imitation,” Winter 1983 *Gems & Gemology*, pp. 228–231). Excellent examples may also be found in the *Photoatlas of Inclusions in Gemstones* (E. J. Gübelin and J. I. Koivula, Vol. 1, Opinio Verlag, Basel, Switzerland, 1986, pp. 437–439).

In an attempt to identify these par-

ticular inclusions, we used confocal Raman spectroscopy on one fibrous bundle that broke the surface of a bezel facet. With both 514 and 830 nm laser excitation, the spectra showed peaks at the same positions, indicating that they were due to Raman scattering from a crystalline substance as opposed to photoluminescence (figure 13). Unfortunately, although we acquired an excellent Raman spectrum, we were unable to match it to any known materials in our mineral reference database.

David M. Kondo
and Donna F. Beaton

PEARL

White Clam Pearl with Original Shell

The New York laboratory recently received a 9.13 ct white non-nacreous pearl (figure 14) for identification. According to the client, it was recovered from Peconic Bay, off the North Fork of Long Island, New York. The client, who has clammed in the area for more than 30 years and has a degree in oceanography, estimated the clam to be about eight years old (based on its growth rings). He submitted the shell to the lab along with the pearl (figure 15). The button-shaped pearl (12.26 \times 8.40 mm) had a clean surface

Figure 13. Raman analysis of one of the devitrified inclusions gave clear results (with major peaks at 855, 650, 622, 426, 269, 226, 185, and 138 cm^{-1}), but they could not be matched to a reference spectrum. The spectrum taken with 830 nm laser excitation is baseline corrected.

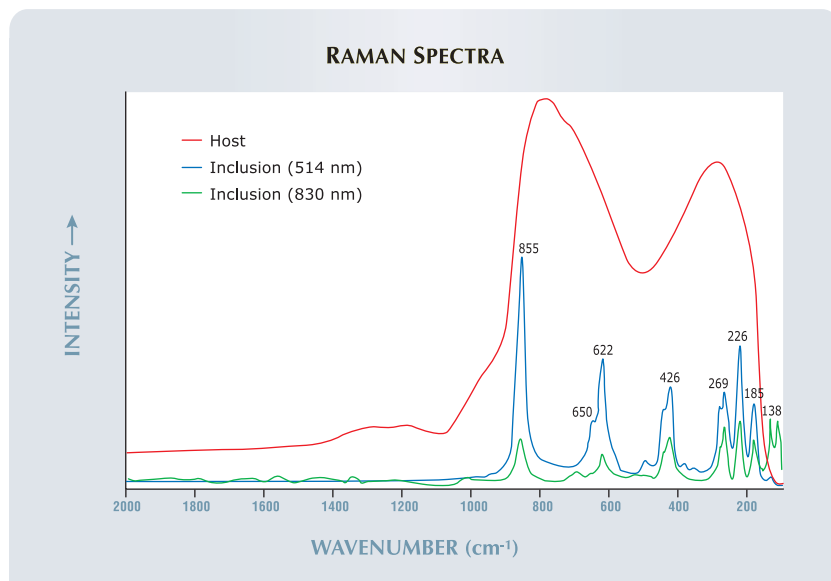


Figure 14. This fine example of a white clam pearl (12.26 \times 8.40 mm) was reportedly recovered from a clam found off the coast of Long Island, New York.





Figure 15. The color of the pearl in figure 14 closely matches that of the shell in which it was found.

with a soft porcelaneous luster, as well as a pure white color that matched the interior of the shell. The X-radiograph showed very subtle growth features, as is typical of clam pearls.

In addition to the opportunity to examine the original shell from which the pearl came, the excellent condition, size, pure white color, and local origin made this an interesting and unusual submission.

Akira Hyatt

Figure 16. This baroque conch pearl (39.45 × 24.55 × 19.15 mm) is unusual for its size and shape, as well as the patches of different colors seen on its surface.



Large Baroque Multicolored Conch Pearl

The New York laboratory recently received a large (125.26 ct) baroque non-nacreous pearl for identification (figure 16). Standard gemological testing established that it was of natural origin and from the *Strombus gigas* mollusk, commonly referred to as the queen conch. The pearl displayed variegated color, with prominent patches of orangy pink, white, orange, orange-brown, and even a small patch of purple. Many of these colors are characteristic of various parts of the conch shell. Additionally, the shape of the pearl suggests that it may have grown in or near one of the folds of the shell. The pearl was chipped at its narrowest edge, but otherwise it showed an intact surface with a porcelaneous luster and a subtle flame structure typical of conch pearls (see, e.g., E. Fritsch and E. Misiorowski, "The history and gemology of Queen conch 'pearls,'" Winter 1987 *Gems & Gemology*, pp. 208–221). The shape and multicolored nature of this pearl, as well as its large size, made it an unusual specimen.

Akira Hyatt

Green SYNTHETIC SAPPHIRE with Vibrant Blue Inclusions

In today's gemological world, synthetic colored stones seldom garner the attention that is bestowed on treated gems. The latter are now available in much greater numbers than ever before and are enhanced using increasingly sophisticated technology, whereas it is not often that a new form of synthetic gem is encountered. Thus, we were intrigued when Leon M. Agee of Agee Lapidary in Deer Park, Washington, sent us a 44.66 ct polished section from a flame-fusion synthetic sapphire boule and a 0.91 ct octagonal step cut fashioned from the same material (figure 17). Both displayed a dull green color that we had never encountered before, as well as numerous vibrant blue solid inclusions (figure 18). Because of their deep blue color (similar to cobalt glass), we suspected that these inclusions contained cobalt.

The standard gemological properties were consistent with synthetic corundum. The material fluoresced moderate chalky orangy red to long-wave UV radiation and was inert to short-wave UV. We observed a very weak cobalt spectrum with the desk-model spectroscope. In addition to the expected elements for corundum, trace elements detected through laser ablative-inductively coupled plasma-mass spectrometry (LA-ICP-MS) analysis included vanadium (~200 ppm), cobalt (150 ppm), and chromium (60 ppm).

Figure 17. This 0.91 ct octagonal step cut represents an unusual color for flame-fusion synthetic sapphire.



Raman analysis could not precisely identify the blue inclusions even though clear target sites were exposed on the surface of the boule section in dramatic dendritic form (figure 19). The closest Raman library match suggested that the blue substance was related to spinel, and polarized light microscopy demonstrated that the inclusions were isotropic.

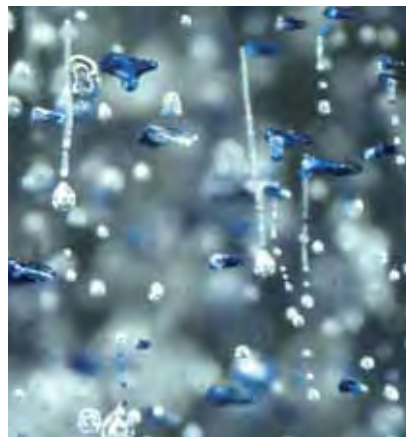
This is the first time we have encountered a synthetic sapphire with this unusual green color and such vibrant blue solid inclusions. Perhaps this material was the result of an “accident” that occurred during crystallization.

John I. Koivula, Alethea Inns, and Andy Hsi-Tien Shen

High-Temperature Heat-Treated ZIRCON

Although zircons are routinely heat treated, the temperatures typically used are considerably lower (near or well below 1000°C) than those used to alter the color in corundum (which may exceed 1500°C). The temperatures used on corundum are capable of doing serious damage to almost any mineral inclusions that might be present.

Figure 18. Intense blue solid inclusions and obvious gas bubbles were discovered in the green flame-fusion synthetic sapphire. Field of view ~0.7 mm.



ent. So while it is common to encounter obviously altered solid inclusions in rubies and sapphires, they are oddities in zircons.

When rubies and sapphires are heat treated, however, it is not unusual for non-corundum gem materials such as chrysoberyl, spinel, or zircon to be accidentally mixed in. This can result in some rather interesting changes in the appearance of these stray gems and even in the corundum itself. As one prominent example of the latter, it has been speculated that the accidental inclusion of chrysoberyl in a sapphire heating run led to the discovery of beryllium treatment of sapphires and the effect that even small traces of Be have on corundum coloration. Consequently, although we don't expect to find visual evidence of high-temperature heating in zircons, observation of any such features is almost always worth documenting.

This was the case with an orangy yellow 0.96 ct transparent mixed-cut zircon from Anakie, Queensland, Australia, that Terry Coldham of Sapphex, in Sydney, loaned the GIA lab for examination. As seen in figure 20, this zircon contained a reflective

Figure 19. LA-ICP-MS and Raman analysis could not conclusively identify these deep blue spinel-like crystalline dendrites exposed on the surface of the flame-fusion synthetic sapphire boule. Field of view ~3.5 mm.

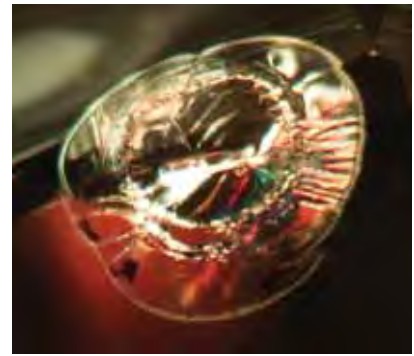
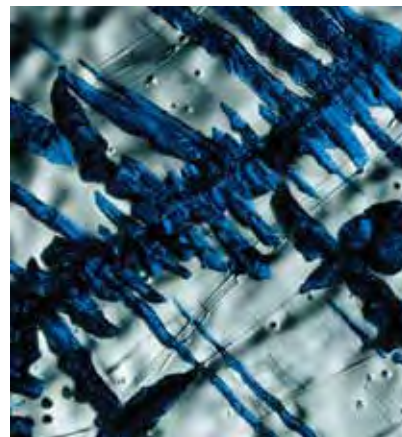


Figure 20. Measuring 0.70 mm in longest dimension, the reflective halo structure surrounding a melted inclusion in this zircon clearly indicates that an atypically high temperature (for zircon) heat treatment has taken place.

decrepitation halo surrounding a melted inclusion, which clearly indicated that the zircon had been subjected to high-temperature heat treatment. A ring of solidified melt droplets surrounded an elongated central inclusion that now appeared to contain a transparent solid with a gas bubble frozen in place at its tip. Beyond the melt droplet ring, the presence of a second reflective discoid rim suggests that this inclusion experienced two rupture events during the heat treatment.

John I. Koivula

ERRATUM

In the Winter 2007 Lab Notes entry on the double-star sapphire (p. 365), the name of the client, Depal Weerasinghe of International-Gem Merchants, Sri Lanka/Rhode Island, was inadvertently left out. *Gems & Gemology* regrets the omission.

PHOTO CREDITS

John I. Koivula—1, 8, 9, 10, 18, 19, and 20; Jian Xin (Jae) Liao—2, 14, 15, and 16; Wuyi Wang—3; Karen M. Chadwick—4 and 5; David M. Kondo—11 and 12; Robert Weldon—17.



EDITOR

Brendan M. Laurs (blaurs@gia.edu)

CONTRIBUTING EDITORS

Emmanuel Fritsch, *IMN, University of Nantes, France* (fritsch@cnrns-immn.fr)

Henry A. Hänni, *SSEF, Basel, Switzerland* (gemlab@ssef.ch)

Franck Notari, *GemTechLab, Geneva, Switzerland* (franck.notari@gemtechlab.ch)

Kenneth V. G. Scarratt, *GIA Research, Bangkok, Thailand* (ken.scarratt@gia.edu)

Tucson

2008

The annual Tucson gem and mineral shows continue to showcase a wide variety of polished material, mineral specimens, and gem rough from around the world. This year saw the introduction of spessartine from a new mine in Tanzania (see report below). Tanzania is also the source of some impressive orangy pinkish red spinel (figure 1), cut from an enormous crystal (reportedly more than 52 kg) that was found near Mahenge in the latter part of 2007 (www.multicolour.com/spinel).

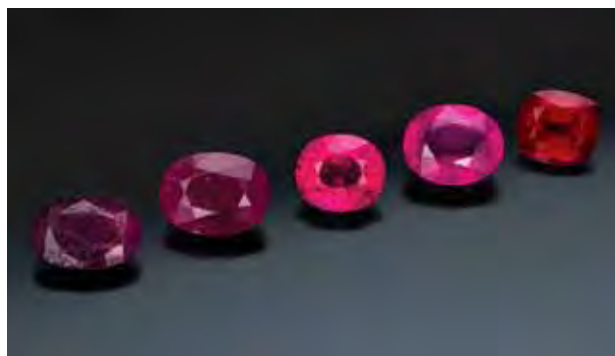
Glass-filled rubies were common at this year's Tucson shows, in a range of qualities and prices (figure 2). Of course, several unusual stones and remarkable oddities were also seen, including a 76.27 ct sphene (figure 3), a 59.58 ct jerejevite (figure 4), and a diamond showing a crystal form that resulted from mixed octahedral and cuboid growth (see figure 5 and C. M. Welbourn et al., "A study of diamonds of cube and cube-related shape from the Jwaneng mine," *Journal of Crystal Growth*, Vol. 94, 1989, pp. 229–252). Additional items seen in Tucson will be described in more detail in future issues of *Gems & Gemology*.

This year's theme for the Tucson Gem and Mineral Society show was "Minerals of the USA," and several superb displays showcased noteworthy specimens from 44 of the most important mineral localities in the United States. Some of the classic sources represented for gem



Figure 1. These spinels (6.77 and 12.07 ct) were reportedly cut from a 52 kg crystal that was recovered near Mahenge, Tanzania, in the latter part of 2007. Courtesy of Nomad's Co., Bangkok; photo by Robert Weldon.

Figure 2. Glass-filled ruby was available at the Tucson gem shows in a wide range of qualities, priced from less than \$1/ct (far left) to \$150/ct (far right). Courtesy of Real Creation Inc., Los Angeles; photo by Robert Weldon.



Editor's note: Interested contributors should send information and illustrations to Brendan Laurs at blaurs@gia.edu or GIA, The Robert Mouawad Campus, 5345 Armada Drive, Carlsbad, CA 92008. Original photos can be returned after consideration or publication.

GEMS & GEMOLOGY, Vol. 44, No. 1, pp. 74–94
© 2008 Gemological Institute of America



Figure 3. This 76.27 ct sapphire is notable for its large size and vibrant display of dispersion. Courtesy of H. Obodda, Short Hills, New Jersey; photo by Robert Weldon.



Figure 4. This Madagascar jeremejevite is an impressive 59.58 ct. Courtesy of Nakoa Gems, Simi Valley, California; photo by Robert Weldon.

material/crystals included California and Maine pegmatites, North Carolina emerald/hiddenite deposits (see report below on one of these emerald mines), and Colorado rhodochrosite, California benitoite, and Utah red beryl. Released in conjunction with the exhibit was a comprehensive book titled *American Mineral Treasures*, edited by G. A. Staebler and W. E. Wilson (Lithographie, East Hampton, Conn., 2008). The 2009 Tucson Gem and Mineral Show will take place February 12–15, 2009, and will feature “Mineral Oddities.”

G&G appreciates the assistance of the many friends who shared material and information with us this year, and also thanks the American Gem Trade Association for providing space to photograph these items during the AGTA show.

Emerald-bearing gem pockets from North Carolina. The 2008 Tucson Gem and Mineral Society show featured a symposium on February 16 titled “Minerals of the USA,”

which was sponsored jointly by the Friends of Mineralogy, the Tucson Gem and Mineral Society, and the Mineralogical Society of America. Of particular interest to *G&G* readers was the presentation by geologist Ed Speer titled “Emerald crystal pockets of the Hiddenite District, Alexander County, North Carolina.” Mr. Speer is a consultant to Jamie Hill’s North American Emerald mine (formerly the Rist mine), located near Hiddenite.

The emeralds occur within “pockets” hosted by subvertical quartz veins intruding foliated migmatitic gneiss (figure 6). A typical, well-developed pocket consists of three distinct components: (1) an uppermost portion filled with massive quartz; (2) a central open cavity that may contain emerald crystals in association with quartz, albite, muscovite, schorl, and, rarely, hiddenite; and (3) a bottom portion that is filled with clay containing mineral fragments and crystals from the overlying cavity (i.e., a

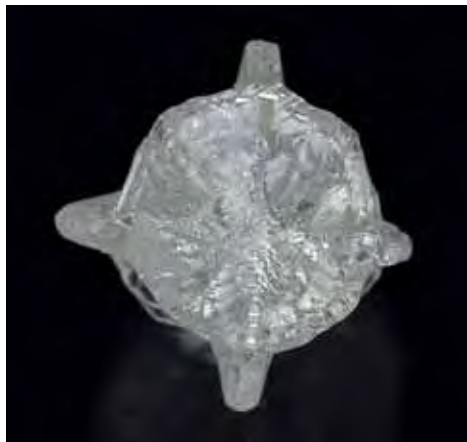


Figure 5. The Orapa mine in Botswana is the source of this unusual diamond crystal (1.1 cm in diameter), which was mined in 2007. Although such crystals have been attributed to hopped growth, this is actually a reentrant cube resulting from mixed octahedral and cuboid growth. Courtesy of North Star Minerals, West Bloomfield, Michigan; photos by Jeff Scovil.



Figure 6. Typical “pockets” at the North American Emerald mine in North Carolina consist of an upper massive quartz portion, a central open cavity lined with various well-formed crystals (including emeralds), and a bottom portion filled with pocket rubble. In the pocket shown here, the latter two components have been excavated by the miners. Photo by Ed Speer.

collapse breccia). The pockets range from a few centimeters to 3 m in the longest dimension, and their distribution varies across the property.

Mr. Speer presented interesting statistics that reflect the small quantity but very high carat weight of the emeralds recovered from the cavities. For example, not all pockets contain emeralds, but when they are present, 50% of the crystals weigh 100+ ct (20+ g). Records and photos provided showed more than 10 emerald crystals exceeding 100 ct, including discoveries made in recent years. Some of the crystals from this mine contain considerable gem-quality areas (figure 7).

North Carolina emeralds are colored by chromium, but Mr. Speer indicated that the source of this element, as well as the mechanism by which it is incorporated into the emerald-bearing fluids, is still unknown. Geologic research is ongoing.

The mining operation excavates significant amounts of country rock to uncover the emerald-bearing veins. In a



Figure 7. North Carolina emeralds have been cut into attractive gemstones. The 14.2 g crystal shown here was faceted into the 18.8 ct Carolina Queen and the 7.85 ct Carolina Prince. Courtesy of Jamie Hill; photo by Robert Weldon.

true entrepreneurial spirit, however, the mine is selling this material as aggregate to the local construction industry. Effectively they are converting their country rock dilution into “ore”—just of another variety. More information on the emerald production and mining activities at various North Carolina localities can be found at www.northcarolinaemeralds.info.

Keith A. Mychaluk (kmychaluk@shaw.ca)
Calgary, Alberta, Canada

Spessartine from Loliondo, Tanzania. Spessartine has been found in a number of locations worldwide and is prized for its vibrant orange hue. This year at the Tucson shows, several dealers exhibited large, well-formed crystals of spessartine from a new deposit in Tanzania (figure 8). According to Werner Radl (Mawingu Gems, Niederwörresbach, Germany), the mine is located ~14 km north-east of Loliondo, near the village of Lemisikio (i.e., just a few kilometers from the border with Kenya). In addition to the crystals and gem rough, Steve Ulatowski (New Era Gems, Grass Valley, California) showed a few faceted stones to one of these contributors (BML). Mr. Ulatowski reported having first seen a few crystals of this garnet during a May 2007 buying trip to Tanzania. Later, in January 2008, he obtained a considerable quantity of the spessartine; local suppliers told him it was mined in late 2007, apparently from a weathered schist host rock. The presence of abundant inclusions has limited the amount of good gem-quality material to an average of approximately 3 kg per month, in pieces weighing up to 4 g.

As of March 2008, Mr. Ulatowski had cut only a few pieces, and faceted stones weighing more than 2 ct were rare. However, the largest stone known to Mr. Ulatowski weighed 10.92 ct (figure 9). This specimen was loaned to GIA for examination, together with a 3.36 g piece of rough, by Brian Cook (Nature’s Geometry, Laguna Beach, California). In addition, Mr. Ulatowski donated a 2.01 ct



Figure 8. Spessartine from a new deposit near Loliondo, Tanzania, has been recovered as relatively large, well-formed crystals. The crystals on the left range from 4.0×4.1 cm to 2.6×3.5 cm, and the sample on the right (with associated reddish purple mica) measures 4.6×9.9 cm (GIA Collection no. 37554). Photos by Robert Weldon.

stone (again, see figure 9) and three pieces of rough (2.07–4.64 g) for our research, while an attractive crystal specimen with some associated purple mica (figure 8, right) was donated to GIA by Abe Suleman (Tuckman Mines and Minerals Ltd., Arusha, Tanzania).

Examination of the two cut stones gave the following properties: color—medium orange and medium yellow-orange; RI—1.780; hydrostatic SG—4.04; inert to long- and short-wave UV radiation; and bands centered at 460, 480, and 520 nm (with a cutoff below 435 nm) when viewed with the desk-model spectroscope. These properties lie between the values listed for spessartine and pyrope-spessartine by C. M. Stockton and D. V. Manson (“A proposed new classification for gem-quality garnets,” Winter 1985 *Gems & Gemology*, pp. 205–218); for spessartine, RI—1.780–<1.810, and bands “at about 410, 421, 430, 460, 480, and 520 nm, but the first three may merge to form a cutoff to about 435 nm”; and for pyrope-spessartine, RI—

1.742–<1.780, and bands “at 410 and 430 nm, and usually at 421 nm, that occasionally merge to form a 435 nm cut-off. Also show some combination of bands at 460, 480, 504, 520, and 573 nm.” M. O’Donoghue (Ed., *Gems*, 6th ed., Butterworth-Heinemann, Oxford, UK, 2006, pp. 233) also reported RI—1.80 and SG—4.04–4.15 for Mandarin garnet (spessartine) from Namibia.

Microscopic examination of the faceted stones revealed numerous mineral inclusions. Using Raman microspectroscopy on the larger sample, we identified some angular euhedral-to-subhedral transparent crystals as quartz (figure 10, left) and rounded anhedral transparent crystals as zircon. We also noted, and identified via Raman analysis, some off-white translucent-to-opaque “snowballs” of zircon that were surrounded by tiny tension cracks (figure 10, middle). Mica inclusions (figure 10, right) were recognized visually and through their reaction in polarized light. Dark, opaque crystals near one of the corners of the smaller stone (figure 11) visually resembled some form of manganese mineral, and a sample of black matrix associated with a spessartine crystal was identified as braunite ($\text{Mn}^{2+}\text{Mn}^{3+}\text{SiO}_3$) by powder X-ray diffraction. However, Raman spectroscopy of the dark inclusions in figure 11 yielded no spectral match to any mineral in our database, including braunite.

One of us (JA) arranged for electron-microprobe analysis of a polished fragment of the spessartine. Data gathered using the instrument’s energy-dispersive spectrometer revealed a significant pyrope component (Mg; $\text{Pyr}_9\%$) and a small grossular content (Ca; $\text{Gro}_\%$)— $\text{Sps}_{77.5}\text{Pyr}_{17.9}\text{Gro}_{4.6}$ —and no measurable almandine component (Fe^{2+}). The high-Mg, low-Fe content of this spessartine is similar to, but more pronounced than, that of the Mandarin garnet from Namibia (derived from Mn-rich gneisses), and it contrasts markedly with the low-Mg spessartine that is typical of granitic pegmatites (see, e.g., table 2 in B. M. Laurs and K. Knox, “Spessartine garnet from Ramona, San Diego County, California,” Winter 2001 *Gems & Gemology*, pp. 278–295). Laurs and Knox (2001) also compiled gemological properties for spessartine from several localities; the RI

Figure 9. The new Tanzanian spessartine is notable for its pure orange color, typically without brown overtones. Due to abundant inclusions, most of the faceted material weighs less than the 2.01 ct stone shown on the right (GIA Collection no. 37555). The 10.92 ct stone on the left is exceptionally large for this locality. Photo by Kevin Schumacher.





Figure 10. Transparent angular crystals of quartz were relatively common inclusions in the spessartine from Tanzania (left, field of view 0.8 mm). The translucent white spheroidal mass (center, 0.09 mm in diameter) was identified by Raman analysis as zircon; it is surrounded by minute tension fractures. Less common were angular subhedral inclusions of transparent-to-translucent brown mica (right, 0.63 mm in longest dimension). Photomicrographs by J. I. Koivula.

value reported here (1.780) is considerably lower than any of those values, but is closest to the Namibian values (1.790–1.797 for $\text{Sps}_{84.0-87.0}\text{Pyr}_{9.8-12.6}\text{Gro}_{1.1-1.4}$).

A fragment of purple mica associated with the specimen in figure 8 (right) was also analyzed by microprobe, and was identified as muscovite containing 3.77 wt.% FeO, 1.92 wt.% MgO, and 0.44 wt.% MnO. Minor amounts of Ba and Ti were also detected. Although the purple color suggested lepidolite, only ~20 ppm Li was recorded by laser ablation-inductively coupled plasma-mass spectrometry (LA-ICP-MS) analysis of another

sample of this muscovite by GIA Laboratory research scientist Dr. Andy H. Shen; the low Li content is consistent with the apparent metamorphic origin of this spessartine. Dark brown to black mica was also seen in association with the spessartine crystals, but none was analyzed for this report.

Some additional mineral samples associated with the spessartine were donated to GIA by Mr. Radl. The first mineral—a 1.71 g crystal of medium yellowish orange color—was identified by Raman analysis as kyanite; basic gemological properties (hydrostatic SG and spot RI) confirmed the spectral identification. The orange hue is noteworthy, since kyanite is generally blue to green (see, e.g., O'Donoghue, 2006, p. 422). A small dark gray crystal on a spessartine sample was identified as rutile using the Raman technique, while an opaque dark gray/brown sample could not be identified, but appeared to be composed of Mn-oxides. Finally, a transparent dark red fragment was identified as dravite by electron-microprobe analysis at the University of New Orleans. An average of five data points showed the following chromophoric elements: 2.69 wt.% FeO, 0.26 wt.% MnO, 0.12 wt.% TiO_2 , and 0.06 wt.% V_2O_3 .

Karen M. Chadwick (karen.chadwick@gia.edu)

and John I. Koivula

GIA Laboratory, Carlsbad

Brendan M. Laurs

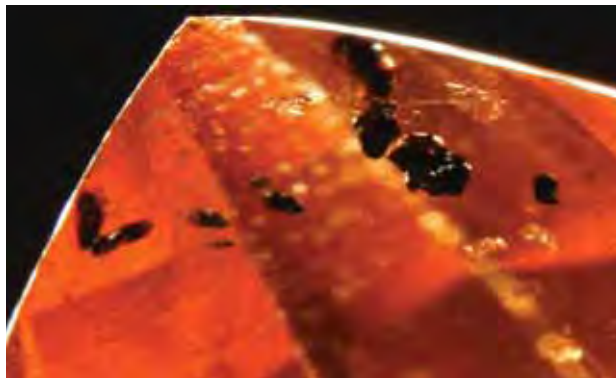
John Attard

Attard's Minerals

San Diego, California

William B. (Skip) Simmons and Alexander U. Falster
University of New Orleans, Louisiana

Figure 11. Situated near the edge of the 2.01 ct stone was this series of nearly opaque inclusions that were reminiscent of senaite previously encountered in other spessartines. However, their identity could not be confirmed by Raman spectroscopy. Photomicrograph by J. I. Koivula; field of view 2.0 mm.





COLORED STONES AND ORGANIC MATERIALS

Gem-quality afghanite and haiüyne from Afghanistan. In April 2007, Farooq Hashmi (Intimate Gems, Jamaica, New York) loaned two parcels of blue rough from Badakhshan, Afghanistan, to GIA for examination. He purchased the parcels in Peshawar, Pakistan. One group was dark blue and sold to him as afghanite, and the other was “turquoise” blue with its identity unknown to the seller (e.g., figure 12). Mr. Hashmi also donated a sample of each color to the RRUFF project (<http://rruff.info>), and both were analyzed by single-crystal X-ray diffraction and electron microprobe. The dark blue fragment (R070558) was identified as afghanite with the formula $(\text{Na}_{19.10}\text{K}_{2.90})_{\Sigma=22}\text{Ca}_{10.00}(\text{Si}_{24.00}\text{Al}_{24.00})_{\Sigma=48}\text{O}_{96}(\text{S}_{1.00}\text{O}_4)_6([\text{OH}]_{3.21}\text{Cl}_{2.79})_{\Sigma=6}$ (OH estimated by difference and charge balance), and the “turquoise” blue sample (R070557) was haiüyne with the formula $\text{Na}_{3.00}(\text{Ca}_{0.84}\text{Na}_{0.16})_{\Sigma=1}(\text{Si}_{3.05}\text{Al}_{2.95})\text{O}_{12}(\text{SO}_4)_{0.89}\text{Cl}_{0.11})_{\Sigma=1}$.

Gem-quality afghanite is quite rare, although the Winter 2003 Gem News International (GNI) section (pp. 326–327) documented some cabochons from Badakhshan containing conspicuous lazurite inclusions. Haiüyne is likewise uncommon in gem quality, and facetable material is principally known from Germany (see, e.g., L. Kiefert and H. A. Hänni, “Gem-quality haiüyne from the Eifel District, Germany,” Fall 2000 *Gems & Gemology*, pp. 246–253).

Some of Mr. Hashmi’s rough afghanite was sufficiently large and transparent to facet, so he had two stones cut by John Bradshaw (Coast-to-Coast Rare Stones International, Nashua, New Hampshire): a 0.34 ct emerald cut and a 0.79 ct modified triangular step cut (figure 13). To stabilize the larger stone and improve its transparency, Mr. Bradshaw filled the fractures with an epoxy resin.

Both faceted afghanites were characterized by standard gemological techniques. These samples had intense blue to moderate blue pleochroism, refractive indices of 1.530–1.538 (birefringence 0.008), and SG values of 2.51 (larger stone, determined hydrostatically) and 2.54 (smaller stone; obtained by DiaVision, a noncontact optical measuring device that was used to calculate SG based on the measured weight and calculated volume, when the hydrostatic method failed due to persistent gas bubbles). The stones were inert to long-wave UV radiation, and had an inert to weak red reaction to short-wave UV (except for very weak to moderate yellowish white fluorescence confined to the fractures in both stones). A desk-model spectroscope showed a weak absorption band at approximately 590 nm. Our RI and birefringence values are somewhat higher than the data reported for afghanite in the Winter 2003 GNI entry and by R. V. Gaines et al. (*Dana’s New*



Figure 12. These afghanite (2.0 g, left) and haiüyne (0.9 g, right) samples are representative of rough material from Badakhshan, Afghanistan, that was purchased in the Peshawar mineral market in 2006–2007. Photo by Robert Weldon.

Mineralogy, John Wiley & Sons, New York, 1997, p. 1634). The SG values determined for this report are lower than those in Gaines et al. (1997), but comparable to those in the Winter 2003 GNI entry.

The smaller stone contained parallel breaks (afghanite has one perfect cleavage) and transparent crystals identified as diopside by Raman microspectroscopy. The larger sample had transparent two-phase inclusions that contained a dark solid material (figure 14, left) as well as colorless prisms (figure 14, right); unfortunately, they were too deep in the stone to be identified by Raman analysis. In both stones, however, the dominant internal features were fractures with evidence of enhancement. Although

Figure 13. Faceted afghanite is extremely rare. These stones from Badakhshan weigh 0.79 and 0.34 ct. Photo by Robert Weldon.





Figure 14. The interior of the 0.79 ct afghanite featured two-phase inclusions that each contained a dark solid grain (left). The stone also hosted a few colorless prisms (right). Photomicrographs by D. M. Kondo; field of view 1.5 mm for both.

Mr. Bradshaw had only filled the fractures in the larger stone, he indicated that the residue in the untreated stone might be due to the “soaking off” process, in which the epoxy used to attach the stone to the dop stick was dissolved by immersion in methylene chloride.

Polarized ultraviolet-visible-near infrared (UV-Vis-NIR) absorption spectroscopy of both samples showed distinct bands at approximately 370, 590, and 895 nm. These bands are quite similar to those documented in häüyne by Kiefert and Hänni (2000). The band at 590 nm is responsible for the blue color. In both of our samples, energy-dispersive X-ray fluorescence (EDXRF) spectroscopy showed major amounts of Si, Al, Ca, K, S, and Cl, which are expected for afghanite, as well as traces of Sr and Ba.

By coincidence, two faceted examples of häüyne from Badakhshan were seen at GIA in 2006–2007. In August 2006, Brad Payne (The Gem Trader, Grand Rapids, Michigan) submitted a 1.21 ct stone to the GIA Laboratory for an identification report (figure 15, left). He had purchased the rough as afghanite, but after cutting the stone he noted properties that were inconsistent for this mineral. The GIA Laboratory recorded the following characteristics: color—greenish blue, with no pleochroism; RI—1.499; optic character—singly refractive; hydrostatic SG—2.44; fluorescence—moderate-to-strong orange to long-wave UV radiation and very weak orange to short-wave UV; and a cutoff at ~450 nm and an absorption band at 600 nm visible with the desk-model spectroscope. These properties are

comparable to those reported for häüyne by Kiefert and Hänni (2000), except for the greener color. Microscopic examination revealed cleavage fractures and slightly flattened whitish crystalline inclusions. EDXRF spectroscopy showed major Si, Al, Ca, Na, K, S, and Cl, which are consistent for both häüyne and afghanite. However, the Raman spectrum provided the best match for häüyne.

Then, in early 2007, Dudley Blauwet (Dudley Blauwet Gems, Louisville, Colorado) sent a 0.92 ct oval cut from Badakhshan to GIA for examination (figure 15, right). He had obtained the piece of rough in December 2006 in Peshawar; he also purchased similar material there in June 2006 and November 2007. The 0.92 ct oval cut was similar in color to the stone from Mr. Payne, but brighter, and Raman analysis of a fragment from the same piece of rough by Dr. Robert Downs (Department of Geosciences, University of Arizona, Tucson) gave a spectrum that was identical to that of Mr. Hashmi’s häüyne. So far Mr. Blauwet has cut 114 of these häüynes (total weight 16.89 carats), and he noted a particularly good demand for this unusual brightly colored gem in the Japanese market.

David M. Kondo
GIA Laboratory, New York
Brendan M. Laurs
Eric Fritz
Denver, Colorado

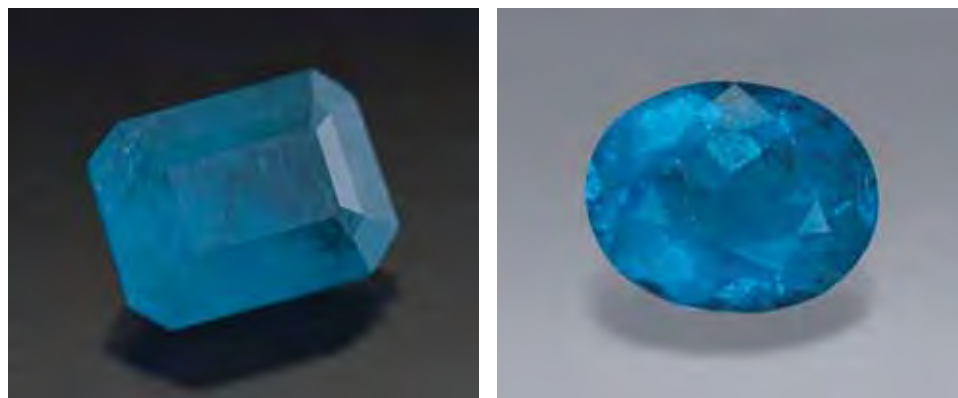


Figure 15. Faceted häüyne from Badakhshan has a distinctive bright greenish blue color, as shown by this 1.21 ct emerald cut (photo by Brad Payne) and 0.92 ct oval (photo by Robert Weldon).



Figure 16. This 0.81 ct piece of light blue rough, originally sold as tanzanite, proved to be manganaxinite. Photo by J.-M. Arlabosse.

A blue manganaxinite. While inspecting a parcel of rough tanzanite, one of these contributors (J-MA) noticed a pale blue sample (figure 16) that stood out from the others because of its moderate-to-strong orange-red fluorescence to long-wave UV radiation (the other pieces were inert). The sample's refractive indices, measured on a polished face, were $n_{\alpha} = 1.665$, $n_{\beta} = 1.672$, and $n_{\gamma} = 1.679$, yielding a birefringence of 0.014, but it was difficult to determine whether the optic sign was biaxial positive or negative. We measured a specific gravity of 3.24 and observed distinct trichroism (blue to brown to purple).

These results were not consistent with zoisite, but instead suggested a member of the axinite group. While kornerupine has similar RI and SG ranges and may also fluoresce orange to long-wave UV, it has different pleochroism. The color was zoned in two faint blue bands, and there were no noticeable inclusions. With a handheld spectroscope, the sample showed only one weak sharp line at about 415 nm. This indicated that it contained Mn^{2+} , so we speculated that it might be manganaxinite. By comparison, a nongem reference sample of blue magnesio-axinite from Tanzania had similar properties, including red fluorescence to long-wave UV, but no 415 nm line. In addition, faceted Tanzanian magnesio-axinite with similar properties (orangy pink UV fluorescence and a 410 nm line) was reported recently (see Winter 2007 GNI, pp. 373–375); those samples were also found in a parcel of tanzanite.

To confirm the identity, we performed quantitative chemical analysis using a JEOL 5800 scanning electron microscope (SEM) with a high-resolution Princeton Gamma Tech IMIX-PTS germanium detector. The results were consistent with axinite: 6.9 wt.% MnO, 2.7 wt.% MgO, and only 0.7 wt.% FeO. The Mn/Mg ratio (~1.5) clearly classified this sample as manganaxinite. Using long count times, we also detected approximately 0.1 wt.% V_2O_5 , as well as traces of chromium that were too small to be quantified.

The UV-Vis absorption spectrum (figure 17) was dominated by a broad band with a maximum at about 597

nm, creating a transmission window in the blue region at about 475 nm. There were also two weak sharp bands at 355 and 368 nm, a moderate sharp band at 413 nm (confirming the handheld spectroscope observations) with a shoulder at 421 nm, and two weak broad bands at approximately 515 and 733 nm. These sharp peaks and the weak broad bands could all be due to Mn^{2+} (R. G. Burns, *Mineralogical Applications of Crystal Field Theory*, 2nd ed., Cambridge University Press, 1993), but they were too weak to affect the color. The broad band around 597 nm is probably from V^{3+} . Even if Cr^{3+} was present, no distinct Cr^{3+} -forbidden transitions could be detected at around 700 nm.

The orange-red fluorescence appeared to be zoned, with a weaker emission in the bluer parts of the sample. The reaction was too weak to obtain a fluorescence spectrum, and we can only hypothesize that its origin might be Mn^{2+} , with possibly a red component imparted by Cr^{3+} .

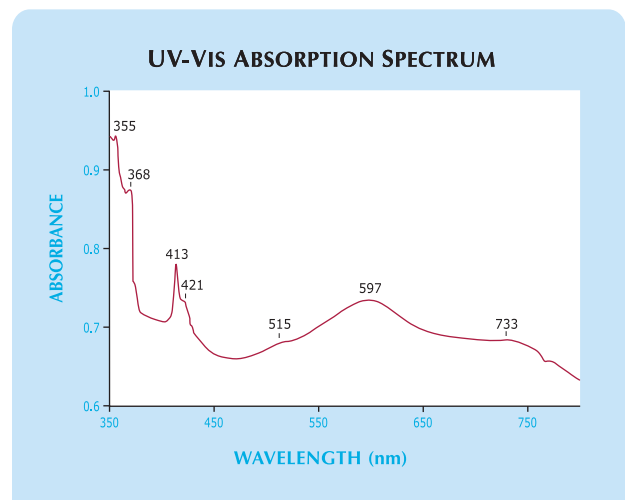
To our knowledge, this is the first report of manganaxinite colored by vanadium. It is also surprising to have two gem materials with such similar properties—the manganaxinite described here and the magnesio-axinite in the Winter 2007 GNI entry—recently appearing in parcels of tanzanite.

Jean-Marie Arlabosse (webmaster@geminterest.com)
Cagnes-sur-Mer, France

Benjamin Rondeau
IMN, University of Nantes, France

Emmanuel Fritsch

Figure 17. The UV-Vis absorption spectrum of the blue manganaxinite shows a broad band with a maximum at approximately 597 nm (due to V^{3+}) that accounts for the color. The sharp peaks at 355, 368, 413, and 421 nm could be due to Mn^{2+} , as could the two broad bands at 515 and 733 nm.



Gem news from Myanmar. From mid-2007 to early 2008, this contributor received information on several new gem occurrences in Myanmar, as described below.

Rubies have been found approximately 32 km north of Namya (Nanyaseik), at a locality called Nam Phyu. This may represent an extension of the Namya deposit, to which the rubies show equivalent quality.

Sapphires have been rediscovered near Mong Ngen village in the Mong Htak township of eastern Shan State. A map published in 1900 (no. 93 O/2) showed a sapphire mine near Mong Ngen, which is located at coordinates 21°40'00" N, 99°50'30" E, at ~1420 m elevation. The sapphires recently found were recovered from a hillside, a paddy field, and a stream. Approximately 15 cabochons and rough samples were examined by this author, and some had been heat treated with a charcoal fire in a clay oven used for home cooking. The heated stones (both rough and cut) weighed ~0.5–1.5 ct and ranged from 40 × 23 mm to 54 × 34 mm. After heating for four hours, dark blue samples changed to medium blue, and greenish blue samples turned light greenish blue. Pale purplish blue and particolored stones were also seen. The largest piece was a 7.5 ct partially polished dark blue *trapiche sapphire* with white "arms." Internal features consisted of color zoning, small colorless inclusions, vague fluid-filled feathers, and parting lines. Some of the sapphires showed prismatic faces. Associated pebbles consisted of quartzite, quartz, and garnet.

Gem-quality *trapiche corundum* has been found in the alluvial gold deposits of Zayatkyin near Mogok, 113 km by road from Mandalay. The material is being sold in the Bogyoke market in Yangon. The corundum consists of irregular pyramidal crystals that are cut in half to make low-domed cabochons. The crystals seen to date by this author range up to about 9 g and measure up to 2.3 × 2.2 cm. The cabochons seen range from 5 to 11 ct and measure 1.2–1.6 cm in diameter and 0.3–1.3 mm thick. They show dark blue and light gray sectors that are neither uniform nor symmetrical. Parting lines, fractures, and small solid inclusions were observed with the microscope.

Green tourmaline is being mined from coarse-grained marbles between Pawn Chaung and the Salween River, southeast of Loikaw (capital of Kayah State). These tourmalines have been referred to as Saw La Phaw (or Loi-Kaw "emerald"; see T. Hlaing, "Hsa-Taw green tourmaline," *Australian Gemmologist*, Vol. 18, No. 11, 1994, pp. 352–353). A piece of marble containing this tourmaline was examined by the author and revealed no additional minerals. The tourmaline was dark green and showed well-developed rhombohedral faces. Microscopic examination revealed parallel tubes and color zoning.

Granitic pegmatites containing *quartz*, *topaz*, *aquamarine*, *amazonite*, *garnet*, and *fluorite* have been found in the Pyethkaye mountain range in the Mandalay region, near coordinates 21°13'40" N, 96°12'30" E. This mountain range attains an elevation of 1094 m and consists of a large batholith measuring 70 km in a north-south direction and

25 km wide. Approximately 50 major pegmatite dikes have been located, striking north-south and measuring up to 150 m long and 4 m wide.

Diamonds were recovered from the Irrawaddy River near Shwegu in southern Kachin State. Gem-quality crystals have ranged up to 3 mm. This contributor also encountered a single 0.65 ct pale yellow hexoctahedral diamond crystal that was purchased in Mong Hsu. Diamonds have recently been reported from the Salween River near Mong Hsu.

U Tin Hlaing
Dept. of Geology (Retired)
Panglong University, Myanmar

Gems on the market in Taunggyi, Myanmar, 1990–2007.

Since 1990, this contributor has conducted regular gemology classes and provided gem identification services for local dealers, retailers, and buyers in Taunggyi, Myanmar (160 km southeast of Mandalay). The clients typically come from the surrounding towns of Kalaw, Shwenyaung, Nyaungshwe, Ho Pong, Lawksawk, and Hsiseng (near Kayah State). Following is a review of the gem materials identified in the market during this period.

Single stones were encountered most often, although jewelry and unprocessed metal ore (gold and other ores) were sometimes presented for identification. Of all the stones tested, 62% were ruby, of which 58% were synthetic (Verneuil) and 42% were natural, mostly of Mong Hsu and Mogok origin. Sapphire (blue and colorless) comprised 27% of the total; over 90% of these proved to be Verneuil synthetics. However, natural colorless sapphires were more common than colorless synthetics.

Other gems seen were quartz (smoky, citrine, and brown chalcedony of unknown origin); peridot from Mogok; pinkish red spinel crystals of good color but small sizes (<1 ct); blue synthetic spinel with a color simulating aquamarine, available in large sizes (one semi-cut from a boule); garnets of good size (>10 ct), though probably not of Burmese origin, as the color was different from local material; topaz; GGG (imitating peridot, although the color was not convincing); YAG; and cubic zirconia. Glass imitations were common and often of large size.

U Tin Hlaing

Large gem pocket discovered at the Oceanview mine, San Diego County, California.

In early fall 2007, a significant pocket was uncovered at the Oceanview mine in the Pala District of San Diego County. This mine is a historic source of quartz and morganite, and is adjacent to the Elizabeth R mine, which has produced tourmaline, kunzite, and other gems (see Fall 2001 GNI, pp. 228–231). The Oceanview was sold in 2000, and current owner Jeff Swanger is mining the pegmatite with a team comprised of Mark Baker, Steve Carter, Phil Osborn, and Peter Renwick. The group had spent more than six years tunneling into the pegmatite with little success. After penetrating 400 feet

into the dike, however, the crew noted some promising mineralization and decided to carefully explore that zone.

On September 22, the miners uncovered the first part of what has become known as the 49er pocket (figure 18). That day happened to be Mr. Swanger's 49th birthday, and this fact along with the mining spirit that prevailed during the 1849 California gold rush inspired the name.

Over the next several months, the 7+ m × 1.5–2 m pocket yielded many kilos of material, including several dozen very fine mineral specimens, especially aquamarine (figure 19) and morganite. In addition, many collector-quality specimens of quartz (pale smoky citrine), albite (clevelandite), and microcline have been recovered. The operation is chiefly aimed at recovering mineral specimens, but some cuttable material has been produced as well; indeed, Mr. Swanger estimates that the rough will yield a minimum of 50,000 carats of polished pale smoky citrine. Although the 49er Pocket appears to be worked out, numerous side pockets have been found (containing quartz, feldspar, and mica), and mining is currently ongoing as of March 2008. Further updates will be posted at <http://digforgems.com>.

Mark Mauthner (mark.mauthner@gia.edu)
GIA Museum, Carlsbad

Green sodic plagioclase from East Africa. Green gem plagioclase is known mainly from Oregon (labradorite: e.g., C. L. Johnston et al., "Sunstone labradorite from the Ponderosa mine, Oregon," Winter 1991 *Gems & Gemology*, pp. 220–233) but has also been reported from China/Tibet and the Democratic Republic of the Congo (andesine-labradorite: see Winter 2005 GNI, pp. 356–357, and references therein). In mid-2007, we were informed about another source of green gem plagioclase—Tanzania—by G. Scott Davies of American-Thai Trading (Bangkok). Mr. Davies donated five faceted stones (1.62–2.70 ct) and three pieces of rough (2.41–6.31 g; e.g., figure 20) to GIA for examination. He indicated that he had obtained 2.5 kg of rough in June 2007, and that stones faceted from this material are seldom larger than 3 ct while those weighing more than 5 ct are quite unusual.

Examination of the five cut stones gave the following properties: color—light green; pleochroism—none to very weak (light green and colorless); RI— $n_{\alpha} = 1.531\text{--}1.533$ and $n_{\gamma} = 1.541\text{--}1.543$; birefringence—0.010–0.012; optic character—biaxial with no sign to biaxial positive; hydrostatic SG—2.63–2.65; inert to both long- and short-wave UV radiation; and no absorption features visible with the desk-model spectroscope. These properties are similar—but with slightly lower RI and SG values—to those published for oligoclase by M. O'Donoghue (Ed., *Gems*, 6th ed., Butterworth-Heinemann, Oxford, UK, 2006, p. 261): RI— $n_{\alpha} = 1.533\text{--}1.543$, $n_{\gamma} = 1.542\text{--}1.552$; birefringence—0.009; optic character—biaxial negative; SG—2.64–2.66. Microscopic examination revealed cleavage fractures, polysynthetic twinning, white "woolly" inclusions, and low-relief wafer-thin transparent crystals that were surrounded by



Figure 18. This view of an early part of the 49er pocket at the Oceanview mine shows smoky citrine crystals being excavated by Peter Renwick (left) and Mark Baker (right). Photo by M. Mauthner.

Figure 19. The 49er pocket has produced some fine crystals of aquamarine (here, 4.5 cm tall) on a matrix of albite (clevelandite). This specimen was collected in October 2007. Photo by M. Mauthner.





Figure 20. These light green feldspars from Tanzania, weighing 2.41–6.31 g (rough) and 1.94–2.38 ct (faceted), were identified as oligoclase. GIA Collection nos. 37517 (rough) and 37518 (faceted); photo by G. Scott Davies.

microfractures and showed spectral colors when tilted. The visual appearance of both the latter types of inclusions suggested they were albite, and Raman microspectroscopy analysis also proved consistent with albite.

Plagioclase feldspars, which include oligoclase, form a solid-solution series from albite ($\text{NaAlSi}_3\text{O}_8$ in its purest form) to anorthite ($\text{CaAl}_2\text{Si}_2\text{O}_8$). Their composition is typically represented by the percentage of the anorthite content ($\text{An}_{\%}$); albite varies from An_0 to An_{10} and anorthite from An_{90} to An_{100} , while oligoclase ranges from An_{10} to An_{30} . RI and SG values systematically increase with anorthite content, while optic sign varies cyclically (figure 21). It is therefore possible to estimate the anorthite content of a sample using these relationships. Our observed values resulted in ranges of $\sim\text{An}_6$ – An_{10} when using n_α , $\sim\text{An}_6$ – An_{10} for n_β , and $\sim\text{An}_4$ – An_{16} for SG, all of which correlate to albite-oligoclase compositions. Further, in conjunction with the RI and SG values, the optic sign (biaxial with no sign to biaxial positive) indicated a composition less than $\sim\text{An}_{17}$.

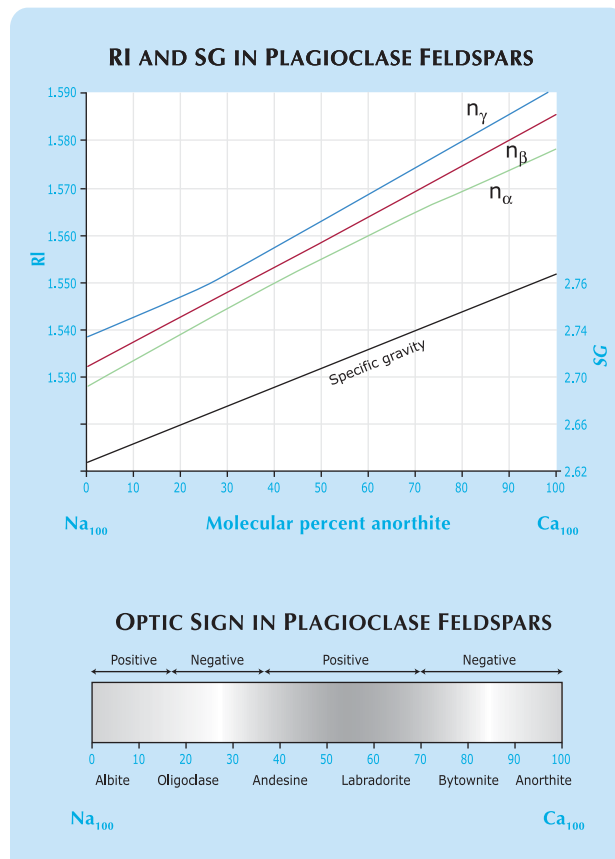
Quantitative chemical analyses were performed by electron microprobe at the University of New Orleans (three rough samples) and at the University of Oklahoma (two of the three rough samples). The data yielded average values of $\sim\text{An}_{10}$ – An_{14} , indicating that the samples were oligoclase or had compositions corresponding to the albite-oligoclase boundary. These values fall within the range of anorthite contents determined from the SG and optic sign, but only border on those estimated from the RIs.

EDXRF analysis of the faceted stones detected major amounts of Na, Al, Si, and Ca; minor K, Fe, and Sr; and traces of Mn, Zn, Ga, Ba, and Pb. LA-ICP-MS analysis corroborated the presence of these elements, and additionally detected Be, B, Mg, and Ti (Mg must be present in significant quantities to be detected by EDXRF, and any traces of Ti in the EDXRF results were obscured by the Ba signal).

None of these elements are unexpected in feldspars.

The LA-ICP-MS analysis did not detect any Cu, which is a known chromophore in green gem labradorite (A. M. Hofmeister and G. R. Rossman, "Exsolution of metallic copper from Lake County labradorite," *Geology*, Vol. 13, 1985, pp. 644–647). Another chromophore in green feldspar—Pb—was present in the oligoclase samples in only very small amounts (~ 18 – 56 ppm). However, the depth of green color in amazonite (and the blue color in plagioclase) appears to be related to a combination of Pb, radiation, and water content (A. M. Hofmeister and G. R. Rossman, "A spectroscopic study of irradiation coloring of amazonite: Structurally hydrous, Pb-bearing feldspar," *American Mineralogist*, Vol. 70, 1985, pp. 794–804; A. M. Hofmeister and G. R. Rossman, "A spectroscopic study of blue radiation coloring in plagioclase," *American Mineralogist*, Vol. 71, 1986, pp. 95–98). FTIR spectroscopy confirmed the presence of a hydrous component (as structural OH groups) in the feldspar. Oriented UV-Vis-NIR absorption spectra (figure 22) showed a transmission win-

Figure 21. The optical properties and specific gravity of plagioclase feldspars vary with anorthite content. Reproduced, with permission, from O'Donoghue (2006), p. 245.



dow located at ~500–530 nm, depending on the direction, which is responsible for the green color. An absorption band was centered at about 615 nm in the β direction that had a full width at half maximum (FWHM) of ~4800 cm^{-1} and an intensity of 0.24 cm^{-1} . These characteristics are similar to those presented for blue plagioclase by Hofmeister and Rossman (1986), suggesting a similar cause of color related to the presence of traces of Pb and water combined with exposure to radiation. The color of this feldspar was represented as natural. We have no reason to believe that it has been laboratory irradiated, and its coloration is consistent with that expected for material exposed to natural radiation in the earth.

A similar light green color was documented in some Tanzanian oligoclase sunstone that was described in the Summer 2002 GNI section (pp. 177–178). It is possible that the material described here came from the same area (northwest of Arusha, near the border with Kenya), but simply lacks the hematite inclusions that were observed in the sunstone.

Furthermore, at the 2007 Tucson gem shows, one of these contributors (BML) was shown some attractive pale slightly bluish green plagioclase from Kenya (figure 23) by Bruce Bridges and Jim Walker (Tavorite USA Inc., Collegeville, Pennsylvania). This material has been known since the mid-1980s from Kioo Hill in the Sultan Hamud area, about 100 km southeast of Nairobi (C. R. Bridges et al., “Ein neuer Edelstein aus der Feldspat-Familie [A new gemstone in the feldspar family],” *Zeitschrift der Deutschen Gemmologischen Gesellschaft*, Vol. 33, No.

Figure 22. The oriented UV-Vis-NIR absorption spectra for one of the rough green oligoclase samples show a transmission window located at ~500–530 nm. Sample thickness in each direction: $\alpha = 22.8$ mm, $\beta = 10.9$ mm, $\gamma = 6.1$ mm.

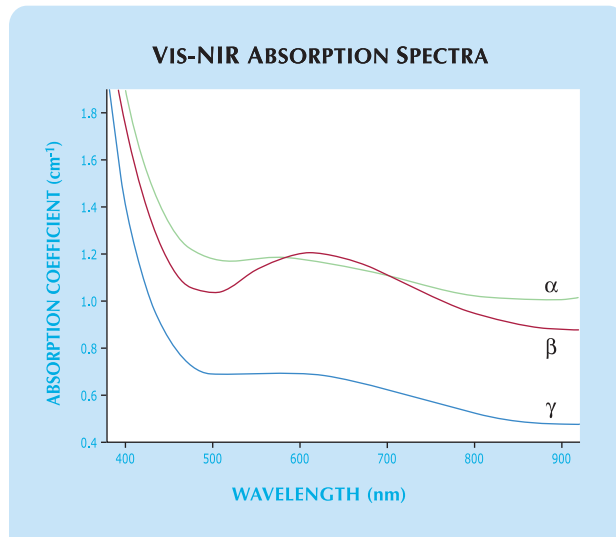


Figure 23. This selection of slightly bluish green plagioclase from Kenya weighs 1.84–15.72 ct. Photo by Robert Weldon.

3–4, 1984, pp. 104–113; C. R. Bridges et al., “A Kenyan gemstone from the feldspar family: Further observations,” *Australian Gemmologist*, Vol. 17, No. 5, 1990, pp. 177–183). These articles documented samples of pale blue-to-green plagioclase that were typically albite, with compositions ranging from An_5 to An_{11} . Although their gemological properties were similar to those described here for the Tanzanian oligoclase, the presence of vermiculite inclusions was indicated by Bridges et al. (1989) as evidence of origin from Kioo Hill. No explanation for the coloration was provided. According to Bruce Bridges, some new production of this feldspar from Kioo Hill occurred in early 2005. The color ranged from near colorless to pale green, and Mr. Bridges knew of faceted stones ranging up to 30 ct.

Karen M. Chadwick and Christopher M. Breeding
GIA Laboratory, Carlsbad

William B. (Skip) Simmons and Alexander U. Falster
Brendan M. Laurs

A blue topaz with 2500+ facets. Terry Lee Martin, a gemstone artist and owner of 5Cs Collectors Gems in Seattle, Washington, recently showed the *G&G* editors a selection of gems he had cut with an unusually large number of facets. Among them was a 16.90 ct blue topaz (figure 24) that he estimates to have about 2,530 facets (the exact number is unknown, as he lost count near the conclusion of the stone). Mr. Martin has completed more than 200 similar gems, though the topaz is by far the most complex. Only one gem is cut from each design, and each can take 20–60 hours to complete. Mr. Martin uses conventional faceting techniques and equipment, but he needed several months of practice to learn how to polish facets that are sometimes less than 0.1 mm across.

One consequence of the large number of facets is a very small table. The optical effects produced by the abundance of tiny facets ranges from billowy light under the crown to micropatterns of light and dark areas that are

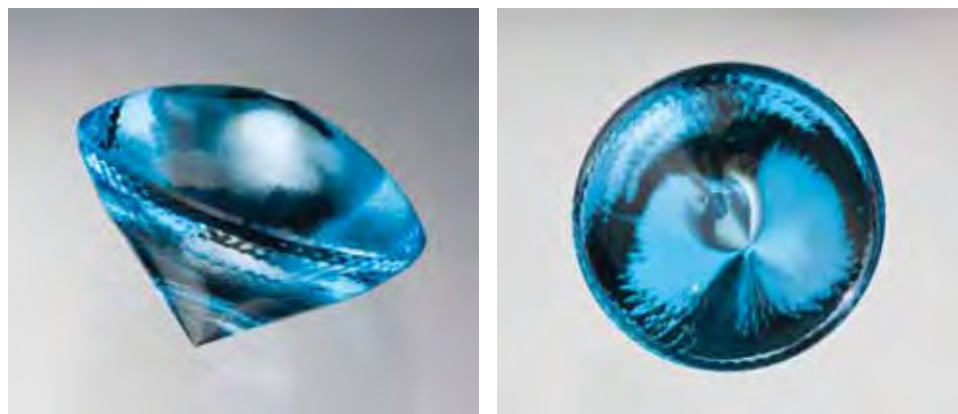


Figure 24. This unique 16.90 ct topaz, created by gem artist Terry Martin, has more than 2,500 facets. Photos by Robert Weldon.

quite unlike those seen in stones faceted with standard cutting styles (e.g., figures 24 and 25).

Thomas W. Overton (toverton@gia.edu)
GIA, Carlsbad

SYNTHETICS AND SIMULANTS

An imitation “elephant pearl.” The “elephant pearl,” or *gajamuthu*, is an ancient and much-revered object in Indian and Sri Lankan culture. Its possession is commonly believed to increase one’s success in life. Elephant pearls are rounded concretions of dentin that are recovered from the soft tissue pulp within tusks of African and Asian elephants as well as the extinct woolly mammoth (B. Mann and G. Brown, “Elephant pearls: True or false?,” *Australian Gemmologist*, Vol. 22, No. 11, 2006, pp. 503–507; G. Brown, “Rare ivories—Challenging identifications,” presentation to the 2007 Federal Conference of the Gemmological Association of Australia, May 19, Hobart, Tasmania, www.australiangemmologist.com.au/images/rareivories.pdf).

The Dubai Gemstone Laboratory recently received for identification a 642 ct opaque, banded, yellow-to-brown and

white sample that the client represented to be an elephant pearl. When viewed from the sides (figure 26, top left and center), the sample showed a near-parallel banded structure; however, when viewed from the bottom (figure 26, top right), the thin white bands appeared wavy. In contrast, genuine elephant pearls consist of a rounded mass of dentin (only) that shows a curved growth layer structure; see the right-hand photo on p. 6 of Brown (2007). In addition, the thin wavy white bands in this sample suggested the appearance of a molar tooth structure from an Asian elephant.

Standard gemological testing revealed spot refractive indices ranging from ~1.50 to 1.55 (the typical range for organic gem materials) and a hydrostatic SG of 1.91. Long-wave UV fluorescence was weak-to-moderate chalky bluish white, with the strongest reaction from some portions of the white bands (figure 26 second row); short-wave UV fluorescence was similar but weaker. No distinguishing spectrum was seen with the desk-model spectroscope. X-radiography in the three directions (figure 26, bottom row) showed significant differences in the opacity to X-rays of the various bands. In addition, microscopic examination with reflected light clearly revealed polishing marks on the surface (figure 27), which indicated that it had been fashioned. EDXRF chemical analysis detected Ca and P as main components, along with minor amounts of Ti and Fe, and traces of Mn, Zn, and Sr. By comparison, the pure dentin of a genuine elephant pearl should show the same range of RI and SG values, moderate chalky bluish white fluorescence to long-wave UV, no significant differences in opacity to X-rays, no obvious polishing marks on the surface, and the same EDXRF results as reported here except no Ti, which was mainly detected in areas containing the white enamel bands.

The structural characteristics and gemological properties of this sample were consistent with those reported for imitation elephant pearls by Mann and Brown (2006). Consequently, it was identified as a manufactured object fashioned from the molar tooth of, most likely, an Asian elephant.

Sutas Singbamroong (sssutas@dm.gov.ae)
and Nazar Ahmed
Dubai Gemstone Laboratory
Dubai, United Arab Emirates

Figure 25. Shown here are five other gems cut by Mr. Martin, from left: a 1.50 ct, 601-facet sunstone; a 5.30 ct, 469-facet topaz; a 13.65 ct, 781-facet sunstone; a 2.45 ct, 474-facet sunstone; and a 2.95 ct, 561-facet sapphire. Photo by Robert Weldon.



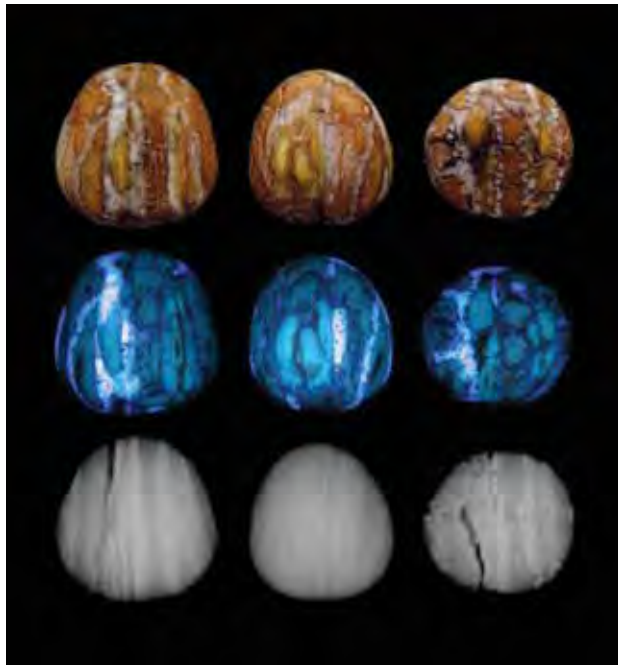


Figure 26. Side (top left and center) and bottom (top right) views of the imitation elephant pearl showed a varying banded structure. Exposure to long-wave UV radiation (second row) gave a variety of reactions that correlated to the structure of the piece; X-radiography also revealed significant differences in its opacity to X-rays (third row). Composite photo by S. Singbamroong, © Dubai Gemstone Laboratory.

An interesting synthetic sapphire. Natural and synthetic gem materials are commonly differentiated on the basis of their microscopic features. Often, however, a natural stone may show characteristics resembling those of synthetic material and vice versa (see, e.g., G. Choudhary and C. Golecha, "A study of nail-head spicule inclusions in natural gemstones," Fall 2007 *Gems & Gemology*, pp. 228–235; and GNI, Fall 2005, pp. 265–266; Summer 2006, pp. 185–186; Summer 2007, p. 177). This contributor recently encountered another such specimen that was submitted to the Gem Testing Laboratory of Jaipur, India.

The sample was a 4.78 ct pear-shape mixed cut, with a brownish orange color similar to that seen in beryllium-diffused sapphire (figure 28). Standard gemological properties (RI and SG) were consistent with corundum, and fine lines in the red region were easily visible in the desk-model spectroscope, indicating the presence of chromium.

With magnification, surface-reaching fingerprint-like inclusions (figure 29, left) were observed. They had a whitish appearance, suggesting they contained a foreign substance, as is commonly seen in corundum exposed to high-temperature heating. A trail of dot-like inclusions giving the impression of a broken (melted) needle (figure 29, right) was also visible, as were fine scattered pinpoints resembling gas bubbles. These features also indicated that



Figure 27. Magnification revealed polishing marks on the surface of the imitation elephant pearl. The object was apparently fashioned from the molar tooth of an elephant, consisting of brown cementum, white enamel, and yellow dentin. Photomicrograph by S. Singbamroong, © Dubai Gemstone Laboratory; magnified 10 \times .

the sapphire had been exposed to high-temperature heat treatment.

Immersion in methylene iodide revealed a colorless girdle area, with most of the color concentrated toward the center (figure 30, left). As the stone was rotated and viewed from various directions, we observed wide color zones that were separated by near-parallel curved boundaries (figure 30, right), which are typical for flame-fusion synthetics. Variations in the color intensity of the bands are consistent with a darker core and paler rim in the original boule. When the sample was viewed in the optic axis direction between crossed polarizers, strong Plato lines confirmed that it was a flame-fusion synthetic. Exposure to short-wave UV produced strong

Figure 28. This 4.78 ct synthetic sapphire shows a brownish orange color similar to that observed in beryllium diffusion-treated corundum.



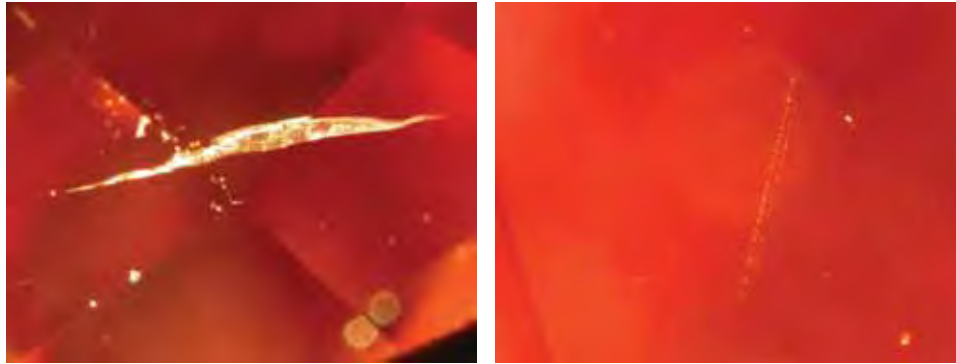


Figure 29. The synthetic sapphire contained a surface-reaching fingerprint-like inclusion (left) and a row of dot-like inclusions resembling a melted needle (right); the latter may also be observed in flame-fusion synthetics. Photomicrographs by G. Choudhary; magnified 30× (left) and 65× (right).

chalky blue fluorescence that was mainly restricted to areas at or near the surface, as would be expected for a heat-treated flame-fusion synthetic sapphire.

EDXRF qualitative chemical analyses revealed the presence of Ca, Ti, Cr, Fe, and Zn as trace elements. Zn was present in unusually high amounts compared to the other impurities.

The presence of surface-reaching fingerprint-like inclusions and rows of dot-like inclusions, along with the surface-related fluorescence, indicated that the synthetic sapphire had undergone some sort of heat treatment. This sample's unusual combination of features could have led to a misidentification, but careful examination with multiple techniques gave useful clues to its synthetic origin.

Gagan Choudhary (gtl@gjepcindia.com)
Gem Testing Laboratory, Jaipur, India

TREATMENTS

Lead glass-filled color-change sapphire. Lead glass-filled rubies were first seen in the market in 2004. Much research has since been conducted to classify these rubies correctly, and the treatment is now well understood. Currently, however, such fillings are being applied to sapphires as well.

Recently, the Gem Testing Laboratory in Jaipur, India, encountered a 3.76 ct oval mixed cut sapphire with numerous eye-visible fissures. The RI and SG values were both

consistent with corundum. The stone appeared brownish green in daylight and fluorescent light (figure 31, left) and brownish purple in incandescent light (figure 31, right). Under long-wave UV radiation, it fluoresced weak reddish orange; it was inert to short-wave UV. Observation with the desk-model spectroscope showed a doublet in the red region (typically associated with chromium in corundum), a weak absorption in the orange-yellow region, and a strong band in the blue region at ~450 nm, probably due to iron.

With magnification, the surface-reaching cracks showed an obvious blue-to-violet flash effect, which changed to greenish blue as the stone was moved. The fractures also contained large, rounded, and highly reflective flattened gas bubbles (figure 32, left and center). In addition, white crystallites were observed in the filled cavities (figure 32, right). These features are consistent with those reported in lead glass-filled rubies (e.g., S. F. McClure et al., "Identification and durability of lead glass-filled rubies," Spring 2006 *Gems & Gemology*, pp. 22–34).

The presence of lead-glass filling in this sapphire was further confirmed by EDXRF analysis, which displayed a strong Pb peak. Other trace elements detected were Cr, Fe, and Ga, as expected in a color-change sapphire of natural origin.

This was the first time we have seen a lead glass-filled sapphire, and we would not be surprised to see the treatment applied to other sapphire colors in the future.

Gagan Choudhary

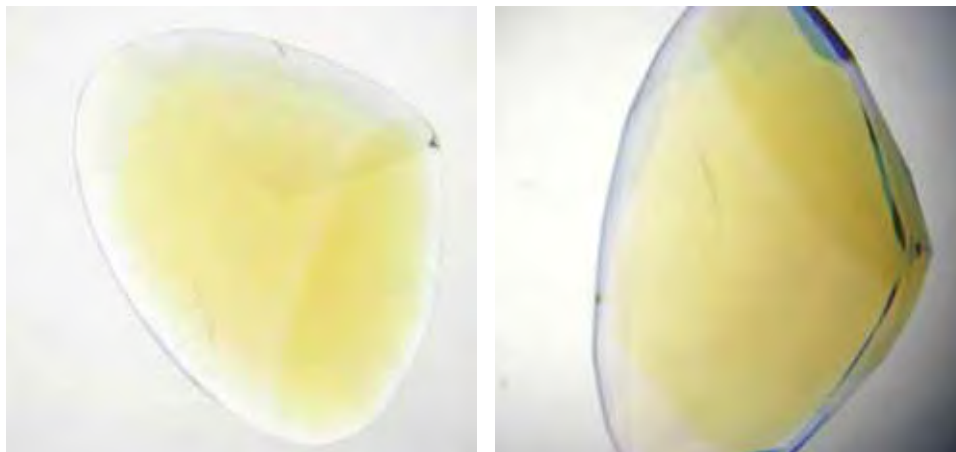


Figure 30. When immersed in methylene iodide, the sample showed a concentration of color toward the center, while the edges appeared colorless (left). This is a common result of beryllium diffusion treatment. In some directions, vague curved colored zones could be seen, indicating synthetic origin (right). Photos by G. Choudhary.



Figure 31. This 3.76 ct color-change sapphire (fluorescent light, left; incandescent light, right) proved to be lead-glass filled. Photos by G. Choudhary.

MISCELLANEOUS

Myanma Gem Emporium offerings for 1992–2007. For many years, the state-run Myanma Gem Enterprise (MGE) has held twice-yearly sales of gem materials produced in Myanmar. This contributor has summarized published sales records for the Myanma Gem Emporium from 1992 to 2007 (although some years are missing) for this report.

Jadeite sales were divided into three categories by quality: Imperial, Commercial, and Utility. Before 2000, jadeite was sold by competitive bidding only, but subsequently 43–92% of the total was sold by tender (i.e., sealed bidding). From 1992 to 2007, jadeite sold by competitive bidding comprised, by number of lots: Imperial 0.1–2%, Commercial 31–96%, and Utility 4–69%. These varying levels generally reflect the quality of material available from year to year. The tender lots offered from 2000 forward ranged from as little as 18% to as high as 48% Commercial, with the balance Utility (Imperial jade constituted less than 1%). Some recent Imperial jadeite lots offered included: two pieces weighing 1,040 kg, for a total reserve price of €1,368,000 (38th Emporium, 2001); 10 pieces weighing 176.6 kg, for a total reserve price of €1,530,000 (39th Emporium, 2002); and three pieces weighing 15 kg, for a total reserve price of €1,688,888 (44th Emporium, 2007). (Since 2002, reserve prices have been given in euros) In 2006, at the mid-year October Emporium,

a lot of Commercial jadeite weighing 1,040 kg was offered at a reserve price of €1,368,000. Approximately one-third of the lots sold at their reserve prices; other actual sale prices are not available.

Lot sizes (smallest and largest) and reserve prices of rough gem materials other than jadeite are summarized in table 1. In addition to ruby and blue sapphire, corundum included pink, yellow, purple, and colorless sapphires, as well as mineral specimens of ruby in marble. Also sold were aquamarine, danburite, diamond, diopside, fluorite, garnet, kyanite, lapis lazuli, moonstone, peridot, quartz (amethyst, citrine, and smoky, as well as quartz crystal specimens), scapolite, spinel, topaz, tourmaline (green), zircon, and parcels described as “assorted gems” (~1–3 carat parcels, usually >90% spinel). Spinel, aquamarine, zircon, peridot, danburite, and yellow sapphire are the highlights (in addition to ruby and sapphire) of most Emporiums in the nonjadeite section.

During the period 1992–1995, on average 500 jadeite lots were offered annually. From 2005 to 2007, this figure was 3,500, representing a seven-fold increase. By comparison, an average of 550 gem lots were offered in 1992–1995. During 2005–2007, that figure fell to 250. Since 1992, gem lots have comprised as little as 2% to as much as 49% of the total lots offered, while jadeite lots comprised 51–98%.

Figure 32. The lead glass-filled fissures showed rounded (left) and flattened (center) gas bubbles, the latter often highly reflective, an important identifying feature for this treatment. Some whitish crystallites were also seen in a few cavities (right). Photomicrographs by G. Choudhary; magnified 45× (left and center) and 35× (right).



TABLE 1. Range of lot sizes and reserve prices for gem materials (other than jadeite) sold at the Myanmar Gem Emporium, 1992–2007.

Gem	Lot size ^a	Reserve price ^b
Aquamarine	94.64–215.9	\$1,000–5,750
Danburite	4.15–31.6	\$700–€2,000
Diamond	1.94–13.68	\$6,600–68,400
Diopside	7.0–14.55	€1,800–\$5,000
Fluorite	28.25	\$3,000
Garnet	10.38–14.7	\$1,000–€2,500
Kyanite	42.42	\$4,200
Lapis lazuli	21–75 kg	\$2,000–3,000
Peridot	29.45–232.2	\$1,500–58,050
Quartz		
Amethyst	239.96	\$5,000
Quartz crystals	3.5 kg	€1200
Ruby	1.22–7.4	€1,000–\$6,000
in marble matrix	317	€8,000
Sapphire		
Blue	2.38–22.30	€1,000–€45,000
Pink	7.7–33.96	\$4,500–€15,000
Yellow	15.62–77.0	\$2,000–€7,000
Purple	6.78–885	\$1,500–4,300
Colorless	12.8–36.68	\$2,300–3,000
Scapolite	118.45	\$2,000
Spinel	8.37–52.32	\$1,000–50,000
Topaz	56.68–316.72	\$2,000–3,200
Tourmaline (green)	25.77	\$2,000
Zircon	21.98–48.9	\$2,000–10,000
Assorted	134.67–349.38	\$4,890–13,800

^a In carats, except where noted.

^b In US\$, except where noted.

Also sold in 2001 and 2002, as part of the jadeite tender, were a total of 25 parcels of petrified wood (*Ingyin*) from central Myanmar. Individual lots were offered at a reserve price of US\$1,000–1,500; these included parcels with a maximum of 470 pieces and a maximum weight of 2,420 kg.

U Tin Hlaing

CONFERENCE REPORTS

2008 Winter Conference on Plasma Spectrochemistry.

Approximately 600 participants from 30 countries attended this 15th biennial meeting sponsored by the ICP Information Newsletter Inc., which was held January 7–12 in Temecula, California. The conference addressed developments in spectrochemical analysis by inductively coupled plasma, direct coupled plasma, microwave plasma, glow discharge, and laser sources. More than 300 presentations covered the applications, fundamentals, and instrumental developments of plasma sources. A few of these were relevant to the gemological community and are summarized here.

In the keynote speech, **Dr. Detlef Günther** (ETH Zurich, Switzerland) discussed new understandings of the principles

behind LA-ICP-MS, such as transport and interface design, and their role in the method's overall performance. He also cited numerous examples of the technique's applications in various disciplines, including gemology. **Dr. Ingo Horn** (University of Hanover, Germany) discussed the application of UV femtosecond laser ablation–multi-collector ICP-MS in accurately measuring iron isotope ratios. Such ratios allow geologists to determine the formation conditions of iron-containing minerals.

Dr. Claude Dalpé (Royal Canadian Mounted Police, Forensic Science and Identification Services, Ottawa, Ontario) reported on the use of LA-ICP-MS to determine the provenance of rough diamonds. His research indicated that as many as 20 trace elements (most on the order of parts per billion) can be used to identify a rough diamond's country of origin. He also indicated, however, that diamond standards containing several different trace elements are very difficult to obtain. **This contributor** reported on the current applications of LA-ICP-MS in the gemological community, specifically in identifying natural versus synthetic materials, gem treatments (such as Be diffusion in corundum), and country of origin for various gem species. A poster presentation by **Dr. Christopher M. Breeding** (GIA Research, Carlsbad) described a normalization method for determining the chemical composition of plagioclase feldspars using LA-ICP-MS. Results from this method were in good agreement ($\pm 10\%$) with electron-microprobe data for the same samples.

*Andy H. Shen (andy.shen@gia.edu)
GIA Research, Carlsbad*

Gemological LA-ICP-MS User Group (GLIUG) workshop and meeting. This gathering, the first of its kind in the gemological community, was held January 6 at GIA in Carlsbad. Organized by researchers from the GIA Laboratory, its theme was "Analysis of trace elements in corundum using LA-ICP-MS."

The workshop featured four invited talks. **Dr. John Emmett** (Crystal Chemistry, Brush Prairie, Washington) gave a presentation on accuracy in trace-element analysis, in which he showed the effect that a 1 ppm Fe-Ti intervalence charge transfer (IVCT) pair can have on the apparent color of a blue sapphire. To detect such small variations in Fe or Ti concentration, he estimated that a chemical analysis with an accuracy of better than 15% is required. **Dr. Detlef Günther** (ETH Zurich, Switzerland) discussed the fundamentals of LA-ICP-MS and the application of ultraviolet femtosecond lasers to the analysis of gems. Some concepts that emerged were the importance of high precision and the need for a sample's absorption characteristics to be very similar to those of the standard. **Dr. George Rossman** (California Institute of Technology, Pasadena, California) discussed various nano-inclusions in gems. The chemical composition of nano-minerals can differ significantly from that of their host minerals, so a spot analysis such as LA-ICP-MS must account for this disparity. **Dr. Alan Koenig** (U.S. Geological

Survey, Denver, Colorado) reported the comparative results of ablating gems using 193, 213, and 266 nm laser emissions. He noted the superiority of the 193 nm laser in analyzing many gem materials. Dr. Koenig also discussed the USGS geological material standard program and some comparative studies on which GIA and USGS have collaborated.

Five other talks were given by **Dr. Ahmadjan Abduriyim** (Gemmological Association of All Japan, Tokyo), **Pierre Lefèvre** (SSEF Swiss Gemmological Institute, Basel), **Thanong Lee** (Gem and Jewelry Institute of Thailand, Bangkok), **Dr. Wuyi Wang** (GIA Research, New York), and **this contributor**. Each reported on the current status and future plans for LA-ICP-MS in their respective institutions, and the last two presenters also covered more specific topics. Dr. Wang presented detailed information on the corundum standards developed at GIA. This contributor discussed natural beryllium-containing inclusions in corundum. From these two presentations, many concerns were raised, including the importance of developing and sharing standards, comparing results with those obtained from other analytical techniques, analyzing gem samples at multiple laboratories, and having interested laboratories pursue certification by the International Association of Geoanalysts (IAG).

Andy H. Shen

First International Pearl Convention. This conference was held in Abu Dhabi, United Arab Emirates (UAE), November 19–20, 2007. Organized by the Dubai-based Pearl Revival Committee to raise the profile of natural pearls from the Persian Gulf (referred to locally as the “Arabian Gulf”) and to discuss related issues, the conference included a seminar dedicated to technical issues and a summit focused on production and marketing.

Kenneth Scarratt (GIA Thailand) described the wide variety of mollusks that can produce pearls, whether for mass production or expensive collectors’ items. He argued that the term *pearl* should be applied to both nacreous and non-nacreous materials, such as conch pearls. He also told participants to “keep their minds open” to the theory that pearls may nucleate on a grain of sand, and displayed X-radiographs of pearls with minuscule shells in their centers. **Elisabeth Strack** (Hamburg, Germany) pointed out that natural freshwater pearls come from numerous locations, including lesser-known ones such as northwest Russia. She also discussed terminology and taxonomy issues (e.g., the vast majority of pearl “oysters” are actually not classified biologically as oysters). Most saltwater cultured pearls in the market come from essentially one oyster genus, *Pinctada*. **Shigeru Akamatsu** (Mikimoto & Co., Tokyo) reviewed the history of pearl culturing. Among other issues, he discussed the present status of the Japanese akoya product, which is suffering from “red tides” and over-warm water temperatures. There are plans to move to a smaller but higher-quality production, mostly by reducing the number of pearl farms and the number of shells under cultivation to reduce stress on the animals.

Nicholas Sturman (Gem & Pearl Testing Laboratory,



Figure 33. These natural pearls, shown here on a shell from the host oyster *Pinctada radiata*, were recovered from the Persian Gulf. Photo by Nicholas Sturman.

Bahrain) reviewed pearl testing techniques, saying he prefers X-ray luminescence over measuring Mn content to separate freshwater from saltwater pearls. He emphasized the importance of proper X-radiography and the difficulty of identifying keshis. He also reminded the audience that production of natural pearls in the Persian Gulf (e.g., figure 33) is quite small today, with pearl fishing more a hobby than a commercial enterprise. For example, only about 4 kg were recovered in Kuwait in 2005. **Stephen Kennedy** (Gem Testing Laboratory of Great Britain, London) reviewed pearl treatments and their detection, noting that some “chocolate” pearls, for example, are created by the bleaching and subsequent dyeing of gray-to-black pearls.

These contributors pointed out the importance of unsubstituted, short, polyacetylenic molecules (“polyenes”) in the coloration of freshwater cultured and many other pearls, rather than carotenoids, which are found only in the pen-shell pearls of the genus *Pinna*. **Sutas Singhamroong** (Dubai Gemstone Laboratory, UAE) presented a preliminary study of Persian Gulf natural pearls, which grow in a variety of shapes and are mainly small, white to “cream” colored (with about 2–3% being yellow). The UV luminescence of the white pearls is typically a strong greenish white. The gray pearls contain more organic matter in their nacre, and typically have a lower SG (down to 2.0).

The technical seminar concluded with a panel discussion on how pearl certification can help the industry. Among other issues, the point was made that nacre quality is as important as nacre thickness. Lower-quality nacre can be recognized by its chalkier appearance, the defects it induces around drill holes, and the presence of thicker-



Figure 34. These cultured pearls (8.6–9.9 mm in diameter) were harvested in 2007 from the Sea of Cortez, Mexico. Photo by Douglas McLaurin.

than-average conchiolin layers just beneath the surface, as seen in X-radiographs.

A number of speakers addressed pearl production during the summit. **Daniele Naveau** (Robert Wan, Tahiti) discussed efforts to reduce the number of Tahitian farms in order to increase quality, in particular to insure nacre thickness above 0.8 mm. In parallel, there is a need for standardization of certification. **Enrique Arizmendi** (Perlas del Mar de Cortez, Guaymas, Mexico) described the history of natural pearl production in Mexico's Sea of Cortez, which ended in 1914. Current efforts with the *Pteria sterna* have resulted in an annual production of about 3.5 kg of multicolored cultured pearls (e.g., figure 34).

Three presenters addressed the incredible boom in Chinese freshwater cultured pearls: **Shi Hongyue** (Gems and Jewellery Trade Association of China), **Dr. Qiu Zhili** (SunYat-sen University, Guangzhou), and **He Naihua** (China's World Pearl Association). Production has risen from the first 0.61 kg of whitish "rice krispies" from *Cristaria plicata* in 1971 to the current 1,500 tonnes of larger, often colored cultured pearls from the *Hyriopsis* genus (an increase of more than two million-fold). This large mollusk has pearl-producing cycles of five-to-six years, with up to 70 grafts per animal. Only about 5% of the cultured pearls are gem grade, 15% are ground into powder for medicinal use, and the rest are incorporated into various ornamental objects. Rounds represent less than 10% of the production. During the summit, Chinese delegates displayed several round white-to-purple freshwater cultured pearls of modest luster but very large size, about 17 mm. There is also a small production of saltwater cultured pearls from the *Pinctada martensii* (but the nacre is thin, 0.2–0.6 mm) and mabe from the *Pteria penguin*.

Stephen Arrow (Arrow Pearls, Broome, Western Australia) presented the history and current status of large

South Sea cultured pearls from *Pinctada maxima* on Australia's northwest coast. Some of the culturing is performed on the seabed, not in suspended baskets, with white being the targeted color, though the production of "golden" colors is around 25%. Good-quality rounds do not exceed 21 mm diameter and take about six years of cultivation. **Sarkis Hajjar** (Belppearl, Antwerp, Belgium) discussed the culturing of pink-to-purple freshwater pearls in Lake Kasumiga, Japan, based on the hybrid *Hyriopsis cumingi* × *H. schlegeli*. About 10 kg of such pearls are produced annually, with other cultivation sites currently being sought.

Both speakers on economics and marketing lamented the lack of reliable statistics for pearl jewelry and the industry. **Tawfique Abdullah** (Dubai Gold & Jewellery Group) lamented the poor communication between producers, manufacturers, and retailers, and argued for harmonization of standards among the various producing regions. He added that the pearl industry spends less than one percent of the production value on promotion, in comparison to 20–40% for other luxury goods. **Naheed Anees** (ARY Academy of Gems & Jewelry, Dubai) pointed out that the Gulf Cooperation Council countries represent 9% of the world's jewelry market, and the per capita jewelry consumption in UAE is about 20 times the world's average. She recommended developing programs to educate consumers about pearls, in particular about imitations, which are still common in the Middle Eastern market. She also proposed developing effective marketing techniques to show that pearl jewelry is no longer "old-fashioned," but rather can be innovative as well as inexpensive.

Emmanuel Fritsch

Stefanos Karampelas

University of Thessaloniki, Greece
IMN, University of Nantes, France

ANNOUNCEMENTS

New Portuguese-language gemology newsletter. A Portuguese language newsletter dedicated to gemology, gems, and jewelry was recently launched by LABGEM gemological laboratory. Called *Portugal Gemas*, the newsletter will be produced on a quarterly basis and be distributed electronically in PDF format. Free subscriptions are available at www.labgem.org.

Association of the Study of Jewelry & Related Arts. This new association, launched in January 2008, will promote jewelry studies in schools, museums, and institutions of higher learning. A quarterly magazine, *Adornment*, and an annual conference are both planned. ASJRA will work for the inclusion of jewelry history courses at the college and graduate level, and encourage the development of study programs for jewelry design students and jewelry history students at museums. Visit www.asjra.net.

CIM Conference and Exhibition. Held May 4–7, in Edmonton, Alberta, the 2008 meeting of the Canadian

Institute of Mining, Metallurgy and Petroleum will feature a session on the geology of diamonds in Canada. Visit www.cim.org/edmonton2008.

INTERTECH 2008. Addressing the latest developments in the manufacture and applications of industrial diamond, CVD synthetic diamond, and related materials, this conference will be held May 5–7, 2008, in Orlando, Florida. Visit www.intertechconference.com.

WDC 2008. The 33rd World Diamond Congress will be held May 12–15, 2008, in Shanghai, China. Visit www.worlddiamondcongress2008.com.

GAA 62nd Federal Conference. The Gemmological Association of Australia will host its 2008 conference on May 16–17 in Coober Pedy, South Australia. Visit www.gem.org.au/newsf.htm.

Santa Fe Symposium 2007. This 22nd annual symposium on jewelry manufacturing technology will be held in Albuquerque, New Mexico, May 18–20. Visit www.santafesymposium.org.

Art2008. Held May 25–30 in Jerusalem, Israel, the *9th International Art Conference on Non-destructive Investigation and Analysis* will focus on items of cultural heritage, but will have implications for gem testing. Visit www.isas.co.il/art2008.

Quebec 2008: GAC-MAC-SEG-SGA. Held May 26–28 in Quebec City, Canada, this joint conference organized by the Geological Association of Canada, Mineralogical Association of Canada, Society of Economic Geologists, and the Society for Geology Applied to Mineral Deposits will include special sessions on “Diamonds: From Mantle to Jewellery” and “Challenges to a Genetic Model for Pegmatites,” as well as a short course called “Rough Diamond Handling.” Visit www.quebec2008.net.

NDNC-2008. The growth, processing, characterization, properties, and applications of diamond and related materials will be covered at the 2nd International Conference on New Diamond and Nano Carbon, held May 26–29 in Taipei, Taiwan. Visit <http://diamond.iams.sinica.edu.tw/NDNC2008>.

Maine Pegmatite Workshop. This short course reviewing current information and theories about pegmatite paragenesis, mineralogy, and petrology will be held May 31 to June 6, 2008, in Poland, Maine. Visit <http://homepage.mac.com/rasprague/PegShop>.

SEG-GSSA2008: Africa Uncovered—Mineral Resources for the Future. Diamond presentations will be covered at this conference, hosted by the Society of Economic Geologists

and the Geological Society of South Africa, in Muldersdrift, South Africa, on July 6–9. Visit www.seg-gssa2008.org.

Goldschmidt 2008. Held July 13–18 in Vancouver, British Columbia, Canada, this geochemistry conference will include a session titled “Fluids Associated with Diamond Formation.” Short courses will include “Laser-Ablation-ICPMS in the Earth Sciences: Current Practices and Outstanding Issues” and “A Hands-On Introductory Tour of Kimberlites.” Visit www.goldschmidt2008.org.

IGC 2008. Held in Oslo, Norway, on August 5–14, the *33rd International Geological Congress* will include sessions with possible applications to gemology: mineral spectroscopy; metallogeny and mineral potential of Russia, Belarus and Ukraine; geology of Africa; and development strategies for the mining sectors of African countries. Visit www.33igc.org.

9th International Kimberlite Conference. Held August 10–15 in Frankfurt, Germany, this conference will bring together the academic and diamond exploration communities to exchange information on kimberlites and related rocks. Visit www.9ikc.com.

IUCr2008. Crystal growth, characterization, and analytical techniques will be covered at the *21st Congress of the International Union of Crystallography*, held in Osaka, Japan, August 23–31. Visit www.congre.co.jp/iucr2008.

6th International Conference on Mineralogy and Museums. Held September 7–9, at the Colorado School of Mines, Golden, Colorado, conference themes are the relationships between museums and research, collection management, and society. Gems will form a significant part of the program, and pre- and post-conference field trips are being planned to kimberlite and pegmatite sites in Colorado. Visit www.mines.edu/outreach/cont_ed/ICMM6.

Diamond 2008. The *19th European Conference on Diamond, Diamond-like Materials, Carbon Nanotubes, and Nitrides* will be held in Sitges, Spain, September 7–11. Presentations will be given on the growth, processing, and characterization of diamond. Visit www.diamond-conference.elsevier.com.

Rapaport International Diamond Conference. This conference will take place September 8, 2008, at the Waldorf Astoria Hotel, New York. Topics will include diamond finance, rough supply, manufacturing, commoditization, and fair trade jewelry. E-mail IDC@diamonds.net.

Exhibits

Exhibits at the GIA Museum. From May 21 through December 2008, “Facets of GIA” will explain the various

gemological services that GIA provides, including diamond grading, gem identification, education, and public outreach. As part of this exhibit, the Aurora Butterfly of Peace—a display comprised of 240 natural fancy-colored diamonds—will be featured through July 2008, courtesy of Alan Bronstein. Also currently on display in the Rosy Blue Student Commons are photo essays by Robert Weldon, manager of photography and visual communications at the GIA Library, and *Gems & Gemology* editor Brendan Laurs, depicting emerald mines in Colombia and the Paraíba-type tourmaline deposit in Mozambique, respectively (for more on the latter, see the article on pp. 4–30 of this issue). Advance reservations are required; to schedule a tour, call 760-603-4116 or e-mail museum@gia.edu.

Diamond Divas. On display at the Diamond Museum Province of Antwerp until June 8, 2008, this exhibit highlights diamond jewelry worn by royalty and celebrities from the past and present. Included will be pieces worn by Empress Josephine, Doris Duke, and Sophia Loren, among others, as well as the rarely seen Moon of Baroda diamond, worn by actress Marilyn Monroe during her iconic scene in the movie “Gentlemen Prefer Blondes.” Visit www.diamonddivas.be.

Gems! Colors of Light and Stone at the Bowers Museum. The Michael Scott collection has returned to the Bowers Museum in Santa Ana, California, with an expanded display of rare colored stones, carvings, and sculptures. The exhibit will run until June 16, 2008. Visit www.bowers.org.

The Aurora Collection at The Vault. “The Vault,” a new permanent collection of rare gemstones and mineral specimens, is now open at the Natural History Museum in London. Headlining the initial exhibit is the Aurora Collection, currently comprising 296 naturally colored diamonds (267.45 carats total weight) assembled by diamond collectors Alan Bronstein and Harry Rodman. Also on display is the 47.69 ct Star of Africa, which helped launch the 1869 diamond rush in South Africa, and the 1,385.95 ct Devonshire emerald crystal. Visit www.nhm.ac.uk/galleries.

Gold: Visions of the Americas. Beginning May 14, 2008, at the Musée de la Civilisation in Quebec City, Quebec, this exhibition will review the importance of gold to the cultures of North and South America, both ancient and modern. The 250 items on display will include gold objects and mineral specimens, as well as paintings, sculptures, and ethnographic objects. Visit www.mcq.org.

IN MEMORIAM

GRAHAME BROWN (1936–2008)

Grahame Brown, distinguished gemologist and longtime editor of *The Australian Gemmologist*, passed away January 15, 2008, after a battle with cancer. He was 71.

Although Dr. Brown was a practicing dentist until the end of his life, gemology became a fitting outlet for his remarkable intellect and energy. At the encouragement of a dentistry colleague in Brisbane, he began taking the Gemmological Association of Australia (GAA) diploma courses in 1973. The following year, Dr. Brown was awarded the association’s diploma with distinction, an accomplishment he repeated with the Gemmological Association of Great Britain in 1975. Numerous other diplomas and professional affiliations would follow.

Dr. Brown began teaching for the GAA in Queensland in 1975. Over the next two decades, he held a series of leadership roles within the association, serving as its president from 1989 to 1993. The GAA named him an honorary life member in 1990. Meanwhile, Dr. Brown was contributing influential articles to the association’s quarterly journal, *The Australian Gemmologist*, for which he served as editor from 1994 until his death. (Grant Pearson has been named the journal’s new editor.)



In addition to operating his own gem identification and appraisal consultancy and teaching for the GAA, Dr. Brown taught gem identification at the University of Queensland from 1989 to 1992. He frequently lectured at conferences worldwide, including GIA’s Second International Gemological Symposium in 1991. He was elected to the International Gemmological Conference (IGC) in 1995 and served as Australia’s delegate to the CIBJO Congress in 2002 and 2004.

Dr. Brown was a prolific author, publishing more than 500 gemological papers. His Summer 1991 *Gems & Gemology* article on treated Andamooka matrix opal remains the definitive work on the subject. He was a contributing editor to the fifth edition of Robert Webster’s *Gems: Their Sources, Descriptions and Identification* in 1994. From 2001 until his death, Dr. Brown was also editor of *The NCJV Valuer*, a gem and jewelry appraisal magazine.

Grahame Brown is survived by his wife, Helen, their three children, and six grandchildren. He will be missed by his many friends and colleagues throughout the world.

Take the Challenge

THE FOLLOWING 25 QUESTIONS are based on information from the Spring, Summer, Fall, and Winter 2007 issues of *GEMS & GEMOLOGY*. Refer to the feature articles, "Notes and New Techniques," and "Rapid Communications" in those issues to find the **single best answer** for each question.



All answers can be found in the 2007 issues—no further research is necessary. Mark your choice on the response card provided in this issue. (Sorry, no photocopies, scans, or facsimiles will be accepted; go to www.gia.edu/gemsandgemology to purchase additional copies of this issue.) Mail the card so that we **receive it no later than Monday, August 4, 2008**. All entries will be acknowledged with a letter and an answer key after the due date, so please remember to include your name and address (and write clearly!).

Score 75% or better, and you will receive a GIA CONTINUING EDUCATION CERTIFICATE, and if you are a member of the GIA Alumni Association, you will earn 10 Carat Points. (Be sure to include your GIA Alumni membership number on your answer card and submit your Carat card for credit.) Earn a perfect score, and your name also will be listed in the Fall 2008 issue of *GEMS & GEMOLOGY*. Good luck!

- In the mid-1990s, Japanese pearl farmers faced their first significant competition in lower price ranges from pearls produced in
 - Australia.
 - China.
 - French Polynesia.
 - the Philippines.
- Testing suggests that, under normal conditions of wear and care, the most durable type of emerald-filling substances are
 - soft fillers.
 - semi-hard fillers.
 - surface-hardened fillers.
 - cedarwood oils.
- Although they are typically associated with _____ synthetic gem materials, nail-head spicules (and similar-appearing inclusions) should not be considered conclusive proof of synthetic origin.
 - chemical vapor deposition-grown
 - flame-fusion
 - flux-grown
 - hydrothermally grown
- The structures of the most common ornamental corals typically consist of a ribbed or striated pattern and a(n)
 - cross-hatch pattern.
 - octahedral growth pattern.
 - lamellar twinning structure.
 - concentric, scalloped structure.
- The vivid yellow tourmaline from the Canary mining area of eastern Zambia is notable for its high manganese and low
 - fluoride.
 - iron.
 - sodium.
 - copper.
- Spectroscopic evidence has shown that _____-related defects can cause a green component in a diamond's bodycolor.
 - magnesium
 - nickel
 - nitrogen
 - oxygen
- Whereas early CVD synthetic diamonds from Apollo Diamond Inc. displayed a weak _____ fluorescence to UV radiation that was considered a strong indicator of CVD synthesis, the company's newer products do not.
 - blue
 - green
 - orange
 - yellow
- According to data for diamond-producing countries from 2001 through 2005, Russia ranks first in carat weight and _____ ranks first in value.
 - Australia
 - Botswana
 - Canada
 - South Africa
- Most Canary tourmaline is heat treated to _____ to pro-

- duce the characteristic bright yellow coloration.
- 400–450°C
 - 450–500°C
 - 500–550°C
 - 550–600°C
- Coated diamonds are not issued GIA Laboratory quality grading reports because
 - their proportions may yield an inconsistent cut grade.
 - it is difficult to view inclusions through the coating.
 - after coatings are applied, inclusions in a diamond become unstable.
 - coatings consist of a foreign material applied to the surface and may be unstable.
 - In a study of colored diamonds, the CCD spectrometer, when compared with the spectrofluorometer, showed a
 - higher resolution and faster collection time.
 - lower resolution and slower collection time.
 - higher resolution and slower collection time.
 - lower resolution and faster collection time.
 - Examination of the Napoleon Necklace with _____ spectroscopy revealed that 13 of its 52 diamonds are the relatively rare type IIa.
 - fluorescence
 - infrared
 - Raman
 - UV-Vis
 - The trapiche pattern in some green tourmalines from northwestern Zambia is formed by a black carbonaceous substance, mostly
 - charcoal.
 - graphite.
 - limestone.
 - shale.
 - The coin-bead/spherical-bead (CBSB) nucleation technique being used by Chinese fresh-
 - water pearl farmers entails a total pearl-growth period of
 - one or two years.
 - two or three years.
 - three or four years.
 - four or five years.
 - In testing of emerald fillers, the most catastrophic damage to individual stones was caused by exposure to
 - chill-thaw cycles.
 - desiccation.
 - mild heat and light.
 - sunlight.
 - _____ dominated world diamond production from 1750 to 1870, followed by _____ from 1870 to 1932.
 - Brazil/South Africa
 - India/Russia
 - Indonesia/South West Africa
 - South Africa/Australia
 - The yellowish green color of diopside and tremolite from Merelani, Tanzania, appears to be related to the presence of trace amounts of vanadium and
 - chromium.
 - iron.
 - manganese.
 - zinc.
 - Which of the following can conclusively and nondestructively identify the origin of color in pink-to-red coral?
 - Microscopy
 - Raman analysis
 - Specific gravity testing
 - UV-Vis-NIR reflectance spectroscopy
 - The most valuable color of “Paraíba” tourmaline, representing some 20% of the production from the new Glorious mine in Brazil, is
 - blue.
 - green-blue.
 - green.
 - violet.
 - Norland Optical Adhesive, a colorless liquid polymer sometimes used to fill turquoise, is cured with
 - epoxy.
 - heat.
 - laser treatment.
 - UV radiation.
 - Pearl retailing has undergone a revolution in recent years, fueled by _____
 - contemporary jewelry designs in a wide variety of styles and prices.
 - the availability of pearls in a variety of colors, shapes, and sizes.
 - a stable supply of high-quality pearls.
 - all of the above.
 - Internal graining and strong _____ are important features observed in CVD-grown synthetic diamonds from Apollo Diamond Inc.
 - birefringence
 - low-order interference colors
 - magnetism
 - twinning
 - On Serenity coated diamonds, the coatings are found
 - on the girdle.
 - on the crown.
 - on the pavilion.
 - over the entire diamond.
 - The natural pink diamonds examined by fluorescence spectroscopy showed _____ fluorescence spectra.
 - category 1 (generally blue)
 - category 2 (generally green)
 - category 3 (generally yellow)
 - other (generally pink to orange)
 - The “fixed-star” pattern in trapiche tourmaline from Zambia, like that of trapiche emeralds and rubies, originates from
 - skeletal growth.
 - pseudomorphism.
 - rotational twinning.
 - variable exsolution of inclusions.

BOOK REVIEWS

EDITORS

Susan B. Johnson
Jana E. Miyahira-Smith
Thomas W. Overton

Rings: Jewelry of Power, Love and Loyalty

By Diana Scarisbrick, 384 pp., illus., publ. by Thames & Hudson Ltd. [www.thamesandhudsonusa.com], London, 2007. US\$50.00

In the course of her rich career, jewelry historian Diana Scarisbrick has written about a variety of arcane, rarefied topics ranging from tiaras and cameo carvings to Tudor and Jacobean jewelry. In *Rings*, she indulges her special interest in some of the smallest yet most potent jewelry objects. The result is a scholarly *tour de force* told by tiny survivors that memorialize mankind's artistic sensibilities and technological advances as much as our beliefs and dreams.

By organizing her book by theme before chronology, Scarisbrick demonstrates how rings embody the spirit of the age in which they were created. She examines eight different themes: rings as signets; love, marriage, and friendship rings; devotional, apotropaic (to "ward off evil"), and ecclesiastical rings; *memento mori* and memorial rings; rings associated with illustrious people and great events; decorative rings; the diamond ring; and the ring as accessory.

The core source for the book's 483 illustrations, most of which are in color, is the Benjamin Zucker Family Collection, supplemented by examples from museums and other collections, both private and public. Insightful legends that underscore significant or archetypal features accompany tidy photographs and illustrations.

The content is rich in anecdote, historical footnotes, and quotations. Scarisbrick leaves no illustrative source unturned, embellishing the academic tone with portraits and oil paintings, engravings, woodcuts, old catalogues, ancient writings, inscriptions, drawings, publicity materials, and early photographs. Beyond familiar sources such as Pliny's *Natural History*, the author cites literature from Greco-Roman classicism to publications of bygone eras that presage the modern age, sampling Lord Byron's letters to *Ladies' Monthly Museum* at the turn of the 18th century and news from *The Tatler* a century later. The scholarly treatise is further supported by source notes for illustrations and text, a bibliography, and an excellent index.

The book ends with its shortest and least expansive chapter, devoted to rings as accessories, which primarily focuses on calendar and watch rings, as well as "poison rings" used to hide lethal substances.

While the book is not suited to casual reading, its thematic organization makes it a valuable resource for those seeking specific insight into design invention or reinvention and jewelry as a reflection of its time. The book deserves recognition beyond its must-have status as a definitive reference for jewelry historians, curators, and designers, to include all those interested in examining civilization through the looking glass of our most personal jewels—rings.

MATILDE PARENTE
Libertine
Indian Wells, California

The Emerald Book

By Yogi Durlabhji, Shyamala Fernandes, and Ruchi Durlabhji, Eds., 143 pp., illus., publ. on behalf of the Jaipur Jewellery Show [info@jaipurjewelleryshow.org], Jaipur, India, 2007. Free [limited distribution]

The Emerald Book was created to provide insight into the world of emeralds and the emerald industry, and to highlight Jaipur as a trading center. As a promotional book published in conjunction with the 2006 Jaipur Jewellery Show, it has a polished, professional look: The layout is attractive, and it is lavishly illustrated and printed on high-quality glossy paper.

However, the text is organized in a way that makes it difficult, at first glance, to grasp the general content. There is no table of contents, and the book starts immediately with the chapter "Romance and Rhapsody," describing the earliest sources of emerald and showing historic pieces of emerald jewelry. It reviews the discovery of Colombian emeralds and their effect on the world market, especially on Indian royalty. Also shown are examples of emerald carvings throughout history, and important emeralds and impressive pieces of jewelry (some with Indian designs), many of which are now owned by royal European families or held in museums throughout the world.

Two brief sections cover beliefs in the magical power of emerald, especially within ancient Indian philosophies. The next section describes the

history and evolution of the emerald trade in Jaipur. It gives the reader a good understanding of how Jaipur built its position as an emerald center, and how its sources of supply changed over the years, with Zambia now the only important one. A very concise overview of the most important commercial emerald mines reveals some interesting facts about the current mining situation. However, a section about “The Great Jewellers” seems a bit out of place. Although much attention is paid to their general impact on the jewelry trade, only one example is given of how a jeweler was inspired to use emeralds in a piece of jewelry. In my opinion, more in-depth information about this jeweler’s thought process would have made this section more interesting and appropriate.

There is little geology or gemology in this book. As a result, a discussion about the term *red emerald* seems sudden and out of place, since the reader must have a thorough understanding of beryl gemology to be able to follow it.

For all those who love emeralds and jewelry, though, this book gives an interesting and honest insider’s look into the emerald trade. The authors express great pride in the profession and in Jaipur’s status within the industry, but they also mention smuggling, robberies, violence at emerald sources, and concerns about the many museum pieces that are meant to be shown to the public, but all too often remain locked away in vaults.

HANCO ZWAAN
*Netherlands Gemmological Laboratory
National Museum of Natural
History Naturalis
Leiden, The Netherlands*

Jewelry Savvy: What Every Jewelry Wearer Should Know

By Cynthia A. Sliwa and Caroline Stanley, 224 pp., illus., publ. by Jewels on Jewels, Los Angeles, [www.jewelrysavvybook.com], 2007. US\$19.99

At some point, every jeweler experi-

ences the dilemma of a customer who returns an item but cannot be specific about the reason, except to say, “It just didn’t look right.” You try to save the sale or come up with an alternative, but in the end both of you walk away shaking your heads.

When faced with this scenario, you have to know that it is not the customer, and it is not the price points; it is the jewelry—the wrong type of jewelry for the body type, personality, and style of the wearer. The art of adornment is very nuanced, and *Jewelry Savvy* is a perfect book for both sides of the counter—a self-help book for the consumer and a marketing book for jewelers.

The authors are a singular collaboration of style consultant and fourth-generation jeweler, with decades of experience between them, who bring practical advice to the choosing and wearing of jewelry. Each chapter starts with a clever quote while addressing the anatomy of choosing the right jewel. Helpful shadow boxes of “Savvy Tips” further drive home the points of the chapter.

The emphasis is on the wearer, with in-depth discussion of physical features, personality, face shapes, and specific body types—in other words, the signature style of the purchaser. The authors encourage jewelers to experiment with color, texture, necklace length, placement, and combinations of pieces.

The primer on metals, diamonds, and gemstones is presented in a conversational, jargon-free tone. Helpful charts that sort gemstones by color, birthstone, anniversaries, and safety in the ultrasonic cleaner, as well as useful terminologies, are liberally sprinkled throughout the book. Further information on cleaning and storage, as well as traveling with jewelry and gemstones, is also included. The section on which jewelry items should be stored in a soft pouch and which ones need to be stored in a plastic bag is a good one to review with your clients.

Considering all this, the “Jewelers and Appraisals” chapter is something

of a disappointment. The appraisal document example is not within industry standards, and may give a false impression of completeness. In addition, the resources chapter does not list any of the major appraisal organizations. The lack of an index is also frustrating when you try to go back to review a topic. However, the overall appeal to consumers is achieved by clear, uncomplicated text, making this book a success.

GAIL BRETT LEVINE, GG
*National Association of
Jewelry Appraisers
Rego Park, New York*

In Gold We Trust: Social Capital and Economic Change in the Italian Jewelry Towns

By Dario Gaggio, 352 pp., publ. by Princeton University Press [press.princeton.edu], Princeton, NJ, 2007. US\$39.50

By the 1960s, despite their relatively small size and spotty-to-nonexistent goldmaking traditions, the small towns of Arezzo, Valenza Po, and Vicenza had come to dominate the Italian gold industry. Each town did it its own way, with Tuscany’s Arezzo eventually identified with global reach and stylized manufacturing, Piedmont’s Valenza Po with craftsmanship and artisanal flair, and the Veneto’s Vicenza with industrialized mass production.

The way each town rapidly transformed into its ultimate brand-incarnation in the gold and jewelry world is the subject of Dario Gaggio’s *In Gold We Trust*. In his rigorous academic and socio-scientific treatise, the University of Michigan assistant professor of history explores each town’s unique socio-cultural and economic factors and how they intertwined with politics, demography, tradition, and trust, among other factors, to spawn the specialized entrepreneurship and small-scale industrialization now recognized as synonymous with quality and style.

Gaggio also examines the decline of Providence, Rhode Island, a city once at the core of America's industrial revolution. With varying success, the author draws parallels and contrasts between the operative dynamics of Providence and that of the Italian towns to examine how and why Providence's jewelry industry eventually lost touch with American modernity. One might also theorize a missing link that emerged in one persona or another in the Italian towns—fire-brand, visionary, or dominant leaders capable of galvanizing industry and the workforce to better adapt to the societal, labor and demographic challenges of the times, as well as emerging competitors. It wasn't always pretty.

This is a high-concept book that cites the writings and polemics of historians, sociologists, political scientists, and philosophers. It is not a book for casual jewelry buffs or romanticist Italophiles. Rather than engage in simplistic arguments about northern Italian prosperity and the corruption and backwardness of the south, the author presents meticulously researched and footnoted arguments in a specialized and often-arcaic academic style more suited to an audience of serious historians and cultural anthropologists. Business school students and their professors, as well as motivated and patient readers interested in Italian culture and its rich jewelry history, may also strike gold.

MATILDE PARENTE

Safety Solutions

63 pp., illus. with DVD, publ. by MISA Press [www.mjasa.org/info_press.php], Providence, RI, 2007. \$49.95 (\$29.95 for DVD alone)

In an increasingly fast-paced world where any assumptions as to a person's understanding of his or her trade are as reliable as winning a late-night game of poker, *Safety Solutions* is a resource no business can afford to do

without. One might call it the North American reference manual on how to set up a jewelry manufacturing operation that minimizes hazards to employees and property, while maintaining efficiency and profitability.

There are two parts: a 56-page booklet and a 20-minute presentation on DVD, both tightly structured and complementing one another.

Besides addressing regulations pertaining to fire safety, building codes, and hazardous materials, the first section specifically introduces California Proposition 65 (intended to keep toxic substances out of consumer products) and national lead poisoning legislation. Although the information is useful, this reviewer would like to have also seen a recommendation that fire alarms and smoke detectors be integrated with security systems, and that fire extinguishers be placed near exits.

The next section discusses the workplace programs for hazard communication. It revolves around material safety data sheets (MSDS) as well as injury and illness prevention. Section three is a selection of excerpts from Charles Lewton-Brain's *Jewelry Workshop Safety Report* (Brain Press Ltd., Calgary, Alberta, Canada, 1998 [www.brainpress.com]), which addresses safe practices in the studio. It takes a closer look at the numerous aspects of safety at the bench and in the casting room, and how to deal with chemicals and chemical inventories. Safety checklists and safety resources are the topics of sections four and five, respectively.

The DVD presentation shares the same objective and covers the topics with comparable emphasis. The order in which topics are presented, however, has been somewhat adapted to the medium.

While most of the information covered in both the publication and the DVD might be shrugged off as common sense, the authors of *Safety Solutions* have kept the content as comprehensive as possible. But make no mistake: The focus is on the *preventive* aspect of safety, with little

about response. You will not find first aid mentioned anywhere in the entire publication. "Is a spill kit available?" or "Is there a procedure in place for dealing with serious injuries that require medical treatment outside the facility?" are as specific as it gets on the subject of response.

Although an ounce of prevention certainly is worth more than a pound of cure, response issues should not be neglected. Thus, purchasers of this work will certainly want to ensure that all emergency numbers remain posted on all their telecom devices.

ROBERT ACKERMAN, GG
Gemological Institute of America
Carlsbad, California

OTHER BOOKS RECEIVED

Diamonds Are Waiting for You. By James R. Holland, 63 pp., illus., publ. by A Bit of Boston Books [www.bitof-boston.com], Boston, MA, 2007, \$12.00. This brief booklet describes the author's trip with his family to the Crater of Diamonds State Park in Murfreesboro, Arkansas. The history of the park and its current status as a public diamond area are reviewed. Also included are tips for would-be diamond diggers. Note that the author incorrectly refers to the site's lamproite deposits as kimberlite.

TWO

Late Antique and Early Christian Gems. By Jeffery Spier, 221 pp. with 154 black-and-white plates, publ. by Reichert Verlag, Wiesbaden, Germany, 2007, \$297.00. This work reviews the history and known examples of carved gems (primarily rings and cameos) from the second through the seventh centuries AD, which are far rarer than examples from periods before the decline of the Roman Empire. More than 1,000 gems from different collections are discussed according to genre, theme, material, and place or time of production.

TWO



GEMOLOGICAL ABSTRACTS

EDITORS

Brendan M. Laurs

Thomas W. Overton

GIA, Carlsbad

REVIEW BOARD

Christopher M. Breeding

GIA Laboratory, Carlsbad

Jo Ellen Cole

Vista, California

Sally Eaton-Magaña

GIA, Carlsbad

Eric A. Fritz

Denver, Colorado

R. A. Howie

Royal Holloway, University of London

HyeJin Jang-Green

GIA Laboratory, New York

Paul Johnson

GIA Laboratory, New York

David M. Kondo

GIA Laboratory, New York

Taijin Lu

Tokyo, Japan

Kyaw Soe Moe

West Melbourne, Florida

Keith A. Mychaluk

Calgary, Alberta, Canada

James E. Shigley

GIA Research, Carlsbad

Boris M. Shmakin

Russian Academy of Sciences, Irkutsk, Russia

Russell Shor

GIA, Carlsbad

Jennifer Stone-Sundberg

Portland, Oregon

Rolf Tatje

Duisburg, Germany

COLORED STONES AND ORGANIC MATERIALS

On the tusks of a dilemma. C. Furness, *Geographical*, November 2006, pp. 47–57.

After ivory poaching brought elephant populations to critically low levels in the 1980s, a worldwide ban on ivory trading in 1990 appeared to address the problem in the eyes of the industry and general public. However, the ivory trade has experienced a renewal in the 21st century, and the means by which different countries handle their elephant populations remains controversial and complex.

The 1990 ban helped in two ways: All ivory crossing a border was known to be illegal, and more importantly, the price of ivory collapsed to the point that poaching was no longer economically viable. Yet by the mid-1990s, wildlife authorities were reporting increased discoveries of poached elephants, and customs officials were noting higher levels of ivory seizures. The rise of a newly affluent middle class in China, long a traditional market for ivory, is thought to be one of the factors, though the consumption of ivory now appears to be higher in Africa—where it is openly sold in many areas, especially Central Africa—than it is in Asia.

Many conservationists were dismayed when the Convention on International Trade in Endangered Species (CITES) voted in 1997 to transfer elephant populations in Botswana, Namibia, and Zimbabwe from Appendix I (the most endangered category, with no trade permitted) to Appendix II (which allows regulated sales), and they blame this action for encouraging new ivory poaching. Many felt this sent a signal that it was okay to purchase ivory again. [*Abstractor's note:* In February 2008, the South African government also voted to

This section is designed to provide as complete a record as practical of the recent literature on gems and gemology. Articles are selected for abstracting solely at the discretion of the section editors and their abstractors, and space limitations may require that we include only those articles that we feel will be of greatest interest to our readership.

Requests for reprints of articles abstracted must be addressed to the author or publisher of the original material.

The abstractor of each article is identified by his or her initials at the end of each abstract. Guest abstractors are identified by their full names. Opinions expressed in an abstract belong to the abstractor and in no way reflect the position of Gems & Gemology or GIA.

© 2008 Gemological Institute of America

transfer their elephants to Appendix II.] Sales of seized ivory stockpiles have also raised concerns, though in October 2006, CITES voted to freeze exports of such ivory from Botswana, Namibia, and South Africa.

Since 2001, worldwide seizures have totaled more than 64 tonnes of raw and worked ivory. For just the period from mid-2005 through 2006, 17 tonnes of ivory were confiscated, a figure that represents 2,750 elephants. However, recent research shows that markets in 25 African and Asian nations may be selling as much as 83 tonnes annually—the equivalent of more than 12,000 elephants—valued at more than US\$8 million. *JEC*

DIAMONDS

Broad-band luminescence in natural brown type Ia diamond. F. De Weerdts [fdw@euphony.net.be] and A. T. Collins, *Diamond and Related Materials*, Vol. 16, No. 3, 2007, pp. 512–516.

The color of type Ia brown diamonds is thought to be due to plastic deformation, since internal strain patterns can be clearly seen with crossed polarizing filters. The visible spectra of these diamonds display absorption that increases significantly below about 550 nm. When illuminated with light from a 514 nm laser, they typically exhibit a broad region of luminescence, composed of two sub-bands, centered at about 710 nm (~1.75 eV). Its occurrence only in the spectra of diamonds containing B-aggregate nitrogen suggests that this feature results from optical transitions at defects that involve this form of nitrogen, perhaps in combination with an intrinsic impurity (a vacancy or interstitial carbon atom) or a structural defect. This broad-band luminescence is absent in type IIa and IaA diamonds. *JES*

The SEM and CCL-SEM study of graphitic inclusions in natural brown diamonds. A. S. Bidny [bidny@mail.ru], O. V. Kononov, A. G. Veresov, and P. V. Ivannikov, *Australian Gemmologist*, Vol. 23, No. 3, 2007, pp. 126–130.

The brown color of some diamonds is believed to be related to vacancy clusters lying on {111} planes or to graphitic microinclusions that are their evolutionary products. The existence of graphitic inclusions in brown diamonds has been confirmed by the use of transmission electron microscopy and is confirmed further here by the use of scanning electron microscopy and color cathodoluminescence scanning electron microscopy to obtain data on the shape, size, and other characteristics of the graphitic inclusions. They are hexagonal lamellar crystals up to 2 μm in size and show recrystallized surface micro-relief; they occur at the corners between the borders of subindividuals. Graphitic, 1–2 μm thick plates measuring 10 μm are found lying parallel to the octahedral diamond faces. *RAH*

A conceptual model for kimberlite emplacement by solitary interfacial mega-waves on the core mantle boundary. B. L. Sim [sim@science.uottawa.ca] and F. P. Agterberg, *Journal of Geodynamics*, Vol. 41, 2006, pp. 451–461.

The authors hypothesize a “mega-wave” model to explain the formation and transportation of core-derived (proto-) kimberlite melts from the earth’s core to the surface. The gravitational forces of the sun and moon, together with accelerated rotation of an inhomogeneous core, caused turbulence in the outer, liquid core. This turbulence triggered lower-density ferrosilicate melts to move out as turbulent jets into the higher-density mantle. Factors such as reduced viscosity at the base of the mantle, irregularities along the core-mantle boundary, and mantle rotation relative to the core (faster than the liquid core and slower than the solid core) provided necessary forces to form extreme amplitude waves or random nonlinear mega-waves. These waves transported (proto-) kimberlite melts with high velocity (~300 m/s) as they approached the surface. The powerful impact of mega-waves at the base of the lithosphere resulted in an upside-down fracture cone of extensional structures (kimberlite pipe complexes) sitting on top of the mega-wave’s apex. An exploration model is proposed for a subduction zone (modern or ancient) that is capable of subducting Archean crust and is also associated with extensional fault complexes.

Future research for this hypothesis may include accurate monitoring of the core-mantle and mantle-crust boundaries, ultra-deep drilling below the kimberlite root zone to look for evidence of the frozen mega-wave, mapping the movement of isolated ferrosilicate melts, and studying fluid dynamics to understand wave mechanics. *KSM*

Diamonds and their mineral inclusions from the A154 South pipe, Diavik diamond mine, Northwest Territories, Canada. C. L. Donnelly [carad@ualberta.ca], T. Stachel, S. Creighton, K. Muehlenbachs, and S. Whiteford, *Lithos*, Vol. 98, No. 1/4, 2007, pp. 160–176.

A study of mineral inclusions in 100 diamond crystals from the A154 South kimberlite at the Diavik mine was undertaken to determine the nature of the diamond source rocks and the conditions of their formation and storage in the mantle. This mine is known for its production of high-quality colorless octahedral diamond crystals. The majority of the diamonds (83%) originated from peridotitic sources in the mantle, while some (12%) were from eclogitic sources, and the others were of undetermined parageneses. Garnet inclusions were slightly enriched in Ca, and olivine inclusions were slightly depleted in Mg, compared to corresponding inclusions in diamonds from southern Africa. The diamonds had carbon isotope compositions similar to those for diamonds from other worldwide sources. Nitrogen concentrations

varied from below detection limits (<10 ppm) to 3800 ppm, and the nitrogen aggregation states ranged from poorly (type IaA) to fully aggregated (type IaB). Some diamonds displayed evidence of plastic deformation. These data suggest that the diamonds formed at temperatures around 1200°C, and then resided at relatively shallow depths in the mantle for an extended period at fairly low temperatures (<1100°C) so as to limit the extent of nitrogen aggregation. *JES*

Diamonds in Western Australia. P. J. Downes and A. W. R. Bevan, *Rocks & Minerals*, Vol. 82, No. 1, 2007, pp. 66–73.

The authors, both curators at the Western Australian Museum in Perth, present a straightforward overview of Australia's main diamond-producing region. The first recorded diamond discovery was in 1895 at Nullagine. Exploration in Australia began in the 1930s and '40s with research by Rex T. Prider, who realized the lamproitic rocks he was studying likely had an origin in the earth's mantle, and therefore had the potential to host diamonds. Diamond exploration reached a pinnacle with the discovery of the Argyle (AK1) lamproite pipe in 1979, but the startup of new mines in the Ellendale field between 2003 and 2005 has shifted attention elsewhere.

A generic account of the geology of the Kimberley region of Western Australia is presented and well-referenced. The Argyle mine is famous for its pink diamonds, which account for less than 0.1% of the diamonds mined in Australia. Quoting other research, the authors state that the pink diamonds are believed to be colored by plastic deformation acting upon nickel impurities and nitrogen defects within the diamond lattice. A donation of several hundred pink diamonds to the Western Australian Museum's collection (from Argyle Diamonds in 2003) is also highlighted.

An interesting side note is that Kimberley, South Africa, which acquired its name in 1873, and the Kimberley region in Western Australia, which received its name in 1880, were both named after John, Baron Wodehouse and Earl of Kimberley, who was the British Secretary of State in the late 19th century. Only by coincidence are the two areas major producers of diamonds. *KAM*

The evolution of diamond morphology in the process of dissolution: Experimental data. A. F. Khokhryakov and Yu. N. Pal'yanov [palyanov@uiggm.nsc.ru], *American Mineralogist*, Vol. 92, No. 5–6, 2007, pp. 909–917.

Experiments on the dissolution of octahedral, pseudo-dodecahedral, and cubic diamond crystals in water-containing carbonate and silicate systems under high-pressure, high-temperature conditions in the diamond stability field are reported. The dissolution agents used included CaCO₃, CaMg(CO₃)₂, and CaMgSi₂O₆, as well as kimberlite from Russia's Udachnaya pipe, with the addition of

distilled water. With dissolution, the diamond morphology changed from octahedra, dodecahedra, and cubes to tetrahedra. Octahedra transformed into tetrahedra when the weight loss was 20–25%, and to a cube when the loss was 50%; pseudo-dodecahedra transformed into tetrahedra when the weight loss was as low as 10%. Crystal morphology, surface features, and goniometric data for diamond dissolution forms produced in these water-bearing systems were identical to those of rounded diamonds found in nature. The results provide a model for evolution of diamond crystal morphology during dissolution by natural processes in the earth. *RAH*

Micrometer-scale cavities in fibrous and cloudy diamonds: A glance into diamond dissolution events. O. Klein-BenDavid [o.k.bendavid@durham.ac.uk], R. Wirth, and O. Navon, *Earth & Planetary Science Letters*, Vol. 264, No. 1–2, 2007, pp. 89–103.

Micrometer-scale cavities found in the inner parts of fibrous and cloudy kimberlitic diamonds may preserve evidence of dissolution events. Combining the methods of focused ion beam sample preparation and transmission electron microscopy enabled the authors to study these features in detail. The fillings in these cavities consisted of amorphous matrix, secondary nanocrystals, volatiles, and in some cases larger resorbed crystals. Trapped minerals included corundum, K-alumina, quartz, olivine, moissanite-6H, and Ca-Mg carbonates. Secondary nanominerals within the amorphous matrix included carbonates, aluminum oxide, fluorite, ilmenite, and secondary diamond crystals. The amorphous matrix was spongy, and its composition was dominated by amorphous carbon, nitrogen, and chlorine; it also contained water. When no crystalline phases were observed, the matrix was also enriched in silica, alumina, and in some cases calcium.

The authors propose that micrometer-scale cavities in diamond form during dissolution events induced by the introduction of oxidizing hydrous fluids. Such fluids are the main dissolving agents for most kimberlitic diamonds. At diamond-forming conditions, silica and alumina are enriched in hydrous fluids that are in equilibrium with eclogites, and this is consistent with the greater solubility of alumina with increased pressure and temperature in the NaCl-bearing fluids. Diamond dissolution will form oxidized carbon species and may decrease the solubility of silica and alumina in the dissolving agent, leading to their precipitation. *RAH*

Morphology of diamonds from kimberlite pipes of Catoca field (Angola). V. N. Linchenko [vlilumir.zln@mail.ru], *Proceedings of the Russian Mineralogical Society*, Vol. 136, No. 6, 2007, pp. 91–102 [in Russian with English abstract].

The morphology of more than 3,200 diamond crystals from kimberlite pipes of the Catoca field in Lunda

Province of northeast Angola was studied in detail. Diamonds from different pipes in this field had distinguishing features in their morphology and in their physical-mineralogical properties. Octahedral forms, which are considered to be indicative of conditions more favorable for diamond growth and preservation, predominated in crystals from the Catoca and Kamitogo pipes, in contrast with diamonds from the Kakele pipe, where rhombododecahedra were the most common form. These morphological and other mineralogical peculiarities of diamond crystals may be used to help evaluate the diamond-bearing potential of their primary sources in northeast Angola.

RAH

GEM LOCALITIES

Ambers from Dominican Republic. P. Guo-Zhen and Z. Li, *Journal of Gems and Gemmology*, Vol. 8, No. 3, 2006, pp. 32–35.

Amber from the Dominican Republic is well known for its rich inclusions of fossil organisms. Gemological and spectroscopic features of this material were studied and compared with amber from other localities. The authors conclude that the gemological characteristics of Dominican amber are similar to those of other ambers except that the Dominican material has greater transparency and more color varieties. In addition, some shows a strong bluish fluorescence. SEM imagery revealed an irregular layered structure with micro-voids or holes and gaps between micro-layers. IR spectra of the different colors of Dominican amber were similar. Despite the similar geologic age of ambers from various localities, they showed clear variations in aggregation state, as determined from IR absorption features. Differential thermal analysis showed that there were two melting points, at 386.2°C and 529.5°C. The lowest temperature that would alter the structure of Dominican amber was 260°C, compared to 310°C for Chinese amber.

Qianwen (Mandy) Liu

Australian opal resources: Outback spectral fire. S. R. Pecover [specover@bigpond.net.au], *Rocks & Minerals*, Vol. 82, No. 2, 2007, pp. 103–115.

A review of the Great Australian Basin's (GAB) opal deposits, remaining resources, and possible genetic models is presented from a nontechnical perspective. The GAB, containing as much as 95% of the world's play-of-color opal, hosts the material within Cretaceous-age sedimentary rocks. Common (locally called *potch*) and play-of-color opal may occur as veins, infillings within ironstone concretions, or replacements of fossils. Clear evidence is provided for both structural (e.g., faults) and sedimentary (e.g., lithologic boundary) controls on the location of opal deposition, with both regional and local examples. Both of these major controls affect the form and texture of the actual opal, whether it is deposited as veins/veinlets (known locally as *seam* opal),

small nodules (*nobbies*), or pseudomorphic replacements.

The author also critiques three widely circulated opal-formation models. He points out that, although they are useful, none of the theories adequately explain all of the depositional features encountered, so they have limited predictive value for exploration. Further, none appear to explain why play-of-color opal is deposited in some areas, while only common opal is deposited in others. The author emphasizes the importance of the collaboration between laboratory scientists and miners in the field to develop a better model of opal formation, which in turn could lead to more effective exploration.

Quoting other sources, the author lists GAB opal resources for individual fields within New South Wales (Lightning Ridge area), South Australia (including Coober Pedy) and western Queensland. Added together, these figures predict an in-ground value of more than Aus\$120 billion.

KAM

Natural gamma radioactivity and exploration for precious opal in Australia. B. R. Senior [seniorgeo@bigpond.com] and L. T. Chadderton, *Australian Gemmologist*, Vol. 23, No. 4, 2007, pp. 160–176.

The authors propose that pre-sedimentation heterogeneous microspherulitic growth of play-of-color opal within siliceous groundwater takes place on a central radioactive catalyst core. Neutron activation analysis and secondary ion mass spectrometry (SIMS) of play-of-color opal revealed Th, U, Pb, and anomalous amounts of daughter nuclides from natural uranium fission. Gamma-ray radioactive logging of drill holes and open-cut mine walls demonstrated the occurrence of natural radioactivity surrounding opal deposits, increasing in intensity toward the central zone of play-of-color opal. The authors maintain that case histories of the discovery of new opal deposits have validated the use of these techniques for exploration.

RAH

Sapphires in the Butte–Deer Lodge area, Montana. R. B. Berg, *Montana Bureau of Mines and Geology Bulletin 134*, 2007, 59 pp.

The state of Montana has numerous sapphire occurrences, several of which have been well documented. The four main deposits (in order of importance) are Yogo Gulch, Rock Creek, Missouri River, and Dry Cottonwood Creek. Except for Yogo, which produces sapphires from a lamprophyre dike, the source rocks for the Montana sapphires are not known. This study focuses on sapphire occurrences in the mountains near Butte (which includes the Dry Cottonwood Creek deposit), with particular emphasis on the search for their host rocks.

For the first time, details are provided on the dimensions and limits to the sapphire placers on the South Fork of the creek, especially its headwaters. A microscopic comparison with sapphires from other deposits showed limited stream abrasion, which suggests a short transport distance. Adhering to the surfaces of a few sapphires was

volcanic rock that is very similar to the Lowland Creek Volcanics (felsic tuffs and lava flows) found at the South Fork's headwaters, which led the author to conclude they were derived from the weathering of these rocks.

Also studied was the distribution and provenance for the historical sapphire occurrences immediately west of Butte ("Browns Gulch and Vicinity"). Again, evidence suggests that at least some of these sapphires (specifically the Silver Bow occurrence) were derived from the weathering of local Lowland Creek Volcanics.

Along Lowland Creek, a small stretch of sapphire- and gold-bearing alluvium was once mined. Microscopic features of these sapphires were similar to those from the other occurrences in the study. The dominant rocks surrounding the deposit are the Lowland Creek Volcanics; it seems probable, once again, that the sapphires were derived from the erosion of these rocks.

The author notes that several corundum-bearing xenoliths have been found in the Butte area. These xenoliths show a metamorphic mineral assemblage very similar to that of corundum-bearing Precambrian rocks located south of Butte, near the city of Bozeman. Neither the Lowland Creek Volcanics nor the Yogo lamprophyre is chemically capable of crystallizing sapphires directly from their magma. Instead, the two opposed rock types (felsic volcanics and ultramafic lamprophyre) contain sapphires because they transported them as xenocrysts.

KAM

Spodumene from Nuristan, Afghanistan. L. Natkaniec-Nowak [natkan@uci.agh.edu.pl], *Australian Gemmologist*, Vol. 23, No. 2, 2007, pp. 51–57.

In spodumene from the Nilaw mine in Nuristan, the substitution of Fe^{2+} and Fe^{3+} for Al in the octahedral sites produces a green-yellow color, whereas the admixture of Mn, Fe, and perhaps Cr ions gives the violet-pink kunzite color. These spodumenes are typical products of post-magmatic pegmatitic-pneumatolytic processes. A significant amount of alkali metals, particularly Na, indicates a petrologic relationship with Li-bearing granitic pegmatites.

RAH

The Sweet Home rhodochrosite specimen mine, Alma District, central Colorado: The porphyry molybdenum-fluorine connection. P. J. Bartos [pbartos@mines.edu], E. P. Nelson, and D. Misantoni, *Mineralium Deposita*, Vol. 42, No. 3, 2007, pp. 235–250.

Mining for silver at the Sweet Home deposit near Alma, Colorado, began in 1873. After 1900, extraction activities occurred only on an intermittent small-scale basis. From 1991 until 2004, however, the mine produced the finest rhodochrosite mineral specimens ever found, including material that was suitable for faceting. Electron-microprobe data indicates that the rhodochrosite is very pure MnCO_3 with minimal solid solution of Fe^{2+} , Ca, or Mg.

The rhodochrosite occurs in quartz-pyrite-sphalerite-fluorite veins that are found in monzonite porphyry and granodiorite. The best crystals occur within open vugs at the larger fault/vein intersections. Based on the mineralization and their mode of occurrence, the veins are interpreted as representing a high-silica porphyry molybdenum hydrothermal deposit. The age of metal deposition (25.8 ± 0.3 Ma) coincides with the end of mineralization of the major molybdenum deposit at the nearby Climax mine. The hydrothermal system at the Sweet Home mine appears to have been a single, relatively small pulse of magmatic fluid that slowly cooled and was diluted with groundwater. Rhodochrosite mineralization occurred at moderate depths of 1.5–2.5 km. Based on fluid-inclusion homogenization temperatures of up to 310°C, the Sweet Home material crystallized at temperatures significantly higher than typical rhodochrosite.

JES

INSTRUMENTS AND TECHNIQUES

Ionoluminescence of diamond, synthetic diamond, and simulants. H. Calvo del Castillo, J. L. Ruvalcaba-Sil, M. Barboza-Flores, E. Belmont, and T. Calderón [tomas.calderon@uam.es], *Nuclear Instruments and Methods in Physics Research A*, Vol. 580, No. 1, 2007, pp. 400–403.

Luminescence is the nonthermal emission of light by matter following excitation by an energy absorption process. Ionoluminescence (IL) is a luminescence phenomenon that is caused by energetic ions penetrating matter to produce light emission. The light originates from electron transitions and recombination processes within the outer electron shells of the atoms in the material. The energy levels of these electron shells are affected by the chemical bonding of the atom. This method can provide information about the chemical form of elements in a material that cannot be obtained by other ion beam analytical techniques.

In this study, IL spectra were recorded for diamond (both natural and CVD synthetic) and simulants such as synthetic sapphire, synthetic spinel, cubic zirconia, strontium titanate, and yttrium aluminum garnet. A 1.9 MeV proton beam of variable intensity from a particle accelerator was used as the excitation source; only a few seconds were needed to record the spectra. The natural diamonds showed broad luminescence peaks (and optical centers) at about 415 (N3), 430 (N-related), 503 (H3), and 637 (N-V) nm, all of which originate from nitrogen impurities. The CVD synthetic diamonds displayed luminescence features related to the N3 and N-V centers. In contrast, the IL spectra of the simulants were completely different, with luminescence bands due to transition metals (Fe, Mn, Cr, and Ti) or rare-earth elements (such as Er). The authors conclude that this type of luminescence may be helpful in rapidly distinguishing diamond from its imitations.

JES

Some new trends in the ionoluminescence of minerals. H. Calvo del Castillo, J. L. Ruvalcaba, and T. Calderón [tomas.calderon@uam.es], *Analytical and Bioanalytical Chemistry*, Vol. 387, 2007, pp. 869–878.

IL is normally used to detect impurities or defects in modern synthetic materials. However, new applications of IL to natural minerals and ancient artifacts are rapidly being developed. Ionoluminescence is the nonthermal emission of light induced by bombardment with accelerated particle beams. The light emitted is related to the valence state of particular atoms (extrinsic luminescence) or to defects within the crystal structure (intrinsic luminescence). The study of these two emissions can provide information related to the chemical composition or structure of the material. With these data, the identity of the material can be determined. IL can help distinguish natural versus synthetic origin, identify polymorphs, or determine whether a material is crystalline or amorphous. Its sensitivity is much higher than that of particle-induced X-ray emission (PIXE).

Aside from its applicability to the study of modern materials and natural minerals, this technique can be used to identify materials in ancient artifacts. One downside to IL is the need for a particle accelerator to provide the excitation beam. Access to particle accelerators is limited and expensive. EAF

Laser induced breakdown spectroscopy. C. Pasquini [paquini@iqm.unicamp.br], J. Cortez, L. M. C. Silva, and F. B. Gonzaga, *Journal of the Brazilian Chemical Society*, Vol. 18, No. 3, 2007, pp. 463–512.

This article reviews in detail the fundamentals, instrumentation, applications, and future trends of laser-induced breakdown spectroscopy (LIBS) for chemical analysis. A short laser pulse (~5 nanoseconds) vaporizes a small portion (a few micrograms) of the sample being analyzed, and excites the emission of electromagnetic radiation from the constituents of the sample. The emitted radiation is analyzed by high-resolution optics and wavelength detectors to provide both qualitative and quantitative information about the chemical composition of the sample. This technique is finding wide application in many fields where the need for chemical composition data must be balanced against the requirement for minimal damage to the sample. JES

Magnetic susceptibility for gemstone discrimination. D. B. Hoover [stonegrouplabs@beargems.com] and B. Williams, *Australian Gemmologist*, Vol. 23, No. 4, 2007, pp. 146–159.

After a brief review of the physics of magnetism and magnetic susceptibility, a simple method is described for the quantitative measurement of magnetic susceptibility on cut gemstones. The method requires a weighing instrument, a few inexpensive magnets, and a simple device to slowly place and then lift the magnet from the stone's cut surface so as to measure the force of attraction. This technique has

been applied to a variety of gems, but the focus here is on corundum and peridot. Magnetic susceptibility may allow the separation of magmatic from metamorphic corundum (results are given for 18 blue sapphires and 15 others). Similarly, peridot may be distinguished from sinhalite. RAH

JEWELRY RETAILING

Goldheart Jewelry: Management decisions in Singapore. C. Patti [c.patti@qut.edu.au] and L. Wee, *International Journal of Management and Decision Making*, Vol. 8, No. 2/3/4, 2007, pp. 241–250.

The article traces the evolution of a Singapore-based gold jewelry retailer from a traditional store selling gold mainly by weight to a large branded jewelry operation. The owner, Johnny Wham, helped guide the company through several regional economic crises by targeting affluent tourists with innovative designs and high levels of customer service. In addition, he upgraded the stores from the traditional “gaudy” gold jeweler by introducing a modern look and feel. At the same time, he pursued the lucrative bridal market by adding contemporary designs and platinum pieces that had become popular in other Asian countries. Today, Goldheart's 20-store chain has attracted similar competitors, prompting the firm's owner to ponder a future change in direction. RS

Jewelry's lack of luster. R. Perks, *Marketing Week*, November 15, 2007, p. 27.

Jewelry retailers continue to lose market share to other consumer products, because retailers have failed to respond to profound changes in the marketplace. Many retail stores still try to be “all-things-to-all-women” when it is clear that other products have more fashion appeal today. In addition, jewelry retailers are losing out to sellers of mobile phones and travel packages. While the market for luxury watches is booming, many retail jewelers fail to devote enough display space to them; in-store watch displays are also problematic because they all tend to look alike. RS

SYNTHETICS AND SIMULANTS

Effects of thermal treatment on optically active vacancy defects in CVD diamonds. J.-M. Maki [jimm@fys-lab.hut.fi], F. Tuomisto, C. Kelly, D. Fisher, and P. Martineau, *Physica B*, Vol. 401–402, 2007, pp. 613–616.

The authors used positron annihilation spectroscopy (PAS) to explore the nature of brown coloration in synthetic diamonds grown by chemical vapor deposition (CVD). Both natural type IIa diamonds and CVD-grown diamonds can display a brown color; however, the origin of color appears to be different. The brown color of natural diamonds

has been observed to be stable up to temperatures of 1900°C, whereas this color in CVD synthetic diamonds can be greatly affected by annealing around 1400°C. Furthermore, natural brown diamond has high dislocation densities, while the CVD product has very low dislocation densities.

The authors analyzed as-grown and annealed single-crystal CVD synthetic diamonds to observe the concentration, size, and optical activity of defects. They grew two pairs of CVD synthetic diamond {100} plates, with low concentrations of nitrogen added to the growth gas to create the brown color. The samples were examined post-growth, after two hours of 1400°C annealing, and after one hour of 1600°C annealing. In both sample sets, the brown color decreased with annealing, but no sample became completely colorless. PAS results point to large open-volume defects in the CVD synthetics. After annealing at 1400°C, the number of these defects increased, indicating smaller vacancies clustering into larger ones due to increased mobility. With the second annealing at 1600°C, the large open-volume defects did not appear to increase, indicating that mobility occurred at temperatures below 1400°C. Optical activity was observed with only the smallest vacancy defects, and a correlation with absorption needs further investigation. JS-S

Synthesis of diamond from a chlorinated organic substance under hydrothermal conditions. S. Korablov [sergiy2@yahoo.com], K. Yokosawa, T. Sasaki, D. Korablov, A. Kawasaki, K. Ioku, E. H. Ishida, and N. Yamasaki, *Journal of Materials Science*, Vol. 42, No. 18, 2007, pp. 7939–7949.

Diamond can be synthesized by several methods: (1) at high pressures and temperatures from a melt of carbon and a catalyst-solvent; (2) at low pressures and high temperatures from a vapor phase consisting of an excited mixture of hydrocarbons and hydrogen; and (3) by direct conversion from graphite by shock detonation. Several other methods have also been attempted. This article reports on the hydrothermal growth of small diamond particles and thin films on seed crystals of either diamond or cubic boron nitride in the presence of a chemical reaction involving a chlorinated carbon liquid (1,1,1-trichloroethane, $C_2H_3Cl_3$) mixed with sodium hydroxide (NaOH). Diamond growth was achieved at temperatures of 300°C and pressures of 10 kbar. The presence of synthetic diamond particles in the reaction products was confirmed by several analytical techniques. The exact mechanism of diamond growth under these hydrothermal conditions is not fully understood, but the results of this experiment may provide new insights into micro-diamond formation in metamorphic rocks. While the synthetic diamonds produced here were small particles, this new method may be further refined to produce larger crystals in the future. JES

TREATMENTS

XPS and ToF-SIMS analysis of natural rubies and sapphires heated in an inert (N_2) atmosphere. S. Achiwanich, B. D. James, and J. Liesegang [j.liesegang@latrobe.edu.au], *Applied Surface Science*, Vol. 253, 2007, pp. 6883–6891.

X-ray photoelectron spectroscopy and time-of-flight secondary ion mass spectrometry were employed to examine the surface concentrations of selected elements in corundum and how those concentrations changed during heat treatment. The authors heated rubies from Mong Hsu, Myanmar, and sapphires from Kanchanaburi, Thailand, to temperatures between 1000°C and 1600°C in an inert nitrogen atmosphere. The blue color in the core of the Mong Hsu rubies was removed, and a gradual transition from near-colorless to blue was noted in the Kanchanaburi sapphires. It was found that the concentration of Fe and Ti increased—and the concentrations of Cu, Cr, and V decreased—on the surface of the rubies and the sapphires as the temperature of heat treatment increased. EAF

MISCELLANEOUS

Better bling. K. Bowers, *Body & Soul*, March 2008, pp. 120–122.

Environmentally friendly jewelry is a popular topic. This article offers guidance to consumers on buying gold, diamond, and colored stone pieces sourced with ethical responsibility in mind. For gold, the article lists companies that have pledged to observe environmentally sound mining practices. Also provided are sources of conflict-free diamonds, as well as information about the humanitarian crisis in Myanmar. The author notes that colored stones tend to cause the least environmental damage because they require less large-scale mining. The article also showcases jewelry from retailers and designers who source from Fair Trade suppliers. RS

Diamonds: Kimberley Process effective. *Africa Research Bulletin: Economic, Financial and Technical Series*, Vol. 44, No. 11, 2008, pp. 17640A–17641A.

As African diamond-producing nations move beyond conflict diamonds, the next issue is “beneficiation”—adding value to their rough diamonds through indigenous cutting and grading operations. Southern Africa produces about 60% of the world’s diamonds, but it still must grapple with problems that include a shortage of skilled labor in its diamond polishing industry and relatively high pay scales as compared to the Asian nations where most diamonds are processed. The article details beneficiation efforts in South Africa, Botswana, and Angola, and discusses a potential producers’ oligopoly formed by these countries and major mining companies such as De Beers and Rio Tinto. RS